Probabilistic numerical methods in finance : valuation of pollution rights and approximate computation for weak hedging

Mohan Yang

Université Paris Cité

École doctorale de Sciences Mathématiques de Paris Centre (386)

Laboratoire de Probabilités, Statistique et Modélisation (LPSM, UMR 8001)

Méthodes numériques probabilistes pour la finance: valorisation des droits à polluer et approximation de couverture faible.

Probabilistic numerical methods in finance: valuation of pollution rights and approximate computation for weak hedging.

Par **Mohan Yang**

Thèse de doctorat de **Mathématiques Appliquées**

Dirigée par **Jean-François Chassagneux**

Présentée et soutenue publiquement le **8 Décembre 2022**

Devant un jury composé de:

Jean-François Chassagneux	Prof. à Université de Paris Cité	Directeur de thèse
Stéphane Crépey	Prof. à Université de Paris Cité	Examinateur
François Delarue	Prof. à Université Côte d'Azur	Examinateur
Roxana Dumitrescu	Prof. à King's College London	Examinatrice
Benjamin Jourdain	Prof. à Ecole des Ponts	Rapporteur
Thomas Kruse	Prof. à University of Wuppertal	Rapporteur
Chao Zhou	Prof. à National University of Singapore	Examinateur

Remerciements

Mes premiers remerciements s'adressent bien évidemment à mon directeur de thèse, Jean-François Chassagneux, sans qui ce travail n'aurait pas vu le jour. Je suis extrêmement reconnaissant pour ta confiance, ton patience à mon égard et bien sûr ta disponibilité durant ces trois années. Tu m'as appris la recherche en mathématiques avec sérieux et rigueur.

Je tiens à remercier sincèrement Benjamin Jourdain et Thomas Kruse qui me font l'honneur de rapporter ma thèse. Je remercie également Stéphane Crépey, François Delarue, Roxana Dumitrescu, et Chao Zhou pour avoir accepté de faire partie de mon jury de thèse.

Je remercie tout le Laboratoire de Probabilités, Statstique et Modélisation, en particulier les doctorants: Aaraona, Azar, Barbara, Bohdan, Côme, Cyril, Enzo, Fabio, Guillaume C., Guillaume S., Hiroshi, Hoang-Dung, Houzhi, Ibrahim, Junchao, Marc, Maximilien, Médéric, Nathan, Nisrine, Simon, Sothea, Sylvain, William, Xuanye, Yann, Yiyang, Ziad et l'équipe de Mathématiques Financières et Actuarielles, Probabilités Numériques pour m'avoir accueilli durant ces trois années. Merci à Nathalie et Valérie qui ont fait un travail remarquable pour m'accompagner dans toutes mes démarches adiministratives.

Je tiens également remercier Cyril pour m'avoir guidé aux problèmes de weak hedging et leurs liens avec transport optimal. Cette collaboration a permis au dernier chapitre de ma thèse de voir le jour.

Je remercie tout les chercheurs et doctorants avec qui j'ai pu avoir des discussions enrichissantes lors de diverses conférences et colloques, que ce soit à Métabief, à île d'Oléron ou à Paris.

Enfin, je remercie ma famille et mes amis qui m'ont accompagné et soutenu, en particulier mes parents et Tonghui.

Abstract

In this thesis, we propose some probabilistic numerical approximation with application in carbon emission market as well as PnL hedging. Including a theoretical splitting scheme by treating differently transport equation and diffusion equation, an alternative particles and tree-based scheme, and approximate computation for PnL hedging.

In the first part of this thesis, we focus on the numerical approximation of a class of Forward-Backward Stochastic Differential Equations(FBSDEs) which have a degenerate forward component and non-regular terminal condition. It is proposed in [20] for carbon emission market modelling and studied in [19]. We propose a new theoretical splitting scheme for solving this FBSDE systems in a high-dimensional setting. This scheme consists of separating diffusion and non-linear transport parts. We also manage to prove a convergence rate results for our theoretical scheme under structural assumptions.

In practice, in order to be able to implement this scheme, we propose a discrete-time version combining finite difference method for transport operator and non-linear regression method for diffusion operator. We employ conservative finite difference methods such as Lax-Friedrichs and Upwind approximation. Concerning non-linear regression part, we propose a backward scheme involving deep neural networks to overcome the curse of dimensionality of process P, inspired by the scheme *DBDP1* in Huré et al. [48].

To validate empirically the numerical results obtained with the non-linear regression scheme, it is necessary to have a proxy. For this purpose, we propose an another numerical scheme in moderate dimension of P based on splitting scheme but combine a particle method with tree-like regression. In particular, we employ the celebrated Sticky Particle Dynamics (SPD) [53, 55] to approximate the transport operator. In the second work, we study the convergence error by decomposition: local error due to transport operator, propagation error, diffusion error as well as splitting error, and we prove a theoretical convergence bound of rate 1/6 with respect to time step for this alternative scheme under some assumptions by considering the convolution with respect to smooth compactly supported probability density function.

In the second part of this thesis, we focus on a class of non standard control problems in which we impose on the controlled process a constraint involving its law at a terminal time. The classical example is the so-called *quantile hedging* see

e.g. [36]. We first introduce *weak hedging problem* and encapsulate all possible cases for target measure μ: discrete and finite or arbitrary in a general setting. Especially, in linear framework we establish an explicit representation via optimal transportation for weak hedging problem in the case where μ a probability measure, and for μ a discrete and finite measure, we also obtain a new dual characterisation for "Kantorovich version" problem. Based on this dual formulation, we propose a new numerical approach using SGD algorithms. Several numerical tests are run showing quite satisfactory results.

Keywords: singular FBSDEs, splitting scheme, non-linear regression, deep learning, sticky particle dynamics, quantile hedging, optimal transport, duality, stochastic gradient descent.

Résumé

Dans cette thèse, nous proposons une approximation numérique probabiliste avec une application au marché des émissions de carbone ainsi qu'à la couverture PnL. Y compris un schéma de splitting théorique en traitant différemment l'équation de transport et l'équation de diffusion, un schéma alternatif basé sur les particules et l'arbre, et le calcul pour l'approximation de la couverture PnL.

Dans la première partie de cette thèse, nous nous concentrons sur l'approximation numérique d'une classe d'équations différentielles stochastiques progressifs et rétrogrades (EDSPRs) qui ont une composante forward dégénérée mais aussi une condition terminale irrégulière. Il est proposé dans [20] pour la modélisation du marché des émissions de carbone et étudié dans [19]. Nous proposons un nouveau schéma de splitting théorique pour résoudre ces systèmes EDSPRs dans un cadre de grande dimension. Ce schéma consiste à séparer les parties de diffusion et celles de transport non linéaire. Nous parvenons également à prouver un résultat de ordre de convergence pour notre schéma théorique sous l'hypothèse minimale.

En pratique, afin de pouvoir implémenter ce schéma, nous proposons ainsi une version en temps discret qui combine la méthode des différences finies pour l'opérateur de transport et la méthode de régression non linéaire pour l'opérateur de diffusion. Nous utilisons des schéma à la loi de conservation aux différences finies comme Lax-Friedrichs et Upwind. Concernant la partie régression non linéaire, nous proposons un schéma rétrograde en utilisant deep learning pour franchir "curse of dimensionality" du processus P, inspiré du schéma *DBDP1* proposé dans Huré et al [48].

Pour valider empiriquement les résultats numériques obtenus avec le schéma de régression non linéaire ci-dessus, il est nécessaire d'avoir un proxy de solution. Pour cela, nous proposons un autre schéma numérique en dimension modérée de P basé sur le schéma de splitting mais avec une méthode particulaire avec une régression par les arbres. En particulier, nous utilisons la célèbre dynamique des particules collantes (SPD) pour approximer l'opérateur de transport. Dans le second travail, nous étudions la décomposition de l'erreur : erreur locale due à l'opérateur de transport, erreur de propagation, erreur de diffusion ainsi que erreur de splitting, et nous prouvons un ordre de convergence théorique pour ce schéma alternatif sous l'hypothèse minimale en introduisant la convolution par rapport à fonction de densité de probabilité smooth avec un support compact.

Dans la deuxième partie de cette thèse, nous nous intéressons à une classe de

problèmes de contrôle non standard dans lesquels nous imposons au processus contrôlé une contrainte sur sa loi au temps terminal. L'exemple classique est ce qu'on appelle la *couverture quantile* voir e.g. [36]. Nous introduisons d'abord *problème de couverture faible* et encapsulons tous les cas possibles pour la mesure cible μ : discrète et finie ou arbitraire dans un cadre général. En particulier, nous établissons une représentation explicite via transport optimal pour le problème de couverture faible dans le cas μ une mesure de probabilité. Et pour μ une mesure discrète et finie, nous obtenons également une nouvelle caractérisation duale pour le problème de "Kantorovich". A partir de cette formulation duale, nous proposons une nouvelle approche numérique qui se base sur des algorithmes de descente de gradient stochastique. A la fin, nous démontrons également numériquement l'efficacité de notre méthode pour plusieurs cas.

Mots clé: EDSPRs singuliers, schéma de splitting, régression non linéaire, deep learning, dynamique de particules collantes, quantile hedging, transport optimal, dualité, descente de gradient stochastique.

Contents

List of Figures

List of Tables

Résumé détaillé

Ce manuscrit étudie les méthodes numériques pour les équations différentielles stochastiques progressives et rétrogrades (EDSPRs) singulières et l'approximation de la couverture PnL.

Partie I : Méthodes numériques pour EDSPRs singulières de grande dimension (Chapitres 2 et 3)

Soit $(\Omega, \mathcal{F}, \mathbb{P})$ une base stochastique qui supporte un mouvement brownien W de dimension d et $T > 0$ un temps de maturité. On note $(\mathcal{F}_t)_{t\geqslant 0}$ la filtration engendrée par le mouvement brownien (augmentée et complétée). On considère tout d'abord une classe générale de système EDSPR singulière qui prend la forme suivante :

$$\mathcal{X}_t = \mathcal{X}_0 + \int_0^t \mathfrak{a}(s, \mathcal{X}_s, \mathcal{Y}_s, \mathcal{Z}_s)\mathrm{d}s + \int_0^t \mathfrak{b}(s, \mathcal{X}_s, \mathcal{Y}_s, \mathcal{Z}_s)\mathrm{d}W_s, \tag{0.0.1}$$

$$\mathcal{Y}_t = \mathfrak{g}(\mathcal{X}_T) + \int_t^T \mathfrak{f}(s, \mathcal{X}_s, \mathcal{Y}_s, \mathcal{Z}_s)\mathrm{d}s - \int_t^T \mathcal{Z}_s \cdot \mathrm{d}W_s, \tag{0.0.2}$$

dans le cas de coefficients de fonctions déterministes et sous des hypothèses appropriées, le processus $\mathcal{X}$ ci-dessus apparaît comme les "caractéristiques aléatoires" de l'EDP quasilinéaire suivante :

$$\partial_t \mathcal{U} + \mathfrak{a}(\cdot)^\top \nabla_x \mathcal{U} + \mathrm{Tr}[\mathfrak{b}^\top \mathfrak{b} \nabla^2 \mathcal{U}(\cdot)] + \mathfrak{f}(\cdot, \mathcal{U}(\cdot), \mathfrak{b}^\top \nabla_x \mathcal{U}(\cdot)) = 0, \tag{0.0.3}$$

et le lien avec (0.0.2) est donné par $\mathcal{Y}_t = \mathcal{U}(t, \mathcal{X}_t)$ et en supposant une certaine régularité, on aura $\mathcal{Z}_t = \mathfrak{b}^\top \nabla_x \mathcal{U}(t, \mathcal{X}_t)$, voir par exemple [63]. De nombreuses difficultés sont rencontrées dans l'étude théorique des systèmes de type (0.0.1)-(0.0.2) en raison du couplage entre deux équations. Même dans le cas Lipschitz pour les coefficients $(\mathfrak{a}, \mathfrak{b}, \mathfrak{f}, \mathfrak{g})$, l'existence et l'unicité ne sont pas garanties sans hypothèses supplémentaires. Néanmoins, un cas particulier du système EDSPR ci-dessus a été initialement introduit par Carmona, Delarue, Espinosa et Touzi dans [20] pour la valorisation des dérivés des émissions de carbone, étudiée ensuite en cas général dans [19], sous des

hypothèses minimales, admet une solution $(P_t, E_t, Y_t, Z_t)_{0\leqslant t\leqslant T}$ telle que :

$$\begin{cases} dP_t &= b(P_t)dt + \sigma(P_t)\mathrm{d}W_t \\ dE_t &= \mu(Y_t, P_t)\mathrm{d}t \\ dY_t &= Z_t \cdot \mathrm{d}W_t \end{cases} \tag{0.0.4}$$

La fonction $b : \mathbb{R}^d \to \mathbb{R}^d$, $\sigma : \mathbb{R}^d \to \mathcal{M}_d$, où $\mathcal{M}_d$ est l'ensemble des matrices $d \times d$ sur $\mathbb{R}$ et $\mu : \mathbb{R} \times \mathbb{R}^d \to \mathbb{R}$ sont Lipschitz continues. Ce système peut modéliser des systèmes "cap-and-trade", dans lesquels une autorité centrale fixe un plafond ou une limite sur le total des émissions de carbone cumulées pour les acteurs du marché, et des pénalités seront payées si l'émission total dépasse la limite d'émission au temps terminal T. Et nous disons que Y est le prix d'un droit de polluer, E est l'émission totale cumulée du polluant et P représente certaines variables d'état de l'émission (demande, prix de l'énergie etc, donc de grande dimension en général). Le coefficient μ est naturellement décroissant en variable y pour traduire le fait qu'un prix plus élevé de droit de polluer entraîne une émission plus faible. La condition terminale est donnée par $\phi(E_T, P_T)$, où $\phi : \mathbb{R} \times \mathbb{R}^d \to \mathbb{R}$ est une fonction mesurable, non-décroissante en variable E et Lipschitz continue en variable P. Un exemple typique est le suivant :

$$e \mapsto \phi(e) = \mathbf{1}_{\{e>\Lambda\}}\,,\ \Lambda > 0. \tag{0.0.5}$$

La constante Λ agit comme une limite d'émissions fixé par le gouvernement ou le régulateur. Elle traduit le fait qu'une pénalité sera payée si les émissions cumulées sont en-dessus de Λ en temps terminal T.

Dans la première partie de cette thèse nous nous intéressons à l'approximation numérique de la solution $u(t, P_t, E_t)$ de l'EDP quasi-linéaire suivante,

$$\begin{cases} \partial_t u(t,p,e) + \mu(u(t,p,e),p)\partial_e u(t,p,e) + \mathcal{L}_p u(t,p,e) = 0, \quad (t,p,e) \in [0,T] \times \mathbb{R}^d \times \mathbb{R}, \\ u(T,p,e) = \phi(e), \quad (p,e) \in \mathbb{R}^d \times \mathbb{R}, \end{cases} \tag{0.0.6}$$

où l'on définit le générateur infinitésimal $\mathcal{L}_p$ par rapport à la variable p, pour φ assez régulière,

$$\mathcal{L}_p\varphi(t,p,e) := b(p) \cdot \nabla_p\varphi(t,p,e) + \frac{1}{2}\mathrm{Tr}[A(p)\nabla_p^2\varphi(t,p,e)], \tag{0.0.7}$$

où ∇_p désigne la jacobienne par rapport à p, $A(p) := (\sigma\sigma^\top)(p)$ et ∇_p^2 est la matrice de l'opérateur de dérivée seconde. Tout d'abord, il a été suggéré et remarqué dans [47] qu'une méthode EDP pourrait s'appliquer à EDSPR singulière ci-dessus pour obtenir une approximation numérique. Cependant, dans le pratique, la variable d'état P est de grande dimension et rend donc ces méthodes EDP peu pratiques. Pour le cas de dimension modérée, certaines méthodes probabilistes classiques pour EDSPRs existent, il est donc naturel d'aborder le problème de (0.0.4) en utilisant les schémas probabilistes déjà connus, voir par exemple méthode Bender-Zhang [4], méthode Delarue-Menozzi [33]. Récemment, des méthodes de réseaux de neurones en profondeur ont été conçues et appliquées pour les problèmes d'approximation des EDSRs, en particulier pour leur utilité dans un cas de très haute dimension.

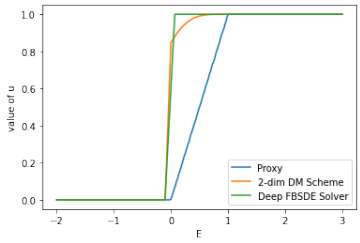

(a) $\sigma = 0.01$

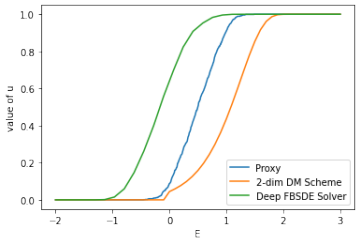

(b) $\sigma = 0.3$

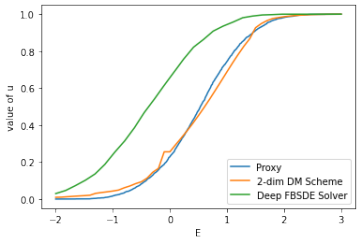

(c) $\sigma = 1.0$

FIGURE 1 : Comparaison de $e \mapsto \mathcal{V}(0, 0, e)$ obtenu par Deep FBSDE Solver et Delarue-Menozzi Scheme (DM Scheme) au proxy, pour différentes volatilités. Nous observons qu'ils ne reproduisent pas correctement le Procuration.

[44] a analysé le *deep BSDE solver* introduit dans [43] à nouveau dans le cadre du petit couplage. Enfin, les méthodes ci-dessus échouent, en pratique, à approximer correctement la solution de (0.0.4). Pour illustrer empiriquement ce fait, nous considérons un "toy model" introduit dans [20]. Le problème vient du fait que la partie transport non-linéaire de l'équation est dégénérée. En effet, les méthodes ci-dessus sont incapables de capturer la bonne solution de l'entropie au sens faible. Ceci est particulièrement clair dans le cas $\sigma = 0.01$ voir Figure 1a, dans lequel la volatilité est relativement faible et la bonne solution devrait correspondre à la solution de l'équation de Burgers non visqueuse avec $\sigma \to 0$.

Cependant, d'un point de vue différent, on sait que les systèmes de particules reproduisent la bonne solution d'entropie de loi de conservation unidimensionnelle ou d'équation de transport dans différents contextes : par exemple en astrophysique ou en dynamique des gaz. Dans ce système, de nombreuses particules évoluent à vitesse constante. Il a été introduit et prouvé pour la première fois dans Brenier et Grenier [17] que la dynamique des particules collantes peut approximer la solution d'entropie des lois de conservation unidimensionnelles avec une condition initiale monotone. Et plus précisément Jourdain et Reygner [53] prouvent et garantissent un taux de convergence théorique d'ordre $\frac{1}{N}$ pour la norme $L1$ en utilisant le multitype SPD (Sticky Particles Dynamics). Dans Bossy et Talay [9, 10], les auteurs proposent un algorithme de particules en interaction, correspondant à un SPD sans collision pour résoudre une équation de type Burgers, une classe d'EDP champ-moyen et prouvent également un taux de convergence théorique d'ordre $N^{-\frac{1}{2}} + \Delta t^{\frac{1}{2}}$ pour la norme $L1$ sous certaines hypothèses. De nombreux autres travaux basés sur des particules stochastiques en interaction ou des SPDs pour résoudre les lois de conservation ou

l'équation de transport sont apparus, voir par exemple [52, 55, 6, 8, 56, 51, 54].

Dans la première partie de cette thèse, nous avons analysé et développé en détail les méthodes d'approximation numérique pour les équations différentielles stochastiques progressifs et rétrogrades singulières et couplées qui présentent une composante forward dégénérée et une condition terminale non régulière, qui sert à modéliser le marché des émissions de carbone, voir par exemple [34, 22, 20].

Pour contourner cette difficulté sur la dégénérescence et la non-régularité, dans le chapitre 2, nous profitons de l'unidimensionnalité de l'opérateur de transport purement non-linéaire et introduisons un schéma théorique de splitting pour approximer la solution de EDSPR singulière en traitant différemment l'approximation numérique de l'opérateur de diffusion de grande dimension et de l'opérateur de transport unidimensionnel rétrograde. Nous avons également étudié la vitesse de convergence ainsi que la stabilité sous l'hypothèse minimale garantissant le caractère bien posé du problème. Notre résultat principal, dans le théorème 2.2.2, prouve que ce schéma de splitting est convergent avec un taux $\frac{1}{2}$ par rapport au pas de temps sous l'hypothèse minimale utilisée dans [19] pour obtenir l'existence et l'unicité de la solution $\mathcal{V}$. Notre deuxième résultat se trouve dans la section 2.3, qui présente, sous les hypothèses précédentes, plusieurs schémas numériquement implémentables, et la procédure globale devient une séquence de problèmes d'optimisation de régression non linéaire et de problèmes d'approximation de l'équation de transport. En pratique, nous nous appuyons sur des méthodes de différences finies (schéma de Lax-Friedrichs ou schéma Upwind), voir par exemple [60] pour l'approximation de l'équation de transport et sur le réseau de neurones, voir par exemple [42, 48, 43] pour la régression non linéaire qui franchit la "malédiction de la dimension". Enfin, nous introduisons un schéma numérique alternatif basé sur SPDs et arbres binomiaux comme proxy et différents tests numériques ont été mis en œuvre et montrent de très bons résultats.

Dans le chapitre 3, basé sur des travaux précédents sur les systèmes de particules et les particules en interaction voir par exemple [53, 55, 8, 9, 10], nous développons et introduisons un schéma de splitting alternatif qui découple l'EDP (0.0.6) séparément en équation de transport unidimensionnelle et en équation de diffusion pour chaque pas de temps. Ce schéma est basé sur la dynamique des particules collantes et l'arbre binomial pour approximer respectivement les parties de transport et de diffusion. Comme mentionné dans le chapitre 2, ce schéma sert de solution "proxy", il est donc intéressant de contrôler l'erreur d'approximation due à ce schéma, qui est l'objectif principal de ce chapitre de thèse. Comme indiqué dans [53], le SPD induit génériquement des solutions faibles exactes, mais pour une condition initiale discrète, et n'a pas besoin de satisfaire la condition d'entropie [58] de Kružkov ou la condition d'entropie de viscosité de Bianchi-Bressan [7], ce qui nous conduit à séparer l'erreur d'approximation totale (pour la norme $L1$) en quatre erreurs : l'erreur de transport, l'erreur de diffusion, l'erreur de splitting ainsi que l'erreur de propagation. L'approximation de l'opérateur de transport est abordée dans la section 3.4.1. L'erreur due à la diffusion a été abordée dans la section 3.4.4. En particulier, pour surmonter la difficulté face à l'explosion du gradient et à la non-régularité au temps terminal T, nous employons une technique de régularisation en considérant sa convolution par rapport à une fonction compacte et régulière φ. L'erreur due au splitting a été étudiée en détail dans Chassagneux [26] et la preuve a été adaptée

dans la section 3.4.3. La principale nouveauté de notre approche par rapport aux travaux précédents est que nous proposons un nouveau schéma numérique basé sur le splitting qui capture la solution d'entropie des EDPs quasi-linéaires et prouvons aussi un taux de convergence théorique $\frac{1}{6}$ par rapport au pas de temps est prouvé sous certaines hypothèses.

Soit une grille en temps discret $\pi = \{0 =: t_0 < \cdots < t_n < \cdots < t_N := T\}$ avec N un entier positif qui désigne le nombre de pas de temps. Pour une utilisation ultérieure, nous notons $|\pi| := \max_{0\leqslant n<N}(t_{n+1} - t_n)$.

Un algorithme de splitting est appliqué itérativement sur les étapes de diffusion et les étapes de transport dans la grille temporelle ci-dessus. L'objectif principal est de prouver une borne supérieure pour le taux de convergence du schéma de splitting en termes de pas de temps sous l'hypothèse suivante.

Assumption 0.0.1 *Nous supposons que $(b, \sigma, \mu) \in \mathcal{A}$ et la condition terminale $\phi \in \mathcal{K}$. où*

1. *$\mathcal{A}$ la classe des fonctions telles que $B : \mathbb{R}^d \to \mathbb{R}^d$, $\Sigma : \mathbb{R}^d \to \mathcal{M}_d$, $F : \mathbb{R} \times \mathbb{R}^d \to \mathbb{R}$ qui sont des fonctions L-Lipschitz continues. De plus, F est strictement décroissante en y et vérifie, pour tout $p \in \mathbb{R}^d$,*

$$\ell_1|y - y'|^2 \leqslant (y - y')(F(y', p) - F(y, p)) \leqslant \ell_2|y - y'|^2. \tag{0.0.8}$$

2. *$\mathcal{K}$ la classe de fonctions $\phi : \mathbb{R}^d \times \mathbb{R} \to [0, 1]$ telle que ϕ soit L_ϕ-Lipschitz dans la première variable pour un certain $L_\phi > 0$ et non décroissante en sa seconde variable,*

$$|\phi(p, e) - \phi(p', e)| \leqslant L_\phi|p - p'| \quad \text{pour tout} \quad (p, p', e) \in \mathbb{R}^d \times \mathbb{R}^d \times \mathbb{R}\,, \tag{0.0.9}$$

$$\phi(p, e') \geqslant \phi(p, e) \quad \text{si} \quad e' \geqslant e\,, \tag{0.0.10}$$

et en plus,

$$\sup_e \phi(p, e) = 1 \quad \text{et} \quad \inf_e \phi(p, e) = 0 \quad \text{pour tout} \quad p \in \mathbb{R}^d\,. \tag{0.0.11}$$

Dans la section 2.2, nous introduisons d'abord le schéma de splitting théorique, qui est un schéma numérique qui traite différemment l'étape de diffusion et l'étape de transport. Nous introduisons l'étape de transport où la partie diffusion est fixée.

Theorem 0.0.1 (Proposition 2.10 dans [19], Proposition 3.2 dans [22]) *Soient $\tau > 0$, $(B, \Sigma, F) \in \mathcal{A}$ et $\Phi \in \mathcal{K}$.*
Étant donnée toute condition initiale $(t_0, p, e) \in [0, \tau) \times \mathbb{R}^d \times \mathbb{R}$, il existe un unique 4-tuple de processus progressivement mesurable $(P_t^{t_0,p,e}, E_t^{t_0,p,e}, Y_t^{t_0,p,e}, Z_t^{t_0,p,e})_{t_0\leqslant t\leqslant\tau} \in \mathcal{S}_c^{2,d}([t_0, \tau]) \times \mathcal{S}_c^{2,1}([t_0, \tau]) \times \mathcal{S}_c^{2,1}([t_0, \tau)) \times \mathcal{H}^{2,d}([t_0, \tau])$ satisfaisant la dynamique

$$\mathrm{d}P_t^{t_0,p,e} = B(P_t^{t_0,p,e})\mathrm{d}t + \Sigma(P_t^{t_0,p,e})\mathrm{d}W_t, \qquad P_{t_0}^{t_0,p,e} = p \in \mathbb{R}^d, \tag{0.0.12}$$

$$\mathrm{d}E_t^{t_0,p,e} = F(Y_t^{t_0,p,e}, P_t^{t_0,p,e})\mathrm{d}t, \qquad E_{t_0}^{t_0,p,e} = e \in \mathbb{R}, \tag{0.0.13}$$

$$\mathrm{d}Y_t^{t_0,p,e} = Z_t^{t_0,p,e} \cdot \mathrm{d}W_t, \tag{0.0.14}$$

et tel que

$$\mathbb{P}\left[\Phi_-(P_\tau^{t_0,p,e}, E_\tau^{t_0,p,e}) \leqslant \lim_{t\uparrow\tau} Y_t^{t_0,p,e} \leqslant \Phi_+(P_\tau^{t_0,p,e}, E_\tau^{t_0,p,e})\right] = 1. \tag{0.0.15}$$

L'unique champ de découplage *défini par*

$$[0,\tau)\times\mathbb{R}^d\times\mathbb{R}\ni(t_0,p,e)\to w(t_0,p,e)=Y_{t_0}^{t_0,p,e}\in\mathbb{R}$$

est continue et satisfait

1. *Pour tout $t\in[0,\tau)$, la fonction $w(t,\cdot,\cdot)$ est $1/(l_1(\tau-t))$-Lipschitz continue par rapport à e,*
2. *Pour tout $t\in[0,\tau)$, la fonction $w(t,\cdot,\cdot)$ est C-Lipschitz continue par rapport à p, où C est une constante dépendant de L, τ et L_ϕ uniquement.*
3. *Soit $(p,e)\in\mathbb{R}^d\times\mathbb{R}$, pour toute famille $(p_t,e_t)_{0\leqslant t<\tau}$ convergeant à (p,e) comme $t\uparrow\tau$, on a*

$$\Phi_-(p,e)\leqslant\liminf_{t\to\tau} w(t,p_t,e_t)\leqslant\limsup_{t\to\tau} w(t,p_t,e_t)\leqslant\Phi_+(p,e)\,. \tag{0.0.16}$$

4. *Pour tout $t\in[0,\tau)$, la fonction $w(t,\cdot,\cdot)\in\mathcal{K}$.*

Definition 0.0.1 (Opérateur de transport) *Nous fixons*

$$(0,\infty)\times\mathcal{K}\ni(h,\psi)\mapsto\mathcal{T}_h(\psi)=\tilde{v}(0,\cdot)\in\mathcal{K}$$

où $\tilde{v}$ est le champ de découplage défini dans le théorème 0.0.1 avec des paramètres $\tau=h$, $B=0$, $\Sigma=0$, $F=\mu$ et condition terminale $\Phi=\psi$.

Dans la définition ci-dessus, $\tilde{v}(\cdot)$ est l'unique solution d'entropie pour

$$\partial_t w+\partial_e(\mathfrak{M}(p,w))=0\,,\qquad \text{où } \mathfrak{M}(p,y)=\int_0^y\mu(p,\upsilon)\mathrm{d}\upsilon\ ,\ 0\leqslant y\leqslant 1, \tag{0.0.17}$$

et $\tilde{v}(h,\cdot)=\psi$. Nous utiliserons ce fait dans la partie numérique.

Comme pour l'étape de transport ci-dessus, il est naturel de fixer le processus E à sa valeur initiale et d'introduire l'étape de diffusion.

Definition 0.0.2 (Opérateur de diffusion) *Nous fixons*

$$(0,\infty)\times\mathcal{K}\ni(h,\psi)\mapsto\mathcal{D}_h(\psi)=\bar{v}(0,\cdot)\in\mathcal{K}$$

où $\bar{v}(0,\cdot)$ est le découplage dans le théorème 0.0.1 avec paramètres $\tau=h$, $B=b$, $\Sigma=\sigma$, $F=0$ et condition terminale $\Phi=\psi$.

Observons que, pour $t\in[0,h)$,

$$\bar{v}(t,p,e)=\mathbb{E}\Big[\psi(P_h^{t,p},e)\Big]\ \text{ et } \bar{v}(t,\cdot)\in\mathcal{K}\,. \tag{0.0.18}$$

Alors, avec les deux étapes d'approximation ci-dessus en tête, nous considérons naturellement le schéma théorique suivant sur la grille π.

Definition 0.0.3 (Schéma de splitting théorique) *Nous fixons*

$$(0,\infty)\times\mathcal{K}\ni(h,\psi)\mapsto\mathcal{S}_h(\psi):=\mathcal{T}_h\circ\mathcal{D}_h(\psi)\in\mathcal{K}.$$

Pour $n\leqslant N$, on note u_n^π la solution de la récurrence suivante sur π :
- pour $n=N$, poser $u_N^\pi:=\phi$,
- pour $n<N$, $u_n^\pi=\mathcal{S}_{t_{n+1}-t_n}(u_{n+1}^\pi)$.

Le $(u_n^\pi)_{0\leqslant n\leqslant N}$ représente l'approximation du champ de découplage $\mathcal{V}(t,\cdot)$ pour $t\in\pi$. De plus, on observe, à partir de la propriété de $\mathcal{T}$ et $\mathcal{D}$, que

$$u_n^\pi\in\mathcal{K},\ \text{pour tout } 0\leqslant n\leqslant N. \tag{0.0.19}$$

Notre résultat principal théorique concernant le taux de convergence du schéma de splitting ci-dessus est le suivant

Theorem 0.0.2 (Taux de convergence) *Selon nos* hypothèses permanentes*, nous avons la borne suivante*

$$\int_{\mathbb{R}}|\mathcal{V}(0,p,e)-u_0^\pi(p,e)|\mathrm{d}e\leqslant CT(1+|p|^2)\sqrt{|\pi|}\,,$$

pour une constante positive C.

Le résultat de convergence ci-dessus garantit l'utilisation de ce schéma de splitting. A partir de ce schéma, nous proposons plusieurs algorithmes numériquement implémentables qui combinent l'approximation par différences finies de l'équation de transport et l'approximation probabiliste de l'opérateur de diffusion.

Soit J un entier positif et $\mathfrak{E}=(e_j)_{1\leqslant j\leqslant J}$ une grille discrète de l'espace $\mathbb{R}$. On note $\mathcal{T}_h^{\mathfrak{E}}$ une approximation de l'opérateur $\mathcal{T}_h$ sur $\mathfrak{E}$. c'est-à-dire $\mathbb{R}^d\times\mathbb{R}^J\ni(p,\theta)\mapsto\mathcal{T}_h^{\mathfrak{E}}(p,\theta)\in\mathbb{R}^J$. Cela signifie que pour chaque $p\in\mathbb{R}^d$, $\mathcal{T}_h^{\mathfrak{E}}(p,\cdot)$ est une approximation sur la grille $\mathfrak{E}$ de l'équation correspondante (0.0.17) sur $[0,h]$. On suppose de plus qu'il vérifie, pour certain $q\geqslant 1$ et $q'\geqslant 1$,

$$|\mathcal{T}_h^{\mathfrak{E}}(p,\theta)|\leqslant C(1+|p|^q+|\theta|^{q'})\,. \tag{0.0.20}$$

La condition terminale $\psi:\mathbb{R}^d\times\mathbb{R}\to\mathbb{R}$ est approximée sur la grille $\mathfrak{E}$ par $\theta^j=\psi(p,e_j)$, pour tout $1\leqslant j\leqslant J$ et $p\in\mathbb{R}^d$. Étant donné cette approximation de transport, nous introduisons une approximation probabiliste de $\mathcal{V}(0,p,\cdot)$ sur $\mathfrak{E}$. Pour cela, on considère le schéma d'Euler associé à P sur π, pour $n\geqslant 0$,

$$\widehat{P}_{t_{n+1}}^\pi=\widehat{P}_{t_n}^\pi+b(\widehat{P}_{t_n}^\pi)(t_{n+1}-t_n)+\ \sigma(\widehat{P}_{t_n}^\pi)\Delta\widehat{W}_n\ \text{ et }\widehat{P}_0^\pi=p\,. \tag{0.0.21}$$

Ici, $(\Delta\widehat{W}_n)_{0\leqslant n\leqslant N-1}$ sont des v.a. indépendantes qui représentent une approximation de la loi de $(W_{t_{n+1}}-W_{t_n})_{0\leqslant n\leqslant N-1}$.
Nous définissons maintenant un processus en temps discret $(\Gamma_n)_{0\leqslant n\leqslant N}$ à valeur dans $\mathbb{R}^J$ comme le suivant.

Definition 0.0.4 *$(\Gamma_n)_{0\leqslant n\leqslant N}$ est la solution du schéma suivant :*

1. *Pour $n=N$, $\Gamma_N^j=\phi(\widehat{P}_{t_N}^\pi,e_j)$ pour $1\leqslant j\leqslant J$.*

2. Pour $n < N$, calculer

$$\Gamma_n = \mathcal{T}_h^{\mathfrak{E}}(\widehat{P}^{\pi}_{t_n}, \mathbb{E}\Big[\Gamma_{n+1}|\widehat{P}^{\pi}_{t_n}\Big]) \,. \tag{0.0.22}$$

Pour une utilisation ultérieure, nous définissons le processus auxiliaire $(\bar{\Gamma}_n)$ par

$$\bar{\Gamma}^j_n = \mathbb{E}\Big[\Gamma^j_{n+1}|\widehat{P}^{\pi}_{t_n}\Big] \quad \text{pour tout } 1 \leqslant j \leqslant J \,. \tag{0.0.23}$$

Nous observons également que, grâce à la propriété Markovienne de $\widehat{P}^{\pi}$ sur π, (Γ_n) satisfait

$$\Gamma_n := \gamma_n(\widehat{P}^{\pi}_{t_n}) \,, \quad 0 \leqslant n \leqslant N \,, \tag{0.0.24}$$

où les fonctions $\gamma_n : \mathbb{R}^d \to \mathbb{R}^J$, sont données par

Definition 0.0.5 *1. Pour $n = N$, $\gamma^j_N(p) = \phi(p, e_j)$, $1 \leqslant j \leqslant J$, $p \in \mathbb{R}^d$.*

2. Puis, calculer pour $n < N$, $p \in \mathbb{R}^d$,

$$\bar{\gamma}^j_n(p) = \mathbb{E}\Big[\gamma^j_{n+1}\Big(p + b(p)h + \sigma(p)\Delta\widehat{W}_n\Big)\Big] \quad \textit{pour tout } 1 \leqslant j \leqslant J, \tag{0.0.25}$$

$$\gamma_n(p) = \mathcal{T}_h^{\mathfrak{E}}(p, \bar{\gamma}_n(p)) \,. \tag{0.0.26}$$

Avec les définitions ci-dessus, nous avons que $\Gamma_0 = \gamma_0(P_0)$ représente une approximation de $\mathcal{V}(0, P_0, \cdot)$ sur la grille $\mathfrak{E}$.
Nous considérons d'abord l'approximation de Lax-Friedrichs de l'équation rétrograde de transport (0.0.17) et définissons $\mathcal{T}^{\mathrm{LF}}_{\mathfrak{E},\mathfrak{R},h} : \mathbb{R}^d \times \mathbb{R}^J \mapsto \mathbb{R}^J$ l'approximation de l'opérateur associé $\mathcal{T}_h$. Il est défini comme suit, voir par ex. [60, Chapitre 12].

Definition 0.0.6 (Lax-Friedrichs) *Pour $p \in \mathbb{R}^d$ et $\theta \in \mathbb{R}^J$ donnés, soit $(V^k_j)_{1\leqslant k\leqslant K, 1\leqslant j\leqslant J}$ l'approximation au point (r_k, e_j). La procédure pour calculer V est :*
- Au temps $r_K = h$: poser $V^K_j = \theta_j$, $1 \leqslant j \leqslant J$,
- pour $0 \leqslant k < K$: définir $V^k_1 = V^{k+1}_1$, $V^k_J = V^{k+1}_J$ et calculer, pour $1 < j < J$:

$$V^k_j = \frac{1}{2}(V^{k+1}_{j+1} + V^{k+1}_{j-1}) + \frac{\delta}{2\mathfrak{d}}\Big(\mathfrak{M}(p, V^{k+1}_{j+1}) - \mathfrak{M}(p, V^{k+1}_{j-1})\Big) \,. \tag{0.0.27}$$

Ensuite, définir $\mathcal{T}^{\mathrm{LF}}_{\mathfrak{E},\mathfrak{R},h}(p, \theta) := V^0$.

Lorsque la fonction μ est de signe constant, la méthode Upwind est meilleure, car elle est moins diffusive. Comme les modèles aux marchés du carbone donnés dans les exemples ci-dessous qui sera bien le cas, nous considérons la méthode upwind pour $\mu \geqslant 0$. On définit donc maintenant $\mathcal{T}^{\mathrm{U}}_{\mathfrak{E},\mathfrak{R},h} : \mathbb{R}^d \times \mathbb{R}^J \mapsto \mathbb{R}^J$ l'approximation de l'opérateur associé $\mathcal{T}_h$, voir par exemple [60].

Definition 0.0.7 (Upwind for $\mu \geqslant 0$) *Pour $p \in \mathbb{R}^d$ et $\theta \in \mathbb{R}^J$ donnés, soit $(V^k_j)_{1\leqslant j\leqslant J, 1\leqslant k\leqslant K}$ l'approximation au point (r_k, e_j). Les étapes pour calculer V sont :*
- au temps $r_K = h$: poser $V^K_j = \theta_j$, $1 \leqslant j \leqslant J$,
- pour $0 \leqslant k < K$: poser $V^k_J = V^{k+1}_J$ et calculer, pour $1 \leqslant j < J$:

$$V^k_j = V^{k+1}_j + \frac{\delta}{\mathfrak{d}}\Big(\mathfrak{M}(p, V^{k+1}_{j+1}) - \mathfrak{M}(p, V^{k+1}_j)\Big) \,. \tag{0.0.28}$$

Ensuite, définir $\mathcal{T}^{\mathrm{U}}_{\mathfrak{E},\mathfrak{R},h}(p, \theta) := V^0$.

Le dernier point est de calculer l'espérance conditionnelle du schéma en Définition 0.0.4, i.e. à chaque pas de temps les quantités $\gamma_n(\widehat{P}^\pi_{t_n}) = \mathbb{E}\Big[\Gamma_{n+1}|\widehat{P}^\pi_{t_n}\Big]$. Pour cela, nous utiliserons deep learning car il est très efficace pour les équations de grande dimension, voir par ex. [43, 48]. On note $\mathcal{NN}_{d_0,d_1,L,m}$ l'ensemble des réseaux de neurones, qui sont des fonctions $\Phi(\cdot;\Theta) : \mathbb{R}^{d_0} \mapsto \mathbb{R}^{d_1}$, paramétrées par Θ et avec les caractéristiques suivantes : la dimension d'entrée est d_0, la dimension de sortie est d_1, $L+1$ est le nombre de couches, $m = (m_l)_{0\leqslant m_l\leqslant L}$ où m_l est le nombre de neurones sur chaque couche, $l = 0, ..., L$: par défaut, $m_0 = d$ et $m_L = d_1$.

Definition 0.0.8 (Schéma de régression non-linéaire par réseaux neurones)

1. *Pour $t_N = T$, $\widehat{\widehat{\gamma}}^j_n(p) = \widehat{\gamma}^j_N(p) = \phi(p, e_j)$, $1 \leqslant j \leqslant J$, $p \in \mathbb{R}^d$.*

2. *Pour $n = N-1, ..., 1$: Etant donné les trajectoires de $P^\pi_{t_n}$, on cherche à optimiser*

$$\widehat{\mathcal{L}}_n(\Theta) = \mathbb{E}\Big|\mathcal{T}^{\mathfrak{E}}_h(\widehat{P}^\pi_{t_{n+1}}, \widehat{\widehat{\gamma}}_{n+1}(\widehat{P}^\pi_{t_{n+1}})) - \Big(\mathcal{Y}_n(\widehat{P}^\pi_{t_n},\Theta) + \mathcal{Z}_n(\widehat{P}^\pi_{t_n},\Theta)(W_{t_{n+1}} - W_{t_n})\Big)\Big|^2 \tag{0.0.29}$$

avec $(\mathcal{Y}_n(\cdot,\Theta), \mathcal{Z}_n(\cdot,\Theta)) \in \mathcal{NN}_{d,(d+1)\times J,L,m}$, telles que

$$\Theta^\star_n \in \arg\min_{\Theta\in\mathbb{R}^{N_m}} \widehat{\mathcal{L}}_n(\Theta) \quad \text{et donc} \quad \widehat{\widehat{\gamma}}_n(\cdot) := \mathcal{Y}_n(\cdot,\Theta^\star_n)\,.$$

3. *En temps initial $t_0 = 0$, calculer $\widehat{\gamma}_0(\widehat{P}^\pi_0) = \mathbb{E}\Big[\mathcal{T}^{\mathfrak{E}}_h(\widehat{P}^\pi_{t_1}, \widehat{\widehat{\gamma}}_1(\widehat{P}^\pi_{t_1}))\Big]$.*

Dans le chapitre 3, nous allons étudier en détail la convergence du schéma numérique alternatif BT & SPD qui consiste se base sur des arbres binomiaux et des dynamiques de particules collantes présenté dans la section 2.3.3.1 du chapitre 2. La convergence est prouvée en utilisant la décomposition des erreurs et quelques résultats intermédiaires dans [26, 53], de plus, certaines techniques comme la convolution sont utilisées pour s'affranchir de l'explosion du gradient près du temps terminal T. En plus, nous nous restreignons dans un cas particulier en faisant l'hypothèse 0.0.2.

Pour valider empiriquement nos résultats obtenus avec le schéma de régression non linéaire dans le chapitre 2, il est intéressant de développer une autre méthode numérique basée sur le schéma de splitting combinant une méthode particulaire en dimension modérée (2 à 5). L'approximation discrète sur la grille π est donnée par le schéma d'Euler classique

$$\widehat{P}_0 = P_0 \text{ et } \widehat{P}_{t_{n+1}} = \widehat{P}_{t_n} + b(\widehat{P}_{t_n})\mathfrak{h} + \sigma(\widehat{P}_{t_n})\Delta\widehat{W}_n\,, \tag{0.0.30}$$

où $(\Delta\widehat{W}_n)$ est une approximation discrète des incréments browniens $(W_{t_{n+1}} - W_{t_n})_{0\leqslant n\leqslant N-1}$. Pour une l'utilisation ultérieure, nous définissons également, pour $p \in \mathbb{R}^d$ et tout $0 \leqslant n \leqslant N-1$,

$$\widehat{P}^{t_n,p}_{t_{n+1}} := p + b(p)\mathfrak{h} + \sigma(p)\Delta\widehat{W}_n\,. \tag{0.0.31}$$

Notons $\mathcal{P}_n$ le support discret et fini de $\widehat{P}_{t_n}$ pour $0 \leqslant n \leqslant N-1$. On observe, grâce à la définition ci-dessus de $(\widehat{P}_{t_n})$, que pour $p \in \mathcal{P}_n$, $\widehat{P}^{t_n,p}_{t_{n+1}} \in \mathcal{P}_{n+1}$.

Dans ce contexte, nous introduisons d'abord une version discrète de l'opérateur $\mathcal{T}$, qui calculera une approximation de (0.0.17) écrite en *forme forward* : nous utiliserons le Sticky Particle Dynamics (SPD) [17] voir [53, Section 1.1]. Le SPD est simple à mettre en œuvre dans notre cas particulier puisqu'il n'y a pas de collision de particules en raison de l'hypothèse de monotonie sur (μ, ψ).

Nous notons $\mathfrak{T}$ l'opérateur discrète, agit sur la CDF empirique appartenant à $\mathcal{I}_M$,

$$(0,\infty)\times\mathbb{R}^d\times\mathcal{I}^M\ni(h,p,\theta)\mapsto\mathfrak{T}_h^M(p,\theta):=H*(\frac{1}{M}\sum_{m=1}^{M}\delta_{e_m^p(h)})\in\mathcal{I}^M\,. \tag{0.0.32}$$

Notons que $(e_m^p(h))_{1\leqslant m\leqslant M}$ est calculé de manière suivante : étant donné la position initiale $\mathrm{e}(0)\in D_M$ et les vitesses $(\bar{F}_m(p))_{1\leqslant m\leqslant M}$ fixées à $\bar{F}_m(p)=-\int_{(m-1)/M}^{m/M}\mu(p,y)\mathrm{d}y$, on considère M particules $(e_m^p)_{1\leqslant m\leqslant M}$, dont les positions au temps $t\in[0,h]$ sont simplement données par

$$e_m^p(t)=e_m(0)+\bar{F}_m(p)t\,. \tag{0.0.33}$$

Ainsi défini $(e_m^p(t))_{1\leqslant m\leqslant M}\in D_M$, pour tout $t\in[0,h]$, puisque $-\mu$ est non décroissante.

Nous définissons maintenant l'approximation utilisée pour l'opérateur de $\mathcal{D}_{\mathfrak{h}}(\psi)$, pour $\psi\in\mathcal{K}_{n+1}^M$ et $\mathrm{p}\in\mathcal{P}_n$. On a

$$\bar{v}_n(\mathrm{p},e):=\mathbb{E}\Big[\psi(\widehat{P}_{t_{n+1}}^{t_n,\mathrm{p}},e)\Big]=\frac{1}{2d}\sum_{i=1}^{2d}\psi(\Big(\widehat{P}_{t_{n+1}}^{t_n,p}\Big)^i,e) \tag{0.0.34}$$

$$=\sum_{i=1}^{2d}H*(\frac{1}{M}\sum_{m=1}^{M}\delta_{e_m^i})(e)\ \text{(puisque }\psi\in\mathcal{K}_{n+1}^M) \tag{0.0.35}$$

$$=H*(\frac{1}{2dM}\sum_{i=1}^{I}\sum_{m=1}^{M}\delta_{e_m^i})(e)\ \text{(par linéarité)} \tag{0.0.36}$$

L'approximation de l'opérateur de diffusion est donc donnée par

$$\mathcal{K}_{n+1}^M\ni\psi\mapsto\mathfrak{D}_n^M(\psi):=\bar{v}_n\in\mathcal{K}_n^{2Md}\,. \tag{0.0.37}$$

Enfin, le schéma aura essentiellement deux versions :

CASE 1 : On garde les particules $2dM$ dans chaque étape n. La procédure globale sera alors l'itération des deux opérateurs $\mathfrak{T}$ et $\mathfrak{D}$, voir Définition 0.0.9 ci-dessous.

CASE 2 : Il n'est pas nécessaire de conserver $2dM$ particules dans chaque étape n, avec la fonction ψ en étape $n+1$ est donnée par M particules (pour chaque $p\in\mathcal{P}_{n+1}$). Pour réduire le nombre de particules, on applique un autre opérateur $\mathfrak{R}$, pour $M\geqslant m\geqslant 1$,

$$\mathcal{I}^M\ni\psi\mapsto\mathfrak{R}^{M,m}(\psi)\in\mathcal{I}^m\,. \tag{0.0.38}$$

Diverses implémentations sont possibles, nous renvoyons à la partie numérique pour une description précise.

Introduisons enfin le schéma formel.

Definition 0.0.9 (Schéma en CASE 1) *Soit $M \geqslant 1$ et on se donne pour $0 \leqslant n \leqslant N$, $M_n := (2d)^{N-n}M$.*

1. *Pour $n = N$: initialiser $\mathrm{e}_N := (\Lambda, \dots, \Lambda) \in D_{M_N}$ dont la CDF empirique est la condition terminale $\phi = \mathbf{1}_{\{e \geqslant \Lambda\}}$. En posant $u_N^{N,M}(p, \cdot) = \phi$, pour tout $p \in \mathcal{P}_N$, on observe que $u_N^{N,M} \in \mathcal{K}_N^{M_N}$.*

2. *Pour $n < N$: étant donné $u_{n+1}^{N,M} \in \mathcal{K}_{n+1}^{M_{n+1}}$, définir*

$$\bar{u}_n^{N,M} = \mathfrak{D}_n^{M_{n+1}}(u_{n+1}^{N,M}) \in \mathcal{K}_n^{M_n}\,, \tag{0.0.39}$$

et pour tout $p \in \mathcal{P}_n$,

$$u_n^{N,M}(p, \cdot) = \mathfrak{T}_{\mathfrak{h}}^{M_n}(p, \bar{u}_n^{N,M}(p, \cdot))\,, \tag{0.0.40}$$

L'approximation de $\mathcal{V}(0, P_0, \cdot)$ est alors donnée par $u_0^{N,M}(P_0, \cdot)$.

Definition 0.0.10 (Schéma en CASE 2) *Soit $M \geqslant 1$.*

1. *Pour $n = N$: initialiser $\mathrm{e}_N := (\Lambda, \cdots, \Lambda) \in D_M$ dont la CDF empirique est la condition terminale $\phi = \mathbf{1}_{\{e \geqslant \Lambda\}}$. En posant $v_N^{N,M}(p, \cdot) := \phi$, pour tout $p \in \mathcal{P}_N$, on observe que $v_N^{N,M} \in \mathcal{K}_N^M$.*

2. *Pour $n < N$: étant donné $v_{n+1}^{N,M} \in \mathcal{K}_{n+1}^M$, définir $\bar{v}_n^{N,M} = \mathfrak{D}_n^M(v_{n+1}^{N,M}) \in \mathcal{K}_n^{2dM}$, rappeler (0.0.37), et alors pour chaque $p \in \mathcal{P}_n$,*

$$\check{v}_n^{N,M} = \mathfrak{R}^{2dM,M}(\bar{v}_n^{N,M}(p, \cdot)) \tag{0.0.41}$$

et enfin,

$$v_n^{N,M}(p, \cdot) = \mathfrak{T}_{\mathfrak{h}}^M(p, \check{v}_n^{N,M}(p, \cdot))\,, \tag{0.0.42}$$

L'approximation de $\mathcal{V}(0, P_0, \cdot)$ est alors donnée par $v_0^{N,M}(P_0, \cdot)$.

Dans la suite, pour chercher à contrôler l'erreur locale de différentes sources, on se restreint dans un cas particulier en faisant l'hypothèse suivante,

Assumption 0.0.2 *Le* champ découplage *$\mathcal{V} \in \mathscr{C}^{1,2,1}([0, T) \times \mathbb{R}^d \times \mathbb{R})$ est la solution d'EDP suivante,*

$$\partial_t \mathcal{V} + \mu(\mathcal{V}, p)\partial_e \mathcal{V} + b(p)\partial_p \mathcal{V} + \frac{1}{2}\bar{\sigma}^2 \Delta_p \mathcal{V} = 0\,. \tag{0.0.43}$$

En particulier, la fonction $\sigma(\cdot)$ est constante $\sigma(\cdot) := \bar{\sigma} I_d$ avec $\bar{\sigma} > 0$ et I_d est le $d \times d$ matrice d'identité. De plus, la fonction b est $\mathscr{C}^2(\mathbb{R}^d)$ avec des dérivées bornées et Lipschitz et la fonction μ est $\mathscr{C}^1(\ R^d \times [0, 1])$ avec Lipschitz et de dérivées bornées.

Décomposition de l'erreur L'erreur totale pourrait être décomposée et contrôlée en quatre parties : erreur due à l'opérateur de transport par les particules, régularisation, diffusion ainsi que diffusion. Cependant, les techniques d'analyse classiques échouent puisque la solution $\mathcal{V}$ n'est pas régulière a priori, ce qui donne une explosion de gradient ainsi que non-régularité en termes de $L1$-norme en général. Pour contourner cette difficulté, nous introduisons la régularisation $\mathcal{V}^\epsilon$ en considérant sa convolution par rapport à une fonction compacte et régulière φ_ϵ comme suit :

$$\mathcal{V}^\epsilon(t,p,e) := \int \mathcal{V}(t,p+q,e)\varphi_\epsilon(q)\mathrm{d}q, \quad \text{où } \varphi_\epsilon(q) := \frac{1}{\epsilon}\varphi(\frac{q}{\epsilon}), \tag{0.0.44}$$

et avec $\varphi(\cdot)$ une fonction de probabilité de densité régulière de support compact.

L'erreur que nous cherchons à contrôler est, pour $\gamma_n = u_n^{N,M}$ ou $\gamma_n = v_n^{N,M}$ (selon CASE 1 our CASE 2),

$$\mathrm{err}(N,M) := \int |\gamma_0(P_0,e) - \mathcal{V}(0,P_0,e)|\mathrm{d}e\,. \tag{0.0.45}$$

Et nous avons d'abord

$$\mathrm{err} \leqslant \mathcal{E}_0(P_0) + \mathcal{E}_0^r\,, \tag{0.0.46}$$

et pour $0 \leqslant n \leqslant N$, et $p \in \mathcal{P}_n$,

$$\mathcal{E}_n^r(p) := \int |\mathcal{V}^\epsilon(t_n,p,e) - \mathcal{V}(t_n,p,e)|\mathrm{d}e\,, \tag{0.0.47}$$

$$\mathcal{E}_n(p) := \int |\gamma_n(p,e) - \mathcal{V}^\epsilon(t_n,p,e)|\mathrm{d}e\,. \tag{0.0.48}$$

L'erreur $\mathcal{E}_n(p)$ pourrait être décomposée en quatre parties dans le CASE 1.

Lemma 0.0.1 *Sous CASE 1, pour* $0 \leqslant n \leqslant N-2$,

$$\mathcal{E}_n(p) \leqslant \mathcal{E}_n^{\mathrm{T}}(p) + \bar{\mathcal{E}}_n(p) + \mathcal{E}_n^D(p) + \mathcal{E}_n^S(p) \tag{0.0.49}$$

et

$$\mathcal{E}_{N-1}(p) \leqslant \mathcal{E}_{N-1}^{\mathrm{T}}(p) + \mathcal{E}_{N-1}^{\mathrm{r}}(p) + \int |\mathcal{S}_{\mathfrak{h}}(\phi(\cdot))(p,e) - \Theta_{\mathfrak{h}}(\phi(\cdot))(p,e)|\mathrm{d}e \tag{0.0.50}$$

où pour $p \in \mathcal{P}_n$,

$$\mathcal{E}_n^{\mathrm{T}}(p) := \int \left|\mathfrak{T}_{\mathfrak{h}}^{M_n}(p,\bar{u}_n^{N,M}(p,\cdot))(e) - \tilde{\mathcal{T}}_h(p,\bar{u}_n^{N,M}(p,\cdot))(e)\right|\mathrm{d}e\,, \tag{0.0.51}$$

$$\bar{\mathcal{E}}_n(p) := \int \left|\tilde{\mathcal{T}}_h(p,\bar{u}_n^{N,M}(p,\cdot))(e) - \tilde{\mathcal{T}}_h(p,\mathbb{E}[\mathcal{V}^\epsilon(t_{n+1},\widehat{P}_{t_{n+1}}^{t_n,p},\cdot)])(e)\right|\mathrm{d}e\,, \tag{0.0.52}$$

et pour $p \in \mathbb{R}^d$,

$$\mathcal{E}_n^D(p) := \int \left|\tilde{\mathcal{T}}_h(p,\mathbb{E}[\mathcal{V}^\epsilon(t_{n+1},\widehat{P}_{t_{n+1}}^{t_n,p},\cdot)])(e) - \tilde{\mathcal{T}}_h(p,\mathbb{E}[\mathcal{V}^\epsilon(t_{n+1},P_{t_{n+1}}^{t_n,p},\cdot)])(e)\right|\mathrm{d}e\ ,, \tag{0.0.53}$$

$$\mathcal{E}_n^S(p) := \int \left|\tilde{\mathcal{T}}_h(p,\mathbb{E}[\mathcal{V}^\epsilon(t_{n+1},P_{t_{n+1}}^{t_n,p},\cdot)])(e) - \mathcal{V}^\epsilon(t_n,p,e)\right|\mathrm{d}e\,, \tag{0.0.54}$$

notons que

$$\mathcal{E}^{\mathrm{T}}_{N-1}(p) = \int |\mathfrak{T}^{M}_{\mathfrak{h}}(p, \phi(\cdot))(e) - \mathcal{T}_{\mathfrak{h}}(p, \phi(\cdot)(e))| \mathrm{d}e \,. \tag{0.0.55}$$

Avec les estimations d'erreur ci-dessus à la main, nous obtenons un contrôle global sur l'erreur de convergence $\mathrm{err}(N, M)$ entre la solution de EDSPR singulier $\mathcal{V}$ et l'approximation numérique γ_0 par le schéma alternatif BT&SPD, plus précisément

Theorem 0.0.3 *Sous l'hypothèse 0.0.2 et dans le cas CASE 1,*

$$\mathrm{err}(N, M) \leqslant C(\frac{1}{M} + \frac{\sqrt{\mathfrak{h}}}{\epsilon^2} + \epsilon) \,, \tag{0.0.56}$$

rappeler (0.0.45). De plus, en posant $\epsilon = \mathfrak{h}^{\frac{1}{6}}$ *et* $M = \frac{1}{\epsilon}$*, on a*

$$\int |\mathcal{V}(0, P_0, e) - u_0^{N,M}(P_0, e)| \mathrm{d}e \leqslant C\mathfrak{h}^{\frac{1}{6}}. \tag{0.0.57}$$

Partie II : Calcul et l'approximation de la couverture PnL (Chapitre 4)

Dans cette deuxième partie de thèse, nous introduisons une classe de problèmes de contrôle non standard dans lesquels nous imposons au processus contrôlé une contrainte sur sa loi au temps terminal. Dans ce cadre, nous nous intéressons au problème de couverture faible, en particulier à la représentation duale dans le cas linéaire. Dans cette partie, nous établissons d'abord un lien entre notre problème de couverture faible général et un problème de transport optimal en considérant à la fois la représentation de Monge et de Kantorovitch. Sous certaines hypothèses, nous prouvons l'équivalence entre la représentation de Monge et la représentation de Kantorovitch dans un cas général. En particulier lorsque le marché est linéaire et avec μ à support fini, nous prouvons et présentons une formulation duale du problème de Kantorovitch. Cette formulation donne naturellement un nouveau schéma numérique utilisant la descente de gradient stochastique. De plus, dans le cas où μ une mesure de probabilité, nous trouvons également une représentation explicite par une résolution directe du problème de transport optimal. La nouveauté de notre approche par rapport aux travaux précédents [15, 11, 13] est que nous arrivons à étendre les résultats théoriques pour une mesure arbitraire μ en assurant l'équivalence de Kantorovitch et de Monge. En plus nous trouvons aussi une nouvelle formulation de dualité pour le problème de Kantorovitch et particulièrement dans le cas linéaire, on développe un schéma numérique basé sur une descente de gradient ainsi qu'une solution explicite basée du transport optimal pour une mesure de probabilité μ.

On considère un processus contrôlé : pour $y \in \mathbb{R}$ et $Z \in \mathscr{H}^2$,

$$Y_t^{y,Z} = y - \int_0^t \mathfrak{f}(s, Y_s, Z_s) \, \mathrm{d}s + \int_0^t Z_s \mathrm{d}W_s, \quad t \in [0, T], \tag{0.0.58}$$

où $(\mathfrak{f}(s, \cdot))_{s\in[0,T]}$ est un processus progressivement mesurable prenant des valeurs dans $\mathbf{Lip}(\mathbb{R} \times \mathbb{R}^d, \mathbb{R})$ et tel que $\mathbb{E}\Big[\int_0^T |\mathfrak{f}(s, 0, 0)|^2 \mathrm{d}s\Big] < +\infty$. De plus, pour tout $\xi \in$

$\mathcal{L}^2(\mathbb{P})$, il existe un unique $(\mathcal{Y}_0, \mathcal{Z}) \in \mathbb{R} \times \mathscr{H}^2$ tel que $Y_T^{\mathcal{Y}_0,\mathcal{Z}} = \xi$. On fixe alors $\mathcal{Y}_t := Y_T^{\mathcal{Y}_0[\xi],\mathcal{Z}[\xi]}$ pour tout $t \in [0,T]$, de sorte que $(\mathcal{Y}, \mathcal{Z})$ est la solution du BSDE avec le driver $\mathfrak{f}$ et la condition terminale ξ,

$$\mathcal{Y}_t = \xi + \int_t^T \mathfrak{f}(s, \mathcal{Y}_s, \mathcal{Z}_s)\mathrm{d}s - \int_t^T \mathcal{Z}_s \mathrm{d}W_s \,, 0 \leqslant t \leqslant T \,,$$

Également donné une $(\mathcal{F}_T \otimes \mathcal{B}(\mathbb{R}), \mathcal{B}(\mathbb{R}))$-fonction aléatoire mesurable $\Omega \times \mathbb{R} \ni (\omega, \gamma) \mapsto G(\omega, \gamma) \in \mathbb{R}$ tel que $\gamma \mapsto G(\gamma)$ est croissant et continu à gauche. Nous introduisons maintenant le problème de la *couverture quantile*. Notons, pour $\mu \in \mathcal{P}(\mathbb{R})$,

$$\mathfrak{H}(\mu) \ := \left\{ y \in \mathbb{R} \,\middle|\, \exists Z \in \mathscr{H}^2, \mathbb{P}(Y_T^{y,Z} \geqslant G(\gamma)) \geqslant F_\mu(\gamma), \forall \gamma \in \mathbb{R} \right\}. \tag{0.0.59}$$

Nous définissons maintenant le *prix de couverture quantile* comme

$$\mathcal{V}_{\mathrm{WH}}(\mu) \ := \inf \mathfrak{H}(\mu). \tag{0.0.60}$$

Problème de Monge relaxé (RM) Pour le problème de Monge, on a l'équivalence suivante

Proposition 0.0.1 *Soit $\mu \in \mathcal{P}_4(\mathbb{R})$. Nous avons l'équivalence suivante*

$$\mathcal{V}_{\mathrm{WH}}(\mu) = \widehat{\mathcal{V}}_{\mathrm{RM}} := \inf_{\chi \in \mathcal{T}_+(\mu)} \mathcal{Y}_0[G(\chi)] \,, \tag{0.0.61}$$

où $\mathcal{T}_+(\mu) = \left\{ \chi \in \mathcal{L}^4(\mathcal{F}_T) \,\middle|\, \chi_\sharp \mathbb{P} \in \mathcal{K}_\mu \right\}$, avec

$$\mathcal{V}_{\mathrm{WH}}(\mu) = \inf \tilde{\mathfrak{H}}(\mu), \ \textit{avec } \tilde{\mathfrak{H}}(\mu) := \left\{ y \in \mathbb{R} | \exists Z \in \mathscr{H}^2, \Psi(Y_T^{y,Z}) \sharp \mathbb{P} \in \mathcal{K}_\mu \right\}, \tag{0.0.62}$$

Problème de Kantorovitch (KP) Nous supposons maintenant

Assumption 0.0.3 *La distribution de probabilité $\mu \in \mathcal{P}_2(\mathbb{R})$ a un support fini, c'est-à-dire $\mu = \sum_{i=1}^d (q_i - q_{i+1})\delta_{\gamma_i}$ avec $d \geqslant 1$, $\gamma_1 < \cdots < \gamma_d$ et $1 = q_1 > \cdots > q_d > q_{d+1} = 0$, soit $\mathrm{supp}[\mu] = \{\gamma_1, \ldots, \gamma_d\}$ et $q_i = F_\mu(\gamma_i)$ pour tout $1 \leqslant i \leqslant d$. Pour chaque $1 \leqslant i \leqslant d$, on pose $p_i := q_i - q_{i+1} = \mu(\{\gamma_i\})$.*

Lemma 0.0.2 *Sous l'hypothèse 0.0.3, nous avons*

$$\mathcal{V}_{\mathrm{WH}}(\mu) = \widehat{\mathcal{V}}_{\mathrm{RM}}(\mu) = \mathcal{V}_{\mathrm{RM}}(\mu) := \inf_{\chi \in \mathcal{T}_+^{\mathrm{r}}(\mu)} \mathcal{Y}_0[G(\chi)] \tag{0.0.63}$$

où $\mathcal{T}_+^{\mathrm{r}}(\mu) = \{\chi \in \mathcal{L}^\infty(\mathcal{F}_T) \,|\, \chi_\sharp \mathbb{P} \in \mathcal{R}_\mu\}$.

Dans le suivant on s'intéresse à établir une équivalence entre le problème de Monge $\mathcal{V}_{\mathrm{RM}}$ et le problème de Kantorovitch $\mathcal{V}_{\mathrm{KP}}$ soit $\mathcal{V}_{\mathrm{KP}} = \mathcal{V}_{\mathrm{RM}}$ dans le cas général ainsi qu'un résultat de dualité pour le problème de Kantorovich $\mathcal{V}_{\mathrm{KP}}(\mu)$ dans le cadre linéaire où $\mathfrak{f}(s, y, z) = \mathfrak{a}_s y + \mathfrak{b}_s^\top z$ et μ à support fini, donné par

$$\mathcal{V}_{\mathrm{KP}}(\mu) = \inf_{(Q_i)_{i=1}^{d+1} \in \mathfrak{Q}_T(\mu)} \mathbb{E}\left[\sum_{i=1}^d H(\gamma_i)(Q_i - Q_{i+1}) \right]. \tag{0.0.64}$$

Pour établir l'équivalence entre les représentations de Monge et de Kantorovitch du problème OT, nous démontrons d'abord l'inégalité $\mathcal{V}_{\mathrm{KP}} \leqslant \mathcal{V}_{\mathrm{RM}}$. En effet, pour $\chi \in \mathfrak{H}^r(\mu)$, il suffit de constater que

$$G(\chi) = \sum_{i=1}^{d} G(\gamma_i)\mathbf{1}_{\chi=\gamma_i} = \sum_{i=1}^{d} G(\gamma_i)\left(\mathbf{1}_{\chi\geqslant\gamma_i} - \mathbf{1}_{\chi\geqslant\gamma_{i+1}}\right),$$

et en considérant $Q_i := \mathbf{1}_{\chi\geqslant\gamma_i}$, ce qui donne $\mathcal{Y}_0[G(\chi)] \geqslant \mathcal{V}_{\mathrm{KP}}(\mu)$. Pour l'inégalité inverse, on construit d'abord une variable aléatoire $\mathfrak{U}^\epsilon$ indépendante de $\mathcal{F}_{T-\epsilon}$ pour tout $\epsilon > 0$, par exemple $\mathfrak{U}^\epsilon = N(\frac{W_T - W_{T-\epsilon}}{\sqrt{\epsilon}})$. Alors en fixant $\eta > 0$ et par définition, il existe $(Q_i^\eta)_{i=1}^{d+1} \in \mathfrak{Q}_T(\mu)$, notant $P_i^\eta := Q_i^\eta - Q_{i+1}^\eta$, tel que

$$\mathcal{V}_{\mathrm{KP}}(\mu) \geqslant \mathcal{Y}_0\left[\sum_{i=1}^{d} G(\gamma_i)(Q_i^\eta - Q_{i+1}^\eta)\right] - \eta =: \mathcal{Y}_0\left[\sum_{i=1}^{d} G(\gamma_i)P_i^\eta\right] - \eta, \tag{0.0.65}$$

Soit $\epsilon > 0$ et on note alors

$$Q_i^{\eta,\epsilon} := \mathbb{E}[Q_i^\eta \,|\, \mathcal{F}_{T-\epsilon}], \quad 1 \leqslant i \leqslant d+1, \text{ et} \tag{0.0.66}$$
$$P_i^{\eta,\epsilon} := Q_i^{\eta,\epsilon} - Q_{i+1}^{\eta,\epsilon} = \mathbb{E}[P_i^\eta \,|\, \mathcal{F}_{T-\epsilon}], \quad 1 \leqslant i \leqslant d. \tag{0.0.67}$$

Introduisons la variable aléatoire $\mathcal{F}_T$-mesurable $\chi^{\eta,\epsilon} = \sum_{i=1}^{d} \gamma_i \mathbf{1}_{\{Q_i^{\eta,\epsilon} \geqslant \mathfrak{U}^\epsilon > Q_{i+1}^{\eta,\epsilon}\}}$, il suffit alors de prouver que

$$\mathcal{Y}_0\left[\sum_{i=1}^{d} G(\gamma_i)P_i^\eta\right] \geqslant \mathcal{Y}_0\left[G(\chi^{\eta,\epsilon})\right] - w(\eta,\epsilon) \geqslant \mathcal{V}_{\mathrm{RM}}(\mu) - o(\epsilon) \tag{0.0.68}$$

pour conclure. Avec contrôle des estimations sur la solution de BSDE non linéaire avec condition terminale $\xi \in \mathcal{L}^2(\mathcal{F}_{T-\epsilon})$ au temps terminal $T-\epsilon$. Avec ces deux points, nous prouvons donc (0.0.68) et concluons que $\mathcal{V}_{\mathrm{KP}}(\mu) \geqslant \mathcal{V}_{\mathrm{RM}}(\mu) - w(\eta,\epsilon) - \eta$, avec $w(\eta,\epsilon)$ qui converge vers 0 lorsque ϵ converge vers 0, soit $\mathcal{V}_{\mathrm{KP}} \geqslant \mathcal{V}_{\mathrm{RM}}$.

Dans le suivant, nous établissons la dualité entre $\mathcal{V}_{\mathrm{KP}}$ et $\mathcal{V}_{\mathrm{DP}}$, donnée par

$$\mathcal{V}_{\mathrm{DP}}(\mu) := \sup_{(X,\Phi)\in\mathfrak{P}_H} \left(\mathbb{E}[X] + \sum_{i=1}^{d} \Phi_i \mu(\{\gamma_i\})\right), \tag{0.0.69}$$

où

$$\mathfrak{P}_{H,\mu} := \left\{(X,\Phi) \in \mathscr{L}^2(\mathcal{F}_T) \times \Delta_+^d \,\middle|\, H(\gamma_i) \geqslant X + \Phi_i, 1 \leqslant i \leqslant d, \mathbb{P}-\text{a.s.}\right\}. \tag{0.0.70}$$

Nous prouvons l'inégalité $\mathcal{V}_{\mathrm{DP}} \leqslant \mathcal{V}_{\mathrm{KP}}$ en considérant le problème KP comme le suivant

$$\inf_{H\in C^r(\mathbb{P},\mu)} \int H(\omega,\gamma)\Pi(\mathrm{d}\omega,\mathrm{d}\gamma).$$

Pour l'inégalité inverse, nous développons $\mathcal{V}_{\mathrm{DP}}$ en transformée de Fenchel,

$$\begin{aligned}\mathcal{V}_{\mathrm{DP}}(\mu) &= \mathbb{E}[H(\gamma_1)] + \mathfrak{V}(p_2,\ldots,p_d)\\ &= \mathbb{E}[H(\gamma_1)] + \mathfrak{W}(q_2,\ldots,q_d),\end{aligned}$$

où

$$\mathfrak{V}(p) = \sup_{\zeta \in \Delta_+^{d-1}} \left(\left(\sum_{i=1}^{d-1} \zeta_i p_{i+1} \right) - \mathbb{E}\Big[\max_{1 \leqslant i \leqslant d-1} \big(\zeta_i - \tilde{H}(\gamma_{i+1})\big)_+ \Big] \right), \tag{0.0.71}$$

$$\mathfrak{W}(q) = \sup_{\theta \in \mathbb{R}_+^{d-1}} \sum_{j=1}^{d-1} \theta_j q_{j+1} - \mathbb{E}\left[\max_{1 \leqslant i \leqslant d-1} \left(\sum_{j=1}^{i} \theta_j - \tilde{H}(\gamma_{i+1}) \right)_+ \right]. \tag{0.0.72}$$

Ensuite, nous prouvons que la fonction définie par

$$w(\omega, \theta) := \sum_{j=1}^{d-1} \theta_j q_{j+1} - \mathbb{E}\left[\max_{1 \leqslant i \leqslant d-1} \left(\sum_{j=1}^{i} \theta_j - \tilde{H}(\omega, \gamma_{i+1}) \right)_+ \right],$$

est continue, concave sur $\mathbb{R}_+^{d-1}$ et $\lim_{|\theta| \to \infty} w(\theta) = -\infty$. Ceci nous permet de déduire une existence de $\theta^\star \in \mathbb{R}_+^{d-1}$ telle que $\sup_{\mathbb{R}_+^{d-1}} w(\theta) = w(\theta^\star) = \mathfrak{W}(q)$. Pour avoir un développement en somme qui nous permet de calculer son sous-différentiel sur $w(\theta)$, on définit pour $1 \leqslant i \leqslant d-1$, $A_i(\theta^{(i)}) := \big\{\Phi_i(\theta^{(i)}) > 0\big\} = \big\{\theta_i + \tilde{H}(\gamma_i) - \tilde{H}(\gamma_{i+1}) + \Phi_{i+1}(\theta^{(i+1)}) > 0\big\}$ et $A_d(\varnothing) := \varnothing$ par convention.

Et pour $2 \leqslant i \leqslant d+1$ et $\theta \in \mathbb{R}^{d-1}$, on définit $Q_i(\theta) := \mathbf{1}_{\bigcap_{k=1}^{i-1} A_k(\theta^{(k)})}$ et $Q_1(\theta) := 1$. On pose aussi, pour $1 \leqslant i \leqslant d$ et $\theta \in \mathbb{R}^{d-1}$, $P_i(\theta) := Q_i(\theta) - Q_{i+1}(\theta) = Q_i(\theta)(1 - \mathbf{1}_{A_i(\theta^{(i)})}) = Q_i(\theta)\mathbf{1}_{A_i(\theta^{(i)})^c}$.

Alors pour $\theta \in \mathbb{R}_+^{d-1}$, on prouve que

$$w(\theta) = \sum_{j=1}^{d-1} \theta_j \left(q_{j+1} - \mathbb{E}[Q_{j+1}(\theta)] \right) + \sum_{j=2}^{d} \mathbb{E}\big[\tilde{H}(\gamma_j) P_j(\theta)\big].$$

et surtout que son sous-différentiel $\partial w(\theta) \subset \Pi_{i=1}^{d-1} [\partial_{i,+} w(\theta), \partial_{i,-} w(\theta)]$, avec pour tout $1 \leqslant i \leqslant d-1$, $\partial_{i,-} w(\theta)$ (resp. $\partial_{i,+} w(\theta)$) est la dérivée partielle gauche (resp. droite) de w en θ,

$$\begin{aligned} \partial_{i,-} w(\theta) &= (+\infty)\mathbf{1}_{\theta_i = 0} + \left(q_{i+1} - \mathbb{E}[Q_{i+1}(\theta)] \right), \\ \partial_{i,+} w(\theta) &= q_{i+1} - \mathbb{E}\big[Q_{i+1}^+(\theta)\big], \end{aligned}$$

avec $Q_{i+1}^+(\theta) := Q_i(\theta)\mathbf{1}_{\left\{\theta_i + \tilde{H}(\gamma_i) - \tilde{H}(\gamma_{i+1}) + \Phi_{i+1}(\theta^{(i+1)}) \geqslant 0\right\}}$. De plus, comme $0 \in \partial_w(\theta^\star)$, on en déduit que pour $1 \leqslant j \leqslant d-1$,

$$q_{j+1} - \mathbb{E}[Q_{j+1}(\theta^\star)] \geqslant 0 \geqslant q_{j+1} - \mathbb{E}\Big[Q_{j+1}^+(\theta^\star)\Big].$$

Avec les conditions ci-dessus et différentes discussions sur les frontières de $\mathbb{R}_+^{d-1}$, nous prouvons que $\mathcal{V}_{\mathrm{DP}} \geqslant \mathcal{V}_{\mathrm{KP}}$.

Chapter 1

Introduction

This manuscript investigates the solution of singular FBSDEs by different numerical schemes and the computation for approximate weak hedging problem. The aim of this chapter is to introduce and motivate the questions we studied and to summarize the main results obtained and also the open questions that could be part of future research.

Contents

1.1 Numerical schemes for high-dimensional singular FBSDEs

1.1.1 Background and limits of classical probabilistic methods for singular FBSDEs

Let $(\Omega, \mathcal{F}, \mathbb{P})$ be a stochastic basis supporting a d-dimensional Brownian motion W and $T > 0$ a terminal time. We denote by $(\mathcal{F}_t)_{t\geqslant 0}$ the filtration generated by the Brownian motion (augmented and completed), and consider first of all a general class of singular FBSDE system which takes the following form:

$$\mathcal{X}_t = \mathcal{X}_0 + \int_0^t \mathfrak{a}(s, \mathcal{X}_s, \mathcal{Y}_s, \mathcal{Z}_s)\mathrm{d}s + \int_0^t \mathfrak{b}(s, \mathcal{X}_s, \mathcal{Y}_s, \mathcal{Z}_s)\mathrm{d}W_s, \tag{1.1.1}$$

$$\mathcal{Y}_t = \mathfrak{g}(\mathcal{X}_T) + \int_t^T \mathfrak{f}(s, \mathcal{X}_s, \mathcal{Y}_s, \mathcal{Z}_s)\mathrm{d}s - \int_t^T \mathcal{Z}_s \cdot \mathrm{d}W_s. \tag{1.1.2}$$

In the case of deterministic function coefficients and under suitable assumptions, the $\mathcal{X}$ process above appears as the "random characteristics" of the following quasilinear PDE:

$$\partial_t \mathcal{U} + \mathfrak{a}(\cdot)^\top \nabla_x \mathcal{U} + \mathrm{Tr}[\mathfrak{b}^\top \mathfrak{b} \nabla^2 \mathcal{U}(\cdot)] + \mathfrak{f}(\cdot, \mathcal{U}(\cdot), \mathfrak{b}^\top \nabla_x \mathcal{U}(\cdot)) = 0, \tag{1.1.3}$$

and the link with (1.1.2) is given by $\mathcal{Y}_t = \mathcal{U}(t, \mathcal{X}_t)$ and, assuming some smoothness, $\mathcal{Z}_t = \mathfrak{b}^\top \nabla_x \mathcal{U}(t, \mathcal{X}_t)$, see e.g. [63]. Many difficulties are encountered in the theoretical study of system of the kind (1.1.1)-(1.1.2) due to the coupling of the two equations. Even in the Lipschitz setting for the coefficients $(\mathfrak{a}, \mathfrak{b}, \mathfrak{f}, \mathfrak{g})$, existence and uniqueness are not guarantee without further assumptions. A special class of the above FBSDE system has been originally introduced by Carmona, Delarue, Espinosa and Touzi in [20] for carbon emission derivatives pricing, and studied thoroughly in [19] under structural assumptions, admits solution $(P_t, E_t, Y_t, Z_t)_{0\leqslant t\leqslant T}$ such that:

$$\begin{cases} dP_t &= b(P_t)dt + \sigma(P_t)\mathrm{d}W_t \\ dE_t &= \mu(Y_t, P_t)\mathrm{d}t \\ dY_t &= Z_t \cdot \mathrm{d}W_t \end{cases} \tag{1.1.4}$$

The function $b : \mathbb{R}^d \to \mathbb{R}^d$, $\sigma : \mathbb{R}^d \to \mathcal{M}_d$, where $\mathcal{M}_d$ is the set of $d \times d$ matrices on $\mathbb{R}$, and $\mu : \mathbb{R} \times \mathbb{R}^d \to \mathbb{R}$ are Lipschitz-continous. This system can be used to model cap-and-trade schemes, in which a central authority sets a cap or limit on the total cumulative carbon emissions for all the market participants, and penalties will be charged if terminal emission is outside of the limit of emission. In this case Y is the price of a pollution permit, E is the total cumulative emission of the pollutant and P represents some state variables influencing the emission (demand, energy prices etc. thus high-dimensional in general). The coefficient μ is naturally decreasing in the y-variable to translate the fact a higher price of pollution permit results in lower emission. The terminal condition is given by $\phi(E_T, P_T)$, where $\phi : \mathbb{R} \times \mathbb{R}^d \to \mathbb{R}$ is a measurable function, non-decreasing in its E-variable and Lipschitz continuous in the P-variable. A typical example is the following:

$$e \mapsto \phi(e) = \mathbf{1}_{\{e>\Lambda\}}\,,\ \Lambda > 0. \tag{1.1.5}$$

The constant Λ here acts as a cap limit on emissions set by government or regulator. It translates the fact that a penalty should be paid if the cumulative emission are above the cap Λ at terminal time T.

In the first part of the thesis we are concerned with the numerical approximation of the solution $u(t, P_t, E_t)$ of the following quasi-linear PDE,

$$\begin{cases} \partial_t u(t,p,e) + \mu(u(t,p,e),p)\partial_e u(t,p,e) + \mathcal{L}_p u(t,p,e) = 0, \quad (t,p,e) \in [0,T] \times \mathbb{R}^d \times \mathbb{R}, \\ u(T,p,e) = \phi(e), \quad (p,e) \in \mathbb{R}^d \times \mathbb{R}, \end{cases} \tag{1.1.6}$$

where we define its infinitesimal generator $\mathcal{L}_p$ with respect to variable p, for φ smooth enough, by

$$\mathcal{L}_p \varphi(t,p,e) := b(p) \cdot \nabla_p \varphi(t,p,e) + \frac{1}{2}\mathrm{Tr}[A(p)\nabla_p^2 \varphi(t,p,e)], \tag{1.1.7}$$

where ∇_p denotes the Jacobian with respect to p, $A(p) := (\sigma\sigma^\top)(p)$ and ∇_p^2 is the matrix of second derivative operator. It was first suggested and noticed in [47] that a PDE method could be applied to above singular FBSDE to obtain a numerical approximation. However in practical economic setting, P is high-dimensional thus it is impractical to apply. For moderate dimension case, some classical probabilistic FBSDE methods exist, thus it is natural to tackle the problem of (1.1.4) by using the already known probabilistic schemes, see. e.g. Bender-Zhang method [4], Delarue-Menozzi method [33]. However neither of them provide a theoretical convergence guarantee in problem under our studies. Recently, deep neural networks methods have been designed and applied for BSDEs approximation problems, especially in high-dimensional setting. In particular, [44] has analysed the *deep BSDE solver* introduced in [43] again in the setting of small coupling. Unfortunately, the above methods fail to approximate correctly the solution to (1.1.4). Indeed, we consider a toy model introduced in [20] as follows.

Example 1.1.1 (Linear model)

$$dP_t = \sigma \mathrm{d}W_t \tag{1.1.8}$$

$$dE_t = \left(\frac{1}{\sqrt{d}} \sum_{\ell=1}^{d} P_t^\ell - Y_t \right) \mathrm{d}t \tag{1.1.9}$$

$$dY_t = Z_t \cdot \mathrm{d}W_t \tag{1.1.10}$$

with terminal function given by (1.1.5) *and where* W *is a* d*-dimensional Brownian motion and* $\sigma > 0$.

And as suggested in Chapter 2, the "classical" probabilistic FBSDEs methods [4, 33, 23] as well as *Deep BSDE solver* [44] fail. The main difficulty comes from the degeneracy of non-linear transport part of equation as well as the non-regularity of terminal condition. In consequence, the above methods are unable to capture the correct weak entropy solution. This is particularly clear when $\sigma = 0.01$ see Figure 1.1a, in which the volatility is relatively small and the correct solution should almost correspond to the solution of the inviscid Burgers' equation as vanishing limit.

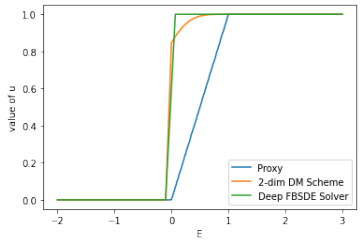

(a) $\sigma = 0.01$

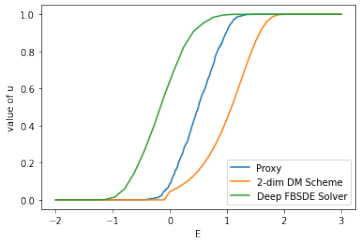

(b) $\sigma = 0.3$

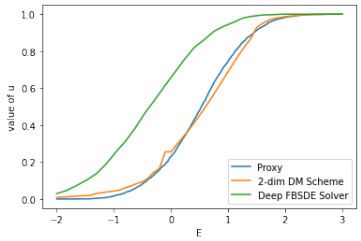

(c) $\sigma = 1.0$

Figure 1.1: Comparison of $e \mapsto \mathcal{V}(0, 0, e)$ obtained by Deep FBSDE Solver and Delarue-Menozzi Scheme (DM Scheme) to the proxy, for different volatilities. We observe that they fail to reproduce correctly the proxy.

However, to tackle the issue of degeneracy of one-dimensional transport equation, by taking a different point of view, particle systems have been known to reproduce the correct entropy solution of one-dimensional conservation laws or transport equations in different contexts: for example in astrophysics or gas dynamics. In this system, many particles evolve at constant velocity and stick together at collisions. It was first introduced and proved in Brenier and Grenier [17] that sticky particle dynamics can approximate the entropy solution of one-dimensional cosnervation laws with monotonic initial condition. And more specifically Jourdain and Reygner [53] proves and guarantees a theoretical convergence rate of order $\frac{1}{N}$ under the $L1$-norm by using multitype SPD (Sticky Particles Dynamics). In Bossy and Talay [9, 10], the authors propose a stochastic interacting particles algorithm, corresponding to a SPD without collisions to solve a Burgers' type equation, a class of Mean field PDE problems and also prove a theoretical convergence rate of order $N^{-\frac{1}{2}} + \Delta t^{\frac{1}{2}}$ for the $L1$-norm under certain assumptions. Many other works based on stochastic interacting particles or sticky particles dynamics to solve conservation laws or transport equation appeared, see for example [52, 55, 6, 8, 56, 51, 54].

1.1.2 Our contributions

In the first part of this thesis, we analyse and develop in details the numerical approximation methods in the framework of singular fully coupled forward backward stochastic differential equations which presents a degenerate forward component and non-smooth terminal condition. They are frequently used for modelling of carbon emission market, see e.g. [34, 22, 20].

To circumvent the mathematical difficulty on degeneracy and non-regularity, in

Chapter 2, we take advantage of the uni-dimensionality of the purely non-linear transport operator and introduce a theoretical splitting approach to approximate the solution of singular FBSDEs by treating differently the numerical approximation of high-dimensional diffusion operator and backward one-dimensional transport operator. We have also studied its convergence rate as well as its stability under the minimal conditions guaranteeing the well posedness of the problem. Our main theoretical result, in Theorem 2.2.2, proves that this splitting scheme is convergent at a rate $\frac{1}{2}$ with respect to the time step under the minimal assumption used in [19] to obtain existence and uniqueness of the solution $\mathcal{V}$. Our second main results are in section 2.3, which presents, under previous standing hypothesis, several fully implementable numerical schemes, and the overall procedure becomes a sequence of combination of non-linear regression optimisation problems and transport operator approximation problems. In practice, we rely on conservative finite difference methods (Lax-Friedrichs scheme or Upwind scheme), see e.g. [60] for transport equation approximation and also on neural network, see e.g. [42, 43, 48] for non-linear regression to tame the "curse of dimensionality. Last, we introduce an alternative particles and tree-based scheme as a proxy and various numerical tests have been implemented in a high-dimensional setting and the tests show very good results.

In Chapter 3, based on previous works of particles systems and interacting particles see e.g. [53, 55, 8, 9, 10], we develop and introduce an alternative scheme which decouples PDE (1.1.33) separately into one-dimensional transport equation and diffusion equation at each time step. This scheme is based on sticky particle dynamics and binomial-tree to approximate respectively transport and diffusion parts. As mentioned in the Chapter 2, this scheme serves as a "proxy" solution, thus it is of interest to control the numerical error due to this procedure, this is the main purpose of this chapter of thesis. As stated in [53], the SPD generically induce exact weak solutions, but for discrete initial condition, and need not satisfy Kružkov's [58] entropy or Bianchi-Bressan's [7] viscosity condition. Thus it leads us to separate the total approximation error (in the $L1$-norm) into four sources of error: the transport part error, the diffusion error, the splitting error as well as the propagation error. The error due to approximation of transport operator is well studied in Jourdain et al [53, 55] and addressed in Section 3.4.1. The error due to diffusion has been addressed in Section 3.4.4. In particular, to overcome the difficulty faced to gradient explosion and non-regularity at terminal time, we employ a regularization technique by considering its convolution of theoretical solution respect to a compactly smooth function φ. The error due to splitting has been thoroughly studied in the Chapter 2 and its proof has been adapted in Section 3.4.3. The main novelty of our approach compared to previous works lies in the fact that a new numerical scheme based on splitting that captures the entropy solution of the quasilinear PDEs and a theoretical convergence rate $\frac{1}{6}$ with respect to time step is proved under assumptions which guarantees the well-posedness of problem and smoothness of value function $\mathcal{V}$.

1.1.3 Splitting scheme

In Chapter 2, given a discrete time grid $\pi = \{0 =: t_0 < \cdots < t_n < \cdots < t_N := T\}$ with N a positive integer which denotes the number of time steps. For later use, we denote $|\pi| := \max_{0 \leqslant n < N}(t_{n+1} - t_n)$.

A splitting algorithm involving a diffusion step and a transport step is applied iteratively within the above time grid. The main goal is to compute an approximation of $u(0, P_0, E_0)$, where u the solution to the PDE (1.1.6) at the initial time and prove an upper bound for the convergence rate of the splitting scheme in terms of the time grid step under the minimal following assumption see e.g. [19, 22].

Assumption 1.1.1 *We assume that $(b, \sigma, \mu) \in \mathcal{A}$ and terminal condition $\phi \in \mathcal{K}$. where*

1. *$\mathcal{A}$ be the class of functions such that $B : \mathbb{R}^d \to \mathbb{R}^d$, $\Sigma : \mathbb{R}^d \to \mathcal{M}_d$, $F : \mathbb{R} \times \mathbb{R}^d \to \mathbb{R}$ which are L-Lipschitz continuous functions. Moreover, F is strictly decreasing in y and satisfies, for all $p \in \mathbb{R}^d$,*

$$\ell_1 |y - y'|^2 \leqslant (y - y')(F(y', p) - F(y, p)) \leqslant \ell_2 |y - y'|^2. \tag{1.1.11}$$

2. *Let $\mathcal{K}$ be the class of functions $\phi : \mathbb{R}^d \times \mathbb{R} \to [0, 1]$ such that ϕ is L_ϕ-Lipschitz in the first variable for some $L_\phi > 0$ and non-decreasing in its second variable, namely*

$$|\phi(p, e) - \phi(p', e)| \leqslant L_\phi |p - p'| \quad \text{for all} \quad (p, p', e) \in \mathbb{R}^d \times \mathbb{R}^d \times \mathbb{R}\,, \tag{1.1.12}$$

$$\phi(p, e') \geqslant \phi(p, e) \quad \text{if} \quad e' \geqslant e\,, \tag{1.1.13}$$

and moreover satisfying,

$$\sup_e \phi(p, e) = 1 \quad \text{and} \quad \inf_e \phi(p, e) = 0 \quad \text{for all} \quad p \in \mathbb{R}^d\,. \tag{1.1.14}$$

1.1.3.1 Theoretical splitting scheme

In Section 2.2, we first introduce the theoretical splitting scheme, which is a numerical scheme that treats separately high-dimensional diffusion step and one-dimensional degenerate transport step. For this purpose, we first introduce the transport step where the diffusion part is frozen.

Theorem 1.1.1 (Proposition 2.10 in [19], Proposition 3.2 in [22]) *Let $\tau > 0$, $(B, \Sigma, F) \in \mathcal{A}$ and $\Phi \in \mathcal{K}$.*
Given any initial condition $(t_0, p, e) \in [0, \tau) \times \mathbb{R}^d \times \mathbb{R}$, there exists a unique progressively measurable 4-tuple of processes $(P_t^{t_0,p,e}, E_t^{t_0,p,e}, Y_t^{t_0,p,e}, Z_t^{t_0,p,e})_{t_0 \leqslant t \leqslant \tau} \in \mathcal{S}_c^{2,d}([t_0, \tau]) \times \mathcal{S}_c^{2,1}([t_0, \tau]) \times \mathcal{S}_c^{2,1}([t_0, \tau)) \times \mathcal{H}^{2,d}([t_0, \tau])$ satisfying the dynamics

$$\begin{aligned} \mathrm{d}P_t^{t_0,p,e} &= B(P_t^{t_0,p,e})\mathrm{d}t + \Sigma(P_t^{t_0,p,e})\mathrm{d}W_t, & P_{t_0}^{t_0,p,e} &= p \in \mathbb{R}^d, \\ \mathrm{d}E_t^{t_0,p,e} &= F(Y_t^{t_0,p,e}, P_t^{t_0,p,e})\mathrm{d}t, & E_{t_0}^{t_0,p,e} &= e \in \mathbb{R}, \\ \mathrm{d}Y_t^{t_0,p,e} &= Z_t^{t_0,p,e} \cdot \mathrm{d}W_t, \end{aligned} \tag{1.1.15}$$

and such that

$$\mathbb{P}\left[\Phi_-(P_\tau^{t_0,p,e}, E_\tau^{t_0,p,e}) \leqslant \lim_{t \uparrow \tau} Y_t^{t_0,p,e} \leqslant \Phi_+(P_\tau^{t_0,p,e}, E_\tau^{t_0,p,e})\right] = 1. \tag{1.1.16}$$

The unique decoupling field *defined by*

$$[0,\tau)\times\mathbb{R}^d\times\mathbb{R}\ni(t_0,p,e)\to w(t_0,p,e)=Y_{t_0}^{t_0,p,e}\in\mathbb{R}$$

is continuous and satisfies

1. *For any $t\in[0,\tau)$, the function $w(t,\cdot,\cdot)$ is $1/(l_1(\tau-t))$-Lipschitz continuous with respect to e,*
2. *For any $t\in[0,\tau)$, the function $w(t,\cdot,\cdot)$ is C-Lipschitz continuous with respect to p, where C is a constant depending on L, τ and L_ϕ only.*
3. *Given $(p,e)\in\mathbb{R}^d\times\mathbb{R}$, for any family $(p_t,e_t)_{0\leqslant t<\tau}$ converging to (p,e) as $t\uparrow\tau$, we have*
$$\Phi_-(p,e)\leqslant\liminf_{t\to\tau}w(t,p_t,e_t)\leqslant\limsup_{t\to\tau}w(t,p_t,e_t)\leqslant\Phi_+(p,e)\,. \tag{1.1.17}$$
4. *For any $t\in[0,\tau)$, the function $w(t,\cdot,\cdot)\in\mathcal{K}$.*

Definition 1.1.1 (Transport step) *We set*

$$(0,\infty)\times\mathcal{K}\ni(h,\psi)\mapsto\mathcal{T}_h(\psi)=\tilde{v}(0,\cdot)\in\mathcal{K},$$

where $\tilde{v}$ is the decoupling field defined in Theorem 1.1.1 with parameters $\tau=h$, $B=0$, $\Sigma=0$, $F=\mu$ and terminal condition $\Phi=\psi$.

And we denote $\tilde{v}(\cdot)$ the unique entropy solution to the following transport equation

$$\partial_t w+\partial_e(\mathfrak{M}(p,w))=0\,,\qquad\text{where }\mathfrak{M}(p,y)=\int_0^y\mu(p,\upsilon)\mathrm{d}\upsilon\ ,\ 0\leqslant y\leqslant 1, \tag{1.1.18}$$

with $\tilde{v}(h,\cdot)=\psi$.

Taking the same idea as before, it is natural to froze the E- process to its initial value and introduce the diffusion step.

Definition 1.1.2 (Diffusion step) *We set*

$$(0,\infty)\times\mathcal{K}\ni(h,\psi)\mapsto\mathcal{D}_h(\psi)=\bar{v}(0,\cdot)\in\mathcal{K},$$

where $\bar{v}(0,\cdot)$ is the decoupling in Theorem 1.1.1 with parameters $\tau=h$, $B=b$, $\Sigma=\sigma$, $F=0$ and terminal condition $\Phi=\psi$.

Observe that, for $t\in[0,h)$,

$$\bar{v}(t,p,e)=\mathbb{E}\Big[\psi(P_h^{t,p},e)\Big]\ \text{ and }\bar{v}(t,\cdot)\in\mathcal{K}\,. \tag{1.1.19}$$

Then, with the above two approximation steps at hand, we consider naturally the following theoretical scheme on π by a backward induction.

Definition 1.1.3 (Theoretical splitting scheme) *We set*

$$(0,\infty)\times\mathcal{K}\ni(h,\psi)\mapsto\mathcal{S}_h(\psi):=\mathcal{T}_h\circ\mathcal{D}_h(\psi)\in\mathcal{K}.$$

For $n\leqslant N$, we denote by u_n^π the solution of the following backward induction on π:
- for $n=N$, set $u_N^\pi:=\phi$,
- for $n<N$, $u_n^\pi=\mathcal{S}_{t_{n+1}-t_n}(u_{n+1}^\pi)$.

The $(u_n^\pi)_{0\leqslant n\leqslant N}$ stands for the approximation of the decoupling field $\mathcal{V}(t,\cdot)$ for $t\in\pi$. Moreover, from the property of $\mathcal{T}$ and $\mathcal{D}$, $u_n^\pi\in\mathcal{K}$, for all $0\leqslant n\leqslant N$.

1.1.3.2 Main results

In Theorem 1.1.2, under some theoretical assumptions such as a structural assumptions which guarantees existence and well-posedness of problem, the $L1$-error of the theoretical splitting numerical scheme is controlled by the truncation error and the error due to the L^1-stability of perturbed scheme. Since the solution itself presents a gradient explosion in the E-variable near the terminal time T, to circumvent it, we employ a smoothed version of decoupling field as in Section 2.2.3.1. We first find a bound on the local truncation error in the norm $L\infty$ see Lemma 2.2.1, and then extend it to global $L1$-error as proposed in Proposition 2.2.1. Combined with the stability of scheme in Proposition 2.2.2, we finally reach the convergence rate of the splitting scheme:

Theorem 1.1.2 *Under our* standing assumptions*, there exists a constant C such that*

$$\int_{\mathbb{R}} |\mathcal{V}(0,p,e) - u_0^\pi(p,e)| \mathrm{d}e \leqslant CT(1+|p|^2)\sqrt{|\pi|}\,,$$

where $u_0^\pi(p,e)$ the solution obtained through theoretical splitting scheme at time $t = 0$.

We show that a convergence rate of order $\frac{1}{2}$ and this guarantees the reasonableness of using a splitting scheme to solve above singular FBSDEs (1.1.4).

1.1.3.3 Implementable schemes

Based on this theoretical splitting approach, we propose several numerically implementable schemes which combines a finite difference approximation of the transport operator and a probabilistic approximation of the diffusion operator.

Let $\mathfrak{E} = (e_j)_{1\leqslant j\leqslant J}$ be a discrete grid of $\mathbb{R}$ with J a positive integer. We denote by $\mathcal{T}_h^{\mathfrak{E}}$ an approximation of the operator $\mathcal{T}_h$ on $\mathfrak{E}$. i.e. $\mathbb{R}^d \times \mathbb{R}^J \ni (p,\theta) \mapsto \mathcal{T}_h^{\mathfrak{E}}(p,\theta) \in \mathbb{R}^J$, which means that $\mathcal{T}_h^{\mathfrak{E}}(p,\cdot)$ is an approximation on the grid $\mathfrak{E}$ of the corresponding equation (1.1.18) on $[0,h]$ for $p \in \mathbb{R}^d$. In addition, we assume that $\mathcal{T}_h^{\mathfrak{E}}(p,\theta)$ has at-most polynomial growth. The terminal condition $\psi : \mathbb{R}^d \times \mathbb{R} \to \mathbb{R}$ is approximated on $\mathfrak{E}$ by $\theta^j = \psi(p,e_j)$, for all $1 \leqslant j \leqslant J$ and $p \in \mathbb{R}^d$. Given this approximate transport operator, we now introduce a probabilistic approximation of decoupling field $\mathcal{V}(0,p,\cdot)$ on $\mathfrak{E}$. For this purpose, we consider the Euler scheme associated to P on π, namely, for $n \geqslant 0$,

$$\widehat{P}^\pi_{t_{n+1}} = \widehat{P}^\pi_{t_n} + b(\widehat{P}^\pi_{t_n})(t_{n+1}-t_n) + \sigma(\widehat{P}^\pi_{t_n})\Delta\widehat{W}_n \quad \text{and } \widehat{P}^\pi_0 = p\,. \tag{1.1.20}$$

Here, $(\Delta\widehat{W}_n)_{0\leqslant n\leqslant N-1}$ are independent random variables that stands for an approximation of the law of $(W_{t_{n+1}} - W_{t_n})_{0\leqslant n\leqslant N-1}$.
We now define a discrete time process $(\Gamma_n)_{0\leqslant n\leqslant N}$ valued in $\mathbb{R}^J$ as follows.

Definition 1.1.4 *$(\Gamma_n)_{0\leqslant n\leqslant N}$ is solution to the following backward scheme:*

1. *For $n = N$, $\Gamma_N^j = \phi(\widehat{P}^\pi_{t_N}, e_j)$ for $1 \leqslant j \leqslant J$.*

2. For $n < N$, compute

$$\Gamma_n = \mathcal{T}_h^{\mathfrak{E}}(\widehat{P}^{\pi}_{t_n}, \mathbb{E}\Big[\Gamma_{n+1}|\widehat{P}^{\pi}_{t_n}\Big]) \,. \tag{1.1.21}$$

For later use, we define the auxiliary process $(\bar{\Gamma}_n)$ by

$$\bar{\Gamma}^j_n = \mathbb{E}\Big[\Gamma^j_{n+1}|\widehat{P}^{\pi}_{t_n}\Big] \quad \text{for all } 1 \leqslant j \leqslant J \,. \tag{1.1.22}$$

We also importantly observe that, due to the Markovian property of $\widehat{P}^{\pi}$ on π, (Γ_n) satisfies

$$\Gamma_n := \gamma_n(\widehat{P}^{\pi}_{t_n}) \,, \quad 0 \leqslant n \leqslant N \,, \tag{1.1.23}$$

where the functions $\gamma_n : \mathbb{R}^d \to \mathbb{R}^J$, are given by

Definition 1.1.5 (Markovian) *1. For $n = N$, $\gamma^j_N(p) = \phi(p, e_j)$, $1 \leqslant j \leqslant J$, $p \in \mathbb{R}^d$.*

2. Then, compute for $n < N$, $p \in \mathbb{R}^d$,

$$\bar{\gamma}^j_n(p) = \mathbb{E}\Big[\gamma^j_{n+1}\Big(p + b(p)h + \sigma(p)\Delta\widehat{W}_n\Big)\Big] \quad \textit{for all } 1 \leqslant j \leqslant J, \tag{1.1.24}$$

$$\gamma_n(p) = \mathcal{T}_h^{\mathfrak{E}}(p, \bar{\gamma}_n(p)) \,. \tag{1.1.25}$$

With the above definitions, we have that $\Gamma_0 = \gamma_0(P_0)$, which is an approximation of $\mathcal{V}(0, P_0, \cdot)$ on the discrete grid $\mathfrak{E}$.

1.1.3.4 Conservative Finite Difference scheme

Concerning the approximation of backward non-linear transport operator (1.1.18), we first consider the Lax-Friedrichs scheme and define $\mathcal{T}^{\mathrm{LF}}_{\mathfrak{E},\mathfrak{R},h} : \mathbb{R}^d \times \mathbb{R}^J \mapsto \mathbb{R}^J$ the approximation of the associated operator $\mathcal{T}_h$. It is defined as follows, see e.g. [60, Chapter 12].

Definition 1.1.6 (Lax-Friedrichs) *For a given $p \in \mathbb{R}^d$ and $\theta \in \mathbb{R}^J$, let $(V^k_j)_{1\leqslant k\leqslant K, 1\leqslant j\leqslant J}$ denotes the approximation at the point (r_k, e_j) The steps to compute V are:*
- at time $r_K = h$: set $V^K_j = \theta_j$, $1 \leqslant j \leqslant J$,
- for $0 \leqslant k < K$: set $V^k_1 = V^{k+1}_1$, $V^k_J = V^{k+1}_J$ and compute, for $1 < j < J$:

$$V^k_j = \frac{1}{2}(V^{k+1}_{j+1} + V^{k+1}_{j-1}) + \frac{\delta}{2\mathfrak{d}}\Big(\mathfrak{M}(p, V^{k+1}_{j+1}) - \mathfrak{M}(p, V^{k+1}_{j-1})\Big) \,. \tag{1.1.26}$$

Then, set $\mathcal{T}^{\mathrm{LF}}_{\mathfrak{E},\mathfrak{R},h}(p, \theta) := V^0$.

When the function μ has constant sign, a more satisfactory method to use is the upwind method, as it is less diffusive. Since in the application to carbon markets given in Example 1.1.2 and 1.1.3 below, this will be the case, we consider the upwind method for $\mu \geqslant 0$. We thus now define $\mathcal{T}^{\mathrm{U}}_{\mathfrak{E},\mathfrak{R},h} : \mathbb{R}^d \times \mathbb{R}^J \mapsto \mathbb{R}^J$ the approximation of the associated operator $\mathcal{T}_h$ as follows, see again e.g. [60].

Definition 1.1.7 (Upwind for $\mu \geqslant 0$) *For a given $p \in \mathbb{R}^d$ and $\theta \in \mathbb{R}^J$ let $(V_j^k)_{1\leqslant j\leqslant J, 1\leqslant k\leqslant K}$ denotes the approximation at the point (r_k, e_j) The steps to compute V are:*
- at time $r_K = h$: set $V_j^K = \theta_j$, $1 \leqslant j \leqslant J$,
- for $0 \leqslant k < K$: set $V_J^k = V_J^{k+1}$ and compute, for $1 \leqslant j < J$:

$$V_j^k = V_j^{k+1} + \frac{\delta}{\mathfrak{d}} \left(\mathfrak{M}(p, V_{j+1}^{k+1}) - \mathfrak{M}(p, V_j^{k+1}) \right). \tag{1.1.27}$$

Then, set $\mathcal{T}^{\mathrm{U}}_{\mathfrak{E},\Re,h}(p,\theta) := V^0$.

In the sequel, we denote for this part our approximation of transport operator by $\mathcal{T}_h^{\mathfrak{E}}$.

1.1.3.5 Non-linear regression scheme

To compute the conditional expectation quantities $\gamma_n(\widehat{P}^\pi_{t_n}) = \mathbb{E}\Big[\Gamma_{n+1}|\widehat{P}^\pi_{t_n}\Big]$ at each time step as defined in Definition 1.1.4 and 1.1.5, we will use deep learning as it was demonstrated to be very efficient for high dimensional system, already in the setting of BSDEs, see e.g. [43, 48, 49]. Indeed, in the past years, neural networks have been used in many fields (such as image recognition, artificial intelligence, NLP etc...) and this resulted in massive improvements, especially to overcome empirically the curse of dimensionality when solving high-dimensional problems. Indeed, using neural networks results in approximations computed in an at-most polynomially growing time.

For this purpose, we choose to use a feed-forward neural network to get the approximation of γ_n. We denote by $\mathcal{NN}_{d_0,d_1,L,m}$ the set of neural nets, functions $\Phi(\cdot;\Theta) : \mathbb{R}^{d_0} \mapsto \mathbb{R}^{d_1}$, with parameter Θ and with the following characteristics: the input dimension is d_0, the output dimension is d_1, $L+1$ is the number of layers, $m = (m_l)_{0\leqslant m_l\leqslant L}$ where m_l is the number of neurons on each layer, $l = 0, ..., L$: by default, $m_0 = d$ and $m_L = d_1$. The neural network has thus $L-1$ hidden layers and the number of total parameters is $N_{L,m} = \sum_{l=0}^{L-1} m_l(1+m_{l+1})$, and thus $\Theta \in \mathbb{R}^{N_{L,m}}$.

Given a discrete approximation of $\mathcal{T}_h^{\mathfrak{E}}$, the scheme to compute $(\hat{\gamma}_n, \hat{\bar{\gamma}}_n)$ approximation of $(\gamma_n, \bar{\gamma}_n)$ in Definition 1.1.5 is given as follows.

Definition 1.1.8 (Non-linear regression by deep neural-networks) *1. At $t_N = T$, $\hat{\widehat{\gamma}}^j_n(p) = \hat{\gamma}^j_N(p) = \phi(p, e_j)$, $1 \leqslant j \leqslant J$, $p \in \mathbb{R}^d$.*

2. For $n = N-1, ..., 1$: given a simulation of $P^\pi_{t_n}$, optimize

$$\widehat{\mathcal{L}}_n(\Theta) = \mathbb{E}\Big|\mathcal{T}_h^{\mathfrak{E}}(\widehat{P}^\pi_{t_{n+1}}, \hat{\widehat{\gamma}}_{n+1}(\widehat{P}^\pi_{t_{n+1}})) - \Big(\mathcal{Y}_n(\widehat{P}^\pi_{t_n}, \Theta) + \mathcal{Z}_n(\widehat{P}^\pi_{t_n}, \Theta)(W_{t_{n+1}} - W_{t_n})\Big)\Big|^2 \tag{1.1.28}$$

where $(\mathcal{Y}_n(\cdot,\Theta), \mathcal{Z}_n(\cdot,\Theta)) \in \mathcal{NN}_{d,(d+1)\times J,L,m}$, so that

$$\Theta^\star_n \in \arg\min_{\Theta\in\mathbb{R}^{N_m}} \widehat{\mathcal{L}}_n(\Theta) \quad \text{and then} \quad \hat{\widehat{\gamma}}_n(\cdot) := \mathcal{Y}_n(\cdot, \Theta^\star_n).$$

3. At the initial time $t_0 = 0$, compute $\hat{\gamma}_0(\widehat{P}^\pi_0) = \mathbb{E}\Big[\mathcal{T}_h^{\mathfrak{E}}(\widehat{P}^\pi_{t_1}, \hat{\widehat{\gamma}}_1(\widehat{P}^\pi_{t_1}))\Big]$.

1.1.3.6 Numerical results

In Section 2.3.3, we work on numerical tests of different models given in Example 1.1.2, 1.1.3 and 1.1.1 under the setting of Assumption 1.1.1, using the non-linear regression and splitting method in 2.3.1. Especially for the linear model, we have plotted the 1-dim proxy of the solution, solution of alternative scheme and solution of Neural nets & LF particularly for linear model 1.1.1 in Figure 1.2.

Example 1.1.2 (BM with positive emission)

$$\mathrm{d}P_t^\ell = \sigma \mathrm{d}W_t^\ell \text{ and } \mathrm{d}E_t = \mu(Y_t, \frac{1}{\sqrt{d}}\sum_{\ell=1}^{d} P_t^\ell)\mathrm{d}t \tag{1.1.29}$$

with $\mu(y,p) = 1 + \frac{1}{1+e^{-p}} - y$ *and* $\phi(p,e) = \mathbf{1}_{\{e \geqslant 0\}}$.

The above model will have non negative μ which is more realistic if one has in mind application to carbon market. A criticism could be however that it is driven by a Brownian Motion and that it will not suffer any discrete time error. We then introduce a multiplicative model as follows.

Example 1.1.3 (Multiplicative model)

$$\mathrm{d}P_t^\ell = \mu P_t^\ell \mathrm{d}t + \sigma P_t^\ell \mathrm{d}W_t^\ell,\ P_0^\ell = 1, \text{ and } \mathrm{d}E_t = \tilde{\mu}(Y_t, P_t)\mathrm{d}t \tag{1.1.30}$$

with $\tilde{\mu}(y,p) = \left(\prod_{\ell=1}^{d} p^\ell\right)^{\frac{1}{\sqrt{d}}} e^{-\theta y}$, *for some* $\theta > 0$ *and* $\phi(p,e) = \mathbf{1}_{\{e \geqslant 0\}}$.

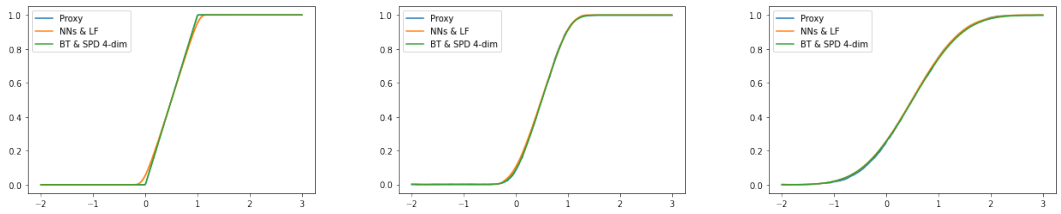

(a) $\sigma = 0.01$ (b) $\sigma = 0.3$ (c) $\sigma = 1.0$

Figure 1.2: Comparison of the two methods Neural Nets & Lax-Friedrichs (NN&LF) with $d = 10$ and the alternative scheme (BT&SPD) with $d = 4$. The Proxy solution is given by the same particle method used in on the one-dimensional PDE.

As what we expected, our schemes are able to reproduce the proxy for the true solution of Example 1.1.1 as reported in Figure 1.2, compared to the results of Figure 1.1 for the "classical" FBSDEs methods. And note the non-linear regression scheme (denoted $NN\&LF$) is tested in dimension $d = 10$ and the alternative scheme (denoted $BT\&SPD$) in dimension $d = 4$.

Empirical order of convergence rate In this part, we estimate the empirical order of convergence rate of introduced by the splitting scheme with respect to time step. In particular, we consider the multiplicative model defined in 1.1.3 with $\sigma = 0.3$, in which there is no simulation error (since the forward process is a Brownian Motion). We have tested for number of time steps $N := \{4, 8, 16, 32, 64, 128\}$, and compute the $L1$ and $L\infty$ error by NN & Upwind method. Note that to reach a better accuracy, the proxy solution is given by one dimensional equivalent model. We found that the empirical convergence rate is close to one, which is slightly better than the upper bound obtained in Theorem 1.1.2.

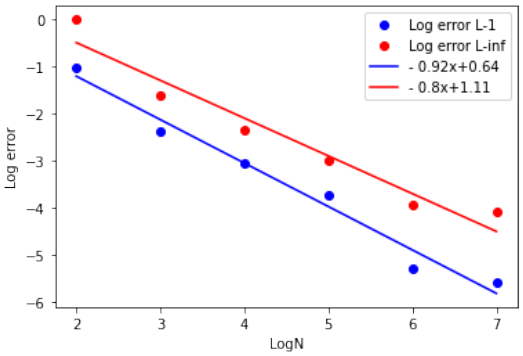

Figure 1.3: Convergence rate on N for model Example 1.1.3 with parameters $d = 10, \sigma = 0.3$ and $K = 20$, $J = 400$.

Numerical results on Dirac mass at the terminal time E_T It was also described in Carmona and Delarue [19, 20] that the fact that the emission process in the singular FBSDE can develop at a Dirac mass at the point of discontinuity of a Heaviside terminal condition at terminal time T. This phenomenon could be thought as a kind of a stochastic residual of the shock wave, as it is known [60], linked to inviscid Burgers' equation with a discontinuous condition. Formally, they prove that in [20, Proposition 3.2] that the marginal distribution of E_t is absolutely continuous with respect to the Lebesgue measure for any $0 \leqslant t < t$, and has a Dirac mass at Λ when $t = T$, i.e. there exists a constant c such that

$$\mathbb{P}\Big(E_T^{t_0,p,e} = \Lambda\Big) \geqslant c$$

We have tested this result numerically via forward simulations of E_T using following Euler scheme:

$$dE_t^{t_0,p,e} = \mu\Big(P_t^{t_0,p}, v(t, P_t^{t_0,p}, E_t^{t_0,p,e})\Big)dt, \tag{1.1.31}$$

$$E_{t_{n+1}}^{t_0,p,e} = E_{t_n}^{t_0,p,e} + \mu\Big(P_{t_n}^{t_0,p}, v_n\big(t_n, P_{t_n}^{t_0,p}, E_{t_n}^{t_0,p,e}\big)\Big)h, \tag{1.1.32}$$

where $h := T/N$ time step and v_n is the numerical solution obtained by neural networks or binomial trees at time step t_n. Empirically, we observed that E_T indeed show a Dirac mass at Λ (see Figures 1.4 and 1.5): it is clear that there are peaks around Λ and we have double-checked that $\mathbb{P}\big(E_T \in [-\epsilon+\Lambda, \epsilon+\Lambda]\big) > 0$ with typically

a small $\epsilon = 10^{-6}$, which validates numerically the theoretical result. Note that for this example we choose initial values $e = 0, 0.1$, the cap $\Lambda = 0$ and $t_0 = 0, p = 0$.

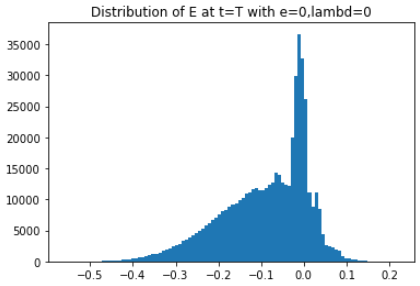

Figure 1.4: Cumulative emission E_T at terminal time with $e = 0, \Lambda = 0$ for model 1.1.1

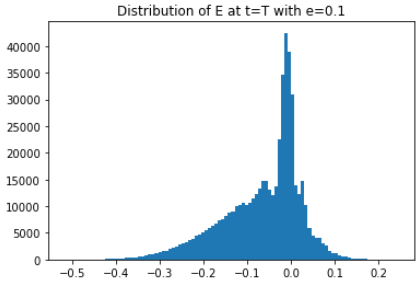

Figure 1.5: Cumulative emission E_T at terminal time with $e = 0.1, \Lambda = 0$ for model 1.1.1

Moreover, as stated in [29, 19] the price (allowance) process $(Y_t)_{0 \leqslant t \leqslant T}$, solution of the singular FBSDE, loses its Markovian property at terminal time: the topological support of the random variable Y_T conditional on event $\{E_T = \Lambda\}$ is the whole interval $[0, 1]$, which means that Y_T is not anymore a deterministic function of variable E_T on $\{E_T = \Lambda\}$. Numerically we have the same result see Figure 1.6.

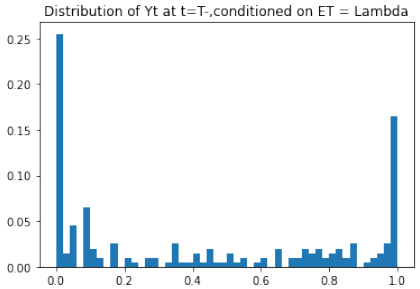

Figure 1.6: $Y_T = Y_{T-}$ conditioned on $E_T = \Lambda$, has the whole of the interval $[0, 1]$ as topological support, for $\Lambda = 0.2$.

Numerical results on decreasing terminal condition Instead of considering increasing terminal condition as (1.1.5), we consider a decreasing terminal condition

ϕ with respect to variable e. For simplicity we choose $\phi(e) = 1_{e<0}$ and also linear model as described in 1.1.1. We plot the curves of numerical solutions at different levels of volatility: $\sigma \in \{0.001, 0.01, 0.1, 0.3, 0.5, 0.7, 0.8, 1.0\}$ using specifically the BT & LF (Binomial Trees and Lax-Friedrichs) method, see Figure 1.7. We observe that its behaviour is different from the increasing terminal function case.

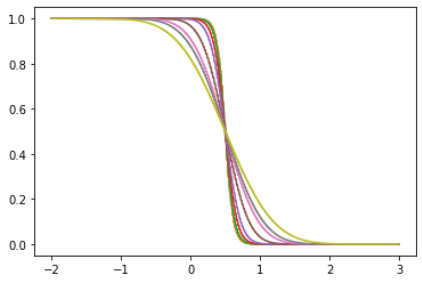

Figure 1.7: Entropy solution for linear model with decreasing terminal condition $\phi(e) = 1_{e<0}$, with different levels of volatility by BT & LF method.

1.1.4 Convergence of particles and tree based scheme

In Chapter 3, we analyse an alternative scheme originally presented in Section 2.3.3.1 of Chapter 2 which treats separately diffusion operator with moderate dimension and one-dimensional non-linear transport operator respectively by Binomial Tree and SPD(Sticky Particle Dynamics), see e.g. [53, 17, 55]. The convergenc of this scheme is proved by using decomposition of errors and also several intermediate results in [26, 53], in addition, to control the local error estimates, we made an additional assumption on the regularity of value function $\mathcal{V}$ and employed regularization to overcome the gradient explosion near the terminal time T. We recall that we are interested in this second chapter of the thesis with an alternative numerical scheme of approximation of solution $u(t, P_t, E_t)$ where u is the value function of the entropy solution to the following quaisi-linear PDE

$$\begin{cases} \partial_t u(t,p,e) + \mu(u(t,p,e),p)\partial_e u(t,p,e) + \mathcal{L}_p u(t,p,e) = 0, \quad (t,p,e) \in [0,T] \times \mathbb{R}^d \times \mathbb{R}, \\ u(T,p,e) = \phi(e), \quad (p,e) \in \mathbb{R}^d \times \mathbb{R} \end{cases} \tag{1.1.33}$$

1.1.4.1 Implementable scheme

Notations: For $M \geqslant 1$, let

$$D_M := \left\{ \mathrm{e} = (e_1, \dots, e_m, \dots, e_M) \in \mathbb{R}^M \,|\, e_1 \leqslant \cdots \leqslant e_m \leqslant \cdots \leqslant e_M \right\} \tag{1.1.34}$$

$$\text{and } \mathcal{I}^M := \left\{ \theta \in \mathscr{I} |\ \theta(\cdot) := H * (\frac{1}{M} \sum_{m=1}^{M} \delta_{e_m}), \mathrm{e} \in D_M \right\} \tag{1.1.35}$$

where H is the Heaviside function $x \mapsto \mathbf{1}_{\{x \geqslant 0\}}$, $*$ the convolution operator and δ_e is the Dirac mass at $e \in \mathbb{R}$. For later use, we also introduce, for $M \geqslant 0$ and $n \in \{0, \dots, N\}$, the set of function

$$\mathcal{K}_n^M = \left\{ \psi : \mathcal{P}_n \times \mathbb{R} \to [0,1] \,|\ \text{for } p \in \mathcal{P}_n,\ \psi(p,\cdot) \in \mathcal{I}^M \right\} . \tag{1.1.36}$$

As mentioned in the above, to validate empirically our results obtained with the non-linear regression scheme, it is thus of interest for us to develop an another numerical method, here based on the splitting scheme combining a particle method with tree-based regression in moderate dimension (say 2 to 5). And this alternative scheme will be efficiently implemented on the various Examples 1.1.2, 1.1.3 and 1.1.1 for the reasons that we work in moderate dimension and the process P can be expressed as a function of the underlying Brownian motion, namely $P_t = \mathfrak{P}(t, W_t)$. We treat the general case where P is solution to a SDE with Lipschitz coefficients as given in (1.1.4). The discrete approximation on the grid π is given by the classical Euler Scheme

$$\widehat{P}_0 = P_0 \text{ and } \widehat{P}_{t_{n+1}} = \widehat{P}_{t_n} + b(\widehat{P}_{t_n})\mathfrak{h} + \sigma(\widehat{P}_{t_n})\Delta\widehat{W}_n\,, \tag{1.1.37}$$

where $(\Delta\widehat{W}_n)$ is discrete approximation of the Brownian increments $(W_{t_{n+1}} - W_{t_n})_{0\leqslant n\leqslant N-1}$. For later use, we also define, for $p \in \mathbb{R}^d$ and any $0 \leqslant n \leqslant N-1$,

$$\widehat{P}^{t_n,p}_{t_{n+1}} := p + b(p)\mathfrak{h} + \sigma(p)\Delta\widehat{W}_n\,. \tag{1.1.38}$$

Let us denote by $\mathcal{P}_n$ the discrete and finite support of $\widehat{P}_{t_n}$ for $0 \leqslant n \leqslant N-1$. We observe, due to the above definition of $(\widehat{P}_{t_n})$, that

$$\text{for } p \in \mathcal{P}_n,\ \widehat{P}^{t_n,p}_{t_{n+1}} \in \mathcal{P}_{n+1}\,. \tag{1.1.39}$$

In this context, we first introduce a discrete version of the operator $\mathcal{T}$, recall Definition 1.1.1, that will compute an approximation to (1.1.18) written in *forward form*: We shall use the celebrated Sticky Particle Dynamics (SPD) [17] see also [53, Section 1.1]. The SPD is simple to implement in our special case since there is no particle colliding due to the monotonicity assumption on (μ, ψ).

We first present the discrete version of $\mathcal{T}$, which we denote $\mathfrak{T}$, acts on empirical CDF belonging to $\mathcal{I}^M$,

$$(0,\infty)\times\mathbb{R}^d\times\mathcal{I}^M \ni (h,p,\theta) \mapsto \mathfrak{T}^M_h(p,\theta) := H*(\frac{1}{M}\sum_{m=1}^{M}\delta_{e^p_m(h)}) \in \mathcal{I}^M\,. \tag{1.1.40}$$

Above $(e^p_m(h))_{1\leqslant m\leqslant M}$ is a set of particles computed as follows. Given the initial position $\mathrm{e}(0) \in D_M$ and velocities $(\bar{F}_m(p))_{1\leqslant m\leqslant M}$ set to $\bar{F}_m(p) = -\int_{(m-1)/M}^{m/M}\mu(p,y)\mathrm{d}y$, we consider M particles $(e^p_m)_{1\leqslant m\leqslant M}$, whose positions at time $t \in [0,h]$ are simply given by

$$e^p_m(t) = e_m(0) + \bar{F}_m(p)t\,. \tag{1.1.41}$$

We observe that $(e^p_m(t))_{1\leqslant m\leqslant M} \in D_M$, for all $t \in [0,h]$, as $-\mu$ is non-decreasing.

We now present the approximation used for the approximation of $\mathcal{D}_{\mathfrak{h}}(\psi)$, recall

Definition 1.1.2 and (1.1.19). For $\psi \in \mathcal{K}_{n+1}^M$ and $\mathrm{p} \in \mathcal{P}_n$. We have, from (1.1.38)

$$\bar{v}_n(\mathrm{p}, e) := \mathbb{E}\Big[\psi(\widehat{P}_{t_{n+1}}^{t_n,\mathrm{p}}, e)\Big] = \frac{1}{2d}\sum_{i=1}^{2d} \psi(\Big(\widehat{P}_{t_{n+1}}^{t_n,p}\Big)^i, e) \tag{1.1.42}$$

$$= \frac{1}{2d}\sum_{i=1}^{2d} H*(\frac{1}{M}\sum_{m=1}^{M} \delta_{e_m^i})(e) \text{ (Since } \psi \in \mathcal{K}_{n+1}^M) \tag{1.1.43}$$

$$= H*(\frac{1}{2dM}\sum_{i=1}^{I}\sum_{m=1}^{M} \delta_{e_m^i})(e) \text{ (By linearity)} \tag{1.1.44}$$

The approximation of the diffusion operator is thus given by

$$\mathcal{K}_{n+1}^M \ni \psi \mapsto \mathfrak{D}_n^M(\psi) := \bar{v}_n \in \mathcal{K}_n^{2Md}\,. \tag{1.1.45}$$

Finally, the scheme will have essentially two versions:

CASE 1: We keep the $2dM$ particles at each step n. The overall procedure will then be the iteration of the two operators $\mathfrak{T}$ and $\mathfrak{D}$, see Definition 1.1.9 below.

CASE 2: There is no need to keep $2dM$ particles at step n, when the function ψ at step $n+1$ is given by M particles (for each $p \in \mathcal{P}_{n+1}$). To reduce the number of particles, we apply another operator $\mathfrak{R}$, namely, for $M \geqslant m \geqslant 1$,

$$\mathcal{I}^M \ni \psi \mapsto \mathfrak{R}^{M,m}(\psi) \in \mathcal{I}^m\,. \tag{1.1.46}$$

Various implementation are possible, we refer to the numerical section for a precise description.

Let us now finally introduce the scheme formally.

Definition 1.1.9 (Scheme in CASE 1) *Fix $M \geqslant 1$ and set for $0 \leqslant n \leqslant N$, $M_n := (2d)^{N-n}M$.*

1. *At $n = N$: Set $\mathrm{e}_N := (\Lambda, \dots, \Lambda) \in D_{M_N}$ whose empirical CDF is the terminal condition $\phi = \mathbf{1}_{\{e \geqslant \Lambda\}}$. Setting simply $u_N^{N,M}(p, \cdot) = \phi$, for all $p \in \mathcal{P}_N$, we do observe that $u_N^{N,M} \in \mathcal{K}_N^{M_N}$.*

2. *For $n < N$: Given $u_{n+1}^{N,M} \in \mathcal{K}_{n+1}^{M_{n+1}}$, define*

$$\bar{u}_n^{N,M} = \mathfrak{D}_n^{M_{n+1}}(u_{n+1}^{N,M}) \in \mathcal{K}_n^{M_n}\,, \tag{1.1.47}$$

recall (1.1.45), and then $u_n^{N,M}$ by, for each $p \in \mathcal{P}_n$,

$$u_n^{N,M}(p, \cdot) = \mathfrak{T}_{\mathfrak{h}}^{M_n}(p, \bar{u}_n^{N,M}(p, \cdot))\,, \tag{1.1.48}$$

recall (1.1.40).

The approximation of $\mathcal{V}(0, P_0, \cdot)$ is then given by $u_0^{N,M}(P_0, \cdot)$.

Definition 1.1.10 (Scheme in CASE 2) *Fix $M \geqslant 1$.*

1. *At $n = N$: Set $\mathrm{e}_N := (\Lambda, \cdots, \Lambda) \in D_M$ whose empirical CDF is the terminal condition $\phi = \mathbf{1}_{\{e \geqslant \Lambda\}}$ is the empirical CDF of $\mathrm{e}_N := (0, \ldots, 0) \in D_M$. Setting simply $v_N^{N,M}(p, \cdot) := \phi$, for all $p \in \mathcal{P}_N$, we do observe that $v_N^{N,M} \in \mathcal{K}_N^M$.*

2. *For $n < N$: Given $v_{n+1}^{N,M} \in \mathcal{K}_{n+1}^M$, define $\bar{v}_n^{N,M} = \mathfrak{D}_n^M(v_{n+1}^{N,M}) \in \mathcal{K}_n^{2dM}$, recall (1.1.45), and then for each $p \in \mathcal{P}_n$,*

$$\check{v}_n^{N,M} = \mathfrak{R}^{2dM,M}(\bar{v}_n^{N,M}(p, \cdot)) \tag{1.1.49}$$

recall (1.1.46), and finally $v_n^{N,M}(p, \cdot)$ by,

$$v_n^{N,M}(p, \cdot) = \mathfrak{T}_{\mathfrak{h}}^M(p, \check{v}_n^{N,M}(p, \cdot)), \tag{1.1.50}$$

recall (1.1.40).

The approximation of $\mathcal{V}(0, P_0, \cdot)$ is then given by $v_0^{N,M}(P_0, \cdot)$.

1.1.4.2 Decomposition of total error

The total error could be decomposed and controlled by four parts: error due to transport operator by the particles, propagation, diffusion as well as splitting. However, classical analysis techniques fail since the solution $\mathcal{V}$ is not smooth a priori, thus its gradient at time t in terms of $L1$-norm leads to an explosion when t approaches the terminal time T. To circumvent this difficulty, we introduce the mollification $\mathcal{V}^\epsilon$ by considering its convolution respect to a smooth compact function φ_ϵ which we defines $\mathcal{V}^\epsilon$ as follows:

$$\mathcal{V}^\epsilon(t, p, e) := \int \mathcal{V}(t, p + q, e)\varphi_\epsilon(q)\mathrm{d}q \quad \text{where} \quad \varphi_\epsilon(q) := \frac{1}{\epsilon}\varphi(\frac{q}{\epsilon}) \tag{1.1.51}$$

and with $\varphi(\cdot)$ a smooth compactly supported density probability function. We first observe that the mollification $\mathcal{V}^\epsilon$ satisfies same PDE in the above 1.1.33 up to an error term as follows

Lemma 1.1.1 *The regularized function $\mathcal{V}^\epsilon$ satisfies on $[0, T) \times \mathbb{R}^d \times R$,*

$$\partial_t \mathcal{V}^\epsilon + \mu(\mathcal{V}(t, p, e), p)\partial_e \mathcal{V}^\epsilon + b(p)\partial_p \mathcal{V}^\epsilon + \frac{1}{2}\bar{\sigma}^2 \nabla_p \mathcal{V}^\epsilon = \theta^\epsilon(t, p, e) \tag{1.1.52}$$

and $w(T, \cdot) = \phi(\cdot)$ with θ a continuous function. Moreover, we have that

$$|\theta^\epsilon(t, p, e)| \leqslant C\epsilon \left(\int |\partial_p \mathcal{V}^\epsilon(t, p + q, e)|\varphi_\epsilon(q)\mathrm{d}q + \partial_e \mathcal{V}^\epsilon(t, p, e) \right). \tag{1.1.53}$$

And we will see that three error terms $\partial_e \mathcal{V}^\epsilon(t, p, e), |\partial_p \mathcal{V}^\epsilon(t, p, e)|, |\partial_{pp}^2 \mathcal{V}^\epsilon(t, p, e)|$ on the right-hand side can be controlled in terms of $L1$-norm. And it is also crucial to have a control of $\partial_p \mathcal{V}^\epsilon$ in terms of norms $L\infty$ and $L1$-norm, indeed, in Proposition 1.1.1, we prove that

$$|\partial_p \mathcal{V}^\epsilon(\cdot)|_\infty \leqslant C \text{ and } \int |\partial_p \mathcal{V}^\epsilon(t, p, e)|\mathrm{d}e \leqslant C(T - t) \tag{1.1.54}$$

In the following ,we perform an analysis on the decomposition of total errors introduced by the scheme given in CASE 1.

The error we seek to control is, for $\gamma_n = u_n^{N,M}$ or $\gamma_n = v_n^{N,M}$ given above,

$$\mathrm{err}(N,M) := \int |\gamma_0(P_0,e) - \mathcal{V}(0,P_0,e)|\mathrm{d}e\,. \tag{1.1.55}$$

And we first observe

$$\mathrm{err} \leqslant \mathcal{E}_0(P_0) + \mathcal{E}_0^r\,, \tag{1.1.56}$$

with for $0 \leqslant n \leqslant N$ and $p \in \mathcal{P}_n$,

$$\mathcal{E}_n^r(p) := \int |\mathcal{V}^\epsilon(t_n,p,e) - \mathcal{V}(t_n,p,e)|\mathrm{d}e\,, \tag{1.1.57}$$

$$\mathcal{E}_n(p) := \int |\gamma_n(p,e) - \mathcal{V}^\epsilon(t_n,p,e)|\mathrm{d}e\,. \tag{1.1.58}$$

Error $\mathcal{E}_n(p)$ could be decomposed further into four parts as follows under CASE1.

Lemma 1.1.2 *Under CASE 1, for* $0 \leqslant n \leqslant N-2$,

$$\mathcal{E}_n(p) \leqslant \mathcal{E}_n^{\mathrm{T}}(p) + \bar{\mathcal{E}}_n(p) + \mathcal{E}_n^D(p) + \mathcal{E}_n^S(p) \tag{1.1.59}$$

and

$$\mathcal{E}_{N-1}(p) \leqslant \mathcal{E}_{N-1}^{\mathrm{T}}(p) + \mathcal{E}_{N-1}^{\mathrm{r}}(p) + \int |\mathcal{S}_\mathfrak{h}(\phi(\cdot))(p,e) - \Theta_\mathfrak{h}(\phi(\cdot))(p,e)|\mathrm{d}e \tag{1.1.60}$$

where for $p \in \mathcal{P}_n$,

$$\mathcal{E}_n^{\mathrm{T}}(p) := \int \left|\mathfrak{T}_\mathfrak{h}^{M_n}(p,\bar{u}_n^{N,M}(p,\cdot))(e) - \tilde{\mathcal{T}}_h(p,\bar{u}_n^{N,M}(p,\cdot))(e)\right|\mathrm{d}e\,, \tag{1.1.61}$$

$$\bar{\mathcal{E}}_n(p) := \int \left|\tilde{\mathcal{T}}_h(p,\bar{u}_n^{N,M}(p,\cdot))(e) - \tilde{\mathcal{T}}_h(p,\mathbb{E}[\mathcal{V}^\epsilon(t_{n+1},\widehat{P}_{t_{n+1}}^{t_n,p},\cdot)])(e)\right|\mathrm{d}e\,, \tag{1.1.62}$$

and for $p \in \mathbb{R}^d$,

$$\mathcal{E}_n^D(p) := \int \left|\tilde{\mathcal{T}}_h(p,\mathbb{E}[\mathcal{V}^\epsilon(t_{n+1},\widehat{P}_{t_{n+1}}^{t_n,p},\cdot)])(e) - \tilde{\mathcal{T}}_h(p,\mathbb{E}[\mathcal{V}^\epsilon(t_{n+1},P_{t_{n+1}}^{t_n,p},\cdot)])(e)\right|\mathrm{d}e\,, \tag{1.1.63}$$

$$\mathcal{E}_n^S(p) := \int \left|\tilde{\mathcal{T}}_h(p,\mathbb{E}[\mathcal{V}^\epsilon(t_{n+1},P_{t_{n+1}}^{t_n,p},\cdot)])(e) - \mathcal{V}^\epsilon(t_n,p,e)\right|\mathrm{d}e\,, \tag{1.1.64}$$

observing that

$$\mathcal{E}_{N-1}^{\mathrm{T}}(p) = \int |\mathfrak{T}_\mathfrak{h}^M(p,\phi(\cdot))(e) - \mathcal{T}_\mathfrak{h}(p,\phi(\cdot)(e))|\mathrm{d}e\,. \tag{1.1.65}$$

1.1.4.3 Control of local errors in a smooth setting

The main assumption we shall use is the following. We mention that it is satisfied in the linear toy model defined in Example 1.1.1.

Assumption 1.1.2 *The* decoupling field $\mathcal{V}$ *is a* $\mathscr{C}^{1,2,1}([0,T)\times\mathbb{R}^d\times\mathbb{R})$ *solution to*

$$\partial_t\mathcal{V}+\mu(\mathcal{V},p)\partial_e\mathcal{V}+b(p)\partial_p\mathcal{V}+\frac{1}{2}\bar{\sigma}^2\Delta_p\mathcal{V}=0\,. \tag{1.1.66}$$

In particular, the function $\sigma(\cdot)$ *is constant* $\sigma(\cdot):=\bar{\sigma}I_d$ *with* $\bar{\sigma}>0$ *and* I_d *is the* $d\times d$ *identity matrix. Moreover, the function* b *is* $\mathscr{C}^2(\mathbb{R}^d)$ *with bounded and Lipschitz derivatives and the function* μ *is* $\mathscr{C}^1(\mathbb{R}^d\times[0,1])$ *with Lipschitz and bounded derivatives.*

We first list some local control estimates of the function $\mathcal{V}$ in the regular setting of the previous assumption.

Proposition 1.1.1 *Under Assumption 1.1.2, the function* $\mathcal{V}$ *satisfies, for* $(t,p,e)\in[0,T)\times\mathbb{R}^d\times\mathbb{R}$,

$$0\leqslant\partial_e\mathcal{V}(t,p,e)\leqslant\frac{C}{T-t}\qquad\text{and}\qquad|\partial_p\mathcal{V}(t,p,e)|\leqslant C\,. \tag{1.1.67}$$

Moreover, for $(t,p)\in[0,T)\times\mathbb{R}^d$,

$$\int|\partial_p\mathcal{V}(t,p,e)|\mathrm{d}e\leqslant C(T-t)\,, \tag{1.1.68}$$

and, thus, for $p'\in\mathbb{R}^d$,

$$\int|\mathcal{V}(t,p,e)-\mathcal{V}(t,p',e)|\mathrm{d}e\leqslant C(T-t)|p-p'|. \tag{1.1.69}$$

From (1.1.52), we observe that since $\mathcal{V}^\epsilon$ *belongs to* $\mathscr{C}^{1,2,1}([0,T)\times\mathbb{R}^d\times\mathbb{R})$, *it satisfies the same bounds in the above as* $\mathcal{V}$.

As well as some control estimates on second and third-order derivatives of $\mathcal{V}^\epsilon$ in terms of norm L_1,

Lemma 1.1.3 *Under assumption 1.1.2, the followings hold, for* $(t,p)\in[0,T)\times\mathbb{R}^d$,

$$\epsilon\int|\partial^2_{p_ip_j}\mathcal{V}^\epsilon(t,p,e)|\mathrm{d}e+\epsilon^2\int|\partial^3_{p_ip_jp_k}\mathcal{V}^\epsilon(t,p,e)|\mathrm{d}e\leqslant C\,, \tag{1.1.70}$$

for $i,j,k\in\{1,\dots,d\}$. *And thus, for* $(t,p,p')\in[0,T)\times\mathbb{R}^d\times\mathbb{R}^d$,

$$\int|\partial_p\mathcal{V}^\epsilon(t,p,e)-\partial_p\mathcal{V}^\epsilon(t,p',e)|\mathrm{d}e+\epsilon\int|\partial^2_{pp}\mathcal{V}^\epsilon(t,p,e)-\partial^2_{pp}\mathcal{V}^\epsilon(t,p',e)|\mathrm{d}e\leqslant\frac{C}{\epsilon}|b-a|\,. \tag{1.1.71}$$

In the following, we will list local error estimates linked to approximation of transport operator, diffusion, regularization, and splitting, as mentioned in the above Section 1.1.4.2, and also our main results in Theorem 1.1.3.

1.1.4.3.1 Approximation of transport operator

Lemma 1.1.4 *Under Assumption 1.1.2 and in CASE 1, the following holds*

$$\mathcal{E}_n^T(p) \leqslant C\frac{\mathfrak{h}}{M_n}\ ,\ p \in \mathcal{P}_n\,. \tag{1.1.72}$$

1.1.4.3.2 Regularization error

Proposition 1.1.2 *Under Assumption 1.1.2, the following holds, for $n \leqslant N$,*

$$\mathcal{E}_n^r(p) \leqslant C\epsilon\,,\ p \in \mathbb{R}^d.$$

1.1.4.3.3 Splitting error In the article [26], the error due the theoretical splitting, has already been studied and the results obtained there can be used in our setting. However, we should point out that here $\mathcal{V}^\epsilon$ appears instead of $\mathcal{V}$. We first present the following lemma.

Lemma 1.1.5 *Under Assumption 1.1.2, the following holds,*

$$\mathcal{E}_n^S(p) \leqslant C(1+|p|^2)h^{\frac{3}{2}} + \mathfrak{E}_n(p) \tag{1.1.73}$$

with

$$\mathfrak{E}_n(p) := \int \Big|\Theta_h(\mathcal{V}^\epsilon(t_{n+1},\cdot))(p,e) - \mathcal{V}^\epsilon(t_n,p,e)\Big|\mathrm{d}e\,. \tag{1.1.74}$$

Concerning control on the term $\mathfrak{E}_n(p)$, we prove the following proposition.

Proposition 1.1.3 *Let Assumption 1.1.2 hold. Then, for $n \leqslant N-2$, $p \in \mathbb{R}^d$,*

$$\mathfrak{E}_n(p) = \int |\Theta_\mathfrak{h}(\mathcal{V}^\epsilon(t_{n+1},\cdot))(p,e) - \mathcal{V}^\epsilon(t_n,p,e)|\mathrm{d}e \leqslant C\mathfrak{h}\epsilon\,. \tag{1.1.75}$$

1.1.4.3.4 Diffusion error

Proposition 1.1.4 *Under Assumption 1.1.2, the following holds*

$$\mathcal{E}_n^D(p) \leqslant C\frac{\mathfrak{h}^{\frac{3}{2}}}{\epsilon^2}$$

for $0 \leqslant n \leqslant N-1$ and $p \in \mathbb{R}^d$.

1.1.4.4 Main results

Based on the above control of local errors linked to approximation of transport and diffusion operators as well as splitting at each stage of the scheme, together with the stability property of propagation error $\bar{\mathcal{E}}_n(p)$, we can decompose iteratively the global error into a sum of local errors, indeed,

$$\begin{aligned}
\text{err} \leqslant \mathcal{E}_0^r(P_0) + \mathcal{E}_0(P_0) &\leqslant \mathcal{E}_0^r(P_0) + \mathcal{E}_1^{\mathrm{T}}(P_0) + \bar{\mathcal{E}}_1(P_0) + \mathcal{E}_1^D(P_0) + \mathcal{E}_1^S(P_0) \\
&\leqslant \ldots \text{(iteration on propagation error } \bar{\mathcal{E}}_i) \\
&\leqslant \mathcal{E}_0^r(P_0) + \sum_{n=0}^{N-2} \mathbb{E}\Big[\mathcal{E}_n^{\mathrm{T}}(\widehat{P}_{t_n}) + \mathcal{E}_n^D(\widehat{P}_{t_n}) + \mathcal{E}_n^S(\widehat{P}_{t_n})\Big] + \mathbb{E}\Big[\mathcal{E}_{N-1}(\widehat{P}_{t_{N-1}})\Big]
\end{aligned}$$

With the above local error estimates at hand, we obtain a global control on the convergence error between the theoretical solution and the numerical approximation by our numerical scheme CASE 1, more precisely, the global $L1$-error is controlled by $\mathcal{O}(\epsilon + \frac{\mathfrak{h}^{\frac{1}{2}}}{\epsilon^2})$. For the purpose of finding an optimal order, we denote $\epsilon := \mathfrak{h}^{\alpha}$, and it's then converted to an optimisation problem which leads to $\alpha^\star = 1/6$.

Theorem 1.1.3 *Let Assumption 1.1.2 hold. Then, under CASE 1,*

$$\mathrm{err}(N, M) \leqslant C(\frac{1}{M} + \frac{\sqrt{\mathfrak{h}}}{\epsilon^2} + \epsilon)\,, \tag{1.1.76}$$

recall (1.1.55). Moreover, setting $\epsilon = \mathfrak{h}^{\frac{1}{6}}$ and $M = \frac{1}{\epsilon}$, we have

$$\int |\mathcal{V}(0, P_0, e) - u_0^{N,M}(P_0, e)|\mathrm{d}e \leqslant C\mathfrak{h}^{\frac{1}{6}}. \tag{1.1.77}$$

1.1.4.5 Numerical results

Comparison between CASE 1, CASE 2 and proxy To view the differences between the various reducing particles implementations in CASE 2 scheme, we test those two numerical schemes in a linear toy model with Brownian setting, recall Example 1.1.1, as plotted in Figure 1.8. And in Figure 1.9, we plot the solutions obtained by CASE 1 and CASE 2 against the proxy solution presented in [9] for different levels of volatility $\sigma = 0.01, 0.3, 1.0$. Both CASE 1 and CASE 2 scheme could reproduce correctly the "entropy" solution.

Comparison between BT&SPD and PDE method Apart from NN & Upwind presented in [26] and method in [9], we would like also compare our CASE1 scheme to a PDE method see e.g. [46] for 2-dimensional toy model 1.1.1, with a discontinuous terminal condition $\phi(e) = \mathbf{1}_{e\geqslant 0}$ and different levels of volatility $\sigma \in \{0.01, 0.3, 1.0\}$, see Figure 1.10a,1.10b and 1.10c. Note that we choose the Lax-Friedrichs scheme for conservation law appearing in the PDE. We observe that both methods could reproduce correctly the weak entropy solution. However in practice we observe that PDE method is not very stable and sometimes its numerical solution is not convergent. To ensure the stability, in practice we need to choose parameters to verify the CNL condition, in our case, we choose number of time steps = 800, number of P-space steps = 50, and number of E steps = 400. Thus by the "diffusive" nature of Lax–Friedrichs scheme as well as the constraints on stability imposed by CNL condition, PDE method require much more time to compute than BT&SPD method for a fixed accuracy.

Empirical convergence rate of CASE1 In this part, we estimate the empirical order of convergence rate of introduced by CASE1 scheme with respect to time step $\mathfrak{h}$. In particular, we consider the linear toy model defined in 1.1.1 with $\sigma = 1.0$. We have tested for number of time steps $N := \{2, 4, 8, 16, 32, 64\}$, and compute the $L1$-error by CASE1 method. Note that to reach a better accuracy, the proxy solution is given by one dimensional equivalent model applied by method in [10]. We found that the empirical convergence rate is very close to one see Figure 1.11, which is better than the upper bound obtained in Theorem 1.1.2.

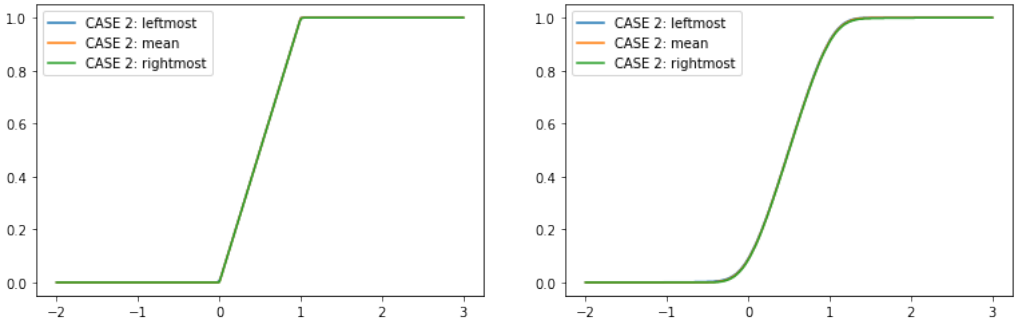

(a) $\sigma = 0.01$

(b) $\sigma = 0.3$

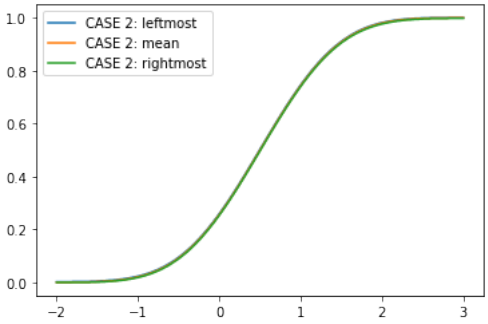

(c) $\sigma = 1.0$

Figure 1.8: Model of Example 1.1.1: Comparison of the different implementations: `leftmost,mean,rightmost` in CASE2 with $d = 4$. The Proxy solution is given by the same particle method on the one-dimensional PDE. For $BT\&SPD$ CASE 2, the number of particles is $M = 3500$ and the number of time steps $N = 20$.

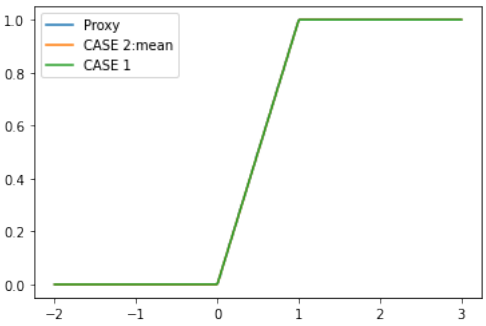

(a) $\sigma = 0.01$

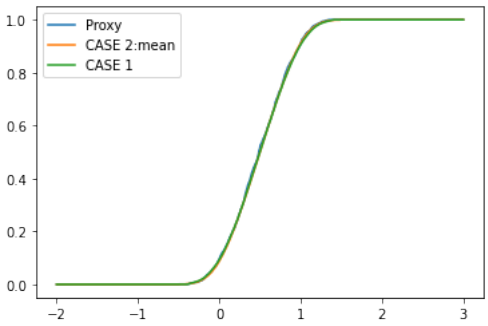

(b) $\sigma = 0.3$

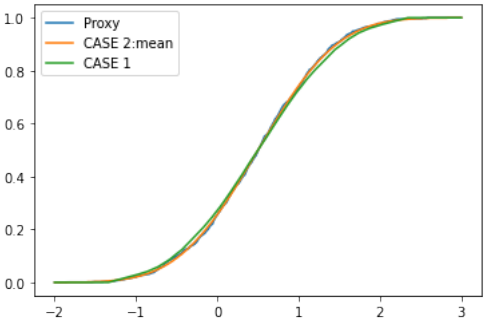

(c) $\sigma = 1.0$

Figure 1.9: Model of Example 1.1.1: Comparison of the two methods CASE 1 & CASE2: `mean` with $d = 4$. The Proxy solution is given by the same particle method on the one-dimensional PDE. For $BT\&SPD$: both CASE 1 and CASE 2, the number of particles is $M = 3500$ and the number of time steps $N = 20$.

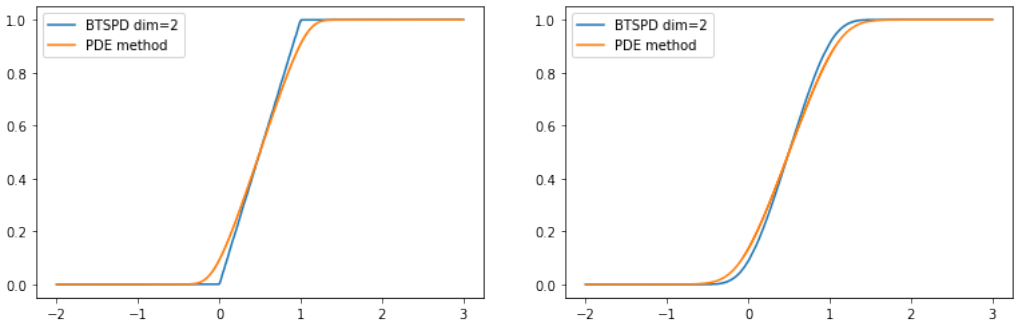

(a) $\sigma = 0.01$

(b) $\sigma = 0.3$

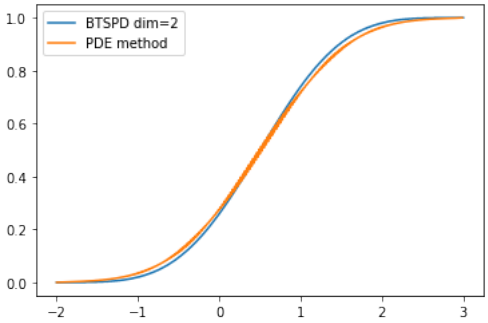

(c) $\sigma = 1.0$

Figure 1.10: Comparison of $e \mapsto \mathcal{V}(0, 0, e)$ obtained by BT&SPD and PDE method, for different volatilities, for the linear model 1.1.1.

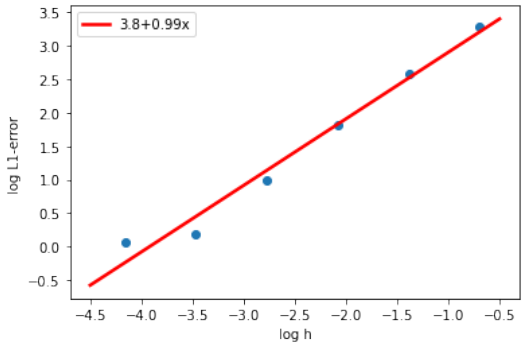

Figure 1.11: Convergence rate on time step $\mathfrak{h} := \frac{T}{N}$ for model Example 1.1.1 with parameters $d = 4, \sigma = 1.0$.

1.2 A dual approach to weak hedging problem

In this second part of thesis, we consider a class of non standard control problems where we impose on the controlled process a constraint involving its law at terminal time T. Within this framework, we are interested in the so-called *weak hedging problem*, especially in a new dual approach in the linear setting case. For this purpose, we first introduce weak hedging problem and its properties in a non-linear setting by encapsulating all possible cases for target measure μ: 1. discrete and finite 2. arbitrary measure, then we establish a link between our general weak hedging problem and a kind of optimal transport problem by considering its "Monge" and "Kantorovitch" version representation. Under suitable assumption, we prove its equivalence in a non-linear setting. Particularly in the linear framework and μ with finite support, we present and prove a dual representation of the "Kantorovitch" problem. This formulation gives naturally a numerical scheme using stochastic gradient descent see e.g. [3]. Besides, in the case where μ a probability measure and $G(\gamma) = \xi + \gamma$, with ξ a fixed random variable, we also find an explicit solution by direct resolution of optimal transport problem. The main novelty of our approach in comparison to the previous works [15, 11, 13] is that we extend theoretical results to an arbitrary target measure μ in a non-linear setting and we find a duality formulation for Kantorovitch problem and especially in the linear framework we find an implementable numerical scheme based on SGD as well as an explicit solution based on OT for the case where μ a probability measure and $G(\gamma) = \xi + \gamma$.

1.2.1 Weak hedging problem

This question named *Quantile hedging* see [36, 14] or in general *PnL hedging* is not new and has been studied before in various settings. In this case, the controlled process is a portfolio of financial assets. The key point is that the value of this portfolio at time T is not supposed to perfectly replicate a given contingent claim. In the *quantile hedging problem*, the agent will seek to replicate the contingent claim with only a 95% (say) probability of success. On a theoretical point of view, the problems of perfect replication and partial replication lead to quite different stochastic control problem. The first one has been generally recognized as a case of stochastic target

problem see e.g. [65, 66]. The second one has been treated as a weak stochastic target problem and needs extra work to be solved, see e.g. [14]. In particular, it leads to a degenerate PDE representing its value function which is quite involved to work with and to approximate numerically, see e.g. [5]. A natural extension to the *quantile hedging problem* is the PnL matching problem introduced in [15]. In this second part of the thesis, we consider a finite number of quantile constraint, representing a given target PnL: in other words, the targeted law for the PnL is discrete and finite. The next step would be naturally to impose any possible law as target PnL. Having in mind financial applications, we have called this more generic problem the *weak hedging problem*.

Notation:

- If $(\Omega, \mathcal{F}, \mathbb{F}, \mathbb{P})$ is a filtered probability space and E a normed space, we define $\mathscr{H}^2(\mathbb{F}, \mathbb{P}; E)$ as the set of progressively measurable processes $U : \Omega \times [0,T] \to E$ with $T > 0$ fixed satisfying

$$\mathbb{E}\left[\int_0^T |U_t|^2 \mathrm{d}t\right] < +\infty$$

  and $\mathscr{S}^2(\mathbb{F}, \mathbb{P}; E)$) as the set of processes $U : \Omega \times [0,T] \to E$ continuous and adapted s.t.

$$\mathbb{E}\left[\sup_{t\in[0,T]} |U_t|^2 \mathrm{d}t\right] < +\infty.$$

- For $(\Omega, \mathcal{F}, \mathbb{P})$ a probability space, we denote $\mathcal{N}_{\mathbb{P}}$ the set of negligible sets, namely

$$\mathcal{N}_{\mathbb{P}} := \{A \in \mathcal{F} \,|\, \mathbb{P}(A) = 0\}.$$

- Given a measurable space $(E, \mathcal{E})$, the set of positive measures on E (resp. the subset probability measures) is denoted $\mathscr{M}_+(E)$ (resp. $\mathcal{P}(E)$). For $p \geqslant 1$, we consider

$$\mathcal{P}_p(\mathbb{R}) = \left\{\nu \in \mathcal{P}(\mathbb{R}) \,\middle|\, \int |x|^p \nu(\mathrm{d}x) < +\infty\right\}.$$

Let $(\Omega, \mathcal{A}, \mathbb{P})$ be a complete probability space supporting a m-dimensional Brownian Motion, where m is a positive integer. We denote by $\mathbb{F} = (\mathcal{F}_t)_{t\geqslant 0}$ the natural $\mathbb{P}$-augmented filtration of W. In the sequel, we work with a finite time horizon $T > 0$. We consider the following class of controlled processes: for $y \in \mathbb{R}$ and $Z \in \mathscr{H}^2$,

$$Y_t^{y,Z} = y - \int_0^t \mathfrak{f}(s, Y_s, Z_s)\, \mathrm{d}s + \int_0^t Z_s \mathrm{d}W_s, \quad t \in [0,T], \tag{1.2.1}$$

where $(\mathfrak{f}(s,\cdot))_{s\in[0,T]}$ is a progressively measurable process taking values in $\mathbf{Lip}(\mathbb{R} \times \mathbb{R}^d, \mathbb{R})$, the set of Lipschitz continuous function from $\mathbb{R} \times \mathbb{R}^d$ to $\mathbb{R}$, and such that

$\mathbb{E}\Big[\int_0^T |\mathfrak{f}(s,0,0)|^2 \mathrm{d}s\Big] < +\infty$. Moreover, for any $\xi \in \mathscr{L}^2(\mathcal{F}_T)$, there exists a unique $(\mathcal{Y}_0, \mathcal{Z}) \in \mathbb{R} \times \mathscr{H}^2$ such that $Y_T^{\mathcal{Y}_0,\mathcal{Z}} = \xi$. We then set $\mathcal{Y}_t := Y_T^{\mathcal{Y}_0[\xi],\mathcal{Z}[\xi]}$ for all $t \in [0,T]$, so that $(\mathcal{Y}, \mathcal{Z})$ is the solution to the BSDE with driver $\mathfrak{f}$ and terminal condition ξ, namely

$$\mathcal{Y}_t = \xi + \int_t^T \mathfrak{f}(s, \mathcal{Y}_s, \mathcal{Z}_s)\mathrm{d}s - \int_t^T \mathcal{Z}_s \mathrm{d}W_s \,, 0 \leqslant t \leqslant T \,,$$

also given a $(\mathcal{F}_T \otimes \mathcal{B}(\mathbb{R}), \mathcal{B}(\mathbb{R}))$-measurable random function $\Omega \times \mathbb{R} \ni (\omega, \gamma) \mapsto G(\omega, \gamma) \in \mathbb{R}$ such that $\gamma \mapsto G(\gamma)$ is non-decreasing and left-continuous. We now introduce the *weak hedging* problem. Denote, for $\mu \in \mathcal{P}(\mathbb{R})$,

$$\mathfrak{H}(\mu) := \Big\{ y \in \mathbb{R} \,\Big|\, \exists Z \in \mathscr{H}^2, \mathbb{P}(Y_T^{y,Z} \geqslant G(\gamma)) \geqslant F_\mu(\gamma), \forall \gamma \in \mathbb{R} \Big\}, \tag{1.2.2}$$

where we denote $F_\mu := \mu([\cdot, \infty])$ for a probability measure μ on $\mathbb{R}$. We now define the *weak hedging price* as

$$\mathcal{V}_{\mathrm{WH}}(\mu) := \inf \mathfrak{H}(\mu). \tag{1.2.3}$$

For later use, we denote $\bar{\Omega} := \Omega \times \mathbb{R}$ and $\bar{\mathcal{F}} := \mathcal{F} \otimes \mathcal{B}(\mathbb{R})$, with $\mathcal{B}(\mathbb{R})$ the Borel sigma-algebra of $\mathbb{R}$. We define the following projections

$$\mathrm{pr}_1 : \bar{\Omega} \ni (\omega, \gamma) \mapsto \omega \in \Omega, \text{ and } \mathrm{pr}_2 : \bar{\Omega} \ni (\omega, \gamma) \mapsto \gamma \in \mathbb{R}.$$

1.2.2 Monge and Kantorovitch representation

In the sequel, for two probability measures μ, ν on $\mathbb{R}$, we denote $\nu \succeq \mu$ as the *first order stochastic dominance*, i.e $\nu([\cdot, \infty)) := F_\nu \geqslant F_\mu =: \mu([\cdot, \infty))$ on $\mathbb{R}$. We define

$$\mathcal{K}_\mu := \{\nu \in \mathcal{P}(\mathbb{R}) | \nu \succeq \mu\} \quad \text{and} \quad \mathcal{K}_\mu^p := \mathcal{K}_\mu \cap \mathcal{P}_p(\mathbb{R}),\ p \geqslant 1 \,.$$

and

$$\mathcal{R}_\mu = \{\nu \in \mathcal{K}_\mu |\ \mathrm{supp}[\nu] \subset \mathrm{supp}[\mu]\} \quad \text{and} \quad \mathcal{R}_\mu^p := \mathcal{R}_\mu \cap \mathcal{P}_p(\mathbb{R}),\ p \geqslant 1 \,,$$

where $\mathrm{supp}[\nu]$ is the support of the measure μ.

1.2.2.1 Relaxed Monge problem (RM)

For Monge problem, we have the following equivalence

Proposition 1.2.1 *Let $\mu \in \mathcal{P}_4(\mathbb{R})$. We have the equivalent formulations*

$$\mathcal{V}_{\mathrm{WH}}(\mu) = \widehat{\mathcal{V}}_{\mathrm{RM}} := \inf_{\chi \in \mathcal{T}_+(\mu)} \mathcal{Y}_0[G(\chi)] \,, \tag{1.2.4}$$

where $\mathcal{T}_+(\mu) = \big\{\chi \in \mathcal{L}^4(\mathcal{F}_T) \,\big|\, \chi_\sharp \mathbb{P} \in \mathcal{K}_\mu\big\}$, and

$$\mathcal{V}_{\mathrm{WH}}(\mu) = \inf \tilde{\mathfrak{H}}(\mu), \ \textit{with } \tilde{\mathfrak{H}}(\mu) := \Big\{ y \in \mathbb{R} | \exists Z \in \mathscr{H}^2, \Psi(Y_T^{y,Z}) \sharp \mathbb{P} \in \mathcal{K}_\mu \Big\}, \tag{1.2.5}$$

1.2.2.2 Kantorovitch problem (KP)

We now assume

Assumption 1.2.1 *The probability distribution $\mu \in \mathcal{P}(\mathbb{R})$ has discrete and finite support, namely* $\mathrm{supp}[\mu] = \{\gamma_1, \dots, \gamma_d\}$ *with* $\gamma_1 < \cdots < \gamma_d$. *We denote* $q_\ell = F_\mu(\gamma_\ell)$ *and* $p_\ell := q_\ell - q_{\ell+1} = \mu(\{\gamma_\ell\})$, *for* $\ell \in \{1, \dots, d\}$ *with the convention* $q_{d+1} = 0$.

Lemma 1.2.1 *Under Assumption 1.2.1, the following holds*

$$\mathcal{V}_{\mathrm{WH}}(\mu) = \widehat{\mathcal{V}}_{\mathrm{RM}}(\mu) = \mathcal{V}_{\mathrm{RM}}(\mu) := \inf_{\chi \in \mathcal{T}_+^{\mathrm{r}}(\mu)} \mathcal{Y}_0[G(\chi)] \tag{1.2.6}$$

and where $\mathcal{T}_+^{\mathrm{r}}(\mu) = \{\chi \in \mathcal{L}^\infty(\mathcal{F}_T) \,|\, \chi_\sharp \mathbb{P} \in \mathcal{R}_\mu\}$.

We now introduce the Kantorovitch representation of the quantile hedging problem. We define

$$\mathcal{V}_{\mathrm{KP}}(\mu) := \inf_{\Pi \in C^{\mathrm{r}}(\mathbb{P}, \mu)} \mathcal{Y}_0 \left[\int G(\omega, \gamma) \rho^\Pi(\omega, \mathrm{d}\gamma) \right], \tag{1.2.7}$$

where ρ^Π is obtained from the disintegration of the measure Π.

1.2.3 Our contributions

Besides the previous representations, we also establish an equivalence between "Monge" problem $\mathcal{V}_{\mathrm{RM}}$ and "Kantorovitch" problem $\mathcal{V}_{\mathrm{KP}}$ i.e. $\mathcal{V}_{\mathrm{KP}} = \mathcal{V}_{\mathrm{RM}}$ in the original general setting as well as a duality result for "Kantorovich" problem $\mathcal{V}_{\mathrm{KP}}(\mu)$ in the linear setting where $\mathfrak{f}(s, y, z) = \mathfrak{a}_s y + \mathfrak{b}_s^\top z$ and μ with discrete and finite support, given by

$$\mathcal{V}_{\mathrm{KP}}(\mu) = \inf_{(Q_i)_{i=1}^{d+1} \in \mathfrak{Q}_T(\mu)} \mathbb{E}\left[\sum_{i=1}^d G(\gamma_i)(Q_i - Q_{i+1}) \right]. \tag{1.2.8}$$

where, for all $t \in [0, T]$,

$$\mathfrak{Q}_t(\mu) := \left\{ (Q_i)_{i=1}^{d+1} \in \mathscr{L}^2(\mathcal{F}_t) \,\middle|\, 1 = Q_1 \geqslant \cdots \geqslant Q_d \geqslant Q_{d+1} = 0 \text{ and } \mathbb{E}[Q_i] \geqslant q_i, 1 \leqslant i \leqslant d \right\} \tag{1.2.9}$$

To establish the equivalence between Monge and Kantorovitch representation of OT problem, we first prove the inequality $\mathcal{V}_{\mathrm{KP}} \leqslant \mathcal{V}_{\mathrm{RM}}$. Indeed, for $\chi \in \mathfrak{H}^r(\mu)$, it suffices to observe that

$$G(\chi) = \sum_{i=1}^d G(\gamma_i) \mathbf{1}_{\chi = \gamma_i} = \sum_{i=1}^d G(\gamma_i) \left(\mathbf{1}_{\chi \geqslant \gamma_i} - \mathbf{1}_{\chi \geqslant \gamma_{i+1}} \right),$$

and considering $Q_i := \mathbf{1}_{\chi \geqslant \gamma_i}$, which leads to $\mathcal{Y}_0[G(\chi)] \geqslant \mathcal{V}_{\mathrm{KP}}(\mu)$. For the converse inequality, we first construct a random variable $\mathfrak{U}^\epsilon$ independent of $\mathcal{F}_{t-\epsilon}$ for any $\epsilon > 0$,

for example $\mathfrak{U}^\epsilon = N(\frac{W_T - W_{T-\epsilon}}{\sqrt{\epsilon}})$. Then fixing $\eta > 0$ and by definition there exists $(Q_i^\eta)_{i=1}^{d+1} \in \mathfrak{Q}_T(\mu)$, denoting $P_i^\eta := Q_i^\eta - Q_{i+1}^\eta$, such that

$$\mathcal{V}_{\mathrm{KP}}(\mu) \geqslant \mathcal{Y}_0\left[\sum_{i=1}^d G(\gamma_i)(Q_i^\eta - Q_{i+1}^\eta)\right] - \eta =: \mathcal{Y}_0\left[\sum_{i=1}^d G(\gamma_i)P_i^\eta\right] - \eta, \tag{1.2.10}$$

Let $\epsilon > 0$ and we then denote

$$Q_i^{\eta,\epsilon} := \mathbb{E}[Q_i^\eta \,|\, \mathcal{F}_{T-\epsilon}], \quad 1 \leqslant i \leqslant d+1, \text{ and} \tag{1.2.11}$$
$$P_i^{\eta,\epsilon} := Q_i^{\eta,\epsilon} - Q_{i+1}^{\eta,\epsilon} = \mathbb{E}[P_i^\eta \,|\, \mathcal{F}_{T-\epsilon}], \quad 1 \leqslant i \leqslant d. \tag{1.2.12}$$

Introducing the $\mathcal{F}_T$-measurable random variable $\chi^{\eta,\epsilon} = \sum_{i=1}^d \gamma_i \mathbf{1}_{\{Q_i^{\eta,\epsilon} \geqslant \mathfrak{U}^\epsilon > Q_{i+1}^{\eta,\epsilon}\}}$, it then suffices to prove that there exists $\omega(\eta,\epsilon) \xrightarrow{\epsilon \longrightarrow 0} 0$ such that

$$\mathcal{Y}_0\left[\sum_{i=1}^d G(\gamma_i)P_i^\eta\right] \geqslant \mathcal{Y}_0\left[G(\chi^{\eta,\epsilon})\right] - w(\eta,\epsilon) \geqslant \mathcal{V}_{\mathrm{RM}}(\mu) - o(\epsilon) \tag{1.2.13}$$

to conclude. Along with control of estimates on the solution of non-linear BSDE with terminal condition $\xi \in \mathcal{L}^2(\mathcal{F}_{T-\epsilon})$ at terminal time $T - \epsilon$. Combining those two points, we prove the above (1.2.13) and make the conclusion that $\mathcal{V}_{\mathrm{KP}}(\mu) \geqslant \mathcal{V}_{\mathrm{RM}}(\mu) - w(\eta,\epsilon) - \eta$, i.e. $\mathcal{V}_{\mathrm{KP}} \geqslant \mathcal{V}_{\mathrm{RM}}$.

In the following, we establish the duality between $\mathcal{V}_{\mathrm{KP}}$ and $\mathcal{V}_{\mathrm{DP}}$, given by

$$\mathcal{V}_{\mathrm{DP}}(\mu) := \sup_{(X,\Phi)\in\mathfrak{P}_H}\left(\mathbb{E}[X] + \sum_{i=1}^d \Phi_i\mu(\{\gamma_i\})\right), \tag{1.2.14}$$

where

$$\mathfrak{P}_{H,\mu} := \left\{(X,\Phi) \in \mathscr{L}^2(\mathcal{F}_T) \times \Delta_+^d \,\middle|\, H(\gamma_i) \geqslant X + \Phi_i, 1 \leqslant i \leqslant d, \mathbb{P}-\text{a.s.}\right\}. \tag{1.2.15}$$

with $\Delta_+^d := \left\{x \in \mathbb{R}^d | 0 \leqslant x_1 \leqslant \cdots \leqslant x_d\right\}$. We prove the inequality $\mathcal{V}_{\mathrm{DP}} \leqslant \mathcal{V}_{\mathrm{KP}}$ by writing KP problem as the following

$$\inf_{H\in C^r(\mathbb{P},\mu)} \int H(\omega,\gamma)\Pi(\mathrm{d}\omega,\mathrm{d}\gamma),$$

where $C^{\mathrm{r}}(\mathbb{P},\mu) := \left\{\Pi \in \mathcal{P}(\bar{\Omega}) \,\middle|\, (\mathrm{pr}_1)_\sharp\Pi = \mathbb{P}, (\mathrm{pr}_2)_\sharp\Pi \in \mathcal{R}_\mu\right\}$, and from which we deduce that for $\Pi \in \mathcal{C}^r(\mathbb{P},\mu)$ and $(X,\Phi) \in \mathfrak{P}_{H,\mu}$, we have

$$\int H(\omega,\gamma)\Pi(\mathrm{d}\omega,\mathrm{d}\gamma) \geqslant \mathbb{E}[X] + \sum_{i=1}^d \Phi_i\mu(\{\gamma_i\}).$$

For the converse inequality, we develop $\mathcal{V}_{\mathrm{DP}}$ into Fenchel transform,

$$\begin{aligned}\mathcal{V}_{\mathrm{DP}}(\mu) &= \mathbb{E}[H(\gamma_1)] + \mathfrak{V}(p_2,\ldots,p_d)\\ &= \mathbb{E}[H(\gamma_1)] + \mathfrak{W}(q_2,\ldots,q_d),\end{aligned}$$

where

$$\mathfrak{V}(p) = \sup_{\zeta \in \Delta_+^{d-1}} \left(\left(\sum_{i=1}^{d-1} \zeta_i p_{i+1} \right) - \mathbb{E}\Big[\max_{1 \leqslant i \leqslant d-1} \big(\zeta_i - \tilde{H}(\gamma_{i+1})\big)_+ \Big] \right), \tag{1.2.16}$$

$$\mathfrak{W}(q) = \sup_{\theta \in \mathbb{R}_+^{d-1}} \sum_{j=1}^{d-1} \theta_j q_{j+1} - \mathbb{E}\left[\max_{1 \leqslant i \leqslant d-1} \left(\sum_{j=1}^{i} \theta_j - \tilde{H}(\gamma_{i+1}) \right)_+ \right]. \tag{1.2.17}$$

Then we prove that the function defined as

$$w(\omega, \theta) := \sum_{j=1}^{d-1} \theta_j q_{j+1} - \mathbb{E}\left[\max_{1 \leqslant i \leqslant d-1} \left(\sum_{j=1}^{i} \theta_j - \tilde{H}(\omega, \gamma_{i+1}) \right)_+ \right],$$

is continuous, concave on $\mathbb{R}_+^{d-1}$ and $\lim_{|\theta| \to \infty} w(\theta) = -\infty$. This allows us to deduce an existence of $\theta^\star \in \mathbb{R}_+^{d-1}$ such that $\sup_{\mathbb{R}_+^{d-1}} w(\theta) = w(\theta^\star) = \mathfrak{W}(q)$. To have a further development on $w(\theta)$, we define for $1 \leqslant i \leqslant d-1$, $A_i(\theta^{(i)}) := \big\{\Phi_i(\theta^{(i)}) > 0\big\} = \big\{\theta_i + \tilde{H}(\gamma_i) - \tilde{H}(\gamma_{i+1}) + \Phi_{i+1}(\theta^{(i+1)}) > 0\big\}$ and $A_d(\varnothing) := \varnothing$ by convention.

And for $2 \leqslant i \leqslant d+1$ and $\theta \in \mathbb{R}^{d-1}$, we define $Q_i(\theta) := \mathbf{1}_{\bigcap_{k=1}^{i-1} A_k(\theta^{(k)})}$ and $Q_1(\theta) := 1$. We also set, for $1 \leqslant i \leqslant d$ and $\theta \in \mathbb{R}^{d-1}$, $P_i(\theta) := Q_i(\theta) - Q_{i+1}(\theta) = Q_i(\theta)(1 - \mathbf{1}_{A_i(\theta^{(i)})}) = Q_i(\theta)\mathbf{1}_{A_i(\theta^{(i)})^c}$.

Then for $\theta \in \mathbb{R}_+^{d-1}$, we prove that

$$w(\theta) = \sum_{j=1}^{d-1} \theta_j \left(q_{j+1} - \mathbb{E}[Q_{j+1}(\theta)]\right) + \sum_{j=2}^{d} \mathbb{E}\big[\tilde{H}(\gamma_j) P_j(\theta)\big].$$

and more importantly that its sub-differential $\partial w(\theta) \subset \Pi_{i=1}^{d-1} [\partial_{i,+} w(\theta), \partial_{i,-} w(\theta)]$, with for all $1 \leqslant i \leqslant d-1$, $\partial_{i,-} w(\theta)$ (resp. $\partial_{i,+} w(\theta)$) is the left (resp. right) partial derivative of w at θ,

$$\begin{aligned} \partial_{i,-} w(\theta) &= (+\infty)\mathbf{1}_{\theta_i = 0} + \left(q_{i+1} - \mathbb{E}[Q_{i+1}(\theta)]\right), \\ \partial_{i,+} w(\theta) &= q_{i+1} - \mathbb{E}\big[Q_{i+1}^+(\theta)\big], \end{aligned}$$

with $Q_{i+1}^+(\theta) := Q_i(\theta)\mathbf{1}_{\left\{\theta_i + \tilde{H}(\gamma_i) - \tilde{H}(\gamma_{i+1}) + \Phi_{i+1}(\theta^{(i+1)}) \geqslant 0\right\}}$. Moreover, since that $0 \in \partial_w(\theta^\star)$, we deduce that for $1 \leqslant j \leqslant d-1$,

$$q_{j+1} - \mathbb{E}[Q_{j+1}(\theta^\star)] \geqslant 0 \geqslant q_{j+1} - \mathbb{E}\Big[Q_{j+1}^+(\theta^\star)\Big].$$

With the above conditions along with different discussion on the frontiers of $\mathbb{R}_+^{d-1}$, we prove that $\mathcal{V}_{\mathrm{DP}} \geqslant \mathcal{V}_{\mathrm{KP}}$ in some cases: one ($d = 2$) and two constraints ($d = 3$) case. For the general case where $d > 3$, we conjecture that it still hold on.

Apart from the above dual characterization, we also obtain an explicit representation for μ a general probability measure via optimal transportation approach. We assume that $G(\gamma) := \xi + \gamma$, where ξ a fixed random payoff. In this case, we recall from (1.2.4) that

$$\widehat{\mathcal{V}}_{\mathrm{RM}}(\mu) = \mathbb{E}[\Gamma_T \xi] + \inf_{\chi \in \mathcal{T}_+(\mu)} \mathbb{E}[\Gamma_T \chi] \ ,$$

and define a more restricted problem

$$\mathcal{V}_{\mathrm{OT}}(\mu) := \inf_{\chi \in \mathcal{T}_\mu} \mathbb{E}[\Gamma_T(\xi + \chi)], \tag{1.2.18}$$

where $\mathcal{T}(\mu) = \{\chi \in \mathcal{L}^2(\mathcal{F}_T) \,|\, \chi_\sharp \mathbb{P} \in \mathcal{K}_\mu\}$.

Theorem 1.2.1 *Suppose that the law of Γ_T is absolutely continuous with respect to the Lebesgue measure, for $\mu \in \mathcal{P}_4$, we have*

$$\mathcal{V}_{\mathrm{OT}}(\mu) = \mathbb{E}[\Gamma_T \xi] - \frac{1}{2}\mathbb{E}\Big[(\Gamma_T)^2\Big] - \frac{1}{2}\int x^2 \mu(\mathrm{d}x) + \frac{1}{2}\mathcal{W}_2^2(\mathcal{L}(-\Gamma_T), \mu). \tag{1.2.19}$$

In addition, $\widehat{\mathcal{V}}_{\mathrm{RM}}(\mu) = \mathcal{V}_{\mathrm{OT}}(\mu)$ and there exists $\chi^\star \in \mathcal{T}_\mu$ such that

$$\mathcal{V}_{\mathrm{OT}}(\mu) = \mathbb{E}[\Gamma_T(\xi + \chi^\star)],$$

which writes explicitely $\chi^\star = N_\mu^{-1} \circ N_{\mathcal{L}(-\Gamma_T)}(-\Gamma_T)$. Here, N_μ stands for the c.d.f. of the law μ and N_μ^{-1} its generalized inverse.

1.2.4 Numerical results

Finally, we now turn to numerical experiments by applying previous results in the linear framework, especially for the Black & Scholes model, already studied in [36, 5]. We recall that in the linear setting, the process Γ is solution to

$$\Gamma_t = 1 + \int_0^t \Gamma_s \alpha(s, X_s)\mathrm{d}s + \int_0^t \Gamma_s \beta(s, X_s)^\top \mathrm{d}W_s, \quad 0 \leqslant t \leqslant T. \tag{1.2.20}$$

Example 1.2.1 (Black & Scholes Model) *The process X satisfies*

$$X_t = X_0 + \int_0^t \hat{b} X_s \mathrm{d}s + \int_0^t \sigma X_s \,\mathrm{d}W_s\,,$$

with $\hat{b} \in \mathbb{R}, \sigma > 0$ and $X_0 > 0$. The function f is given by:

$$f(t, x, y, z) = -ry - \frac{\hat{b} - r}{\sigma} z =: -ry - \lambda z, \tag{1.2.21}$$

where $r \geqslant 0$ the interest rate, and $\lambda := \frac{\hat{b}-r}{\sigma}$ the risk premium. The Radon-Nikodym derivative defined in (1.2.20) is thus:

$$\Gamma_T = \frac{\mathrm{d}\mathbb{Q}}{\mathrm{d}\mathbb{P}}\Big|_T = \exp\Big(\frac{r - \hat{b}}{\sigma} W_T - \frac{1}{2}\frac{(r - \hat{b})^2}{\sigma^2} T\Big).$$

One constraint We consider a target measure $\mu = (1 - p)\delta_0 + p\delta_\gamma$. We have tested numerical results by SGD algorithm against OT-Approach, and results are reported in Table 1.1. The SGD algorithm is applied to function $\mathfrak{W}$ defined in (1.2.17). We note that the number of simulations of trajectories of brownian motion is $N = 100000$, European claim payoff function $g(x) = (x - K)+$ with $K = 100$. Concerning the dynamics of X, we take $X_0 = 100$, $r = 0, \hat{b} = 0.1, \sigma = 0.2$, and time

Probability p	$p = 0.01$	$p = 0.1$	$p = 0.5$	$p = 0.9$	$p = 0.99$
Computation time of SGD	17.89s	18.14s	19.17s	17.88s	18.93s
SGD algorithm	7.99	8.36	11.08	15.72	17.81
Optimal transport	7.94	8.36	11.15	15.78	17.78

Table 1.1: Numerics of measure $\mu = (1-p)\delta_0 + p\delta_\gamma$ with different probabilities with SGD algorithm and OT-Approach.

Quantiles p_1, p_2	γ_1, γ_2	SGD	OT	Computation time of SGD
(0.3,0.5)	(10,20)	17.38	17.48	30.66s
(0.05,0.05)		8.48	8.41	30.31s
(0.05,0.9)		24.41	24.44	29.46s
(0.3,0.5)	(10,100)	42.07	42.19	32.47s
(0.05,0.05)		9.57	9.62	31.40s
(0.05,0.9)		87.89	87.57	30.68s

Table 1.2: Numerics of measure $\mu = (1-p_1-p_2)\delta_0 + p_1\delta_{\gamma_1} + p_2\delta_{\gamma_2}$ with different probabilities and quantiles with SGD algorithm and OT-Approach.

horizon $T = 1.0$. We also note that the solution of OT-Approach is obtained by computing (1.2.1) in Theorem 1.2.1.

One can see in Table 1.1 that SGD algorithm performs very well compared to OT-Approach and we also plot the learning curves of quantile $\theta^\star$ during the SGD algorithm, see Figure 1.12, we observe that they all converge and verify the convex constraint.

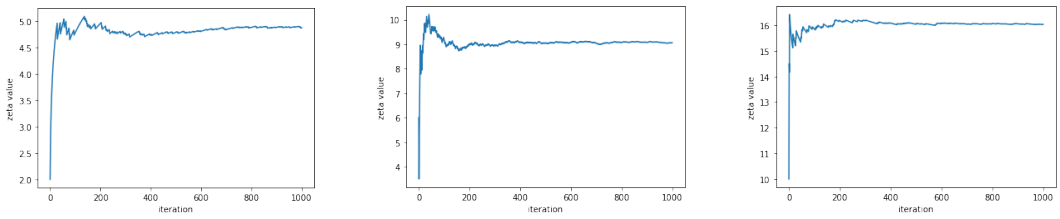

(a) $p = 0.1$ (b) $p = 0.5$ (c) $p = 0.9$

Figure 1.12: Numerical convergence of $\theta^\star$ for different values of quantiles $p = 0.1, 0.5, 0.9$ and $\gamma = 10$ by SGD algorithm.

Two constraints We consider in this part a discrete measure with two constraints $\mu = (1-p_1-p_2)\delta_0 + p_1\delta_{\gamma_1} + p_2\delta_{\gamma_2}$. The numerical results are reported in the Table 1.2. Again we observe that the numerical solutions by SGD perform well in comparison to the OT-Approach.

Quantile hedging In this part, we want to validate our numerical methods by comparison with some theoretical quantile hedging results see e.g. [5, 36, 11]. In this setting, it presents two following constraints: $\mathbb{P}(Y_T \geqslant 0) = 1$ and $\mathbb{P}(Y_T \geqslant$

$g(X_T)) = p$. We consider a set of probabilites $p := \{\frac{i}{100}, 0 \leqslant i \leqslant 100\}$. We have tested our numerical scheme for classical European call and put option claims against theoretical price see e.g. [36]. We first observe that our numerical scheme is able to reproduce correctly the true solution of call option claim, even for extreme values of p, as reported in Figure 1.13. However we note that SGD algorithm does not work pretty well for put option as reported in Figure 1.13.

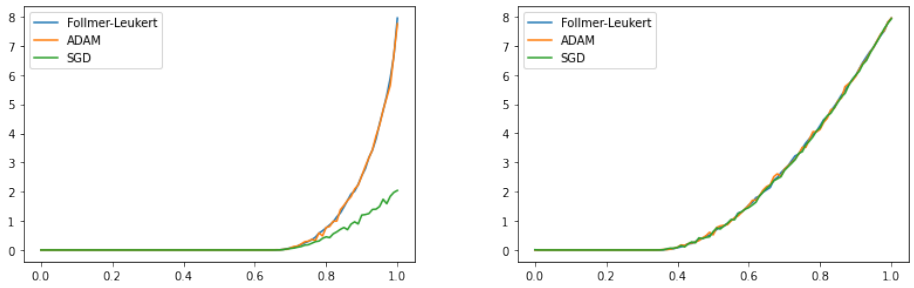

(a) Put option $(K - S)_+$ (b) Call option $(S - K)_+$

Figure 1.13: Comparison of the three methods: SGD algorithm, ADAM optimizer & Exact solution [5, 36] for put and call options, with parameters $X_0 = 100$, $r = 0$, $\sigma = 0.2$ and $\hat{b} = 0.1$, strike $K = 100$, terminal time $T = 1$.

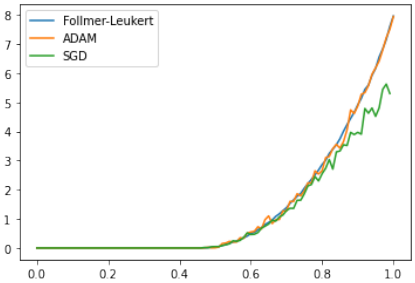

Figure 1.14: Comparison of the three methods: SGD algorithm, ADAM optimizer & Exact solution [5, 36] for put option with $\hat{b} = r = 0$, other parameters are same as above.

We think it is largely because of the trapping in a saddle point: this phenomenon suggests us using an adaptive gradient descent method such as ADAM optimizer [57]. Concerning the ADAM optimiser, we tested two cases mentioned in the above: $\hat{b} = 0.1, r = 0$ and $\hat{b} = r = 0$, see in the Figure 1.13 and 1.14, note that we choose parameters $\beta_1 = 0.9, \beta_2 = 0.999$ as well as a batchsize $= 256$. We observe that Adam optimizer caputres quite well the extreme quantiles than vanilla SGD.

Part I

Schemes for solving singular FBSDEs

Chapter 2

Numerical approximation of singular FBSDEs

The content of this chapter is from an article in collaboration with Jean-François Chassagneux [26]. Published in *Journal of Computational Physics*.

Contents

2.1 Introduction

In this work, we study the approximation of a class of singular fully coupled Forward Backward Stochastic Differential Equations (FBSDE). Let $(\Omega, \mathcal{F}, \mathbb{P})$ be a stochastic basis supporting a d-dimensional Brownian motion W and $T > 0$ a terminal time.

We denote by $(\mathcal{F}_t)_{t\geqslant 0}$ the filtration generated by the Brownian motion (augmented and completed). The singular FBSDE system, with solution $(P_t, E_t, Y_t, Z_t)_{0\leqslant t\leqslant T}$, has the following form:

$$\begin{cases} dP_t &= b(P_t)dt + \sigma(P_t)\mathrm{d}W_t \\ dE_t &= \mu(Y_t, P_t)\mathrm{d}t \\ dY_t &= Z_t \cdot \mathrm{d}W_t \end{cases} \tag{2.1.1}$$

The function $b : \mathbb{R}^d \to \mathbb{R}^d$, $\sigma : \mathbb{R}^d \to \mathcal{M}_d$[1], where $\mathcal{M}_d$ is the set of $d\times d$ matrices on $\mathbb{R}$, and $\mu : \mathbb{R}\times\mathbb{R}^d \to \mathbb{R}$ are Lipschitz-continous. These equations have been introduced in [20] as models for carbon emission market. They can model, more generally, cap-and-trade scheme used by government to limit the emission of certain pollutant. In these models, Y is the price of a pollution permit, E is the cumulative emission of the pollutant and P represents some state variables influencing the emission (demand, energy prices etc.). The coefficient μ is naturally decreasing in the y-variable. The initial condition for (P, E) in (2.1.1) is given by some $(P_0, E_0) = (p, e) \in \mathbb{R}^d \times \mathbb{R}$. The terminal condition is given by $\phi(E_T, P_T)$, where $\phi : \mathbb{R}\times\mathbb{R}^d \to \mathbb{R}$ is a measurable function, non-decreasing in its E-variable and Lipschitz continuous in the P-variable. In its simplest form, it is given typically by:

$$e \mapsto \phi(e) = \mathbf{1}_{\{e>\Lambda\}}\,,\ \Lambda > 0. \tag{2.1.2}$$

The constant Λ appears as a cap on emissions set by the regulator. The shape given in (2.1.2) translates the fact that a penalty (here set to one) is paid if the emission are above the regulatory cap at T.
We observe that (2.1.1) has a forward one dimensional E-component of bounded variation and a backward component with an irregular terminal condition (2.1.2). This renders the mathematical analysis of the FBSDE system difficult. Nevertheless, the well-posedness and main features of (2.1.1) have been thoroughly studied in [19], see also Section 2.2.1 below. Notably, the authors of [19] prove existence and uniqueness of the solution to (2.1.1) but show at the same time that the terminal condition can only be attained in the following weak sense:

$$\mathbf{1}_{(\Lambda,+\infty)}(E_T) \leqslant Y_T \leqslant \mathbf{1}_{[\Lambda,+\infty)}(E_T)\,, \tag{2.1.3}$$

using to simplify the presentation at this point the terminal function (2.1.2). Their study is based on the celebrated markovian representation of Y as

$$Y_t = \mathcal{V}(t, P_t, E_t), \quad \text{for } \ t < T, \tag{2.1.4}$$

and the careful analysis of the property of $\mathcal{V}$, where $\mathcal{V}$, known as the *decoupling fields*, is solution to a quasilinear PDE. As mentioned in [19], the FBSDE system can be seen as a random perturbation of a scalar conservation law. The behavior at the terminal time is reminiscent of shocks appearing in conservation law. Let us

[1] To alleviate the notation, we assume that P and W have the same dimension and the coefficient functions of P are time-homogeneous. Note however that σ will not be assumed to be uniformly elliptic, which allows to consider a dimension of P as time and to embed the case of different dimension for P and W in our framework.

note that the markovian representation breaks down at T as indicated by (2.1.3). Moreover, the function $\mathcal{V}$ is only locally Lipschitz-continuous on $[0,T)$:

$$|\mathcal{V}(t,p,e) - \mathcal{V}(t,p',e')| \leqslant c_1|p-p'| + \frac{1}{c_2(T-t)}|e-e'|\,, \tag{2.1.5}$$

for some constants $c_1, c_2 > 0$, $(p,p',e,e') \in \mathbb{R}^d \times \mathbb{R}^d \times \mathbb{R} \times \mathbb{R}$.

The application to carbon market is also a key motivation for our numerical study here: efficient numerical simulation of the price Y would allow to calibrate properly the model to market data and validate its efficiency in practice. A first approach for the numerical approximation of Y or $\mathcal{V}$ would be to use PDE methods, and this is suggested in [47]. However, in the economic applications we have in mind, the dimensionality of the process P prevents generally the use of these methods. In order to work on problems in moderate dimension, say 5 to 10, some probabilistic methods could be introduced. Probabilistic schemes have already been designed for FBSDEs and one could be tempted (as we were) to use the already known methods to tackle the numerical approximation of (2.1.1). In [4], the authors use a Picard Iteration method to decouple the FBSDE system and then obtain an approximation of $\mathcal{V}$ by performing iteratively linear regression. Unfortunately, this method has only been shown to be convergent in the case of Lipschitz coefficient and for small coupling between the forward and backward part (or equivalently small time horizon), see [4] for details. Recently, machine learning methods have been considered for BSDEs approximation, especially for their applicability in very high-dimensional setting. In particular, [44] has analysed the *deep BSDE solver* introduced in [43] again in the setting of small coupling. In [33], a grid algorithm is introduced where the decoupling is obtained by a predictor: there, the time horizon or the coupling is arbitrary but the diffusion coefficient of the forward process must be uniformly elliptic. As observed, the FBSDE system under study is degenerate in the E-component and the terminal condition is not Lipschitz, so that none of the known methods for FBSDEs are proved to be convergent in the setting of (2.1.1). Moreover, the above methods fail, in practice, to approximate correctly the solution to (2.1.1). To empirically illustrate this fact, we consider the following toy model borrowed from [20]:

Example 2.1.1 (Linear model)

$$dP_t = \sigma \mathrm{d}W_t \tag{2.1.6}$$

$$dE_t = \left(\frac{1}{\sqrt{d}}\sum_{\ell=1}^{d} P_t^\ell - Y_t\right)\mathrm{d}t \tag{2.1.7}$$

$$dY_t = Z_t \cdot \mathrm{d}W_t \tag{2.1.8}$$

with terminal function given by (2.1.2) *and where* W *is a* d*-dimensional Brownian motion and* $\sigma > 0$.

By using a change of variable, this $d+1$ dimensional model can be reduced to a one dimension model. Indeed, from [20, Proposition 6], there exists $\nu \in C^{1,2}([0,T),\mathbb{R})$, solution to

$$\partial_t \nu - \nu\partial_\xi \nu + \frac{\sigma^2(T-t)^2}{2}\partial^2_{\xi\xi}\nu = 0 \quad \text{and} \quad \nu(T,\xi) = \phi(\xi)\,. \tag{2.1.9}$$

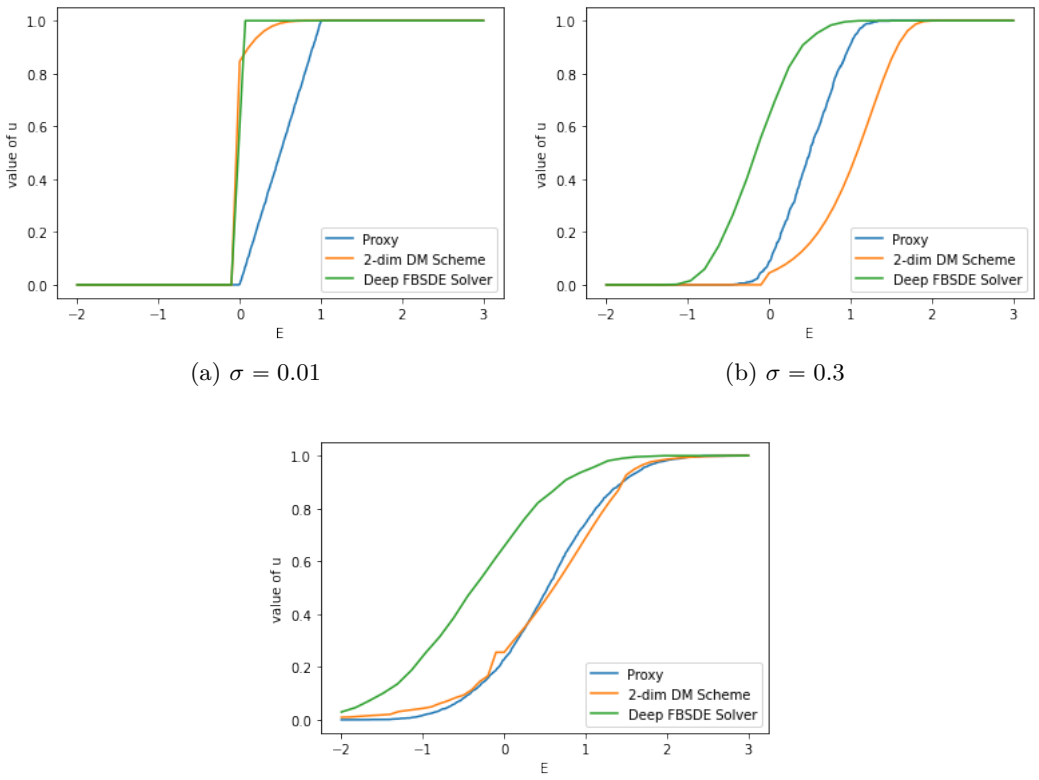

(a) $\sigma = 0.01$ (b) $\sigma = 0.3$

(c) $\sigma = 1.0$

Figure 2.1: Comparison of $e \mapsto \mathcal{V}(0,0,e)$ obtained by Deep FBSDE Solver and Delarue-Menozzi Scheme (DM Scheme) to the proxy, for different level of volatility. The methods fail to reproduce correctly the proxy.

By essentially applying Ito's formula (see the proof of [20, Proposition 7] for details on proving (2.1.9)), one obtains that $\mathcal{V}(t,p,e) = \nu(t, e + (T-t)\frac{1}{\sqrt{d}}\sum_{\ell=1}^{d} p_\ell)$. This observation allows us to use efficient methods to solve (2.1.9) numerically and to compare them to numerical solutions obtained by "classical" FBSDE scheme. In particular, we use a probabilistic method studied in [10] using interacting particle system, a class of mean field SDE, to obtain a "proxy" for $e \mapsto \mathcal{V}(0,0,e)$, see also [9, 51].
Going back to the approximation of (2.1.6)-(2.1.7)-(2.1.8) by "classical" FBSDEs methods, we first note that, in [23, Chapter 4], the authors report an application of the Bender-Zhang scheme [4]. The main issue is then that the Picard iteration does not converge to a single limit. Next, we have tested the Delarue-Menozzi scheme [33] and the *deep FBSDE solver* [44] for different value of σ, the results are given in Figure 2.1.

Except maybe for the Delarue-Menozzi scheme in Figure 2.1c, the methods fail clearly to approximate the correct solution $\mathcal{V}(0,0,\cdot)$. The problem comes from the nonlinear transport part of the equation in this degenerate setting. Indeed, the methods seem unable to recover the correct weak entropy solution. This is particularly clear on Figure 2.1a, where the level of noise is extremely small and the correct

solution is almost the solution to the inviscid Burger's equation. This leads us to introduce a new method to approximate the FBSDE system (2.1.1).

As already mentioned, in the socio-economic applications, the dimension of the P-variable is generally large. On the contrary, the E-variable is constrained to be of dimension one. We note also that approximating the dynamics of the P-variable corresponds to approximating simply a diffusion process, which can be easily done. To take into account these key differences in the two variables, we follow a splitting approach to compute numerically the solution $\mathcal{V}$. On a discrete time grid, we iterate backward in time, a diffusion operator where the E-variable is fixed to capture the effect of the P-dynamics in (2.1.1), and a transport operator where the P variable is fixed to capture the effect of E-dynamics in (2.1.1). Our main theoretical result, see Theorem 2.2.2, proves that this scheme is convergent at a rate $\frac{1}{2}$ with respect to the time step. Our analysis is done under the minimal assumption used in [19] to obtain existence and uniqueness of the solution $\mathcal{V}$. One of the main difficulty encountered is therefore due to the gradient explosion at the end of the time interval (2.1.5).

Then, we propose various implementations of the splitting scheme. They have however a common structure: given a discrete transport operator, the diffusion part is computed by means of probabilistic methods. The overall scheme is a then a sequence of (non linear) regressions in the high dimensional space where lives the approximation of $\mathcal{V}$ with respect to the E-variable. In our numerical experiments, we consider approximations of the transport operator by conservative finite difference methods (Lax-Friedrichs scheme or Upwind scheme), see e.g. [60]. As we do not always have access to a proxy for the tested models, we introduce an alternative implementation of the splitting scheme to validate our numerical results. It combines a particle approximation of the transport operator with a tree based regression for the diffusion operator. We validate empirically both approaches on Example 2.1.1 for which we have a one dimensional proxy at hand. We then test models with no equivalent one-dimensional PDE but whose $d+1$ dimensional version can be reduced to 2-dimensional specification, see Section 2.3.3 for details. The tree-based algorithm is then used as a proxy as it is very efficient in low-dimension (we test dimension 4) for the models under consideration. When combining feedforward neural networks to compute the regression step and finite difference scheme for the transport step, we show that our splitting procedure can compute precisely and in reasonable amount of time the solutions of $10 + 1$ dimensional models.

The rest of this chapter is organised as follows. In Section 2.2, we first recall key properties of the theoretical solution. We then introduce the splitting approach and prove the convergence of the splitting scheme. In Section 2.3, we present a regression method for the splitting scheme at a theoretical level, which uses a grid approximation of the transport operator. We then introduce various implementation of the transport operator and a neural network approximation for the regression part. We finally present various numerical experiments to validate the efficiency of our method in practice.

Notation.

In the following we will use the following spaces

- For fixed $0 \leqslant a < b < +\infty$ and $I = [a, b]$ or $I = [a, b)$, $\mathcal{S}^{2,k}(I)$ is the set of $\mathbb{R}^k$-valued càdlàg[2] $\mathcal{F}_t$-adapted processes Y, s.t.

$$\|Y\|^2_{\mathcal{S}^2} := \mathbb{E}\left[\sup_{t\in I} |Y_t|^2\right] < \infty.$$

  Note that we may omit the dimension and the terminal date in the norm notation as this will be clear from the context. $\mathcal{S}^{2,k}_{\mathrm{c}}(I)$ is the subspace of processes with continuous sample paths.

- For fixed $0 \leqslant a < b < +\infty$, and $I = [a, b]$, we denote by $\mathcal{H}^{2,k}(I)$ the set of $\mathbb{R}^k$-valued progressively measurable processes Z, such that

$$\|Z\|^2_{\mathcal{H}^2} := \mathbb{E}\left[\int_I |Z_t|^2 dt\right] < \infty.$$

For $\varphi : \mathbb{R}^d \times \mathbb{R} \to \mathbb{R}$, measurable and non-decreasing in its second variable, the functions φ_- and φ_+ are the left and right continuous versions, respectively defined, for $(p, e) \in \mathbb{R}^d \times \mathbb{R}$, by,

$$\begin{aligned} \varphi_-(p, e) &= \sup_{e'<e} \varphi(p, e') \\ \varphi_+(p, e) &= \inf_{e'>e} \varphi(p, e'). \end{aligned} \tag{2.1.10}$$

Moreover, we denote by $\|\cdot\|_\infty$ the essential supremum:

$$\|\varphi\|_\infty = \mathrm{esssup}_{(p,e)\in\mathbb{R}^d\times\mathbb{R}} |\varphi(p, e)| .$$

2.2 A splitting scheme

In this section, we introduce a theoretical splitting scheme to compute the solution of the singular FBSDEs. This scheme consists into iterating a "diffusion step" and a "transport step" on a discrete time grid

$$\pi := \{0 =: t_0 < \cdots < t_n < \cdots < t_N := T\},$$

where N is a positive integer. For latter use, we denote by $|\pi| := \max_{0\leqslant n<N}(t_{n+1} - t_n)$.

Before defining the splitting scheme for the system (2.1.1), we recall some key theoretical properties of the solution obtained in [19], with slight extensions for the case of P-dependent terminal condition in [22]. The rest of the section is then dedicated to the proof of an upper bound for the convergence rate of the splitting scheme in terms of $|\pi|$. This is our main theoretical result, given in Theorem 2.2.2. Numerical implementations are presented in the next section.

[2] French acronym for right continuous with left limits.

2.2.1 Well-posedness and properties of singular FBSDEs

We first introduce two classes of functions, that will be useful in the sequel. The terminal condition function for (2.1.1) will belong to the first one.

Definition 2.2.1 *Let $\mathcal{K}$ be the class of functions $\phi : \mathbb{R}^d \times \mathbb{R} \to [0,1]$ such that ϕ is L_ϕ-Lipschitz in the first variable for some $L_\phi > 0$ and non-decreasing in its second variable, namely*

$$|\phi(p,e) - \phi(p',e)| \leqslant L_\phi |p - p'| \quad \text{for all} \quad (p,p',e) \in \mathbb{R}^d \times \mathbb{R}^d \times \mathbb{R}\,, \tag{2.2.1}$$

$$\phi(p,e') \geqslant \phi(p,e) \quad \text{if} \quad e' \geqslant e\,, \tag{2.2.2}$$

and moreover satisfying,

$$\sup_e \phi(p,e) = 1 \quad \text{and} \quad \inf_e \phi(p,e) = 0 \quad \text{for all} \quad p \in \mathbb{R}^d\,. \tag{2.2.3}$$

Note that the bounds given in (2.2.3) are motivated by our main application, but up to a rescalling they can be arbitrary changed. We now introduce a class of admissible coefficient functions, for which the singular BSDE is well-posed, see Theorem 2.2.1 below. This class will be also useful to define the splitting scheme.
We consider three positive constants L, ℓ_1 and ℓ_2.

Definition 2.2.2 *Let $\mathcal{A}$ be the class of functions $B : \mathbb{R}^d \to \mathbb{R}^d$, $\Sigma : \mathbb{R}^d \to \mathcal{M}_d$, $F : \mathbb{R} \times \mathbb{R}^d \to \mathbb{R}$ which are L-Lipschitz continuous functions. Moreover, F is strictly decreasing in y and satisfies, for all $p \in \mathbb{R}^d$,*

$$\ell_1 |y - y'|^2 \leqslant (y - y')(F(y',p) - F(y,p)) \leqslant \ell_2 |y - y'|^2. \tag{2.2.4}$$

Standing assumptions: From now on, we assume that $(b, \sigma, \mu) \in \mathcal{A}$, recalling (2.1.1).

Theorem 2.2.1 (Proposition 2.10 in [19], Proposition 3.2 in [22]) *Let $\tau > 0$, $(B, \Sigma, F) \in \mathcal{A}$ and $\Phi \in \mathcal{K}$.*
Given any initial condition $(t_0, p, e) \in [0,\tau) \times \mathbb{R}^d \times \mathbb{R}$, there exists a unique progressively measurable 4-tuple of processes $(P_t^{t_0,p,e}, E_t^{t_0,p,e}, Y_t^{t_0,p,e}, Z_t^{t_0,p,e})_{t_0 \leqslant t \leqslant \tau} \in \mathcal{S}_c^{2,d}([t_0,\tau]) \times \mathcal{S}_c^{2,1}([t_0,\tau]) \times \mathcal{S}_c^{2,1}([t_0,\tau)) \times \mathcal{H}^{2,d}([t_0,\tau])$ satisfying the dynamics

$$\begin{aligned} \mathrm{d}P_t^{t_0,p,e} &= B(P_t^{t_0,p,e})\mathrm{d}t + \Sigma(P_t^{t_0,p,e})\mathrm{d}W_t, & P_{t_0}^{t_0,p,e} &= p \in \mathbb{R}^d, \\ \mathrm{d}E_t^{t_0,p,e} &= F(Y_t^{t_0,p,e}, P_t^{t_0,p,e})\mathrm{d}t, & E_{t_0}^{t_0,p,e} &= e \in \mathbb{R}, \\ \mathrm{d}Y_t^{t_0,p,e} &= Z_t^{t_0,p,e} \cdot \mathrm{d}W_t, \end{aligned} \tag{2.2.5}$$

and such that

$$\mathbb{P}\left[\Phi_-(P_\tau^{t_0,p,e}, E_\tau^{t_0,p,e}) \leqslant \lim_{t \uparrow \tau} Y_t^{t_0,p,e} \leqslant \Phi_+(P_\tau^{t_0,p,e}, E_\tau^{t_0,p,e})\right] = 1. \tag{2.2.6}$$

The unique decoupling field *defined by*

$$[0,\tau) \times \mathbb{R}^d \times \mathbb{R} \ni (t_0,p,e) \to w(t_0,p,e) = Y_{t_0}^{t_0,p,e} \in \mathbb{R}$$

is continuous and satisfies

1. *For any $t \in [0,\tau)$, the function $w(t,\cdot,\cdot)$ is $1/(l_1(\tau-t))$-Lipschitz continuous with respect to e,*
2. *For any $t \in [0,\tau)$, the function $w(t,\cdot,\cdot)$ is C-Lipschitz continuous with respect to p, where C is a constant depending on L, τ and L_ϕ only.*
3. *Given $(p,e) \in \mathbb{R}^d \times \mathbb{R}$, for any family $(p_t,e_t)_{0\leqslant t<\tau}$ converging to (p,e) as $t \uparrow \tau$, we have*
$$\Phi_-(p,e) \leqslant \liminf_{t\to\tau} w(t,p_t,e_t) \leqslant \limsup_{t\to\tau} w(t,p_t,e_t) \leqslant \Phi_+(p,e)\,. \tag{2.2.7}$$
4. *For any $t \in [0,\tau)$, the function $w(t,\cdot,\cdot) \in \mathcal{K}$.*

Remark 2.2.1 *From the previous Theorem, we observe that the function w is only locally Lipschitz continuous before τ, in the E-variable. This will need some special care in the convergence's proof of the splitting method. Nevertheless, one can also see this property as a regularization provided by the dynamics, since the terminal condition is discontinuous. This smoothing effect is due to the structural monotonicity assumptions made on the coefficient functions F and Ψ. In the example given in Figure 2.1a, this fact is clearly illustrated as w is close to be a solution to Burger's inviscid equation (seen backward in time) in the setting of a* rarefaction wave.

Using the previous result, we define the following operator associated to (2.1.1).

Definition 2.2.3 *We define the operator Θ by*
$$(0,\infty) \times \mathcal{K} \ni (h,\psi) \mapsto \Theta_h(\psi) = v(0,\cdot) \in \mathcal{K} \tag{2.2.8}$$
where v is the decoupling field given in Theorem 2.2.1 with parameters $\tau = h$, $B = b$, $\Sigma = \sigma$, $F = \mu$ and $\Phi = \psi$.

We also deduce from Theorem 2.2.1 that $(\Theta_t)_{0<t}$ is a semi-group of non-linear operators. In particular, we observe that $\mathcal{V}(0,\cdot) := \Theta_T(\phi) = \prod_{0\leqslant n<N} \Theta_{t_{n+1}-t_n}(\phi)$, recall (2.1.4).

The following result arises from the proof of the previous Theorem, see [22].

Corollary 2.2.1 (Approximation result) *Let $\tau > 0$, $(B,\Sigma,F) \in \mathcal{A}$ and $\Phi \in \mathcal{K}$. Let $(\phi^k)_{k\geqslant 0}$ be a sequence of smooth functions belonging to $\mathcal{K}$ and converging pointwise towards ϕ as k goes to $+\infty$. For $\epsilon > 0$, consider then $w^{\epsilon,k}$ the solution to:*
$$\partial_t u + F(u,p)\partial_e u + \mathcal{L}_p u + \frac{1}{2}\epsilon^2(\partial^2_{ee}u + \Delta_{pp}u) = 0 \quad \text{and} \quad u(\tau,\cdot) = \phi^k \tag{2.2.9}$$
where Δ_{pp} is the Laplacian with respect to p, and $\mathcal{L}_p$ is the operator
$$\mathcal{L}_p(\varphi)(t,p,e) = \partial_p\varphi(t,p,e)B(p) + \frac{1}{2}\mathrm{Tr}\left[A(p)\partial^2_{pp}\right](\varphi)(t,p,e), \tag{2.2.10}$$
with ∂_p denotes the Jacobian with respect to p, and $A = \Sigma\Sigma^\top$, where $\top$ is the transpose and ∂^2_{pp} is the matrix of second derivative operators. (For later use, we define $\mathcal{L}^\epsilon := \mathcal{L}_p + \frac{1}{2}\epsilon^2(\partial^2_{ee} + \Delta_{pp})$.)

Then the functions $w^{\epsilon,k}$ are $C^{1,2}$ (continuously differentiable in t and twice continuously differentiable in both p and e) and $\lim_{k\to\infty}\lim_{\epsilon\to 0} w^{\epsilon,k} = w$ where the convergence is locally uniform in $[0,\tau)\times\mathbb{R}^d\times\mathbb{R}$. Moreover, for all k,ϵ, $w^{k,\epsilon}(t,\cdot) \in \mathcal{K}$.

2.2.2 Scheme Definition

Let us first introduce the transport step where the diffusion part is frozen.

Definition 2.2.4 (Transport step) *We set*

$$(0,\infty)\times\mathcal{K}\ni(h,\psi)\mapsto\mathcal{T}_h(\psi)=\tilde{v}(0,\cdot)\in\mathcal{K}$$

where $\tilde{v}$ is the decoupling field defined in Theorem 2.2.1 with parameters $\tau=h$, $B=0$, $\Sigma=0$, $F=\mu$ and terminal condition $\Phi=\psi$.

In the definition above, $\tilde{v}(\cdot)$ is the unique entropy solution, see e.g. [18], to

$$\partial_t w+\partial_e(\mathfrak{M}(p,w))=0\,,\qquad\text{where }\mathfrak{M}(p,y)=\int_0^y\mu(\upsilon,p)\mathrm{d}\upsilon\,,\ 0\leqslant y\leqslant 1,\tag{2.2.11}$$

and $\tilde{v}(h,\cdot)=\psi$. We will use this fact in the numerical section.

We now introduce the diffusion step, where conversely, the E - process is frozen to its initial value.

Definition 2.2.5 (Diffusion step) *We set*

$$(0,\infty)\times\mathcal{K}\ni(h,\psi)\mapsto\mathcal{D}_h(\psi)=\bar{v}(0,\cdot)\in\mathcal{K}$$

where $\bar{v}(0,\cdot)$ is the decoupling in Theorem 2.2.1 with parameters $\tau=h$, $B=b$, $\Sigma=\sigma$, $F=0$ and terminal condition $\Phi=\psi$.

Observe that, for $t\in[0,h)$,

$$\bar{v}(t,p,e)=\mathbb{E}\Big[\psi(P_h^{t,p},e)\Big]\ \text{ and }\bar{v}(t,\cdot)\in\mathcal{K}\,.\tag{2.2.12}$$

with $P_h^{t,p}=P_h^{t,p,e}$ process at time h when starting from (t,p,e). We can now define the theoretical scheme on π by a backward induction.

Definition 2.2.6 (Theoretical splitting scheme) *We set*

$$(0,\infty)\times\mathcal{K}\ni(h,\psi)\mapsto\mathcal{S}_h(\psi):=\mathcal{T}_h\circ\mathcal{D}_h(\psi)\in\mathcal{K}.$$

For $n\leqslant N$, we denote by u_n^π the solution of the following backward induction on π:
- for $n=N$, set $u_N^\pi:=\phi$,
- for $n<N$, $u_n^\pi=\mathcal{S}_{t_{n+1}-t_n}(u_{n+1}^\pi)$.

The $(u_n^\pi)_{0\leqslant n\leqslant N}$ stands for the approximation of the decoupling field $\mathcal{V}(t,\cdot)$ for $t\in\pi$. Moreover, we observe, from the property of $\mathcal{T}$ and $\mathcal{D}$, that

$$u_n^\pi\in\mathcal{K},\ \text{for all }0\leqslant n\leqslant N.\tag{2.2.13}$$

2.2.3 Convergence analysis

Our main theoretical result concerning the splitting is the following

Theorem 2.2.2 *Under our* standing assumptions*, the following holds*

$$\int_{\mathbb{R}} |\mathcal{V}(0,p,e) - u_0^\pi(p,e)| \mathrm{d}e \leqslant CT(1+|p|^2)\sqrt{|\pi|}\,,$$

for a positive constant C.

The proof of the Theorem is postponed to the end of the section. It is classically based on the study of the scheme's stability and its truncation error.

2.2.3.1 Truncation error

We need to compare, for $\psi \in \mathcal{K}$, $\Theta_h(\psi)$ and $\mathcal{S}_h(\psi)$, $h > 0$, to assess the truncation error. As already mentioned, the true solution $\mathcal{V}$ has minimal locally Lipschitz regularity and it exhibits a gradient explosion in the E-variable near the terminal time T. In the proof below, we thus need to consider smoothed version of the decoupling fields introduced in the definition of Θ, $\mathcal{T}$, $\mathcal{D}$ and $\mathcal{S}$.
First of all, for a given $\psi \in \mathcal{K}$, we consider a smooth approximation sequence ψ^k as in Corollary 2.2.1. In particular, $v^{k,\epsilon}$ is the smooth approximation of the decoupling field $v = \Theta_h(\psi)$ in Definition 2.2.3 and the associated FBSDEs, for $0 \leqslant t \leqslant h$, $Y_t^{k,\epsilon} = v^{k,\epsilon}(t, E_t^{k,\epsilon}, P_t^\epsilon)$

$$P_t^\epsilon = p + \int_0^t b(P_s^\epsilon)\mathrm{d}s + \int_0^t \sigma(P_s^\epsilon)\mathrm{d}W_s + \epsilon W_t' \,, \tag{2.2.14}$$

$$E^{k,\epsilon} = e + \int_0^t \mu(Y_s^{k,\epsilon}, P_s^\epsilon)\mathrm{d}s + \epsilon B_t \,, \tag{2.2.15}$$

where (W', B) is a Brownian motion independent from W. Note that for the reader's convenience, we omit the dependence upon the starting point $(0,p,e)$ in the FBSDEs notation. The convergence of $v^{k,\epsilon}$ to v is given in Corollary 2.2.1.
We also need to consider a smooth version of $\mathcal{S}_h(\psi)$, that we define now:

1. for $0 \leqslant t \leqslant h$, set:

$$\bar{v}^{k,\epsilon}(t,p,e) = \mathbb{E}\Big[\psi^k(P_{h-t}^\epsilon, e)\Big] \tag{2.2.16}$$

2. then, $\tilde{v}^{k,\epsilon}$ is the decoupling of the following FBSDE, for all $p \in \mathbb{R}^d$, $e \in \mathbb{R}$:

$$\mathrm{d}\tilde{Y}_t^{k,\epsilon} = \tilde{Z}_t^{k,\epsilon}\mathrm{d}B_t \,, \tag{2.2.17}$$

$$\mathrm{d}\tilde{E}_t^{k,\epsilon} = \mu(\tilde{Y}_t^{k,\epsilon}, p)\mathrm{d}t + \epsilon \mathrm{d}B_t \tag{2.2.18}$$

with terminal condition $\tilde{Y}_h^{k,\epsilon} = \bar{v}^{k,\epsilon}(0,p,\tilde{E}_h^{k,\epsilon})$ and initial condition $\tilde{E}_0^{k,\epsilon} := e$. Observe that the P-variable is frozen in the above definition and that $\tilde{Y}_t^{k,\epsilon} = \tilde{v}^{k,\epsilon}(t,p,\tilde{E}_t^{k,\epsilon})$, for $0 \leqslant t \leqslant h$.

Before studying the truncation error, we give a strong local error control between the smooth approximations $v^{k,\epsilon}$ and $\tilde{v}^{k,\epsilon}$. Note that this local error control in $\sqrt{h}$ does not allow obtaining a converging global error control. We will however use it to obtain a better local control error in $L1$-norm, see the proof of Proposition 2.2.1.

Lemma 2.2.1 *Under our* standing assumptions *on* (μ, b, σ)*, the following holds, for* $p \in \mathbb{R}^d$*,* $h > 0$*,*

$$\sup_{t\in[0,h], e\in\mathbb{R}} |v^{k,\epsilon}(t,p,e) - \tilde{v}^{k,\epsilon}(t,p,e)| \leqslant C_{L_\psi}(1+|p|)\sqrt{h}.$$

Importantly, C_{L_ψ} *does not depend on* k *nor* ϵ*, however it depends on the Lipschiz constant of* ψ *in the* P*-variable.*

Proof. For $t \leqslant h$, let $V_t^{k,\epsilon} = \tilde{v}^{k,\epsilon}(t,p,\tilde{E}_t^{k,\epsilon}) - v^{k,\epsilon}(t,P_t^\epsilon,\tilde{E}_t^{k,\epsilon})$ with $(P_0^\epsilon,\tilde{E}_0^{k,\epsilon}) = (p,e)$. Applying Ito's formula, we compute, since $\tilde{Y}^{k,\epsilon}$ is a martingale, recall (2.2.17),

$$V_t^{k,\epsilon} = V_0^{k,\epsilon} - \int_0^t \Big(\partial_t v^{k,\epsilon}(s,P_s^\epsilon,\tilde{E}_s^{k,\epsilon}) + \mu(\tilde{Y}_s^{k,\epsilon},p)\partial_e v^{k,\epsilon}(s,P_s^\epsilon,\tilde{E}_s^{k,\epsilon}) + \mathcal{L}^\epsilon v^{k,\epsilon}(s,P_s^\epsilon,\tilde{E}_s^{k,\epsilon})\Big)\,\mathrm{d}s + M_t^{k,\epsilon},$$

where $M^{k,\epsilon}$ is a square-integrable martingale.
From the PDE (2.2.9) satisfied by $v^{k,\epsilon}$, we get

$$V_t^{k,\epsilon} = V_0^{k,\epsilon} - \int_0^t \Big(\mu(\tilde{Y}_s^{k,\epsilon},p) - \mu(v^{k,\epsilon}(s,P_s^\epsilon,\tilde{E}_s^{k,\epsilon}),P_s^\epsilon)\Big)\,\partial_e v^{k,\epsilon}(s,P_s^\epsilon,\tilde{E}_s^{k,\epsilon})\mathrm{d}s + M_t^{k,\epsilon}\,. \tag{2.2.19}$$

We set, for $0 \leqslant s \leqslant h$, $\delta P_s = P_s^\epsilon - p$ and we observe

$$\begin{aligned}\mu(v^{k,\epsilon}(s,P_s^\epsilon,\tilde{E}_s^{k,\epsilon}),P_s^\epsilon) - \mu(\tilde{Y}_s^{k,\epsilon},p) &= \mu(v^{k,\epsilon}(s,P_s^\epsilon,\tilde{E}_s^{k,\epsilon}),P_s^\epsilon) - \mu(\tilde{Y}_s^{k,\epsilon},P_s^\epsilon) + \mu(\tilde{Y}_s^{k,\epsilon},P_s^\epsilon) - \mu(\tilde{Y}_s^{k,\epsilon},p)\\ &= -c_s V_s^{k,\epsilon} + d_s\delta P_s,\end{aligned}$$

with

$$c_s := \frac{\mu(v^{k,\epsilon}(s,P_s^\epsilon,\tilde{E}_s^{k,\epsilon}),P_s^\epsilon) - \mu(\tilde{Y}_s^{k,\epsilon},P_s^\epsilon)}{v^{k,\epsilon}(s,P_s^\epsilon,\tilde{E}_s^{k,\epsilon}) - \tilde{Y}_s^{k,\epsilon}}\mathbf{1}_{\left\{v^{k,\epsilon}(s,P_s^\epsilon,\tilde{E}_s^{k,\epsilon})-\tilde{Y}_s^{k,\epsilon}\neq 0\right\}}, \tag{2.2.20}$$

$$d_s := \frac{\mu(\tilde{Y}_s^{k,\epsilon},P_s^\epsilon) - \mu(\tilde{Y}_s^{k,\epsilon},p)}{P_s^\epsilon - p}\mathbf{1}_{\{P_s^\epsilon\neq p\}}. \tag{2.2.21}$$

From Definition 2.2.2 and (2.2.4), we know that, for all $0 \leqslant s \leqslant h$,

$$c_s\mathbf{1}_{\{c_s\neq 0\}} \leqslant -\ell_1 < 0 \text{ and } |d_s| \leqslant L\,. \tag{2.2.22}$$

Then, (2.2.19) reads

$$V_t^{k,\epsilon} = V_0^{k,\epsilon} - \int_0^t c_s\mathbf{1}_{\{c_s\neq 0\}}V_s^{k,\epsilon}\partial_e v^{k,\epsilon}(s,P_s^\epsilon,\tilde{E}_s^{k,\epsilon})\mathrm{d}s + \int_0^t d_s\delta P_s\partial_e v^{k,\epsilon}(s,P_s^\epsilon,\tilde{E}_s^{k,\epsilon})\mathrm{d}s + M_t^{k,\epsilon} \tag{2.2.23}$$

We set, for $0 \leqslant t \leqslant h$, $\mathcal{E}_t = e^{\int_0^t c_s\mathbf{1}_{\{c_s\neq 0\}}\partial_e v^{k,\epsilon}(s,P_s^\epsilon,\tilde{E}_s^{k,\epsilon})\mathrm{d}s}$ and, we have

$$0 \leqslant \mathcal{E}_t \leqslant 1\,, \quad \text{for all } 0 \leqslant t \leqslant h\,, \tag{2.2.24}$$

since $v^{k,\epsilon} \in \mathcal{K}$, recall (2.2.22). We then compute

$$\mathcal{E}_t V_t^{k,\epsilon} = V_0^{k,\epsilon} + \int_0^t d_s \delta P_s \partial_e v^{k,\epsilon}(s, P_s^\epsilon, \tilde{E}_s^{k,\epsilon}) \mathcal{E}_s \mathrm{d}s + N_t^{k,\epsilon} \tag{2.2.25}$$

where $N^{k,\epsilon}$ is a square-integrable martingale. In particular, we get

$$|V_0^{k,\epsilon}| \leqslant \mathbb{E}\Big[|V_h^{k,\epsilon}| - \int_0^h \frac{|d_s|}{|c_s|} |\delta P_s| c_s \mathbf{1}_{\{c_s \neq 0\}} \partial_e v^{k,\epsilon}(s, P_s^\epsilon, \tilde{E}_s^{k,\epsilon}) \mathcal{E}_s \mathrm{d}s \Big] \tag{2.2.26}$$

recall (2.2.22). Observe that, for all $0 \leqslant s \leqslant h$,

$$\dot{\mathcal{E}}_s := c_s \mathbf{1}_{\{c_s \neq 0\}} \partial_e v^{k,\epsilon}(s, P_s^\epsilon, \tilde{E}_s^{k,\epsilon}) \mathcal{E}_s \tag{2.2.27}$$

where the dot denotes classicaly the time derivative. We thus deduce from (2.2.26)

$$\begin{aligned} |V_0^{k,\epsilon}| &\leqslant \mathbb{E}\Big[|V_h^{k,\epsilon}| + C \sup_{s \in [0,h]} |\delta P_s| (\mathcal{E}_0 - \mathcal{E}_h) \Big] \\ &\leqslant \mathbb{E}\Big[|V_h^{k,\epsilon}| \Big] + C(1 + |p|)\sqrt{h} \,. \end{aligned} \tag{2.2.28}$$

Now, we observe that

$$\mathbb{E}\Big[|V_h^{k,\epsilon}| \Big] = \mathbb{E}\Big[|\bar{v}^{k,\epsilon}(0, p, \tilde{E}_h^{k,\epsilon}) - \psi(P_h^\epsilon, \tilde{E}_h^{k,\epsilon})| \Big] \tag{2.2.29}$$

$$= \mathbb{E}\Big[|\mathbb{E}[\psi(P_h^\epsilon, e)]_{e = \tilde{E}_h^{k,\epsilon}} - \psi(P_h^\epsilon, \tilde{E}_h^{k,\epsilon})| \Big] \tag{2.2.30}$$

$$\leqslant 2 L_\psi \mathbb{E}[|\delta P_h|] \ . \tag{2.2.31}$$

We thus get $\mathbb{E}\Big[|V_h^{k,\epsilon}| \Big] \leqslant C(1 + |p|)\sqrt{h}$, which, combined with (2.2.28), concludes the proof. □

We now turn to the main result for this part, which gives an upper bound to the error between $\mathcal{S}_h(\psi)$ and $\Theta_h(\psi)$ that is effectively a control on the truncation error of the scheme.

Proposition 2.2.1 (truncation error) *Under our standing assumptions on the coefficients (μ, b, σ), the following holds, for $\psi \in \mathcal{K}$:*

$$\int |\mathcal{S}_h(\psi)(p, e) - \Theta_h(\psi)(p, e)| \mathrm{d}e \leqslant C_{L_\psi}(1 + |p|^2) h^{\frac{3}{2}} \ , \tag{2.2.32}$$

for $p \in \mathbb{R}^d$, $h > 0$.

Proof. 1. We first consider the regularised version of the decoupling fields, as introduced in (2.2.16)-(2.2.17). Let $V_t^{e,k,\epsilon} = \tilde{Y}_t^{k,\epsilon} - v^{k,\epsilon}(t, P_t^\epsilon, \tilde{E}_t^{k,\epsilon})$, for $t \leqslant h$, with $(P_0^\epsilon, \tilde{E}_0^{k,\epsilon}) = (p, e)$. We first observe that by definition (2.2.16) and the fact that P^ϵ and B (and thus subsequently $\tilde{E}^{e,k,\epsilon}$) are independent,

$$\mathbb{E}\Big[V_h^{e,k,\epsilon} | B \Big] = \bar{v}(0, p, \tilde{E}_h^{k,\epsilon}) - \mathbb{E}\Big[\psi^k(P_h^\epsilon, \tilde{E}_h^{k,\epsilon}) | B \Big] = 0 \ . \tag{2.2.33}$$

We also observe that, for $0 \leqslant t \leqslant h$,

$$\begin{aligned}|V_t^{e,k,\epsilon}| &\leqslant |\tilde{v}^{k,\epsilon}(t,p,\tilde{E}_t^{k,\epsilon}) - v^{k,\epsilon}(t,p,\tilde{E}_t^{k,\epsilon})| + |v^{k,\epsilon}(t,p,\tilde{E}_t^{k,\epsilon}) - v^{k,\epsilon}(t,P_t^\epsilon,\tilde{E}_t^{k,\epsilon})| \\ &\leqslant C(1+|p|)\sqrt{h} + C|P_t^\epsilon - p| \ ,\end{aligned}$$

where for the last inequality we used Lemma 2.2.1 and the uniform Lipschitz continuity of $v^{k,\epsilon}$ (Note that C depends upon the Lispchitz constant of ψ). This leads to

$$\sup_{t\in[0,h]} \mathbb{E}\Big[\text{esssup}_e |V_t^{e,k,\epsilon}|\Big] \leqslant C(1+|p|)\sqrt{h} \ . \tag{2.2.34}$$

2. Let us consider the tangent process $\partial_e \tilde{E}^{k,\epsilon}$ given by

$$\partial_e \tilde{E}_t^{k,\epsilon} = 1 + \int_0^t \partial_y \mu(\tilde{Y}_s^{k,\epsilon},p)\partial_e \tilde{v}^{k,\epsilon}(s,p,\tilde{E}_s^{k,\epsilon})\partial_e \tilde{E}_s^{k,\epsilon}\mathrm{d}s \tag{2.2.35}$$

$$= e^{\int_0^t \partial_y \mu(\tilde{Y}_s^{k,\epsilon},p)\partial_e \tilde{v}^{k,\epsilon}(s,p,\tilde{E}_s^{k,\epsilon})\mathrm{d}s}. \tag{2.2.36}$$

And we observe that $0 \leqslant \partial_e \tilde{E}_t^{k,\epsilon} \leqslant 1$, for all $0 \leqslant t \leqslant h$.
In order to bound the error $\int |V_0^{e,k,\epsilon}|\mathrm{d}e$, we will study the dynamics of $t \mapsto \int |\mathbb{E}\Big[V_t^{e,k,\epsilon}\partial_e \tilde{E}_t^{k,\epsilon}\Big]|\mathrm{d}e$. Using (2.2.19), we compute

$$V_t^{e,k,\epsilon}\partial_e \tilde{E}_t^{k,\epsilon} = V_0^{e,k,\epsilon} + \int_0^t V_s^{e,k,\epsilon}\partial_y \mu(\tilde{Y}_s^{k,\epsilon},p)\partial_e \tilde{v}^{k,\epsilon}(s,p,\tilde{E}_s^{k,\epsilon})\partial_e \tilde{E}_s^{k,\epsilon}\mathrm{d}s + N_t^{k,\epsilon} \tag{2.2.37}$$

$$- \int_0^t \Big(\mu(\tilde{Y}_s^{k,\epsilon},p) - \mu(v^{k,\epsilon}(s,P_s^\epsilon,\tilde{E}_s^{k,\epsilon}),P_s^\epsilon)\Big)\partial_e v^{k,\epsilon}(s,P_s^\epsilon,\tilde{E}_s^{k,\epsilon})\partial_e \tilde{E}_s^{k,\epsilon}\mathrm{d}s \tag{2.2.38}$$

where $N^{k,\epsilon}$ is a square-integrable martingale. Taking expectation on both sides of the above equality, we get

$$|V_0^{e,k,\epsilon}| \leqslant |\mathbb{E}\Big[\int_0^h \Big(\mu(\tilde{Y}_s^{k,\epsilon},p) - \mu(v^{k,\epsilon}(s,P_s^\epsilon,\tilde{E}_s^{k,\epsilon}),P_s^\epsilon)\Big)\partial_e v^{k,\epsilon}(s,P_s^\epsilon,\tilde{E}_s^{k,\epsilon})\partial_e \tilde{E}_s^{k,\epsilon}\mathrm{d}s\Big]| \tag{2.2.39}$$

$$+ |\mathbb{E}\Big[\int_0^h V_s^{e,k,\epsilon}\partial_y \mu(\tilde{Y}_s^{k,\epsilon},p)\partial_e \tilde{v}^{k,\epsilon}(s,p,\tilde{E}_s^{k,\epsilon})\partial_e \tilde{E}_s^{k,\epsilon}\mathrm{d}s\Big]| \tag{2.2.40}$$

recall (2.2.33). Since $\partial_e \tilde{v}^{k,\epsilon}()$, $\partial_e \tilde{E}^{k,\epsilon}$ and $-\partial_y \mu()$ are non-negative, we deduce

$$|V_0^{e,k,\epsilon}| \leqslant \mathbb{E}\Big[\int_0^h |\mu(\tilde{Y}_s^{k,\epsilon},p) - \mu(v^{k,\epsilon}(s,P_s^\epsilon,\tilde{E}_s^{k,\epsilon}),P_s^\epsilon)|\partial_e v^{k,\epsilon}(s,P_s^\epsilon,\tilde{E}_s^{k,\epsilon})\partial_e \tilde{E}_s^{k,\epsilon}\mathrm{d}s\Big] \tag{2.2.41}$$

$$- \mathbb{E}\Big[\int_0^h |V_s^{e,k,\epsilon}|\partial_y \mu(\tilde{Y}_s^{k,\epsilon},p)\partial_e \tilde{v}^{k,\epsilon}(s,p,\tilde{E}_s^{k,\epsilon})\partial_e \tilde{E}_s^{k,\epsilon}\mathrm{d}s\Big] \ . \tag{2.2.42}$$

Integrating the previous inequality, we get

$$\int |V_0^{e,k,\epsilon}|\mathrm{d}e \leqslant \mathbb{E}\Big[\int\int_0^h \Big|\mu(\tilde{Y}_s^{k,\epsilon},p) - \mu(v^{k,\epsilon}(s,P_s^\epsilon,\tilde{E}_s^{k,\epsilon}),P_s^\epsilon)\Big|\,\partial_e[v^{k,\epsilon}(s,P_s^\epsilon,\tilde{E}_s^{k,\epsilon})]\mathrm{d}s\mathrm{d}e\Big] =: A_1$$
$$- \mathbb{E}\Big[\int\int_0^h |V_s^{e,k,\epsilon}|\partial_e[\mu(\tilde{v}^{k,\epsilon}(s,p,\tilde{E}_s^{k,\epsilon}),p)]\mathrm{d}s\mathrm{d}e\Big] =: A_2\,. \tag{2.2.43}$$

We now study the term A_2 above: Since, $\tilde{v}^{k,\epsilon}$ is bounded i.e. $\tilde{v}^{k,\epsilon}$ uniformly bounded by a constant: $|\tilde{v}^{k,\epsilon}| \leqslant C$ and μ is Lipschitz continuous, we have

$$|\int \partial_e[\mu(\tilde{v}^{k,\epsilon}(s,p,\tilde{E}_s^{k,\epsilon}),p)]\mathrm{d}e| \leqslant C(1+|p|) \tag{2.2.44}$$

the factor $(1+|p|)$ above comes from the fact μ is Lipschitz continuous

$$|\mu(\cdot,p) - \mu(\cdot,0)| \leqslant C(1+|p|)$$

and then

$$\begin{aligned} A_2 &\leqslant C(1+|p|)\mathbb{E}\Big[\int_0^h \mathrm{esssup}_e|V_s^{e,k,\epsilon}|\mathrm{d}s\Big] \\ &\leqslant C(1+|p|^2)h^{\frac{3}{2}}\,, \end{aligned}$$

recalling (2.2.34).
We now compute an upper bound for A_1. Since μ is Lipschitz-continuous, we have

$$\begin{aligned} A_1 &\leqslant C\mathbb{E}\Big[\int\int_0^h \Big(|V_s^{e,k,\epsilon}| + |P_s^\epsilon - p|\Big)\,\partial_e[v^{k,\epsilon}(s,P_s^\epsilon,\tilde{E}_s^{k,\epsilon})]\mathrm{d}s\mathrm{d}e\Big] \\ &\leqslant C\mathbb{E}\Big[\int_0^h (\mathrm{esssup}_e|V_s^{e,k,\epsilon}| + |P_s^\epsilon - p|)\int \partial_e[v^{k,\epsilon}(s,P_s^\epsilon,\tilde{E}_s^{k,\epsilon})]\mathrm{d}e\mathrm{d}s\Big] \end{aligned}$$

Since $v^{k,\epsilon}$ is (uniformly) bounded and using (2.2.34), we obtain

$$A_1 \leqslant C(1+|p|^2)h^{\frac{3}{2}}\,. \tag{2.2.45}$$

Combining the estimate for A_1 and A_2, we conclude:

$$\int |\tilde{v}^{k,\epsilon}(0,p,e) - v^{k,\epsilon}(0,p,e)|\mathrm{d}e \leqslant C(1+|p|^2)h^{\frac{3}{2}}\,. \tag{2.2.46}$$

Then passing to the limits in k,ϵ and using the dominated convergence theorem conclude the proof. □

2.2.3.2 Scheme stability

We now study the scheme's stability by a introducing a perturbed version of the scheme given in Definition 2.2.6.

Definition 2.2.7 (Perturbed scheme) *For $n \leqslant N$, let $\eta_n : \mathbb{R}^d \times \mathbb{R} \to \mathbb{R}$ be measurable functions satisfying*

$$\int |\eta_n(p,e)|\mathrm{d}e \leqslant \mathfrak{c}(1+|p|^\kappa) \ \text{ for some } \kappa \geqslant 1, \mathfrak{c} > 0, \tag{2.2.47}$$

where κ, $\mathfrak{c}$ do not depend on n. We denote by $(u'_n)_{0\leqslant n\leqslant N}$ the solution of the following backward induction:
- for $n = N$, set $u'_N := \phi + \eta_N$,
- for $n < N$, $u'_n = \mathcal{S}_{t_{n+1}-t_n}(u'_{n+1}) + \eta_n$.

Proposition 2.2.2 (L^1-stability) *Under our* standing assumptions, *the following holds true for (η_n),satisfying (2.2.47), perturbation of the scheme given in Definition 2.2.6 :*

$$\max_{0\leqslant n\leqslant N} \mathbb{E}\Big[\int |u^\pi_n - u'_n|(P^{0,p}_{t_n}, e)\mathrm{d}e\Big] \leqslant \sum_{n=0}^{N} \mathbb{E}\Big[\int |\eta_n|(P^{0,p}_{t_n}, e)\mathrm{d}e\Big] \ . \tag{2.2.48}$$

Proof. 1.a In the proof, we denote $\delta u^\pi_n = u_n - u'_n$, for all $n \leqslant N$.
We observe that

$$\int |\delta u_N|(p,e)\mathrm{d}e \leqslant \int |\eta_N|(p,e)\mathrm{d}e \leqslant \mathfrak{c}(1+|p|^\kappa)\,, \tag{2.2.49}$$

where we used (2.2.47) for the last inequality. We have then

$$\mathbb{E}\Big[\int |\delta u_N|(P^{0,p}_T, e)\mathrm{d}e\Big] \leqslant \mathbb{E}\Big[\int |\eta_N|(P^{0,p}_T, e)\mathrm{d}e\Big] < \infty\,. \tag{2.2.50}$$

We used the fact that for any $q > 0$,

$$\mathbb{E}\Big[\sup_{t\in[0,T]} |P^{0,p}_t|^q\Big] \leqslant C_q(1+|p|^q). \tag{2.2.51}$$

1.b Assume (induction hypothesis)

$$|\delta u_{n+1}|(p,e)\mathrm{d}e \leqslant K_{n+1}(1+|p|^\kappa)\,. \tag{2.2.52}$$

for some positive $K_{n+1} < +\infty$ (Note that $K_N = \mathfrak{c}$ from (2.2.49)). Denoting $\bar{u}_{n+1} = \mathcal{D}_{(t_{n+1}-t_n)}(u^\pi_{n+1})$ and $\bar{u}'_{n+1} = \mathcal{D}_{(t_{n+1}-t_n)}(u'_{n+1})$, we have

$$|u^\pi_n - u'_n| \leqslant |\mathcal{T}_{(t_{n+1}-t_n)}(\bar{u}_{n+1}) - \mathcal{T}_{(t_{n+1}-t_n)}(\bar{u}'_{n+1})| + |\eta_n| \tag{2.2.53}$$

From Lemma 3.6 in [22] applied to $\mathcal{T}$, we obtain

$$\int |\mathcal{T}_{(t_{n+1}-t_n)}(\bar{u}_n) - \mathcal{T}_{(t_{n+1}-t_n)}(\bar{u}'_n)|(p,e)\mathrm{d}e \leqslant \int |\bar{u}_{n+1} - \bar{u}'_{n+1}|(p,e)\mathrm{d}e \tag{2.2.54}$$

Moreover,

$$\bar{u}_{n+1} - \bar{u}'_{n+1} = \mathbb{E}\Big[u^\pi_{n+1}(P^{0,p}_{t_{n+1}-t_n}, e) - u'_{n+1}(P^{0,p}_{t_{n+1}-t_n}, e)\Big] \tag{2.2.55}$$

which leads to

$$\int |\delta u_n|(p,e)\mathrm{d}e \leqslant \int \mathbb{E}\Big[|\delta u_{n+1}|(P^{0,p}_{t_{n+1}-t_n},e)\mathrm{d}e\Big] + \int |\eta_n|(p,e)\mathrm{d}e\,. \tag{2.2.56}$$

From the induction hypothesis, we know that

$$\mathbb{E}\Big[|\delta u_{n+1}|(P^{0,p}_{t_{n+1}-t_n},e)\mathrm{d}e\Big] \leqslant K_{n+1}(1+\mathbb{E}\Big[|P^{0,p}_{t_{n+1}-t_n}|^\kappa\Big])$$

leading to $\mathbb{E}\Big[|\delta u_{n+1}|(P^{0,p}_{t_{n+1}-t_n},e)\mathrm{d}e\Big] \leqslant K_{n+1}C_\kappa(1+|p|^\kappa)$, where we used (2.2.51). Using (2.2.47), we then obtain

$$\int |\delta u_n|(p,e)\mathrm{d}e \leqslant K_n(1+|p|^\kappa) \text{ with } K_n = K_{n+1}C_\kappa + \mathfrak{c}\,,$$

proving the induction hypothesis (2.2.52) for the next step. Moreover, this shows that $\mathbb{E}\Big[\int |\delta u_{n+1}|(P^{0,p}_{t_{n+1}},e)\mathrm{d}e\Big] < +\infty$ and $\mathbb{E}\Big[\int |\delta u_n|(P^{0,p}_{t_n},e)\mathrm{d}e\Big] < +\infty$. Thus, we deduce from (2.2.56),

$$\mathbb{E}\Big[|\delta u_n|(P^{0,p}_{t_n},e)\mathrm{d}e\Big] \leqslant \mathbb{E}\Big[|\delta u_{n+1}|(P^{0,p}_{t_{n+1}},e)\mathrm{d}e\Big] + \mathbb{E}\Big[\int |\eta_n|(P^{0,p}_{t_n},e)\mathrm{d}e\Big] \tag{2.2.57}$$

2. From step 1.a and 1.b above, we deduce that (2.2.57) holds for all $n < N$. Iterating the inequality on n concludes the proof. □

2.2.3.3 Proof of Theorem 2.2.2

We classicaly writes the true solution given by the decoupling field as a perturbed splitting scheme, for a perturbation $(\zeta_n)_{0\leqslant n\leqslant N}$ given as follows: $\zeta_N = 0$ and $\zeta_n(\cdot) = \Theta_{t_{n+1}-t_n}(\mathcal{V}(t_{n+1},\cdot)) - \mathcal{S}_{t_{n+1}-t_n}(\mathcal{V}(t_{n+1},\cdot))$. We observe that, indeed, for all $n \leqslant N$,

$$\mathcal{V}(t_n,\cdot) = \mathcal{S}_{t_{n+1}-t_n}(\mathcal{V}(t_{n+1},\cdot)) + \zeta_n(\cdot)\,. \tag{2.2.58}$$

From Proposition 2.2.1, we know that ζ_n satisfies (2.2.47) with $\kappa = 2$, recall (2.2.32), and then

$$\mathbb{E}\Big[\int |\zeta_n|(P_{t_n},e)\mathrm{d}e\Big] \leqslant C(1+|p|^2)(t_{n+1}-t_n)^{\frac{3}{2}}. \tag{2.2.59}$$

Using Proposition 2.2.2, we obtain that for $n = 0$ in particular,

$$\int |\mathcal{V}(0,p,e) - u_0^\pi(p,e)|\mathrm{d}e \leqslant CT(1+|p|^2)\sqrt{|\pi|}\,.$$

□

2.3 Numerical schemes

The possible difference in the dimension between the E-variable and the P-variable leads us to treat these variables very differently in the numerical procedure. The convergence result obtained in the previous section indicates that it is indeed reasonable to use a splitting scheme. We then work toward a fully implementable scheme building on this approach.

2.3.1 A regression method for the splitting scheme

We present here a – still theoretical – discrete-time scheme which combines a finite difference approximation of the transport operator and a probabilistic approximation of the diffusion operator. In the next section, we discuss various possible implementations.

We first suppose that the approximation of the transport operator is given as follows. Let J be a positive integer and $\mathfrak{E} = (e_j)_{1\leqslant j\leqslant J}$ a discrete grid of $\mathbb{R}$. We denote by $\mathcal{T}_h^{\mathfrak{E}}$ an approximation of the operator $\mathcal{T}_h$ on $\mathfrak{E}$. Namely,

$$\mathbb{R}^d \times \mathbb{R}^J \ni (p,\theta) \mapsto \mathcal{T}_h^{\mathfrak{E}}(p,\theta) \in \mathbb{R}^J. \tag{2.3.1}$$

This means that for each $p \in \mathbb{R}^d$, $\mathcal{T}_h^{\mathfrak{E}}(p,\cdot)$ is an approximation on the grid $\mathfrak{E}$ of the corresponding equation (2.2.11) on $[0,h]$. We assume moreover that it satisfies, for some $q \geqslant 1$ and $q' \geqslant 1$,

$$|\mathcal{T}_h^{\mathfrak{E}}(p,\theta)| \leqslant C(1+|p|^q+|\theta|^{q'})\,. \tag{2.3.2}$$

The terminal condition $\psi : \mathbb{R}^d\times\mathbb{R} \to \mathbb{R}$ is simply approximated on $\mathfrak{E}$ by $\theta^j = \psi(p,e_j)$, for all $1 \leqslant j \leqslant J$ and $p \in \mathbb{R}^d$.

Given this approximate transport operator, we now introduce a probabilistic approximation of $\mathcal{V}(0,p,\cdot)$ on $\mathfrak{E}$. To this end, let us consider the Euler scheme associated to P on π, namely, for $n \geqslant 0$,

$$\widehat{P}^{\pi}_{t_{n+1}} = \widehat{P}^{\pi}_{t_n} + b(\widehat{P}^{\pi}_{t_n})(t_{n+1}-t_n) + \sigma(\widehat{P}^{\pi}_{t_n})\Delta\widehat{W}_n \ \text{ and } \widehat{P}^{\pi}_0 = p\,. \tag{2.3.3}$$

Here, $(\Delta\widehat{W}_n)_{0\leqslant n\leqslant N-1}$ are independent random variables that stands for an approximation of the law of $(W_{t_{n+1}}-W_{t_n})_{0\leqslant n\leqslant N-1}$ and we assume that their moments verify $\mathbb{E}\Big[|\Delta\widehat{W}_n|^\rho\Big] \leqslant C_\rho|t_{n+1}-t_n|^{\frac{\rho}{2}}$, $\rho \geqslant 1$. It is well known from the Lipschitz continuity assumption on b and σ that, for any $\rho \geqslant 1$,

$$\mathbb{E}\Big[\sup_{t\in\pi}|\widehat{P}^{\pi}_t|^\rho\Big] \leqslant C_\rho(1+|p|^\rho)\,. \tag{2.3.4}$$

We now define a discrete time process $(\Gamma_n)_{0\leqslant n\leqslant N}$ valued in $\mathbb{R}^J$ as follows.

Definition 2.3.1 *$(\Gamma_n)_{0\leqslant n\leqslant N}$ is solution to the following backward scheme:*

1. *For $n = N$, $\Gamma^j_N = \phi(\widehat{P}^{\pi}_{t_N}, e_j)$ for $1 \leqslant j \leqslant J$.*
2. *For $n < N$, compute*

$$\Gamma_n = \mathcal{T}_h^{\mathfrak{E}}(\widehat{P}^{\pi}_{t_n}, \mathbb{E}\Big[\Gamma_{n+1}|\widehat{P}^{\pi}_{t_n}\Big])\,. \tag{2.3.5}$$

For later use, we define the auxiliary process $(\bar{\Gamma}_n)$ by

$$\bar{\Gamma}^j_n = \mathbb{E}\Big[\Gamma^j_{n+1}|\widehat{P}^{\pi}_{t_n}\Big] \ \text{ for all } 1 \leqslant j \leqslant J\,. \tag{2.3.6}$$

We also importantly observe that, due to the Markovian property of $\widehat{P}^\pi$ on π, (Γ_n) satisfies

$$\Gamma_n := \gamma_n(\widehat{P}^\pi_{t_n}) \,, \quad 0 \leqslant n \leqslant N \,, \tag{2.3.7}$$

where the functions $\gamma_n : \mathbb{R}^d \to \mathbb{R}^J$, are given by

Definition 2.3.2 *1. For $n = N$, $\gamma^j_N(p) = \phi(p, e_j)$, $1 \leqslant j \leqslant J$, $p \in \mathbb{R}^d$.*

2. Then, compute for $n < N$, $p \in \mathbb{R}^d$,

$$\bar{\gamma}^j_n(p) = \mathbb{E}\Big[\gamma^j_{n+1}\Big(p + b(p)h + \sigma(p)\Delta\widehat{W}_n\Big)\Big] \quad \textit{for all } 1 \leqslant j \leqslant J, \tag{2.3.8}$$

$$\gamma_n(p) = \mathcal{T}^{\mathfrak{E}}_h(p, \bar{\gamma}_n(p)) \,. \tag{2.3.9}$$

With the above definitions, we have that $\Gamma_0 = \gamma_0(P_0)$ which stands for an approximation of $\mathcal{V}(0, P_0, \cdot)$ on the grid $\mathfrak{E}$.

To obtain the wellposedness of the previous definitions, we check that the conditional expectations at each step of the scheme are well defined. This follows from a direct backward induction using (2.3.2) and (2.3.4).
Depending on how large d, the dimension of the P-variable, is, we may choose various probabilistic schemes to compute (2.3.6). This has been thoroughly studied in the context of BSDEs approximation and various methods have been suggested: linear regression [38, 39, 40], quantization methods [2, 1, 62], cubature methods [30, 31, 25] or Malliavin calculus approach [16, 32]. In the next section, we present a non-linear regression method used e.g. in [48].

2.3.2 Implementation using non linear regression

We now turn to an implementation that can work in a high dimensional setting for P. To perform the regression step in Definition 2.3.1, we will use Neural Networks representation of the value function. This will be coupled with conservative finite difference approximation of the transport operator that we first recall.

2.3.2.1 Conservative Finite Difference approximation of transport equation

We shall now consider conservative methods for the transport operator associated to the backward equation (2.2.11).

Recall that, for a given positive integer J, $\mathfrak{E} = (e_j)_{1 \leqslant j \leqslant J}$ is a uniform grid of $\mathbb{R}$ where we set $\delta := e_{j+1} - e_j$. We also introduce $\mathfrak{R} = \{r_0 = 0 < \cdots < r_k < \cdots < r_K = h\}$ a uniform grid for a given positive integer K, and we set $\mathfrak{d} := h/K$.

We first consider the Lax-Friedrichs approximation to the backward transport equation (2.2.11) and define $\mathcal{T}^{\mathrm{LF}}_{\mathfrak{E},\mathfrak{R},h} : \mathbb{R}^d \times \mathbb{R}^J \mapsto \mathbb{R}^J$ the approximation of the associated operator $\mathcal{T}_h$. It is defined as follows, see e.g. [60, Chapter 12].

Definition 2.3.3 (Lax-Friedrichs) *For a given $p \in \mathbb{R}^d$ and $\theta \in \mathbb{R}^J$, let $(V_j^k)_{1\leqslant k\leqslant K, 1\leqslant j\leqslant J}$ denotes the approximation at the point (r_k, e_j) The steps to compute V are:*
- at time $r_K = h$: set $V_j^K = \theta_j$, $1 \leqslant j \leqslant J$,
- for $0 \leqslant k < K$: set $V_1^k = V_1^{k+1}$, $V_J^k = V_J^{k+1}$ and compute, for $1 < j < J$:

$$V_j^k = \frac{1}{2}(V_{j+1}^{k+1} + V_{j-1}^{k+1}) + \frac{\delta}{2\mathfrak{d}}\left(\mathfrak{M}(p, V_{j+1}^{k+1}) - \mathfrak{M}(p, V_{j-1}^{k+1})\right). \tag{2.3.10}$$

Then, set $\mathcal{T}^{\mathrm{LF}}_{\mathfrak{E},\Re,h}(p,\theta) := V^0$.

When the function μ has constant sign, a more satisfactory method to use is the upwind method, as it is less diffusive. Since in the application to carbon markets given in Example 2.3.2 and 2.3.1 below, this will be the case, we consider the upwind method for $\mu \geqslant 0$. We thus now define $\mathcal{T}^{\mathrm{U}}_{\mathfrak{E},\Re,h} : \mathbb{R}^d \times \mathbb{R}^J \mapsto \mathbb{R}^J$ the approximation of the associated operator $\mathcal{T}_h$ as follows, see again e.g. [60].

Definition 2.3.4 (Upwind for $\mu \geqslant 0$) *For a given $p \in \mathbb{R}^d$ and $\theta \in \mathbb{R}^J$ let $(V_j^k)_{1\leqslant j\leqslant J, 1\leqslant k\leqslant K}$ denotes the approximation at the point (r_k, e_j) The steps to compute V are:*
- at time $r_K = h$: set $V_j^K = \theta_j$, $1 \leqslant j \leqslant J$,
- for $0 \leqslant k < K$: set $V_J^k = V_J^{k+1}$ and compute, for $1 \leqslant j < J$:

$$V_j^k = V_j^{k+1} + \frac{\delta}{\mathfrak{d}}\left(\mathfrak{M}(p, V_{j+1}^{k+1}) - \mathfrak{M}(p, V_j^{k+1})\right). \tag{2.3.11}$$

Then, set $\mathcal{T}^{\mathrm{U}}_{\mathfrak{E},\Re,h}(p,\theta) := V^0$.

2.3.2.2 Non-linear regression and implemented scheme

We first mention that for this part the Euler scheme (2.3.3) is computed using real Brownian increment, namely $\widehat{\Delta W}_n = (W_{t_{n+1}} - W_{t_n})$, $0 \leqslant n \leqslant N-1$. We have seen in the last section two possible implementations of the transport operator $\mathcal{T}_h$ on the spatial grid $\mathfrak{E}$, that we shall denote for this part simply by $\mathcal{T}_h^{\mathfrak{E}}$. The last point to precise is the computation of the conditional expectation part of the scheme in Definition 2.3.1, where at each time step the quantities $\gamma_n(\widehat{P}^\pi_{t_n}) = \mathbb{E}\Big[\Gamma_{n+1}|\widehat{P}^\pi_{t_n}\Big]$ has to be estimated, recall Definition 2.3.2. In order to do so, we will use deep learning as it was demonstrated to be very efficient for high dimensional system, already in the setting of FBSDEs, see e.g. [43, 48]. The functions (γ_n) will be optimally approximated by a feedforward neural network. We denote by $\mathcal{NN}_{d_0,d_1,L,m}$ the set of neural nets, which are functions $\Phi(\cdot;\Theta) : \mathbb{R}^{d_0} \mapsto \mathbb{R}^{d_1}$, parametrised by Θ and with the following characteristics: the input dimension is d_0, the output dimension is d_1, $L+1$ is the number of layers, $m = (m_l)_{0\leqslant m_l\leqslant L}$ where m_l is the number of neurons on each layer, $l = 0, ..., L$: by default, $m_0 = d$ and $m_L = d_1$. The neural network has thus $L-1$ hidden layers. We refer, to e.g. [48, Section 2] for a detailed description of feedforward neural network. The number of total parameters is $N_{L,m} = \sum_{l=0}^{L-1} m_l(1+m_{l+1})$, and thus $\Theta \in \mathbb{R}^{N_{L,m}}$.

Given $\mathcal{T}_h^{\mathfrak{E}} = \mathcal{T}^{\mathrm{U}}_{\mathfrak{E},\Re,h}$ or $\mathcal{T}_h^{\mathfrak{E}} = \mathcal{T}^{\mathrm{LF}}_{\mathfrak{E},\Re,h}$, the scheme to compute $(\hat{\gamma}_n, \hat{\bar{\gamma}}_n)$ approximation of $(\gamma_n, \bar{\gamma}_n)$ in Definition 2.3.2 is given as follows.

Definition 2.3.5 *1. At* $t_N = T$, $\widehat{\bar{\gamma}}_N^j(p) = \widehat{\gamma}_N^j(p) = \phi(p, e_j)$, $1 \leqslant j \leqslant J$, $p \in \mathbb{R}^d$.

2. For $n = N-1, ..., 1$*: given a simulation of* $P_{t_n}^\pi$*, optimize*

$$\widehat{\mathcal{L}}_n(\Theta) = \mathbb{E}\Big|\mathcal{T}_h^{\mathfrak{E}}(\widehat{P}^\pi_{t_{n+1}}, \widehat{\bar{\gamma}}_{n+1}(\widehat{P}^\pi_{t_{n+1}})) - \Big(\mathcal{Y}_n(\widehat{P}^\pi_{t_n}, \Theta) + \mathcal{Z}_n(\widehat{P}^\pi_{t_n}, \Theta)(W_{t_{n+1}} - W_{t_n})\Big)\Big|^2 \tag{2.3.12}$$

where $(\mathcal{Y}_n(\cdot, \Theta), \mathcal{Z}_n(\cdot, \Theta)) \in \mathcal{NN}_{d,(d+1)\times J, L, m}$*, so that*

$$\Theta_n^\star \in \arg\min_{\Theta \in \mathbb{R}^{N_m}} \widehat{\mathcal{L}}_n(\Theta) \quad \text{and then} \quad \widehat{\bar{\gamma}}_n(\cdot) := \mathcal{Y}_n(\cdot, \Theta_n^\star)\,.$$

3. At the initial time $t_0 = 0$*, compute* $\widehat{\gamma}_0(\widehat{P}_0^\pi) = \mathbb{E}\Big[\mathcal{T}_h^{\mathfrak{E}}(\widehat{P}^\pi_{t_1}, \widehat{\bar{\gamma}}_1(\widehat{P}^\pi_{t_1}))\Big]$.

The function $\widehat{\gamma}_0(\cdot)$ stands for the numerical approximation of $\mathcal{V}(0, P_0, \cdot)$.

Remark 2.3.1 *(i) The loss minimisation in (2.3.12) is done using a Stochastic Gradient Descent algorithm: we use Adam Optimizer [57] provided in the Keras API [28]. The good approximation of the function* $\bar{\gamma}_n$ *is guaranteed by universal approximation theorem for neural networks [45] and is quite efficient in practice, as demonstrated by our numerical examples below.*

(ii) Definition 2.3.5 should be compared with the scheme DBDP1 in [48, Section 3]. In this paper, the authors compute a non-linear conditional expectation (related to BSDEs) at each step: Here, we only compute a conditional expectation and use $\mathcal{Z}$ *as a control variate. In particular, differently to DBDP1, we have to apply* $\mathcal{T}_h^{\mathfrak{E}}$ *in* $\widehat{\mathcal{L}}_n(\cdot)$ *at each step. Note also that one can not apply directly DBDP1 to the singular FBSDE (2.1.1) under study as it is a fully-coupled FBSDE.*

(iii) A key point is to ensure the stability of the finite difference scheme for the transport equation, namely that the CFL condition is satisfied. For example, for the Lax-Friedrichs scheme given in Definition 2.3.3, one has to enforce, for each time t_n*:*

$$\sup_{1\leqslant k\leqslant K, 1\leqslant j\leqslant J} \Big|\mu(V_k^j, \widehat{P}^\pi_{t_n})\frac{\delta}{\mathfrak{d}}\Big| < 1,$$

see e.g. [60, Chapter 13]. In practice, we choose B*, such that*

$$\sup_{y\in[0,1], p\in[-B,B]^d} \Big|\mu(y,p)\frac{\delta}{\mathfrak{d}}\Big| < 1.$$

The constant B *depends obviously on the parameters* $\delta, \mathfrak{d}$ *and should be large enough. Then, in the simulation,* $\widehat{P}^\pi_{t_n}$ *is projected on* $[-B, B]^d$*. We also ensure that* $0 \leqslant V_k^j \leqslant 1$ *by truncating* $\bar{\gamma}_n^j$ *if necessary and relying on the scheme monotony.*

2.3.3 Numerical experiments

In this section, we present the results of our numerical experiments that show that the splitting scheme is efficient in practice to approximate $\mathcal{V}(\cdot)$. The method presented in the previous section, will be tested on two complementary models to Example 2.1.1. The first one reads as follows.

Example 2.3.1 (BM with positive emission)

$$\mathrm{d}P_t^\ell = \sigma \mathrm{d}W_t^\ell \text{ and } \mathrm{d}E_t = \mu(Y_t, \frac{1}{\sqrt{d}}\sum_{\ell=1}^{d} P_t^\ell)\mathrm{d}t \tag{2.3.13}$$

with $\mu(y,p) = 1 + \frac{1}{1+e^{-p}} - y$ *and* $\phi(p,e) = \mathbf{1}_{\{e\geqslant 0\}}$.

The above model will have non negative μ which is more realistic if one has in mind application to carbon market. A critic could be however that it is driven by a Brownian Motion and that it will not suffer any discrete time error. We then introduce a multiplicative model as follows.

Example 2.3.2 (Multiplicative model)

$$\mathrm{d}P_t^\ell = \mu P_t^\ell \mathrm{d}t + \sigma P_t^\ell \mathrm{d}W_t^\ell,\ P_0^\ell = 1, \text{ and } \mathrm{d}E_t = \tilde{\mu}(Y_t, P_t)\mathrm{d}t \tag{2.3.14}$$

with $\tilde{\mu}(y,p) = \left(\prod_{\ell=1}^d p^\ell\right)^{\frac{1}{\sqrt{d}}} e^{-\theta y}$, *for some* $\theta > 0$ *and* $\phi(p,e) = \mathbf{1}_{\{e\geqslant 0\}}$.

We are not aware of any explicit solution for these models but they have the property that any $d+1 > 2$ dimensional model can be recast as a 2-dimensional model (one dimension for the P-variable, one dimension for the E-variable). This will be used for numerical validation of the non-linear regression scheme used for the multi-dimensional models by introducing an alternative scheme efficient in low dimension (see next Section). However, one should notice that there is no simple equivalent one-dimensional PDE available for Examples 2.3.2 or 2.3.13 as it is the case for Example 2.1.1, recall (2.1.9).

2.3.3.1 An alternative scheme

To validate empirically the results obtained with the non-linear regression scheme, we could use a PDE method in low dimension. However, we chose to use here another method based on the splitting scheme that will combine a particle method with tree-like regression. This method will be efficiently implemented on the Examples 2.3.1, 2.3.2 and 2.1.1 for two main reasons: We work in moderate dimension and the process P can be expressed as a function of the underlying Brownian motion, namely $P_t = \mathfrak{P}(t, W_t)$.
Here, contrarily to the previous section, $(\Delta\widehat{W}_n := \widehat{W}_{t_{n+1}} - \widehat{W}_{t_n})_{0\leqslant n\leqslant N-1}$ stands for discrete approximation of the Brownian increments $(W_{t_{n+1}} - W_{t_n})_{0\leqslant n\leqslant N-1}$. We also assume that the time grid π is equidistant and thus $|\pi| = \frac{T}{N} =: \mathfrak{h}$. One could then use, for all $1 \leqslant \ell \leqslant d$, $\mathbb{P}(\widehat{W}_n^\ell = \sqrt{h}) = \mathbb{P}(\widehat{W}_n^\ell = -\sqrt{h}) = \frac{1}{2}$ in (2.3.3) but this requires 2^d points in total for the approximation. We use instead the cubature

formula introduced in [41, Section A.2] which requires only $2d$ points. Denoting $(\mathfrak{e}^\ell)_{1\leqslant\ell\leqslant d}$ the canonical basis of $\mathbb{R}^d$, we set, for $1 \leqslant i \leqslant I = 2d$, $\mathbb{P}(\Delta\widehat{W}_n = \omega_\mathfrak{h}^i) = \frac{1}{2d}$ and $\omega_\mathfrak{h}^i = -\sqrt{d\mathfrak{h}}\mathfrak{e}^\ell$, if $i = 2\ell$ or $\omega_\mathfrak{h}^i = \sqrt{d\mathfrak{h}}\mathfrak{e}^\ell$ if $i = 2\ell - 1$. At a given point $(t_n, \widehat{P}^\pi_{t_n} = \mathfrak{P}(t_n, \widehat{W}_{t_n}), e)$, the approximation of $\mathcal{D}_\mathfrak{h}(\psi)$, recall Definition 2.2.5, reads then simply

$$\mathbb{E}\Big[\psi(\widehat{P}^\pi_{t_{n+1}}, e)|\widehat{P}^\pi_{t_n}\Big] = \frac{1}{2d}\sum_{i=1}^{I}\psi(\mathfrak{P}(t_{n+1}, \widehat{W}_{t_n} + \omega_\mathfrak{h}^i), e)\ . \tag{2.3.15}$$

For $0 \leqslant n \leqslant N$, we denote by $\mathfrak{S}_n$, the discrete support of the random variable $\widehat{W}_{t_n}$. We observe that $\mathfrak{S}_n \subset \mathfrak{S}_{n+1}$ and for $x \in \mathfrak{S}_n$, $x + \Delta\widehat{W}_n \in \mathfrak{S}_{n+1}$. Thus, when computing (2.3.15), there is no need for an interpolation step, if $\psi(\cdot, e)$ is known on $\mathfrak{S}_{n+1}$. We will obviously exploit this fact and compute recursively, backward in time, the approximation of $\mathcal{V}$ on the discrete sets $(\mathfrak{S}_n)_{0\leqslant n\leqslant N}$. The full approximation of the diffusion operator $\mathcal{D}_{(t_{n+1}-t_n)}$ that acts at time t_n, will be given after discussing the discrete version of the operator $\mathcal{T}$, as it will be then more easily justified.

Let us thus now introduce a discrete version of the operator $\mathcal{T}$, recall Definition 2.2.4, that will compute an approximation to (2.2.11) written in *forward form*: We shall use the celebrated Sticky Particle Dynamics (SPD) [17] see also [53, Section 1.1]. The SPD is particularly simple to implement in our case, since, due to the monotonicity assumption on (μ, ψ), there is no particle colliding! For $M \geqslant 1$, let $D_M = \big\{\mathrm{e} = (e_1, \dots, e_m, \dots, e_M) \in \mathbb{R}^M \,|\, e_1 \leqslant \dots \leqslant e_m \leqslant \dots \leqslant e_M\big\}$. The discrete version of $\mathcal{T}$ will act on empirical CDF or equivalently on empirical distribution $\frac{1}{M}\sum_{m=1}^M \delta_{e_m}$ (δ_e is the Dirac mass at e). Generally, $\psi(p, .)$, which is a CDF for each $p \in \mathbb{R}^d$, would need to be approximated in an optimal way on D_M. We observe here that the terminal condition ϕ to Examples 2.3.1, 2.3.2 and 2.1.1, is simply represented by $\mathrm{e} = (0, \dots, 0)$. The iterative algorithm allows us to restrict our study to terminal condition ψ, such that $\psi(p, \cdot) = H*(\frac{1}{M}\sum_{m=1}^M \delta_{e_m})$ for some $\mathrm{e} \in D_M$, where H is the Heaviside function and $*$ the convolution operator. The approximation of $\mathcal{T}$ is then given by

$$\mathbb{R}^d \times D_M \ni (p, \mathrm{e}) \mapsto \mathcal{T}_h^M(p, \mathrm{e}) = (E_h^{p,m})_{1\leqslant m\leqslant M} \in D_M\ , \tag{2.3.16}$$

where $(E_h^{p,m})_{1\leqslant m\leqslant M}$ is a set (of positions) of particles computed as follows. Given the initial position $\mathrm{e} \in D_M$ (representing ψ) and velocities $(\bar{F}_m(p))_{1\leqslant m\leqslant M}$ set to $\bar{F}_m(p) = -\int_{(m-1)/M}^{m/M}\mu(p, y)\mathrm{d}y$, we consider M particles $(E^{p,m})_{1\leqslant m\leqslant M}$, whose positions at time $t \in [0, h]$ are simply given by

$$E_t^{p,m} = e_m + \bar{F}_m(p)t\ . \tag{2.3.17}$$

We observe that $(E_t^{p,m})_{1\leqslant m\leqslant M} \in D_M$, for all $t \in [0, h]$, as $-\mu$ is non-decreasing.

We are now ready to define the approximation of the diffusion operator $\mathcal{D}_{t_{n+1}-t_n}$, denoted $\mathcal{D}_n^M$: it will take into account that $\mathcal{T}_h^M$ acts at the level of particles. Introduce, to ease the presentation, $\mathcal{P}_{n+1} = \{p = \mathfrak{P}(t_{n+1}, \mathrm{w}), \mathrm{w} \in \mathfrak{S}_{n+1}\}$, which is simply the (discrete) support of $\widehat{P}^\pi_{t_{n+1}}$. Assume that

$$\mathfrak{S}_{n+1} \ni \mathrm{w} \mapsto \Psi(\mathrm{w}) = \mathrm{e}^\mathrm{w} \in D_M$$

is given such that for $p \in \mathcal{P}_{n+1}$, $p = \mathfrak{P}(t_{n+1}, \mathrm{w})$, we have $\psi(p, \cdot) = H*(\frac{1}{M}\sum_{m=1}^{M} \delta_{e_m^{\mathrm{w}}})$. Then, for $\mathrm{w} \in \mathfrak{S}_n$, setting $\mathrm{w}_{n+1}^i = \mathrm{w} + \omega_{\mathfrak{h}}^i$, (2.3.15) reads

$$\begin{aligned}\bar{v}_n(\mathrm{w}, e) &:= \mathbb{E}\Big[\psi(\widehat{P}^{\pi}_{t_{n+1}}, e) | \widehat{P}^{\pi}_{t_n} = \mathfrak{P}(t_n, \mathrm{w})\Big] \\ &= \frac{1}{2d}\sum_{i=1}^{I} H*(\frac{1}{M}\sum_{m=1}^{M} \delta_{e_m^{\mathrm{w}_{n+1}^i}})(e) \ , \\ &= H*(\frac{1}{2dM}\sum_{i=1}^{I}\sum_{m=1}^{M} \delta_{e_m^{\mathrm{w}_{n+1}^i}})(e) \ .\end{aligned}$$

This means that, the function $e \mapsto \bar{v}(\mathrm{w}, e)$ is an empirical CDF and is determined by the particles $\mathcal{E} = \bigcup_{i=1}^{I} \left\{\mathrm{e}^{\mathrm{w}_{n+1}^i}\right\}$. There is no need to keep $2dM$ particles at step n, when the function ψ at step $n+1$ is given by M particles (for each $p \in \mathcal{P}_{n+1}$). To reduce the number of particles, we first sort the cloud of particles $\mathcal{E}$ to obtain $\tilde{\mathrm{e}}^{\mathrm{w}} \in D_{2dM}$, then we consider $\bar{\mathrm{e}}^{\mathrm{w}} := (\tilde{e}^{\mathrm{w}}_{2dm})_{1 \leqslant m \leqslant M}$. The approximation operator $\mathcal{D}_n^M$ is finally defined by

$$(D_M)^{\mathfrak{S}_{n+1}} \ni \Psi \mapsto \mathcal{D}_n^M(\Psi)(\mathrm{w}) = \bar{\mathrm{e}}^{\mathrm{w}} \in (D_M)^{\mathfrak{S}_n} \ . \tag{2.3.18}$$

The overall procedure is as follows

Definition 2.3.6 (Alternative scheme) *1. At $n = N$: Set $\mathrm{e}_N := (0, \cdots, 0)$ whose empirical CDF is ϕ. Then define, γ_N by*

$$\mathfrak{S}_N \ni \mathrm{w} \mapsto \gamma_N(\mathrm{w}) = \mathrm{e}_N \ .$$

2. For $n < N$: Given $\gamma_{n+1} : \mathfrak{S}_{n+1} \to D_M$, define $\bar{\gamma}_n : \mathfrak{S}_n \to D_M$ by $\bar{\gamma}_n = \mathcal{D}_n^M(\gamma_{n+1})$ and then γ_n by

$$\mathfrak{S}_n \ni \mathrm{w} \mapsto \gamma_n(\mathrm{w}) = \mathcal{T}_{\mathfrak{h}}^M(\mathfrak{P}(t_n, \mathrm{w}), \bar{\gamma}_n(\mathrm{w})) \in D_M \ . \tag{2.3.19}$$

The approximation of $\mathcal{V}(0, 0, \cdot)$ is then given by $H*\gamma_0$.

2.3.3.2 Numerical results

In this section, we report the findings of the numerical tests we performed on the models given in Examples 2.3.1, 2.3.2 and 2.1.1, using the non-linear regression and splitting method of Definition 2.3.1 and the alternative scheme, presented in Definition 2.3.6.

Concerning the non-linear regression, we use a common structure in all our experiments for the feedforward neural networks used in (2.3.12) to represent $(\mathcal{Y}, \mathcal{Z})$, namely:
- The output layer is of dimension $(J+1) \times d$, where J is size of the E-variable grid;
- Two intermediate layers of dimension $\kappa_J \times d + 10$ (κ_J is fixed to 20 below);
- An input layer of dimension d.

As already mentionned, the training is done using the Adam optimiser using 100

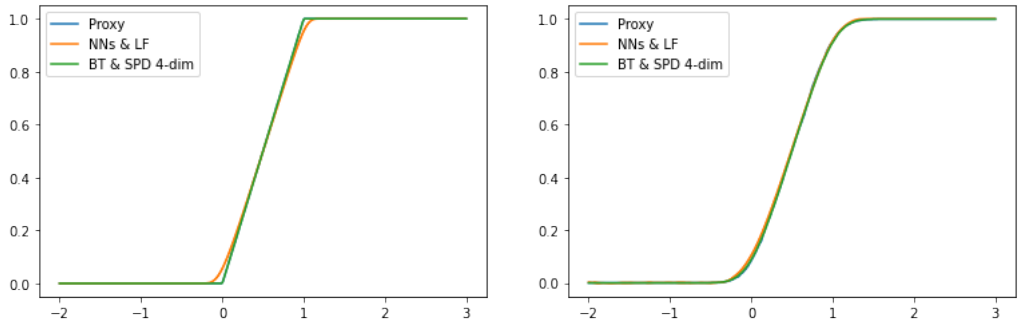

(a) $\sigma = 0.01$ (b) $\sigma = 0.3$

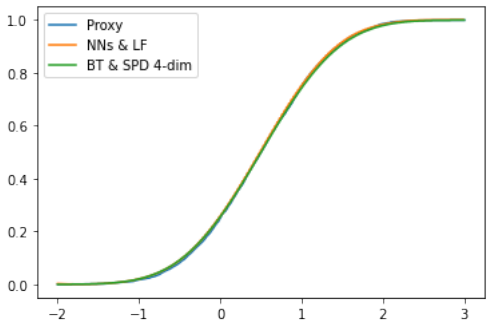

(c) $\sigma = 1.0$

Figure 2.2: Model of Example 2.1.1: Comparison of the two methods Neural Nets & Lax-Friedrichs (NN&LF) with $d = 10$ and the alternative scheme (BT&SPD) with $d = 4$. The Proxy solution is given by the same particle method used in Figure 2.1 on the one-dimensional PDE (2.1.9). Lax-Friedrichs scheme implemented with discretization of space $J = 1500, 1000, 500$, for $\sigma = 0.01, 0.3, 1$ respectively and number of time step $K = 30$. The number of time step for the splitting is $N = 64$. For $BT\&SPD$, the number of particles is $M = 3500$ and the number of time steps $N = 20$.

mini-batches with size 50 and batch normalization. We check validation loss every 30 iterations with the validation batch of size 500. The learning rate is initially fixed at $\eta = 0.001$.

We first observe that our schemes are able to reproduce the proxy for the true solution of Example 2.1.1 as reported in Figure 2.2. This has to be compared with the results of Figure 2.1 for the "classical" FBSDEs methods. Let us emphasize that the non-linear regression scheme (denoted $NN\&LF$) is tested in dimension $d = 10$ and the alternative scheme (denoted $BT\&SPD$) in dimension $d = 4$. Since the Lax-Friedrichs scheme presents a diffusive phenomenon, we increase the space discretization steps to overcome this effect when σ decreases. In the numerical computations, we choose respectively $J = 500, 1000, 1500$ for $\sigma = 1.0, 0.3, 0.01$ to obtain satisfactory approximations.

Next, we tested our scheme on the models of Example 2.3.1 and Example 2.3.2. The results are reported on the graphs in Figure 2.3 and 2.4 respectively. Since the function μ is always positive in these two examples, we can use an Upwind scheme. Unlike the Lax-Friedrichs scheme, the Upwind scheme is less diffusive, and we can

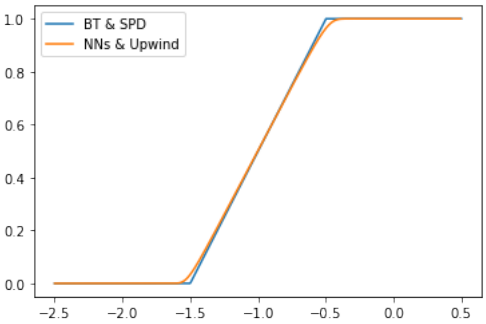

(a) $\sigma = 0.01$

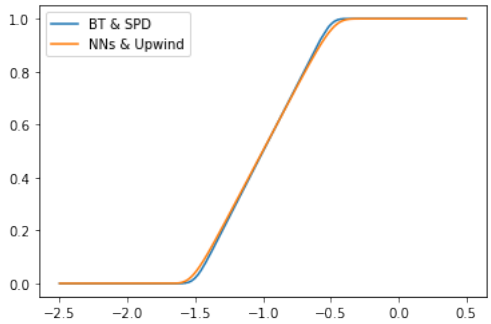

(b) $\sigma = 0.3$

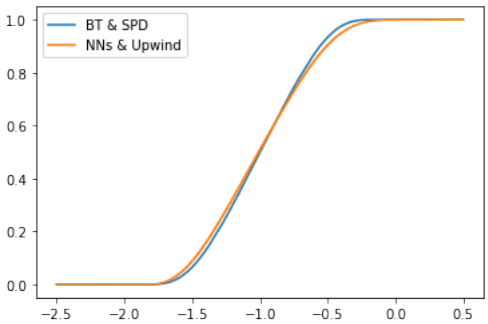

(c) $\sigma = 1.0$

Figure 2.3: Example 2.3.1 in dimension $d = 10$: Comparison of two methods Neural nets & Upwind scheme and solution obtained using the alternative scheme on equivalent 4-dimensional model. The Upwind scheme used discretization of space $J = 100, 300, 400$ respectively for $\sigma = 1, 0.3, 0.01$ and number of time step $K = 20$. The number of time step for the splitting is $N = 32$. For $BT\&SPD$, the number of particles is $M = 3500$, and the number of time steps $N = 20$.

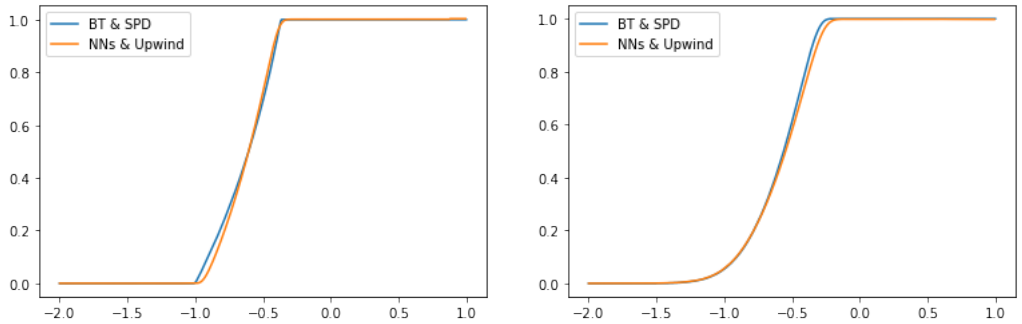

(a) $\sigma = 0.01$ (b) $\sigma = 0.3$

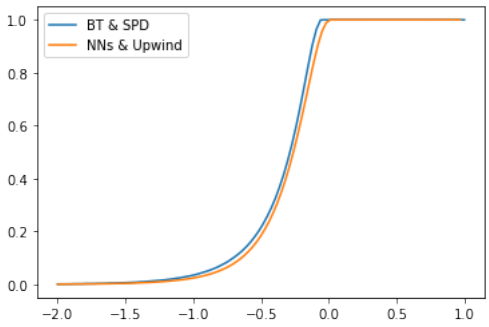

(c) $\sigma = 1.0$

Figure 2.4: Example 2.3.2 in dimension $d = 10$: Comparison of two methods Neural nets & Upwind scheme and solution obtained using the alternative scheme on equivalent 4-dimensional model (BT&SPD). The Upwind scheme used discretization of space $J = 100, 400, 500$ respectively for $\sigma = 1, 0.3, 0.01$ and number of time step $K = 20$. The number of time step for the splitting is $N = 32$. For $BT\&SPD$, the number of particles is $M = 3500$, and the number of time steps $N = 20$.

lower the number of space discretization. In our example, we take $J = 100, 300, 400$ respectively for $\sigma = 1.0, 0.3, 0.01$. We are not aware of an exact solution for this model, so we compare both the non-linear regression scheme (NN&U) for $d = 10$ and the alternative scheme (BT&SPD) on an equivalent four dimensional model.

As we pointed out before, Lax-Friedrichs scheme is more diffusive than Upwind scheme: this is illustrated on Figure 2.5, by considering the case where $\sigma = 0.01$, and taking $J = 400$ only for the LF space discretisation. On this graph and the computations below, the 'Proxy' to the true solution is obtained by running an equivalent one-dimensional model using the alternative scheme (BT&SPD) with parameters: number of particles $M = 3500$, number of time step $N = 20$. Table 2.1 presents the error obtained by comparing the non-linear regression scheme to this proxy, the computational times is also given[3] The $L1$-error is the error used in the theoretical part, but one can see that the $L\infty$-error behaves also very well. The computational times can still be reduced on our examples by diminishing the batch size but this would certainly not generalise to other models more challenging for

[3]Intel Core i5-8265U, 16.0 GB RAM.

the training of the neural networks. We remark that increasing number of layers, number of neurons as well as number of samples, the improvements are small even barely significant.

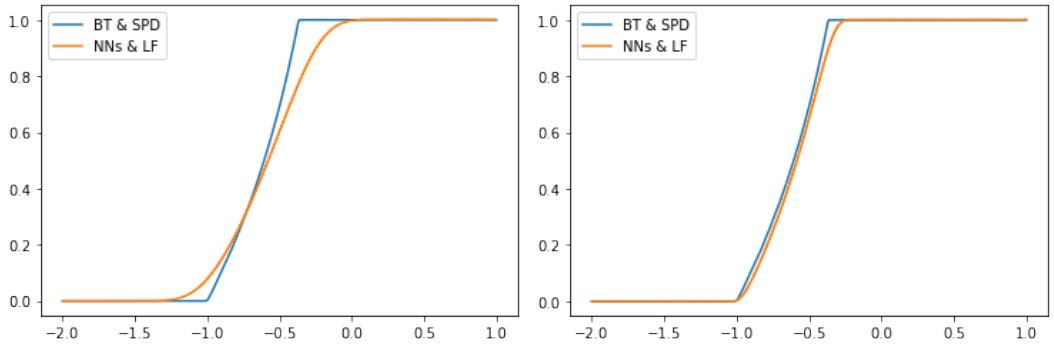

(a) $\sigma = 0.01, J = 500$ (b) $\sigma = 0.01, J = 1500$

Figure 2.5: Example 2.3.2 in dimension $d = 10$: Neural nets & Lax-Friedrichs with $J = 500$ and 1500, compared with the Proxy (BT&SPD in dimension one).

Model	Sigma	Method	Parameters	$L1$	$L\infty$	Time
Ex 2.1.1	1.0	NN & LF	$J = 500$	0.0233	0.0283	3813s
Ex 2.3.1		NN & Upwind	$J = 500$	0.0116	0.0142	1687s
Ex 2.3.2		NN & Upwind	$J = 100$	0.0206	0.0856	336s
Ex 2.1.1	0.3	NN & LF	$J = 1000$	0.0183	0.0250	7660s
Ex 2.3.1		NN & Upwind	$J = 500$	0.0147	0.0220	1693s
Ex 2.3.2		NN & Upwind	$J = 400$	0.0756	0.1253	1488s
Ex 2.1.1	0.01	NN & LF	$J = 2000$	0.0055	0.0215	15139s
Ex 2.3.1		NN & Upwind	$J = 500$	0.0141	0.0365	1712s
Ex 2.3.2		NN & Upwind	$J = 500$	0.0410	0.0843	1701s

Table 2.1: Numerics of model 2.1.1, 2.3.1 and 2.3.2 with different parameters in dimension $d = 10$.

Finally, we want to empirically estimate the convergence rate of the error introduced by the splitting. We consider the model 2.3.2 where $\sigma = 0.3$ and for which there is no discrete-time simulation error (as the forward process is a Brownian Motion). We consider a set of number of time steps $N := \{4, 8, 16, 32, 64, 128\}$, and compute the $L1$ and $L\infty$-error by NN & Upwind method (with $K = 20$, $J = 400$). The proxy solution is always given by alternative scheme in one dimensional equivalent model, to achieve a better precision. The empirical convergence rate with respect to the number of time step is close to one see Figure 2.6, which is slightly better than the upper bound obtained in Theorem 2.2.2.

Finally, in Table 2.2, we report the computational time and the error associated to different dimensions $d = 1, 5, 10$ in Example 2.3.2 where $\sigma = 0.3$ with NNs & Upwind scheme ($K = 20$, $J = 400$) and with fixed number of time step for the splitting

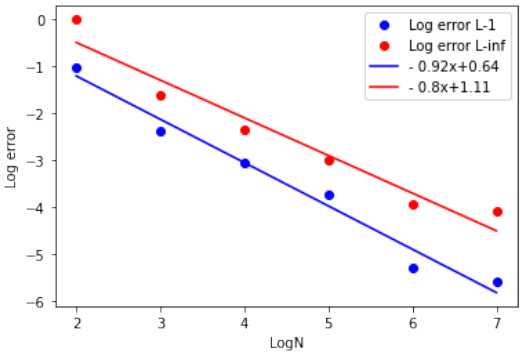

Figure 2.6: Convergence rate on N for model Example 2.3.2 with parameters $d = 10, \sigma = 0.3$ and $K = 20$, $J = 400$.

$N = 32$. Per our specification, the computational time does not increase exponentially and, importantly, neither the empirical error. This behaviour is expected from the non-linear regression using neural networks.

Dimension	$d = 1$	$d = 5$	$d = 10$
Time	673s	1077s	1488s
$L1$ Error	0.0431	0.0594	0.0756
$L\infty$ Error	0.0867	0.1041	0.1253

Table 2.2: Computational cost in example 2.3.2 for different dimension d (for the P-variable).

Chapter 3

Convergence of particles and tree based scheme for singular FBSDEs

The content of this chapter is from a work in collaboration with Jean-François Chassagneux.

Contents

3.1 Introduction

In this work, we study the theoretical and numerical convergence of particles and tree based scheme for singular FBSDEs. The class of singular Forward Backward

Stochastic Differential Equations (FBSDE) is motivated by application in the modeling of carbon markets [47, 20, 22]. Let $(\Omega, \mathcal{F}, \mathbb{P})$ be a stochastic basis supporting a d-dimensional Brownian motion W and $T > 0$ a terminal time. We denote by $(\mathcal{F}_t)_{t\geqslant 0}$ the filtration generated by the Brownian motion (augmented and completed). The singular FBSDE system, with solution $(P_t, E_t, Y_t, Z_t)_{0\leqslant t\leqslant T}$, has the following form:

$$\left\{\begin{array}{rcl} dP_t &=& b(P_t)dt + \sigma(P_t)dW_t \\ dE_t &=& \mu(Y_t, P_t)dt \\ dY_t &=& Z_t dW_t \end{array}\right. \tag{3.1.1}$$

The terminal condition is typically given by

$$Y_T = \phi(E_T) \text{ where } \phi(e) = \mathbf{1}_{e\geqslant\Lambda}\,, \tag{3.1.2}$$

for some $\Lambda > 0$. Existence and uniqueness to the above FBSDE is not straightforward has it is fully coupled (the backward process Y appears in the coefficient of the forward process E), it is degenerate in the forward direction E and the terminal condition is discontinuous. However, assuming some structural conditions, see Theorem 3.2.1 below for a precise statement, Carmona and Delarue [20] managed to prove the wellposedness of such singular FBSDEs. They also show that for $0 \leqslant t < T$, the following Markovian representation holds true for the Y-process, namely:

$$Y_t := \mathcal{V}(t, P_t, E_t) \tag{3.1.3}$$

where the measurable function $\mathcal{V} : [0, T] \times \mathbb{R}^d \times \mathbb{R} \to \mathbb{R}$ is classically named the *decoupling field*.
The decoupling field $\mathcal{V}$ associated to (3.1.1) is a weak solution to

$$\partial_t u + \partial_e(\mathfrak{M}(p, u)) + \partial_p u b(p) + \frac{1}{2}\mathrm{Tr}[\sigma(p)\sigma^\top(p)\partial^2_{pp}] = 0 \;\text{ and }\; u(T, p, e) = \phi(e), \tag{3.1.4}$$

with

$$\mathfrak{M}(p, y) := \int_0^y \mu(p, \upsilon)\mathrm{d}\upsilon\;,\; 0 \leqslant y \leqslant 1, \tag{3.1.5}$$

where ∂_p denotes the Jacobian with respect to p, ∂_t the time derivative, ∂_e the derivative with respect to the e variable, $\top$ is the transpose and ∂^2_{pp} is the matrix of second derivatives with respect to the p variable.

The algorithm we study is based on a splitting scheme designed for this kind of equation and introduced in [26]. Though it could be defined at a general level for the PDE, we should note that the convergence proof rely on the FBSDE setting. Indeed, under appropriate conditions, the FBSDE appears as well-posed random characteristics for the PDE (3.1.4). The splitting scheme rely on the iteration on a discrete time grid of the composition of two operators : a transport operator $\mathcal{T}$ (in this case the P variable is fixed) and a diffusion operator $\mathcal{D}$ (in this case the E variable is fixed). Precise definitions are given in the next section. From [26], we already know that the theoretical splitting scheme is convergent with a rate one half. This result is obtained under the same structural conditions which

guarantee the well-posedness of the FBSDE. In [26], the splitting scheme is then implemented using various finite difference approximations of the transport operator and a non-linear regression using Deep Neural Networks for the diffusion operator. An alternative scheme [26, Section 3.3.1] is also suggested to verify the convergence result of the main numerical procedure. In this paper, we analyse precisely this alternative scheme by proving its convergence with a rate under some conditions.

The rest of this chapter is organized as follows. In the next Section, we recall the theoretical setting for the study of singular FBSDEs and introduce the theoretical splitting scheme. We also give some properties of the solution in the framework used to study the convergence of the numerical method. In Section 3.3, we present the numerical algorithm and some of its variant that will be used for numerical tests. We also state our main convergence result in Theorem 3.3.1. Section 3.4 is dedicated to the proof of the convergence by studying precisely all sources of errors. The last section presents numerical results for the various schemes introduced, illustrating the theoretical convergence.

Notations In the following we will use the following spaces

- For fixed $0 \leqslant a < b < +\infty$ and $I = [a, b]$ or $I = [a, b)$, $\mathcal{S}^{2,k}(I)$ is the set of $\mathbb{R}^k$-valued càdlàg[1] $\mathcal{F}_t$-adapted processes Y, s.t.

$$\|Y\|^2_{\mathcal{S}^2} := \mathbb{E}\left[\sup_{t\in I} |Y_t|^2\right] < \infty.$$

  Note that we may omit the dimension and the terminal date in the norm notation as this will be clear from the context. $\mathcal{S}^{2,k}_{\mathrm{c}}(I)$ is the subspace of processes with continuous sample paths.

- For fixed $0 \leqslant a < b < +\infty$, and $I = [a, b]$, we denote by $\mathcal{H}^{2,k}(I)$ the set of $\mathbb{R}^k$-valued progressively measurable processes Z, such that

$$\|Z\|^2_{\mathcal{H}^2} := \mathbb{E}\left[\int_I |Z_t|^2 dt\right] < \infty.$$

We denote by $\mathscr{P}(\mathbb{R})$ the space of probability measure on $\mathbb{R}$ and $\mathscr{P}_q(\mathbb{R})$, $q \geqslant 1$ the subset of probability measure which have a q-moment finite.
We denote by $\mathscr{I}$ the space of cumulative distribution function (CDF) namely functions θ given by

$$\mathbb{R} \ni x \mapsto \theta(x) = \mu((-\infty, x]) \in [0, 1]$$

for some $\mu \in \mathscr{P}(\mathbb{R})$.

3.2 Review of theoretical result for singular FBSDEs

In this section, we first recall the main properties of solution to (3.1.1). We then define the theoretical splitting scheme studied in [26] and used to build our implemented algorithms introduced in the next section. Finally, we consider a smooth

[1] French acronym for right continuous with left limits.

framework for the solution of (3.1.4) and obtain some properties useful to prove the convergence of the numerical schemes.

3.2.1 Well-posedness of Singular FBSDEs

We first define a class of function whose the solution belongs to.

Definition 3.2.1 *Let $\mathcal{K}$ be the class of functions $\Phi : \mathbb{R}^d \times \mathbb{R} \to [0,1]$ such that Φ is L_ϕ-Lipschitz in the first variable for some $L_\Phi > 0$, namely*

$$|\Phi(p,e) - \Phi(p',e)| \leqslant L_\Phi |p - p'| \quad \text{for all} \quad (p,p',e) \in \mathbb{R}^d \times \mathbb{R}^d \times \mathbb{R}\,, \tag{3.2.1}$$

and moreover satisfying, for all $p \in \mathbb{R}^d$

$$\Phi(p,e) = \mu(p,(-\infty,e]) \text{ where } \mu(p,\cdot) \in \mathcal{P}_0(\mathbb{R})\,. \tag{3.2.2}$$

From the above definition that $\Phi(p,\cdot) \in \mathscr{I}$ and is thus non-decreasing, right continuous function and satisfies, for all $p \in \mathbb{R}^d$,

$$\lim_{e\to-\infty} \Phi(p,e) = 0 \text{ and } \lim_{e\to-\infty} \Phi(p,e) = 1\,. \tag{3.2.3}$$

We now recall the existence and uniqueness result for the singular FBSDE. It is also key to define the theoretical splitting scheme. This result is obtained for the following class of admissible coefficient functions.

Definition 3.2.2 *Let $\mathcal{A}$ be the class of functions $B : \mathbb{R}^d \to \mathbb{R}^d$, $\Sigma : \mathbb{R}^d \to \mathcal{M}_d$, $F : \mathbb{R} \times \mathbb{R}^d \to \mathbb{R}$ which are L-Lipschitz continuous functions. Moreover, F is strictly decreasing in y and satisfies, for all $p \in \mathbb{R}^d$,*

$$\ell_1 |y - y'|^2 \leqslant (y - y')(F(y',p) - F(y,p)) \leqslant \ell_2 |y - y'|^2, \tag{3.2.4}$$

where L, ℓ_1 and ℓ_2 are positive constants.

The well-posedness result in this setting reads as follows.

Theorem 3.2.1 (Proposition 2.10 in [20], Proposition 3.2 in [22]) *Let $\tau > 0$, $(B,\Sigma,F) \in \mathcal{A}$ and $\Phi \in \mathcal{K}$.*
Given any initial condition $(t_0,p,e) \in [0,\tau) \times \mathbb{R}^d \times \mathbb{R}$, there exists a unique progressively measurable 4-tuple of processes $(P_t^{t_0,p,e}, E_t^{t_0,p,e}, Y_t^{t_0,p,e}, Z_t^{t_0,p,e})_{t_0 \leqslant t \leqslant \tau} \in \mathcal{S}_{\mathrm{c}}^{2,d}([t_0,\tau]) \times \mathcal{S}_{\mathrm{c}}^{2,1}([t_0,\tau]) \times \mathcal{S}_{\mathrm{c}}^{2,1}([t_0,\tau)) \times \mathcal{H}^{2,d}([t_0,\tau])$ satisfying the dynamics

$$\begin{aligned}
\mathrm{d}P_t^{t_0,p,e} &= B(P_t^{t_0,p,e})\mathrm{d}t + \Sigma(P_t^{t_0,p,e})\mathrm{d}W_t, & P_{t_0}^{t_0,p,e} &= p \in \mathbb{R}^d,\\
\mathrm{d}E_t^{t_0,p,e} &= F(P_t^{t_0,p,e}, Y_t^{t_0,p,e})\mathrm{d}t, & E_{t_0}^{t_0,p,e} &= e \in \mathbb{R},\\
\mathrm{d}Y_t^{t_0,p,e} &= Z_t^{t_0,p,e}\mathrm{d}W_t,
\end{aligned} \tag{3.2.5}$$

and such that

$$\mathbb{P}\left[\Phi_-(P_\tau^{t_0,p,e}, E_\tau^{t_0,p,e}) \leqslant \lim_{t\uparrow\tau} Y_t^{t_0,p,e} \leqslant \Phi_+(P_\tau^{t_0,p,e}, E_\tau^{t_0,p,e})\right] = 1. \tag{3.2.6}$$

The unique decoupling field *defined by*

$$[0,\tau) \times \mathbb{R}^d \times \mathbb{R} \ni (t_0,p,e) \to w(t_0,p,e) = Y_{t_0}^{t_0,p,e} \in \mathbb{R}$$

is continuous and satisfies

1. *For any $t \in [0,\tau)$, the function $w(t,\cdot,\cdot)$ is $1/(l_1(\tau-t))$-Lipschitz continuous with respect to e,*

2. *For any $t \in [0,\tau)$, the function $w(t,\cdot,\cdot)$ is C-Lipschitz continuous with respect to p, where C is a constant depending on L, τ and L_ϕ only.*

3. *Given $(p,e) \in \mathbb{R}^d \times \mathbb{R}$, for any family $(p_t,e_t)_{0\leqslant t<\tau}$ converging to (p,e) as $t \uparrow \tau$, we have*

$$\Phi_-(p,e) \leqslant \liminf_{t\to\tau} w(t,p_t,e_t) \leqslant \limsup_{t\to\tau} w(t,p_t,e_t) \leqslant \Phi_+(p,e)\,. \tag{3.2.7}$$

4. *For any $t \in [0,\tau)$, the function $w(t,\cdot,\cdot) \in \mathcal{K}$.*

The previous result leads us to define a non-linear operator associated to (3.1.1) under the following assumption on the coefficient function appearing in (3.1.1).

Standing assumptions: From now on, we assume that $(b,\sigma,\mu) \in \mathcal{A}$.

Definition 3.2.3 *We define the operator Θ by*

$$(0,\infty) \times \mathcal{K} \ni (h,\psi) \mapsto \Theta_h(\psi) = v(0,\cdot) \in \mathcal{K} \tag{3.2.8}$$

where v is the decoupling field given in Theorem 3.2.1 with parameters $\tau = h$, $B = b$, $\Sigma = \sigma$, $F = \mu$ and $\Phi = \psi$.

In particular, we observe that $\mathcal{V}(0,\cdot) := \Theta_T(\phi) = \prod_{0\leqslant n<N} \Theta_{t_{n+1}-t_n}(\phi)$.

The next result arises from the proof of the previous Theorem, see [22].

Corollary 3.2.1 (Approximation result) *Let $\tau > 0$, $(B,\Sigma,F) \in \mathcal{A}$ and $\Phi \in \mathcal{K}$. Let $(\Phi^k)_{k\geqslant 0}$ be a sequence of smooth functions belonging to $\mathcal{K}$ and converging pointwise towards ϕ as k goes to $+\infty$. For $\eta > 0$, consider then $w^{\eta,k}$ the solution to:*

$$\partial_t u + F(u,p)\partial_e u + \mathcal{L}_p u + \frac{1}{2}\eta^2(\partial^2_{ee} u + \Delta_{pp} u) = 0 \quad \text{and} \quad u(\tau,\cdot) = \Phi^k \tag{3.2.9}$$

where Δ_{pp} is the Laplacian with respect to p, and $\mathcal{L}_p$ is the operator

$$\mathcal{L}_p(\varphi)(t,p,e) = \partial_p\varphi(t,p,e)B(p) + \frac{1}{2}\mathrm{Tr}\left[A(p)\partial^2_{pp}\right](\varphi)(t,p,e), \tag{3.2.10}$$

with ∂_p denotes the Jacobian with respect to p, and $A = \Sigma\Sigma^\top$, where $\top$ is the transpose and ∂^2_{pp} is the matrix of second derivative operators. (For later use, we define $\mathcal{L}^\eta := \mathcal{L}_p + \frac{1}{2}\eta^2(\partial^2_{ee} + \Delta_{pp})$.)

Then the functions $w^{\eta,k}$ are $C^{1,2}$ (continuously differentiable in t and twice continuously differentiable in both p and e) and $\lim_{k\to\infty}\lim_{\eta\to 0} w^{\eta,k} = w$ where the convergence is locally uniform in $[0,\tau)\times\mathbb{R}^d\times\mathbb{R}$. Moreover, for all k,η, $w^{k,\eta}(t,\cdot) \in \mathcal{K}$.

For later use, we introduce the associated system of FBSDEs. We consider $(W,\tilde{B},\tilde{\tilde{B}})$ to be independent Brownian motions. For $t_0 \in [0,T)$ and $(p,e) \in \mathbb{R}^d \times \mathbb{R}$,

let $(P^\eta, E^{\eta,k}) \in \mathcal{S}_c^{2,d}([t_0,T]) \times \mathcal{S}_c^{2,1}([t_0,T])$ and $(Y^{\eta,k}, Z^{\eta,k}, \tilde{Z}^{\eta,k}, \tilde{\tilde{Z}}^{\eta,k}) \in \mathcal{S}_c^{2,d}([t_0,T]) \times \mathcal{H}^{2,d}([t_0,T]) \times \mathcal{H}^{2,d}([t_0,T]) \times \mathcal{H}^{2,1}([t_0,T])$ be the solution to

$$\begin{cases} \mathrm{d}P_t^\eta = B(P_t^\eta)\mathrm{d}t + \Sigma(P_t^\eta)\mathrm{d}W_t + \eta \mathrm{d}\tilde{B}_t, \ P_{t_0}^\eta = p\,, \\ \mathrm{d}E_t^{\eta,k} = F(P_t^\eta, Y_t^{\eta,k})\mathrm{d}t + \eta \mathrm{d}\tilde{\tilde{B}}_t, \ E_{t_0}^\eta = e\,, \\ \mathrm{d}Y^{\eta,k} = Z^{\eta,k}\mathrm{d}W_t + \tilde{Z}^{\eta,k}\mathrm{d}\tilde{B}_t + \tilde{\tilde{Z}}^{\eta,k}\tilde{\tilde{B}}_t. \end{cases} \tag{3.2.11}$$

Observe that $Y_t^{\eta,k} = w^{\eta,k}(t, P_t^\eta, E_t^{\eta,k})$ for $t \in [t_0,T]$, in particular $Y_T^{\eta,k} = \Phi^k(P_T, E_t)$. Let us note that the above processes depend upon the initial condition (t_0,p,e) but we slightly abuse the notation in this regard by omitting to indicate it.

3.2.2 A theoretical splitting scheme

The numerical algorithm is based on a splitting method for the quasilinear PDE (3.1.4), which has been introduced in [26]. We first recall quickly the splitting approach at a theoretical level.

We first introduce the transport step where the diffusion part is frozen.

Definition 3.2.4 (Transport step) *We set*

$$(0,\infty) \times \mathcal{K} \ni (h,\psi) \mapsto \mathcal{T}_h(\psi) = \tilde{v}(0,\cdot) \in \mathcal{K}$$

where $\tilde{v}$ is the decoupling field defined in Theorem 3.2.1 with parameters $\tau = h$, $B = 0$, $\Sigma = 0$, $F = \mu$ and terminal condition $\Phi = \psi$.

In the definition above, $\tilde{v}(\cdot)$, defined on $[0,h] \times \mathbb{R}^d \times \mathbb{R}$, is the unique entropy solution to

$$\partial_t w + \partial_e(\mathfrak{M}(p,w)) = 0 \ \text{ and } \ \tilde{v}(h,\cdot) = \psi \tag{3.2.12}$$

recall (3.1.4).

Remark 3.2.1 *For later use in the convergence analysis, we introduce a small modification of the previous operator that acts on function in $\mathscr{I}$ instead of $\mathcal{K}$. Namely, we set*

$$(0,\infty) \times \mathbb{R}^d \times \mathscr{I} \ni (h,p,\theta) \mapsto \tilde{\mathcal{T}}_h(p,\theta) = \hat{v}_p(0,\cdot) \in \mathscr{I}$$

where $\hat{v}_p(0,\cdot)$ is the unique entropy solution to

$$\partial_t w + \partial_e(\mathfrak{M}(p,w)) = 0 \ \text{ and } \ \hat{v}_p(h,\cdot) = \theta \tag{3.2.13}$$

One observes that $\mathcal{T}_h(\psi)(p,\cdot) = \tilde{\mathcal{T}}_h(p,\psi(p,\cdot))$.

From e.g. [53, Theorem 1.1], we have the following stability result:

$$\int |\tilde{\mathcal{T}}_h(p,\psi_1(p,\cdot))(e) - \tilde{\mathcal{T}}_h(p,\psi_2(p,\cdot))(e)|\mathrm{d}e \leqslant \int |\psi_1(p,e)) - \psi_2(p,e)|\mathrm{d}e\,, \tag{3.2.14}$$

for $\psi_1, \psi_2 \in \mathcal{K}$.

We now introduce the diffusion step, where conversely, the E - process is frozen to its initial value.

Definition 3.2.5 (Diffusion step) *We set*

$$(0,\infty)\times\mathcal{K}\ni(h,\psi)\mapsto\mathcal{D}_h(\psi)=\bar{v}(0,\cdot)\in\mathcal{K}$$

where $\bar{v}(0,\cdot)$ is the decoupling field in Theorem 3.2.1 with parameters $\tau=h$, $B=b$, $\Sigma=\sigma$, $F=0$ and terminal condition $\Phi=\psi$.

Observe that, for $t\in[0,h)$,

$$\bar{v}(t,p,e)=\mathbb{E}\Big[\psi(P_h^{t,p},e)\Big]\quad\text{and }\bar{v}(t,\cdot)\in\mathcal{K}\,. \tag{3.2.15}$$

Let us now be given a discrete time grid of $[0,T]$:

$$\pi:=\{t_0:=0\leqslant\cdots\leqslant t_n\leqslant\ldots t_N:=T\}\,, \tag{3.2.16}$$

for $N\geqslant 1$. For ease of presentation, we assume that the time grid π is equidistant and thus, for $0\leqslant n\leqslant N-1$,

$$t_{n+1}-t_n=\frac{T}{N}=:\mathfrak{h}\,. \tag{3.2.17}$$

We can now define the theoretical scheme on π by a backward induction. Since

$$\mathcal{V}(0,\cdot)=\Theta_T(\phi)=\prod_{0\leqslant n<N}\Theta_{t_{n+1}-t_n}(\phi)\,, \tag{3.2.18}$$

the main point of the scheme is to replace one step of Θ by one step of $\mathcal{T}\circ\mathcal{D}$. This leads to the following.

Definition 3.2.6 (Theoretical splitting scheme) *We set*

$$(0,\infty)\times\mathcal{K}\ni(h,\psi)\mapsto\mathcal{S}_h(\psi):=\mathcal{T}_h\circ\mathcal{D}_h(\psi)\in\mathcal{K}.$$

For $n\leqslant N$, we denote by u_n^π the solution of the following backward induction on π:
- for $n=N$, set $u_N^\pi:=\phi$,
- for $n<N$, $u_n^\pi=\mathcal{S}_{t_{n+1}-t_n}(u_{n+1}^\pi)$.

The $(u_n^\pi)_{0\leqslant n\leqslant N}$ stands for the approximation of the decoupling field $\mathcal{V}(t,\cdot)$ for $t\in\pi$. It is proven in [26, Proposition 2.1] a key result concerning the scheme's truncation error.

Proposition 3.2.1 (truncation error) *Under our standing assumptions on the coefficients $(\mu,b,\sigma)\in\mathcal{A}$, the following holds, for $\psi\in\mathcal{K}$:*

$$\int|\mathcal{S}_h(\psi)(p,e)-\Theta_h(\psi)(p,e)|\mathrm{d}e\leqslant C_{L_\psi}(1+|p|^2)h^{\frac{3}{2}}\,, \tag{3.2.19}$$

for $p\in\mathbb{R}^d$, $h>0$.

This allows in particular to obtain the convergence with a rate $\frac{1}{2}$ of the theoretical splitting scheme to the decoupling field $\mathcal{V}$, namely

$$\int_{\mathbb{R}}|\mathcal{V}(0,p,e)-u_0^\pi(p,e)|\mathrm{d}e\leqslant C(1+|p|^2)\sqrt{\mathfrak{h}}\,,\qquad p\in\mathbb{R}^d\,,$$

for a positive constant C.

3.2.3 Smooth setting for convergence results

We now consider a more restricted framework. In this setting, we give further properties of the value function $\mathcal{V}$ that will be used to prove our convergence results. Indeed, even if the scheme can be defined in a quite general setting, the convergence with a rate is obtained in more regular framework.

Therefore, the main assumption we shall use is the following, see Remark 3.2.2 below.

Assumption 3.2.1 *The* decoupling field $\mathcal{V}$ *is a* $\mathscr{C}^{1,2,1}([0,T)\times\mathbb{R}^d\times\mathbb{R})$ *solution to*

$$\partial_t\mathcal{V}+\mu(\mathcal{V},p)\partial_e\mathcal{V}+b(p)\partial_p\mathcal{V}+\frac{1}{2}\bar{\sigma}^2\Delta_p\mathcal{V}=0\,. \tag{3.2.20}$$

In particular, the function $\sigma(\cdot)$ *is constant* $\sigma(\cdot):=\bar{\sigma}I_d$ *with* $\bar{\sigma}>0$ *and* I_d *is the* $d\times d$ *identity matrix, recall* (3.1.4)*. Moreover, the function* b *is* $\mathscr{C}^2(\mathbb{R}^d)$ *with bounded and Lipschitz derivatives and the function* μ *is* $\mathscr{C}^1(\mathbb{R}^d\times[0,1])$ *with Lipschitz and bounded derivatives.*

We first list some further properties of the function $\mathcal{V}$ in the regular setting of the previous assumption.

Proposition 3.2.2 *Under Assumption 3.2.1, the function* $\mathcal{V}$ *satisfies, for* $(t,p,e)\in[0,T)\times\mathbb{R}^d\times\mathbb{R}$*,*

$$0\leqslant\partial_e\mathcal{V}(t,p,e)\leqslant\frac{C}{T-t}\qquad\text{and}\qquad|\partial_p\mathcal{V}(t,p,e)|\leqslant C\,. \tag{3.2.21}$$

Moreover, for $(t,p)\in[0,T)\times\mathbb{R}^d$*,*

$$\int|\partial_p\mathcal{V}(t,p,e)|\mathrm{d}e\leqslant C(T-t)\,, \tag{3.2.22}$$

and, thus, for $p'\in\mathbb{R}^d$*,*

$$\int|\mathcal{V}(t,p,e)-\mathcal{V}(t,p',e)|\mathrm{d}e\leqslant C(T-t)|p-p'|. \tag{3.2.23}$$

Proof. The estimates (3.2.21) are obtained directly from the property of $\mathcal{V}$ given in Theorem 3.2.1. We now study the L^1-control.
Let $\mathcal{V}^{\eta,k}$ be the smooth approximation given in Corollary 3.2.1 to $\mathcal{V}$. We consider also the associated FBSDE $(P^\eta,E^{\eta,k},Y^{\eta,k})$ in (3.2.11). We adapt the computations in the proof of Lemma 3.8 in [22], to obtain the equivalent of equation (3.35) there. In our simpler framework ($r=0$, ϕ does not depend on p), it reads

$$\partial_p\mathcal{V}^{\eta,k}(t_0,p,e)=\mathbb{E}\Big[\int_{t_0}^T\partial_p\mu(P_t^\eta,Y_t^{\eta,k})\partial_pP_t^\eta\partial_eE_t^{\eta,k,e}\partial_e\mathcal{V}^{\eta,k}(t,P_t^\eta,E_t^{\eta,k,e})\mathrm{d}t\Big] \tag{3.2.24}$$

where $(\partial_p P^\eta, \partial_e E^{\eta,k,e})$ are the tangent processes associated to $(P^\eta, E^{\eta,k,e})$. They are given by

$$\partial_e E_t^{\eta,k,e} = 1 + \int_{t_0}^t \partial_y \mu(P_s^\eta, \mathcal{V}^{\eta,k}(s, P_s^\eta, E_s^{\eta,k,e}))\partial_e \mathcal{V}^{\eta,k}(s, P_s^\eta, E_s^{\eta,k,e})\partial_e E_s^{\eta,k,e} \mathrm{d}s\,, \tag{3.2.25}$$

$$(\partial_{p^{\ell'}} P_t^\eta)^\ell = \mathbf{1}_{\{\ell=\ell'\}} + \int_{t_0}^t \partial_p b^\ell(P_s^\eta)\partial_{p^{\ell'}} P_s^\eta \mathrm{d}s \quad \text{for} \quad \ell, \ell' \in \{1, \dots, d\}\,. \tag{3.2.26}$$

It is well known in our setting that

$$\mathbb{E}\left[\sup_{t\in[t_0,T]} |\partial_p P_t^\eta|^\kappa\right] \leqslant C_\kappa\,, \tag{3.2.27}$$

for $\kappa \geqslant 1$.
For a positive real number R, we obtain from (3.2.24) that

$$\int_{-R}^R |\partial_p \mathcal{V}^{\eta,k}(t_0, p, e)|\mathrm{d}e \leqslant \mathbb{E}\left[\int_{t_0}^T \int_{-R}^R |\partial_p \mu(P_t^\eta, Y_t^{\eta,k})\partial_p P_t^\eta| \partial_e[\mathcal{V}^{\eta,k}(t, P_t^\eta, E_t^{\eta,k,e})]\mathrm{d}e\mathrm{d}t\right] \tag{3.2.28}$$

recalling that $\partial_e E^{\eta,k,e}$ and $\partial_p \mathcal{V}^{\eta,k}(\cdot)$. Moreover, since $\mathcal{V}^{\eta,k}$ is bounded and μ Lipschitz continuous, we compute

$$\int_{-R}^R |\partial_p \mathcal{V}^{\eta,k}(t_0, p, e)|\mathrm{d}e \leqslant 2\|\mathcal{V}^{\eta,k}\|_\infty \|\partial_p \mu\|_\infty (T - t_0)\mathbb{E}\left[\sup_{t\in[t_0,T]} |\partial_p P_t^\eta|\right].$$

Using (3.2.27), we eventually obtain

$$\int_{-R}^R |\partial_p \mathcal{V}^{\eta,k}(t_0, p, e)|\mathrm{d}e \leqslant C(T - t_0)\,. \tag{3.2.29}$$

Since $\mathcal{V}^{\eta,k}(t_0, p+\delta, e) - \mathcal{V}^{\eta,k}(t_0, p, e) = \delta \int_0^1 \partial_p \mathcal{V}^{\eta,k}(t_0, p + \lambda\delta, e)\mathrm{d}\lambda$, we have

$$\int_{-R}^R |\mathcal{V}^{\eta,k}(t_0, p+\delta, e) - \mathcal{V}^{\eta,k}(t_0, p, e)|\mathrm{d}e \leqslant \delta \int_0^1 \int_{-R}^R |\partial_p \mathcal{V}^{\eta,k}(t_0, p + \lambda\delta, e)|\mathrm{d}e\lambda\,, \tag{3.2.30}$$

$$\leqslant C(T - t_0)\delta \tag{3.2.31}$$

where we used (3.2.29) for the last inequality. The dominated convergence theorem leads to

$$\int_{-R}^R \frac{1}{\delta}|\mathcal{V}(t_0, p+\delta, e) - \mathcal{V}(t_0, p, e)|\mathrm{d}e \leqslant C(T - t_0)\,, \tag{3.2.32}$$

recalling Corollary 3.2.1. Taking limit as $\delta \to 0$, we obtain

$$\int_{-R}^R |\partial_p \mathcal{V}(t_0, p, e)|\mathrm{d}e \leqslant C(T - t_0)\,. \tag{3.2.33}$$

The estimate (3.2.22) is then obtained by letting $R \to +\infty$ and invoking monotone convergence. □

The study of the regularity of the decoupling field is outside the scope of this paper. We, however, give now an example of model for which Assumption 3.2.1 is known to hold.

Remark 3.2.2 *Let us consider the following* toy model*, which has been studied in [20]*

$$\begin{cases} dP_t = \bar{\sigma} \mathrm{d}\mathcal{W}_t \,, \; P_0 = p \,, \\ dE_t = (P_t - Y_t)\, \mathrm{d}t \,, \; E_0 = e \,, \\ dY_t = Z_t \mathrm{d}\mathcal{W}_t. \end{cases} \tag{3.2.34}$$

Here, $\bar{\sigma}$ is a positive constant, $\mathcal{W}$ is a one-dimensional Brownian Motion and the terminal condition (in the weak sense of (3.2.6)) for Y is given by $\phi(E_T)$, recall (3.1.2). By Theorem 3.2.1 above, it has a unique solution and we denote by v its decoupling field. In particular, we have $v(0,p,e) = Y_0$. Now, we introduce, as in [20], the following process

$$\bar{E}_t = E_t + (T-t)P_t \,, \tag{3.2.35}$$

and observe then that $(\bar{E}, Y)$ satisfies

$$\begin{cases} \mathrm{d}\bar{E}_t = -Y_t \mathrm{d}t + (T-t)\mathrm{d}W_t \\ \mathrm{d}Y_t = Z_t \mathrm{d}W_t \end{cases} \tag{3.2.36}$$

with the same terminal condition since $\bar{E}_T = E_T$. Independently from (3.2.34), the system (3.2.36) is thoroughly studied in [20, Section 4], this system has also a unique solution with a decoupling field $Y_0 = \bar{v}(0, \bar{E}_0)$, and from Proposition 6 in [20] again, $\bar{v}$ is $\mathscr{C}^{1,2}([0,T) \times \mathbb{R})$. We deduce that $v(0,p,e) = \bar{v}(0, e + Tp)$ and more generally $v(t,p,e) = \bar{v}(t, e + (T-t)p)$ for $t \in [0,T)$. This yields that v is $\mathscr{C}^{1,2,2}([0,T) \times \mathbb{R}^d \times \mathbb{R})$.

Let us observe that Proposition 3.2.2 states estimates for the first order derivatives of $\mathcal{V}$. And even though $\mathcal{V}$ is assumed to be smooth in Assumption 3.2.1, nothing is said on the control of higher order derivatives. And, as we will see later on, the control of the second order derivative and third order derivative with respect to p, will be needed. This should not come as a surprise as we will approximate the P process by a discrete in time and space process, see Section 3.3.1.1. We will not make further assumption on the behavior of $\mathcal{V}$ and its derivatives. Instead, we introduce a proxy to $\mathcal{V}$ that will be used in the proof of convergence of our numerical algorithm.

Let then $\mathcal{V}^\epsilon$ be a smoothing of the decoupling field $\mathcal{V}$, namely: For $\epsilon \in (0,1)$,

$$\mathcal{V}^\epsilon(t,p,e) := \int \mathcal{V}(t, p+q, e)\varphi_\epsilon(q)\mathrm{d}q \quad \text{where} \quad \varphi_\epsilon(q) := \frac{1}{\epsilon}\varphi(\frac{q}{\epsilon}) \tag{3.2.37}$$

and with $\varphi(\cdot)$ a smooth compactly supported probability density function.

We now show that $\mathcal{V}^\epsilon$ satisfies the same PDE as $\mathcal{V}$ up to an error term that we can control. From the previous Assumption 3.2.1, we first observe that $\mathcal{V}^\epsilon$, defined in

(3.2.37) belongs also to $\mathscr{C}^{1,2,1}([0,T)\times\mathbb{R}^d\times\mathbb{R})$ and that it satisfies the same bounds as $\mathcal{V}$, namely

$$0 \leqslant \partial_e \mathcal{V}^\epsilon(t,p,e) \leqslant \frac{C}{T-t}\,, \tag{3.2.38}$$

$$|\partial_p \mathcal{V}^\epsilon(t,p,e)| \leqslant C \text{ and } \int |\partial_p \mathcal{V}^\epsilon(t,p,e)|\mathrm{d}e \leqslant C(T-t)\,. \tag{3.2.39}$$

Proposition 3.2.3 *Under Assumption 3.2.1, the function $\mathcal{V}^\epsilon$ satisfies on $[0,T)\times\mathbb{R}^d\times\mathbb{R}$,*

$$\partial_t \mathcal{V}^\epsilon + b(p)\partial_p \mathcal{V}^\epsilon + \frac{1}{2}\bar{\sigma}^2\Delta_p \mathcal{V}^\epsilon + \mu(\mathcal{V}(t,p,e),p)\partial_e \mathcal{V}^\epsilon = \theta^\epsilon(t,p,e) \tag{3.2.40}$$

with

$$|\theta^\epsilon(t,p,e)| \leqslant C\epsilon\left(\int |\partial_p \mathcal{V}^\epsilon(t,p+q,e)|\varphi_\epsilon(q)\mathrm{d}q + \partial_e \mathcal{V}^\epsilon(t,p,e)\right)\,. \tag{3.2.41}$$

Proof. Recall that $\mathcal{V}$ satisfies (3.2.20), and that,

$$\partial_t \mathcal{V}^\epsilon(t,p,e) = \int \partial_t \mathcal{V}(t,p+q,e)\varphi_\epsilon(q)\mathrm{d}q \text{ and } \partial^2_{pp}\mathcal{V}^\epsilon(t,p,e) = \int \partial^2_{pp}\mathcal{V}(t,p+q,e)\varphi_\epsilon(q)\mathrm{d}q. \tag{3.2.42}$$

We thus compute, by linearity of ∂_t, Δ_p,

$$\partial_t \mathcal{V}^\epsilon(t,p,e) + \frac{1}{2}\bar{\sigma}^2\Delta_p \mathcal{V}^\epsilon(t,p,e) = -\int b(p+q)\partial_p \mathcal{V}(t,p+q,e)\varphi_\epsilon(q)\mathrm{d}q \tag{3.2.43}$$

$$-\int \mu(\mathcal{V}(t,p+q,e),p+q)\partial_e \mathcal{V}(t,p+q,e)\varphi_\epsilon(q)\mathrm{d}q \tag{3.2.44}$$

which leads to

$$\partial_t \mathcal{V}^\epsilon(t,p,e) + b(p)\partial_p \mathcal{V}^\epsilon(t,p,e) + \frac{1}{2}\bar{\sigma}^2\Delta_p \mathcal{V}^\epsilon(t,p,e) \tag{3.2.45}$$

$$+ \mu(\mathcal{V}(t,p,e),p)\partial_e \mathcal{V}^\epsilon(t,p,e) = \theta^\epsilon(t,p,e) \tag{3.2.46}$$

with

$$\theta^\epsilon(t,p,e) := \int \{b(p) - b(p+q)\}\,\partial_p \mathcal{V}(t,p+q,e)\varphi_\epsilon(q)\mathrm{d}q \tag{3.2.47}$$

$$+ \int \{\mu(\mathcal{V}(t,p,e),p) - \mu(\mathcal{V}(t,p+q,e),p+q)\}\,\partial_e \mathcal{V}(t,p+q,e)\varphi_\epsilon(q)\mathrm{d}q \tag{3.2.48}$$

We compute, using the uniform Lipschitz property of b, μ and $\mathcal{V}$ in the p variable and $\partial_e \mathcal{V} \geqslant 0$ that

$$|\theta^\epsilon(t,p,e)| \leqslant C\int |q||\partial_p \mathcal{V}(t,p+q,e)|\varphi_\epsilon(q)\mathrm{d}q + C\int |q|\partial_e \mathcal{V}(t,p+q,e)\varphi_\epsilon(q)\mathrm{d}q \tag{3.2.49}$$

$$\leqslant C\epsilon\left(\int |\partial_p \mathcal{V}(t,p+q,e)|\varphi_\epsilon(q)\mathrm{d}q + \partial_e \mathcal{V}^\epsilon(t,p,e)\right) \tag{3.2.50}$$

where we use the fact that φ has compact support to get the last inequality. □

To conclude this section, we collect some useful control in the L^1-sense of the function $\mathcal{V}^\epsilon$ and its derivatives.

Lemma 3.2.1 *Assumption 3.2.1, the followings hold, for* $(t,p) \in [0,T) \times \mathbb{R}^d$,

$$\epsilon \int |\partial^2_{p_i p_j} \mathcal{V}^\epsilon(t,p,e)| \mathrm{d}e + \epsilon^2 \int |\partial^3_{p_i p_j p_k} \mathcal{V}^\epsilon(t,p,e)| \mathrm{d}e \leqslant C \,, \tag{3.2.51}$$

for $i,j,k \in \{1,\dots,d\}$. *And thus, for* $(t,p,p') \in [0,T) \times \mathbb{R}^d \times \mathbb{R}^d$,

$$\int |\partial_p \mathcal{V}^\epsilon(t,p,e) - \partial_p \mathcal{V}^\epsilon(t,p',e)| \mathrm{d}e + \epsilon \int |\partial^2_{pp} \mathcal{V}^\epsilon(t,p,e) - \partial^2_{pp} \mathcal{V}^\epsilon(t,p',e)| \mathrm{d}e \leqslant \frac{C}{\epsilon} |b-a| \,. \tag{3.2.52}$$

Proof. For sake of clarity, we recall the main arguments in dimension one. From the definition of $\mathcal{V}^\epsilon$ in (3.2.37), we observe

$$\partial^2_{pp} \mathcal{V}^\epsilon(t,p,e) = \frac{1}{\epsilon} \int \partial_p \mathcal{V}(t,p+q,e) \frac{1}{\epsilon} \varphi'(\frac{q}{\epsilon}) \mathrm{d}q. \tag{3.2.53}$$

and

$$\partial^3_{ppp} \mathcal{V}^\epsilon(t,p,e) = \frac{1}{\epsilon^2} \int \partial_p \mathcal{V}(t,p+q,e) \frac{1}{\epsilon} \varphi''(\frac{q}{\epsilon}) \mathrm{d}q \tag{3.2.54}$$

Then classical computations, using the estimate (3.2.22), allow to conclude. □

3.3 Numerical algorithm

In this section, we first introduce various version of the splitting scheme that will be implemented in practice. We then introduce the numerical errors that have to be taken into account in order to obtain the convergence of the scheme. The main error decomposition is given at the end of this section together with our main convergence result. Precise study of each error is postponed to the next section.

3.3.1 Fully implementable schemes

The schemes we consider are all based on the approximation of the Wiener measure by a discrete and finite set of path. Indeed, on the grid π, the Brownian motion is approximated by a discrete time process denoted $\widehat{W}$. At each date t_n, $\mathfrak{S}_n \subset \mathbb{R}^d$ denotes the support of the law of the random variable $\widehat{W}_{t_n}$. To define $\widehat{W}$, we first define $(\Delta \widehat{W}_n := \widehat{W}_{t_{n+1}} - \widehat{W}_{t_n})_{0 \leqslant n \leqslant N-1}$ which stands for discrete approximation of the Brownian increments $(W_{t_{n+1}} - W_{t_n})_{0 \leqslant n \leqslant N-1}$.

Definition 3.3.1 (Brownian increments approximation) *We use the cubature formula introduced in [41, Section A.2] which requires only* $2d$ *points. Denoting* $(\mathfrak{e}^\ell)_{1 \leqslant \ell \leqslant d}$ *the canonical basis of* $\mathbb{R}^d$, *we set, for* $1 \leqslant i \leqslant I = 2d$, $\mathbb{P}(\Delta \widehat{W}_n = \omega^i_{\mathfrak{h}}) = \frac{1}{2d}$ *and* $\omega^i_{\mathfrak{h}} = -\sqrt{d\mathfrak{h}}\mathfrak{e}^\ell$, *if* $i = 2\ell$ *or* $\omega^i_{\mathfrak{h}} = \sqrt{d\mathfrak{h}}\mathfrak{e}^\ell$ *if* $i = 2\ell - 1$.

By construction, we observe that

$$\text{for } x \in \mathfrak{S}_n,\ x + \Delta \widehat{W}_n \in \mathfrak{S}_{n+1} \,. \tag{3.3.1}$$

Moreover, the set $\mathfrak{S}_n$ are discrete and finite.

3.3.1.1 Schemes for generic diffusion

In this section, we treat the general case where P is solution to a SDE with Lipschitz coefficients as given in (3.1.1). The discrete approximation on the grid π is given by the classical Euler Scheme

$$\widehat{P}_0 = P_0 \text{ and } \widehat{P}_{t_{n+1}} = \widehat{P}_{t_n} + b(\widehat{P}_{t_n})\mathfrak{h} + \sigma(\widehat{P}_{t_n})\Delta\widehat{W}_n\,, \tag{3.3.2}$$

where $(\Delta\widehat{W}_n)$ is introduced in Definition 3.3.1. For later use, we also define, for $p \in \mathbb{R}^d$ and any $0 \leqslant n \leqslant N-1$,

$$\widehat{P}^{t_n,p}_{t_{n+1}} := p + b(p)\mathfrak{h} + \sigma(p)\Delta\widehat{W}_n\,, \tag{3.3.3}$$

and, for $1 \leqslant i \leqslant 2d$,

$$\left(\widehat{P}^{t_n,p}_{t_{n+1}}\right)^i := p + b(p)\mathfrak{h} + \sigma(p)\omega^i_{\mathfrak{h}}\,. \tag{3.3.4}$$

Let us denote by $\mathcal{P}_n$ the discrete and finite support of $\widehat{P}_{t_n}$ for $0 \leqslant n \leqslant N-1$. We observe, due to the very definition of $(\widehat{P}_{t_n})$, that

$$\text{for } p \in \mathcal{P}_n,\ \widehat{P}^{t_n,p}_{t_{n+1}} \in \mathcal{P}_{n+1}\,. \tag{3.3.5}$$

In this context, we first introduce a discrete version of the operator $\mathcal{T}$, recall Definition 3.2.4, that will compute an approximation to (3.2.12) written in *forward form*: We shall use the celebrated Sticky Particle Dynamics (SPD) [17] see also [53, Section 1.1]. The SPD is particularly simple to implement in our case, since, due to the monotonicity assumption on (μ, ψ), there is no particle colliding!
For $M \geqslant 1$, let

$$D_M := \left\{\mathrm{e} = (e_1, \dots, e_m, \dots, e_M) \in \mathbb{R}^M \,|\, e_1 \leqslant \cdots \leqslant e_m \leqslant \cdots \leqslant e_M\right\} \tag{3.3.6}$$

$$\text{and } \mathcal{I}^M := \left\{\theta \in \mathscr{I} |\ \theta(\cdot) := H*(\frac{1}{M}\sum_{m=1}^{M}\delta_{e_m}), \mathrm{e} \in D_M\right\} \tag{3.3.7}$$

where H is the Heaviside function $x \mapsto \mathbf{1}_{\{x\geqslant 0\}}$, $*$ the convolution operator and δ_e is the Dirac mass at $e \in \mathbb{R}$.
For later use, we introduce, for $M \geqslant 0$ and $n \in \{0, \dots, N\}$, the set of function

$$\mathcal{K}^M_n = \left\{\psi : \mathcal{P}_n \times \mathbb{R} \to [0,1] \,|\ \text{for } p \in \mathcal{P}_n,\ \psi(p,\cdot) \in \mathcal{I}^M\right\}\,. \tag{3.3.8}$$

The discrete version of $\mathcal{T}$, denoted $\mathfrak{T}$, acts on empirical CDF belonging to $\mathcal{I}^M$ and is given by

$$(0,\infty) \times \mathbb{R}^d \times \mathcal{I}^M \ni (h,p,\theta) \mapsto \mathfrak{T}^M_h(p,\theta) := H*(\frac{1}{M}\sum_{m=1}^{M}\delta_{e^p_m(h)}) \in \mathcal{I}^M\,. \tag{3.3.9}$$

Above $(e^p_m(h))_{1\leqslant m\leqslant M}$ is a set (of positions) of particles computed as follows. Given the initial position $\mathrm{e}(0) \in D_M$ (representing θ) and velocities $(\bar{F}_m(p))_{1\leqslant m\leqslant M}$

set to $\bar{F}_m(p) = -\int_{(m-1)/M}^{m/M} \mu(p,y)\mathrm{d}y$, we consider M particles $(e_m^p)_{1\leqslant m\leqslant M}$, whose positions at time $t \in [0,h]$ are simply given by

$$e_m^p(t) = e_m(0) + \bar{F}_m(p)t\,. \tag{3.3.10}$$

We observe that $(e_m^p(t))_{1\leqslant m\leqslant M} \in D_M$, for all $t \in [0,h]$, as $-\mu$ is non-decreasing.

We now present the approximation used for the approximation of $\mathcal{D}_{\mathfrak{h}}(\psi)$, recall Definition 3.2.5 and (3.2.15).
Let $\psi \in \mathcal{K}_{n+1}^M$ and fix $\mathrm{p} \in \mathcal{P}_n$. We observe

$$\bar{v}_n(\mathrm{p},e) := \mathbb{E}\Big[\psi(\widehat{P}^{t_n,\mathrm{p}}_{t_{n+1}},e)\Big] = \frac{1}{2d}\sum_{i=1}^{2d}\psi(\Big(\widehat{P}^{t_n,p}_{t_{n+1}}\Big)^i,e) \tag{3.3.11}$$

recall (3.3.4).
Since $\psi \in \mathcal{K}_{n+1}^M$, recall (3.3.8), we know that there is some $\mathrm{e}^i \in D_M$, such that

$$\psi(\Big(\widehat{P}^{t_n,p}_{t_{n+1}}\Big)^i,e) = H*(\frac{1}{M}\sum_{m=1}^{M}\delta_{e_m^i})(e)\,.$$

By linearity, (3.3.11) reads

$$\bar{v}_n(\mathrm{p},e) = H*(\frac{1}{2dM}\sum_{i=1}^{I}\sum_{m=1}^{M}\delta_{e_m^i})(e)\,. \tag{3.3.12}$$

The approximation of the diffusion operator is thus given by

$$\mathcal{K}_{n+1}^M \ni \psi \mapsto \mathfrak{D}_n^M(\psi) := \bar{v}_n \in \mathcal{K}_n^{2Md}\,. \tag{3.3.13}$$

Finally, the scheme will have essentially two versions:

CASE 1: We keep the $2dM$ particles at each step n. The overall procedure will then be the iteration of the two operators $\mathfrak{T}$ and $\mathfrak{D}$, see Definition 3.3.2 below.

CASE 2: There is no need to keep $2dM$ particles at step n, when the function ψ at step $n+1$ is given by M particles (for each $p \in \mathcal{P}_{n+1}$). To reduce the number of particles, we apply another operator $\mathfrak{R}$, namely, for $M \geqslant m \geqslant 1$,

$$\mathcal{I}^M \ni \psi \mapsto \mathfrak{R}^{M,m}(\psi) \in \mathcal{I}^m\,. \tag{3.3.14}$$

Various implementation are possible, we refer to the numerical section for a precise description. The overall procedure for this case is given in Definition 3.3.3.

Let us now finally introduce the scheme formally.

Definition 3.3.2 (Scheme in CASE 1) *Fix $M \geqslant 1$ and set for $0 \leqslant n \leqslant N$, $M_n := (2d)^{N-n}M$.*

1. *At $n = N$: Set $\mathrm{e}_N := (\Lambda, \dots, \Lambda) \in D_{M_N}$ whose empirical CDF is the terminal condition $\phi = \mathbf{1}_{\{e \geqslant \Lambda\}}$, recall (3.1.2). Setting simply $u_N^{N,M}(p, \cdot) = \phi$, for all $p \in \mathcal{P}_N$, we do observe that $u_N^{N,M} \in \mathcal{K}_N^{M_N}$.*

2. *For $n < N$: Given $u_{n+1}^{N,M} \in \mathcal{K}_{n+1}^{M_{n+1}}$, define*

$$\bar{u}_n^{N,M} = \mathfrak{D}_n^{M_{n+1}}(u_{n+1}^{N,M}) \in \mathcal{K}_n^{M_n}, \tag{3.3.15}$$

recall (3.3.13), and then $u_n^{N,M}$ by, for each $p \in \mathcal{P}_n$,

$$u_n^{N,M}(p, \cdot) = \mathfrak{T}_{\mathfrak{h}}^{M_n}(p, \bar{u}_n^{N,M}(p, \cdot)), \tag{3.3.16}$$

recall (3.3.9).

The approximation of $\mathcal{V}(0, P_0, \cdot)$ is then given by $u_0^{N,M}(P_0, \cdot)$.

Definition 3.3.3 (Scheme in CASE 2) *Fix $M \geqslant 1$.*

1. *At $n = N$: Set $\mathrm{e}_N := (\Lambda, \cdots, \Lambda) \in D_M$ whose empirical CDF is the terminal condition $\phi = \mathbf{1}_{\{e \geqslant \Lambda\}}$ is the empirical CDF of $\mathrm{e}_N := (0, \dots, 0) \in D_M$. Setting simply $v_N^{N,M}(p, \cdot) := \phi$, for all $p \in \mathcal{P}_N$, we do observe that $v_N^{N,M} \in \mathcal{K}_N^M$.*

2. *For $n < N$: Given $v_{n+1}^{N,M} \in \mathcal{K}_{n+1}^M$, define $\bar{v}_n^{N,M} = \mathfrak{D}_n^M(v_{n+1}^{N,M}) \in \mathcal{K}_n^{2dM}$, recall (3.3.13), and then for each $p \in \mathcal{P}_n$,*

$$\check{v}_n^{N,M} = \mathfrak{R}^{2dM,M}(\bar{v}_n^{N,M}(p, \cdot)) \tag{3.3.17}$$

recall (3.3.14), and finally $v_n^{N,M}(p, \cdot)$ by,

$$v_n^{N,M}(p, \cdot) = \mathfrak{T}_{\mathfrak{h}}^M(p, \check{v}_n^{N,M}(p, \cdot)), \tag{3.3.18}$$

recall (3.3.9).

The approximation of $\mathcal{V}(0, P_0, \cdot)$ is then given by $v_0^{N,M}(P_0, \cdot)$.

3.3.1.2 A simplified functional Brownian setting

We now consider a special case for the process P for which the numerical implementation is less computationally demanding, see Remark 3.3.2 below.

Assumption 3.3.1 *The process P is given as a function of the Brownian motion, namely*

$$P_t = \mathfrak{P}(t, W_t) \quad \text{for} \quad \mathfrak{P} : [0, T] \times \mathbb{R}^d \mapsto \mathbb{R}^d.$$

Remark 3.3.1 *The main application of this case is when P is the Brownian motion itself (also known as the Bachelier model in financial application) or a Geometric Brownian Motion (also known as Black-Scholes model in financial application).*

Compared to the previous section, the only difference is the approximation of P. In this context, it is naturally given by

$$\widehat{P}_t := \mathfrak{P}(t, \widehat{W}_t)\,,\ t \in \pi\,. \tag{3.3.19}$$

Note that we slightly abuse the notation here by keeping the same ones as the ones introduced in the previous section.
So, for $0 \leqslant n \leqslant N$,

$$\mathcal{P}_n = \{\mathrm{p} = \mathfrak{P}(t_n, \mathrm{w}), \mathrm{w} \in \mathfrak{S}_n\}\ , \tag{3.3.20}$$

which is the (discrete) support of $\widehat{P}_{t_n}$. We also define, for $p = \mathfrak{P}(t_n, \mathrm{w})$,

$$\widehat{P}^{t_n,p}_{t_{n+1}} = \mathfrak{P}(t_{n+1}, \mathrm{w} + \Delta\widehat{W}_n) \text{ and } \left(\widehat{P}^{t_n,p}_{t_{n+1}}\right)^i = \mathfrak{P}(t_{n+1}, \mathrm{w} + \omega^i_{\mathfrak{h}})\,, \tag{3.3.21}$$

for $1 \leqslant i \leqslant 2d$, recall Definition 3.3.1.

Now that the approximation of P has been precised in this context, we can use the various schemes given in Definition 3.3.2 and Definition 3.3.3.

Remark 3.3.2 *The main difference between the generic diffucion case and the functional Brownian setting comes from the numerical complexity associated to their implementation. Indeed, it is the case that the growth size of $\mathfrak{S}_n$ with respect to n is tamed (for low dimensional problem) because the "tree" associated to the brownian motion is naturally recombining. It is a priori not the case for generic diffusion and in particular the growth of $\mathcal{P}_n$ is exponential in n. For implementation purposes, we just use the Brownian setting. A well known way to control the growth for generic diffusion is to introduce some interpolation on a grid as e.g. in [25], this method is well known and we do not present it here. It introduces a further error that would need to be controlled. Note that all the method we have described here and we study are impacted by the "curse of dimensionality" associated to the dimension of P. However, we should also note that for dimension around 5 and in the case of the brownian setting, the problems are tractable numerically, see section 3.5.*

3.3.2 Error decomposition and main result

We first present the various sources of errors introduced by the schemes above. In the sequel, we shall mainly conduct our analysis for the scheme given in CASE 1.

The error we seek to control is, for $\gamma_n = u^{N,M}_n$ or $\gamma_n = v^{N,M}_n$ given above,

$$\mathrm{err}(N, M) := \int |\gamma_0(P_0, e) - \mathcal{V}(0, P_0, e)|\mathrm{d}e\ . \tag{3.3.22}$$

And we first observe

$$\mathrm{err} \leqslant \mathcal{E}_0(P_0) + \mathcal{E}^r_0\,, \tag{3.3.23}$$

with for $0 \leqslant n \leqslant N$ and $p \in \mathcal{P}_n$,

$$\mathcal{E}_n^r(p) := \int |\mathcal{V}^\epsilon(t_n, p, e) - \mathcal{V}(t_n, p, e)| \mathrm{d}e\,, \tag{3.3.24}$$

$$\mathcal{E}_n(p) := \int |\gamma_n(p, e) - \mathcal{V}^\epsilon(t_n, p, e)| \mathrm{d}e\,. \tag{3.3.25}$$

In CASE 1, we define, for $p \in \mathcal{P}_n$,

$$\mathcal{E}_n^{\mathrm{T}}(p) := \int \left| \mathfrak{T}_{\mathfrak{h}}^{M_n}(p, \bar{u}_n^{N,M}(p, \cdot))(e) - \tilde{\mathcal{T}}_h(p, \bar{u}_n^{N,M}(p, \cdot))(e) \right| \mathrm{d}e\,, \tag{3.3.26}$$

$$\bar{\mathcal{E}}_n(p) := \int \left| \tilde{\mathcal{T}}_h(p, \bar{u}_n^{N,M}(p, \cdot))(e) - \tilde{\mathcal{T}}_h(p, \mathbb{E}[\mathcal{V}^\epsilon(t_{n+1}, \widehat{P}_{t_{n+1}}^{t_n,p}, \cdot)])(e) \right| \mathrm{d}e\,. \tag{3.3.27}$$

recall Definition 3.3.2 and Remark 3.2.1.
Moreover for $p \in \mathbb{R}^d$, we set

$$\mathcal{E}_n^D(p) := \int \left| \tilde{\mathcal{T}}_h(p, \mathbb{E}[\mathcal{V}^\epsilon(t_{n+1}, \widehat{P}_{t_{n+1}}^{t_n,p}, \cdot)])(e) - \tilde{\mathcal{T}}_h(p, \mathbb{E}[\mathcal{V}^\epsilon(t_{n+1}, P_{t_{n+1}}^{t_n,p}, \cdot)])(e) \right| \mathrm{d}e\,, \tag{3.3.28}$$

$$\mathcal{E}_n^S(p) := \int \left| \tilde{\mathcal{T}}_h(p, \mathbb{E}[\mathcal{V}^\epsilon(t_{n+1}, P_{t_{n+1}}^{t_n,p}, \cdot)])(e) - \mathcal{V}^\epsilon(t_n, p, e) \right| \mathrm{d}e\,. \tag{3.3.29}$$

We have the following.

Lemma 3.3.1 *Under CASE 1, for $0 \leqslant n \leqslant N-2$,*

$$\mathcal{E}_n(p) \leqslant \mathcal{E}_n^{\mathrm{T}}(p) + \bar{\mathcal{E}}_n(p) + \mathcal{E}_n^D(p) + \mathcal{E}_n^S(p) \tag{3.3.30}$$

and

$$\mathcal{E}_{N-1}(p) \leqslant \mathcal{E}_{N-1}^{\mathrm{T}}(p) + \mathcal{E}_{N-1}^{\mathrm{r}}(p) + \int |\mathcal{S}_{\mathfrak{h}}(\phi(\cdot))(p, e) - \Theta_{\mathfrak{h}}(\phi(\cdot))(p, e)| \mathrm{d}e \tag{3.3.31}$$

observing that

$$\mathcal{E}_{N-1}^{\mathrm{T}}(p) = \int |\mathfrak{T}_{\mathfrak{h}}^M(p, \phi(\cdot))(e) - \mathcal{T}_{\mathfrak{h}}(p, \phi(\cdot)(e))| \mathrm{d}e\,. \tag{3.3.32}$$

Proof. The first inequality is straightforward. For the second, we observe that $u_N^{M,N} = \phi$ and does not depend on p variable so that $\bar{u}_{N-1}^{M,N} = \phi$.

$$\begin{aligned}
\mathcal{E}_{N-1}(p) &:= \int |u_{N-1}^{M,N}(p, e) - \mathcal{V}^\epsilon(t_{N-1}, p, e)| \mathrm{d}e \\
&= \int |\mathfrak{T}_{\mathfrak{h}}^M(p, \phi(\cdot))(e) - \mathcal{V}^\epsilon(t_{N-1}, p, e)| \mathrm{d}e \\
&\leqslant \int |\mathfrak{T}_{\mathfrak{h}}^M(p, \phi(\cdot))(e) - \mathcal{T}_{\mathfrak{h}}(p, \phi(\cdot))(e)| \mathrm{d}e + \int |\mathcal{T}_{\mathfrak{h}}(p, \phi(\cdot))(e) - \mathcal{V}(t_{N-1}, p, e)| \mathrm{d}e \\
&\quad + \int |\mathcal{V}(t_{N-1}, p, e) - \mathcal{V}^\epsilon(t_{N-1}, p, e)| \mathrm{d}e
\end{aligned}$$

We then observe that $\mathcal{T}_{\mathfrak{h}}(p,\phi(\cdot))(e) = \mathcal{S}_{\mathfrak{h}}(\phi(\cdot))(p,e)$ as again ϕ does not depend on p. □

We now comment quickly the various errors appearing above: The term $\mathcal{E}_n^{\mathrm{T}}(p)$ is the local error due to the approximation of the transport operator by the SPD. The term $\bar{\mathcal{E}}_n(p)$ will allow to propagate the local errors thanks to the L^1 stability of $\mathcal{T}_h(\cdot)$. The term $\mathcal{E}^D$ is linked to the approximation of the diffusion by the tree and $\mathcal{E}^S$ is the splitting error applied to the proxy $\mathcal{V}^\epsilon$.

Proposition 3.3.1 (Stability) *Under CASE 1, the following hold*

$$\mathcal{E}_0(P_0) \leqslant \sum_{n=0}^{N-2} \mathbb{E}\Big[\mathcal{E}_n^{\mathrm{T}}(\widehat{P}_{t_n}) + \mathcal{E}_n^D(\widehat{P}_{t_n}) + \mathcal{E}_n^S(\widehat{P}_{t_n})\Big] + \mathbb{E}\Big[\mathcal{E}_{N-1}(\widehat{P}_{t_{N-1}})\Big]\,. \tag{3.3.33}$$

Proof. Since $\tilde{\mathcal{T}}_h$ is L^1-stable, (3.3.27) yields for $p \in \mathcal{P}_n$,

$$\bar{\mathcal{E}}_n(p) \leqslant \int |\bar{u}^{N,M}(t_n,p,e) - \mathbb{E}[\mathcal{V}^\epsilon(t_{n+1},\widehat{P}^{t_n,p}_{t_{n+1}},e)]|\mathrm{d}e$$

Under CASE 1, recall (3.3.15), we then get

$$\bar{\mathcal{E}}_n(p) \leqslant \mathbb{E}\Big[\int |u^{N,M}(t_{n+1},\widehat{P}^{t_n,p}_{t_{n+1}},e) - \mathcal{V}^\epsilon(t_{n+1},\widehat{P}^{t_n,p}_{t_{n+1}},e)|\mathrm{d}e\Big]\,. \tag{3.3.34}$$

Thus,

$$\mathbb{E}\Big[\bar{\mathcal{E}}_n(\widehat{P}_{t_n})\Big] \leqslant \mathbb{E}\Big[\mathcal{E}_{n+1}(\widehat{P}_{t_{n+1}})\Big]\,. \tag{3.3.35}$$

We thus deduce from Lemma 3.3.1

$$\mathbb{E}\Big[\mathcal{E}_n(\widehat{P}_{t_n})\Big] \leqslant \mathbb{E}\Big[\mathcal{E}_n^{\mathrm{T}}(\widehat{P}_{t_n}) + \mathcal{E}_n^D(\widehat{P}_{t_n}) + \mathcal{E}_n^S(\widehat{P}_{t_n})\Big] + \mathbb{E}\Big[\mathcal{E}_{n+1}(\widehat{P}_{t_{n+1}})\Big]\,. \tag{3.3.36}$$

The proof is concluded by induction observing $\mathbb{E}\Big[\mathcal{E}_N(\widehat{P}_{t_N})\Big] = 0$. □

The next section is dedicated to the study of the various error appearing above. We prove there the main theoretical result of the paper:

Theorem 3.3.1 *Let Assumption 3.2.1 hold. Then, under CASE 1,*

$$\mathrm{err}(N,M) \leqslant C\Big(\frac{1}{M} + \frac{\sqrt{\mathfrak{h}}}{\epsilon^2} + \epsilon\Big)\,, \tag{3.3.37}$$

recall (3.3.22). Moreover, setting $\epsilon = \mathfrak{h}^{\frac{1}{6}}$ and $M = \frac{1}{\epsilon}$, we have

$$\int |\mathcal{V}(0,P_0,e) - u_0^{N,M}(P_0,e)|\mathrm{d}e \leqslant C\mathfrak{h}^{\frac{1}{6}}\,. \tag{3.3.38}$$

3.4 Study of the errors

3.4.1 Approximation of transport operator

We discuss here the error introduced by the use of the SPD approximation in our framework. The numerical analysis of this method is now well known see e.g. [53].

Lemma 3.4.1 *Under Assumption 3.2.1 and in CASE 1, the following holds*

$$\mathcal{E}_n^T(p) \leqslant C\frac{\mathfrak{h}}{M_n}\ , p \in \mathcal{P}_n\,. \tag{3.4.1}$$

Proof. By Definition 3.3.2, for $p \in \mathcal{P}_n$ and $n \leqslant N-2$, we have

$$\mathcal{E}_n^T(p) = \int \left|\mathfrak{T}_{\mathfrak{h}}^{M_n}(\bar{u}_n^{N,M}(p,\cdot),p) - \tilde{\mathcal{T}}_{\mathfrak{h}}(\bar{u}_n^{N,M}(p,\cdot),p)\right|\mathrm{d}e \tag{3.4.2}$$

with $\bar{u}_n^{N,M}(p,\cdot) \in \mathcal{I}_{M_n}$. For fixed p, the property of $\mathfrak{T}_{\mathfrak{h}}^M$ are discussed in [53, Section 1.1]. We use here the estimate given in [53, Theorem 3.1], observing that, in our context, there is no error due to the discretization of the initial condition. Indeed, $\bar{u}_n^{N,M}(p,\cdot)$ appears already as the CDF of an empirical distribution. Thus, straightforwardly, we get

$$\mathcal{E}_n^T(p) \leqslant C\frac{\mathfrak{h}}{M_n}, \tag{3.4.3}$$

where C does not depend on p but depends on the Lipschitz constant of $\partial_y\mu$, recall Assumption 3.2.1.
For the step $n = N-1$, we have,

$$\mathcal{E}_{N-1}^{\mathrm{T}}(p) = \int |\mathfrak{T}_{\mathfrak{h}}^M(p,\phi(\cdot))(e) - \mathcal{T}_{\mathfrak{h}}(p,\phi(\cdot)(e))|\mathrm{d}e \tag{3.4.4}$$

recall (3.3.32). It turns out that for our application ϕ is trivially the CDF of an empirical distribution, recall (3.1.2). Thus, we indeed have, $\mathcal{E}_{N-1}^T(p) \leqslant C\frac{\mathfrak{h}}{M_{N-1}}$. □

3.4.2 Regularization error

Proposition 3.4.1 *Under Assumption 3.2.1, the following holds, for $n \leqslant N$,*

$$\mathcal{E}_n^r(p) \leqslant C\epsilon\,,\ p \in \mathbb{R}^d.$$

Proof. We first observe that $\mathcal{E}_N^r(p) = 0$ as ϕ does not depend on p. For $n < N$, we have that

$$\mathcal{E}_n^r(p) = \int |\mathcal{V}^\epsilon(t_n,p,e) - \mathcal{V}(t_n,p,e)|\mathrm{d}e \tag{3.4.5}$$

$$= \int |\int \{\mathcal{V}(t_n,p+q,e) - \mathcal{V}(t_n,p,e)\}\,\varphi_\epsilon(q)\mathrm{d}q|\mathrm{d}e \tag{3.4.6}$$

$$\leqslant \int\int |\mathcal{V}(t_n,p+q,e) - \mathcal{V}(t_n,p,e)|\mathrm{d}e\varphi_\epsilon(q)\mathrm{d}q \tag{3.4.7}$$

Thus, using (3.2.23), we compute

$$\mathcal{E}_0^r(p) \leqslant C \int |q|\varphi_\epsilon(q)\mathrm{d}q \leqslant C\epsilon\,, \tag{3.4.8}$$

which concludes the proof. □

3.4.3 Splitting error

Recall that the splitting error is given by

$$\mathcal{E}_n^S(p) = \int \left|\tilde{\mathcal{T}}_h(p, \mathbb{E}[\mathcal{V}^\epsilon(t_{n+1}, P_{t_{n+1}}^{t_n,p}, \cdot)])(e) - \mathcal{V}^\epsilon(t_n, p, e)\right|\mathrm{d}e\,. \tag{3.4.9}$$

for $0 \leqslant n \leqslant N-1$, $p \in \mathbb{R}^d$.
In [26], the error due the theoretical splitting, has already been studied and the results obtained there can be used in our setting. However, we should point out that here $\mathcal{V}^\epsilon$ appears instead of $\mathcal{V}$. We thus first observe the following.

Lemma 3.4.2 *Under Assumption 3.2.1, the following holds,*

$$\mathcal{E}_n^S(p) \leqslant C(1+|p|^2)h^{\frac{3}{2}} + \mathfrak{E}_n(p) \tag{3.4.10}$$

with

$$\mathfrak{E}_n(p) := \int \left|\Theta_h(\mathcal{V}^\epsilon(t_{n+1}, \cdot))(p, e) - \mathcal{V}^\epsilon(t_n, p, e)\right|\mathrm{d}e\,. \tag{3.4.11}$$

Proof. We compute

$$\begin{aligned}\mathcal{E}_n^S(p) \leqslant & \int \left|\tilde{\mathcal{T}}_h(p, \mathbb{E}[\mathcal{V}^\epsilon(t_{n+1}, P_{t_{n+1}}^{t_n,p}, \cdot)])(e) - \Theta_h(\mathcal{V}^\epsilon(t_{n+1}, \cdot))(p, e)\right|\mathrm{d}e \\ & + \int \left|\Theta_h(\mathcal{V}^\epsilon(t_{n+1}, \cdot))(p, e) - \mathcal{V}^\epsilon(t_n, p, e)\right|\mathrm{d}e\,.\end{aligned}$$

The first term in the RHS above is then controlled by invoking Proposition 3.2.1. □

It remains to study $\mathfrak{E}_n$. The upper bound for this term is obtained in Proposition 3.4.2 below, which allows to conclude for the splitting error in Corollary 3.4.1. We first need the following result.

Lemma 3.4.3 *Let Assumption 3.2.1 hold. Then, for $n \leqslant N-2$,*

$$\sup_{(t,p,e)\in[t_n,t_{n+1}]\times\mathbb{R}^d\times\mathbb{R}} |\Theta_{t_{n+1}-t}(\mathcal{V}^\epsilon(t_{n+1}, \cdot))(p, e) - \mathcal{V}^\epsilon(t, p, e)| \leqslant C\epsilon\,. \tag{3.4.12}$$

Proof. Without loss of generality, we do the proof for $n = 0$, working on $[0, t_1 = \mathfrak{h}]$. We denote $w(s, \cdot) = \Theta_{t_1-s}(\mathcal{V}^\epsilon(t_1, \cdot))$ for $s \in [0, t_1]$. Recall that the following FBSDE is well posed: for $s \in [0, t_1]$,

$$\begin{cases} P_s = \mathrm{p} + \displaystyle\int_0^s b(P_t)\mathrm{d}t + \bar{\sigma}W_s, \\ E_s = \mathrm{e} + \displaystyle\int_0^s \mu(Y_t, P_t)\mathrm{d}t, \\ Y_s = \mathcal{V}^\epsilon(t_1, P_{t_1}, E_{t_1}) - \displaystyle\int_s^{t_1} Z_t \mathrm{d}W_t, \end{cases} \tag{3.4.13}$$

with $Y_s = w(s, P_s, E_s)$ for $s \in [0, t_1]$. Without loss of generality, we will prove (3.4.12) at the point $(0, \mathrm{p}, \mathrm{e})$ (and for $n = 0$).
Let $V_t = Y_t - \mathcal{V}^\epsilon(t, P_t, E_t)$. Applying Ito's formula and using the martingale property of Y we get,

$$\mathrm{d}V_t = \mathrm{d}M_t - \mu(Y_t, P_t)\partial_e \mathcal{V}^\epsilon(t, P_t, E_t)\mathrm{d}t \tag{3.4.14}$$

$$- \left\{ \partial_t \mathcal{V}^\epsilon(t, P_t, E_t) + b(P_t)\partial_p \mathcal{V}^\epsilon(t, P_t, E_t) + \frac{1}{2}\Delta_p \mathcal{V}^\epsilon(t, P_t, E_t) \right\} \mathrm{d}t \tag{3.4.15}$$

where M is a square integrable martingale with $M_0 = 0$.
Using the PDE (3.2.40) satisfied by $\mathcal{V}^\epsilon$ we get

$$\mathrm{d}V_t = \mathrm{d}M_t - (\{\mu(Y_t, P_t)) - \mu(\mathcal{V}^\epsilon(t, P_t, E_t), P_t))\}\, \partial_e \mathcal{V}^\epsilon(t, P_t, E_t) + \theta^\epsilon(t, P_t, E_t))\, \mathrm{d}t \tag{3.4.16}$$

Observe that

$$\mu(Y_t, P_t) - \mu(\mathcal{V}^\epsilon(t, P_t, E_t), P_t)) = c_t V_t \quad \text{with} \quad c_t := \int_0^1 \partial_y \mu(\mathcal{V}^\epsilon(t, P_t, E_t) + \lambda V_t, P_t)\mathrm{d}\lambda \tag{3.4.17}$$

and from the property of μ, recall (3.2.4), we have

$$c_t \leqslant -\ell_1 < 0\,. \tag{3.4.18}$$

We get, for $s \in [0, t_1]$

$$V_s - V_0 = -\int_0^s (c_t V_t \partial_e \mathcal{V}^\epsilon(t, P_t, E_t) + \theta^\epsilon(t, P_t, E_t))\, \mathrm{d}t + M_s \tag{3.4.19}$$

We set, for $0 \leqslant t \leqslant t_1$, $\mathcal{E}_t = e^{\int_0^t c_s \partial_e \mathcal{V}^\epsilon(s, P_s, E_s)\mathrm{d}s}$ and, we have

$$0 \leqslant \mathcal{E}_t \leqslant 1\,, \quad \text{for all } 0 \leqslant t \leqslant t_1\,, \tag{3.4.20}$$

since $\partial_e \mathcal{V}^\epsilon$ is non negative, recall also (3.4.18). We then compute

$$\mathcal{E}_s V_s - V_0 = -\int_0^s \theta^\epsilon(t, P_t, E_t)\mathcal{E}_t \mathrm{d}t + N_s \tag{3.4.21}$$

with N a square integrable martingale such that $N_0 = 0$. In particular, recalling (3.2.41), we get

$$V_0 \leqslant |\mathbb{E}[\mathcal{E}_s V_s]\,| + C\mathfrak{h}\epsilon + C\epsilon\mathbb{E}\left[\int_0^s \partial_e \mathcal{V}^\epsilon(t, P_t, E_t)\mathcal{E}_t \mathrm{d}t\right] \tag{3.4.22}$$

where we use the fact that $|\partial_p \mathcal{V}|$ is bounded and $\partial_e \mathcal{V}^\epsilon(t, P_t, E_t) \geqslant 0$. The above inequality reads also

$$|V_0| \leqslant |\mathbb{E}[\mathcal{E}_s V_s]\,| + C\mathfrak{h}\epsilon - C\epsilon\mathbb{E}\left[\int_0^s \frac{c_t}{|c_t|}\partial_e \mathcal{V}^\epsilon(t, P_t, E_t)\mathcal{E}_t \mathrm{d}t\right] \tag{3.4.23}$$

Observing that

$$\dot{\mathcal{E}}_t = c_t \partial_e \mathcal{V}^\epsilon(t, P_t, E_t)\mathcal{E}_t,$$

since $|c_t| \geqslant \ell_1 > 0$, we obtain

$$|V_0| \leqslant |\mathbb{E}[\mathcal{E}_s V_s]| + C(1+\mathfrak{h})\epsilon \tag{3.4.24}$$

and since $V_{t_1} = 0$

$$|w(0,\mathrm{p},\mathrm{e}) - \mathcal{V}^\epsilon(0,\mathrm{p},\mathrm{e})| = |V_0| \leqslant C\epsilon\,,$$

which concludes the proof. □

Proposition 3.4.2 *Let Assumption 3.2.1 hold. Then, for $n \leqslant N-2$, $p \in \mathbb{R}^d$,*

$$\mathfrak{E}_n(p) = \int |\Theta_\mathfrak{h}(\mathcal{V}^\epsilon(t_{n+1},\cdot))(p,e) - \mathcal{V}^\epsilon(t_n,p,e)|\mathrm{d}e \leqslant C\mathfrak{h}\epsilon\,. \tag{3.4.25}$$

Proof. Without loss of generality, we prove the statement in the same setting as the one used for the proof of Lemma 3.4.3. We just stress here the dependence upon the initial condition: $V_t^{\mathrm{e}} = Y_t^{\mathrm{e}} - \mathcal{V}^\epsilon(t, P_t, E_t^{\mathrm{e}})$ since $E_0 = \mathrm{e}$. We consider the tangent process $\partial_e E$ given by

$$\partial_e E_t = 1 + \int_0^t \partial_y \mu(Y_s, P_s)\partial_e w(s, P_s, E_s)\partial_e E_s \mathrm{d}s, \tag{3.4.26}$$

$$= e^{\int_0^t \partial_y \mu(Y_s,P_s)\partial_e w(s,P_s,E_s)\mathrm{d}s}. \tag{3.4.27}$$

And we observe that $0 \leqslant \partial_e E_t \leqslant 1$, for all $0 \leqslant t \leqslant t_1$, since $\partial_e w \geqslant 0$ and μ is decreasing in y, recall (3.2.4).
In order to bound the error $\int |V_0^e|\mathrm{d}e$, we will study the dynamics of $t \mapsto \int |\mathbb{E}[V_t^e \partial_e E_t^e]|\mathrm{d}e$.

Recalling (3.4.19), we compute

$$\mathrm{d}(V_t^e \partial_e E_t) = \mathrm{d}N_t + V_t^e \partial_y \mu(Y_t, P_t)\partial_e w(t, P_t, E_t)\partial_e E_t \mathrm{d}t \tag{3.4.28}$$

$$-(c_t V_t^e \partial_e \mathcal{V}^\epsilon(t, P_t, E_t)\partial_e E_t + \theta^\epsilon(t, P_t, E_t^e)\partial_e E_t)\,\mathrm{d}t, \tag{3.4.29}$$

where N is a square integrable martingale satisfying $N_0 = 0$.

$$\mathbb{E}\big[V_\mathfrak{h}^e \partial_e E_\mathfrak{h} - V_0^e\big] = \mathbb{E}\bigg[\int_0^\mathfrak{h} V_t^e\big(\partial_y \mu(Y_t, P_t)\partial_e[w(t, P_t, E_t^e)] - c_t V_t^e \partial_e[\mathcal{V}^\epsilon(t, P_t, E_t^e)]\big)\mathrm{d}t\bigg] \tag{3.4.30}$$

$$+ \mathbb{E}\bigg[\int_0^\mathfrak{h} \theta^\epsilon(t, P_t, E_t)\partial_e E_t \mathrm{d}t\bigg]\,. \tag{3.4.31}$$

Since $V_\mathfrak{h} = 0$ and $\partial_e w \geqslant 0$, $\partial_e \mathcal{V}^\epsilon \geqslant 0$, $\partial_e E_t \geqslant 0$, we obtain

$$\int |V_0^e|\mathrm{d}e \leqslant \int_0^\mathfrak{h} \mathbb{E}\bigg[\int |V_t^e \partial_y \mu(Y_t, P_t)|\partial_e[w(t, P_t, E_t^e)]\mathrm{d}e\bigg]\mathrm{d}t \tag{3.4.32}$$

$$+ \int_0^\mathfrak{h} \mathbb{E}\bigg[\int |c_t V_t^e|\partial_e[\mathcal{V}^\epsilon(t, P_t, E_t^e)]\mathrm{d}e\bigg]\mathrm{d}t$$

$$+ \int_0^\mathfrak{h} \mathbb{E}\bigg[\int |\theta^\epsilon(t, P_t, E_t)|\partial_e E_t \mathrm{d}e\bigg]\mathrm{d}t.$$

We obtain, using Lemma 3.4.3 and the bound on $\|\partial_y \mu\|_\infty$,

$$\int |V_t^e \partial_y \mu(Y_t, P_t)| \partial_e [w(t, P_t, E_t^e)] \mathrm{d}e \leqslant C\epsilon \int \partial_e [w(t, P_t, E_t^e)] \mathrm{d}e, \\ \leqslant C\epsilon, \tag{3.4.33}$$

where we used the fact that w is bounded in the last inequality. Similar arguments, since c is bounded, lead to

$$\int |c_t V_t^e| \partial_e [\mathcal{V}^\epsilon(t, P_t, E_t^e)] \mathrm{d}e \leqslant C\epsilon \,. \tag{3.4.34}$$

From (3.2.41), we know that

$$|\theta^\epsilon(t, P_t, E_t)| \leqslant C\epsilon \left(\int |\partial_p \mathcal{V}(t, P_t + q, E_t^e)| \varphi_\epsilon(q) \mathrm{d}q + \partial_e \mathcal{V}^\epsilon(t, P_t, E_t) \right). \tag{3.4.35}$$

We compute, using the change of variable $e \mapsto \zeta = E_t^e$

$$\int \int |\partial_p \mathcal{V}(t, P_t + q, E_t^e)| \varphi_\epsilon(q) \mathrm{d}q \partial_e E_t^e \mathrm{d}e = \int \int |\partial_p \mathcal{V}(t, P_t + q, \zeta)| \varphi_\epsilon(q) \mathrm{d}q \mathrm{d}\zeta, \tag{3.4.36}$$

$$\leqslant C, \tag{3.4.37}$$

where we used the L^1-bound on $\partial_p V$ given in (3.2.22) . We then compute

$$\mathbb{E}\left[\int |\theta^\epsilon(t, P_t, E_t)| \partial_e E_t \mathrm{d}e \right] \leqslant C\epsilon (1 + \mathbb{E}\left[\int \partial_e \mathcal{V}^\epsilon(t, P_t, E_t) \partial_e E_t \mathrm{d}e \right]), \tag{3.4.38}$$

$$\leqslant C\epsilon. \tag{3.4.39}$$

The proof is concluded by combining the previous inequality, the estimates given in (3.4.33)-(3.4.34) with (3.4.32). □

Combining Lemma 3.4.2 with the result Proposition 3.4.2, we obtain straightforwardly the following.

Corollary 3.4.1 *Let Assumption 3.2.1 hold. Then, for $n \leqslant N-2$, $p \in \mathbb{R}^d$,*

$$\mathcal{E}_n^S(p) \leqslant C(1 + |p|^2)\mathfrak{h}^{\frac{3}{2}} + C\epsilon\mathfrak{h} \,. \tag{3.4.40}$$

3.4.4 Diffusion error

We now study the term given in (3.3.28) and we straightforwardly observe

$$\mathcal{E}_n^D(p) = \int \left| \tilde{\mathcal{T}}_h(p, \mathbb{E}[\mathcal{V}^\epsilon(t_{n+1}, \hat{P}_{t_{n+1}}^{t_n,p}, \cdot)])(e) - \tilde{\mathcal{T}}_h(p, \mathbb{E}[\mathcal{V}^\epsilon(t_{n+1}, P_{t_{n+1}}^{t_n,p}, \cdot)])(e) \right| \mathrm{d}e \,, \tag{3.4.41}$$

$$\leqslant \int \left| \mathbb{E}[\mathcal{V}^\epsilon(t_{n+1}, \hat{P}_{t_{n+1}}^{t_n,p}, e)] - \mathbb{E}[\mathcal{V}^\epsilon(t_{n+1}, P_{t_{n+1}}^{t_n,p}, e)] \right| \mathrm{d}e \,, \tag{3.4.42}$$

where we use the L^1-stability of $\tilde{\mathcal{T}}_h$.

This motivates the introduction of the following auxiliary result.

Proposition 3.4.3 *Let Assumption 3.2.1 hold. For $0 \leqslant n \leqslant N-1$, let w_n be the solution on $[t_n, t_{n+1}] \times \mathbb{R}^d$ to the following PDE:*

$$\partial_t w + b(p)\partial_p w + \frac{1}{2}\bar{\sigma}^2 \Delta_{pp} w = 0 \text{ and } w(t_{n+1}, \cdot) := \mathcal{V}^\epsilon(t_{n+1}, \cdot, e)\,, \tag{3.4.43}$$

for a fixed $e \in \mathbb{R}$. Then, under Assumption 3.2.1, the followings hold, for $q, q' \in \mathbb{R}^d$ and $t \in [0, T)$,

$$\int |\partial_{p^\ell} w_n(t,q,e) - \partial_{p^\ell} w_n(t,q',e)|\mathrm{d}e \leqslant \frac{C}{\epsilon}|q-q'| \tag{3.4.44}$$

and

$$\int |\partial^2_{p^\ell p^{\ell'}} w_n(t,q,e) - \partial^2_{p^\ell p^{\ell'}} w_n(t,q',e)|\mathrm{d}e \leqslant \frac{C}{\epsilon^2}|q-q'|, \tag{3.4.45}$$

for all $\ell, \ell' \in \{1, \dots, d\}$. Moreover,

$$\int |\partial_p w_n(t,p,e)|\mathrm{d}e \leqslant C. \tag{3.4.46}$$

Proof. For ease of presentation, the proof is done in the one-dimensional case. By Theorem 2.3.5 in Zhang [68], we have the following expressions for the first and second order derivative with respect to vector p, for $(t,p,e) \in [t_n, t_{n+1}] \times \mathbb{R} \times \mathbb{R}$,

$$\partial_p w_n(t,p,e) = \mathbb{E}\Big[\partial_p \mathcal{V}^\epsilon(t_{n+1}, P^{t,p}_{t_{n+1}}, e)\partial_p P^{t,p}_{t_{n+1}}\Big]\,, \tag{3.4.47}$$

$$\partial^2_{pp} w_n(t,p,e) = \mathbb{E}\Big[\partial^2_{pp}\mathcal{V}^\epsilon(t_{n+1}, P^{t,p}_{t_{n+1}}, e)(\partial_p P^{t,p}_{t_{n+1}})^2 + \partial_p \mathcal{V}^\epsilon(t_{n+1}, P^{t,p}_{t_{n+1}}, e)\partial^2_{pp} P^{t,p}_{t_{n+1}}\Big]\,, \tag{3.4.48}$$

where, for $t \leqslant s \leqslant t_{n+1}$,

$$P^{t,p}_s = p + \int_t^s b(P^{t,p}_r)\mathrm{d}r + \bar{\sigma}(W_s - W_t)\,, \tag{3.4.49}$$

$$\partial_p P^{t,p}_s = 1 + \int_t^s b'(P^{t,p}_r)\partial_p P^{t,p}_r \mathrm{d}r\,, \tag{3.4.50}$$

$$\partial^2_{pp} P^{t,p}_s = \int_t^s \left(b''(P_r)|\partial_p P^{t,p}_r|^2 + b'(P_r)\partial^2_{pp} P^{t,p}_r\right)\mathrm{d}r\,. \tag{3.4.51}$$

In this setting, classical arguments lead to,

$$\mathbb{E}\left[\sup_{s\in[t,t_{n+1}]}|\partial_p P^{t,p}_s|^\kappa + \sup_{s\in[t,t_{n+1}]}|\partial^2_{pp} P^{t,p}_s|^\kappa\right] \leqslant C_\kappa, \tag{3.4.52}$$

and for $q, q' \in \mathbb{R}$, $s \in [t,T]$, $\kappa \geqslant 1$,

$$\mathbb{E}\Big[|P^{t,q}_s - P^{t,q'}_s|^\kappa + |\partial_p P^{t,q}_s - \partial_p P^{t,q'}_s|^\kappa + |\partial^2_{pp} P^{t,q}_s - \partial^2_{pp} P^{t,q'}_s|^\kappa\Big] \leqslant C|q-q'|^\kappa\,. \tag{3.4.53}$$

We now study the second order derivative given in (3.4.48).
We compute, for $(t,q,q') \in [t_n, t_{n+1}] \times \mathbb{R} \times \mathbb{R}$,

$$\int |\partial^2_{pp} w_n(t,q,e) - \partial^2_{pp} w_n(t,q',e)| \mathrm{d}e \tag{3.4.54}$$

$$\leqslant \mathbb{E}\Big[\int |\partial^2_{pp}\mathcal{V}^\epsilon(t_{n+1}, P^{t,q}_{t_{n+1}}, e)(\partial_p P^{t,q}_{t_{n+1}})^2 - \partial^2_{pp}\mathcal{V}^\epsilon(t_{n+1}, P^{t,q'}_{t_{n+1}}, e)(\partial_p P^{t,q'}_{t_{n+1}})^2| \mathrm{d}e\Big] := B_1 \tag{3.4.55}$$

$$+ \mathbb{E}\Big[\int |\partial_p \mathcal{V}^\epsilon(t_{n+1}, P^{t,q}_{t_{n+1}}, e)\partial^2_{pp} P^{t,q}_{t_{n+1}} - \partial_p \mathcal{V}^\epsilon(t_{n+1}, P^{t,q'}_{t_{n+1}}, e)\partial^2_{pp} P^{t,q'}_{t_{n+1}}| \mathrm{d}e\Big] := B_2 \tag{3.4.56}$$

For the first term B_1,

$$\begin{aligned} B_1 \leqslant{}& \mathbb{E}\Big[\int |\partial^2_{pp}\mathcal{V}^\epsilon(t_{n+1}, P^{t,q}_{t_{n+1}}, e)(\partial_p P^{t,q}_{t_{n+1}})^2 - \partial^2_{pp}\mathcal{V}^\epsilon(t_{n+1}, P^{t,q}_{t_{n+1}}, e)(\partial_p P^{t,q'}_{t_{n+1}})^2| \mathrm{d}e\Big] \\ &+ \mathbb{E}\Big[\int |\partial^2_{pp}\mathcal{V}^\epsilon(t_{n+1}, P^{t,q}_{t_{n+1}}, e)(\partial_p P^{t,q'}_{t_{n+1}})^2 - \partial^2_{pp}\mathcal{V}^\epsilon(t_{n+1}, P^{t,q'}_{t_{n+1}}, e)(\partial_p P^{t,q'}_{t_{n+1}})^2| \mathrm{d}e\Big] \end{aligned}$$

We then compute

$$\mathbb{E}\Big[\int |\partial^2_{pp}\mathcal{V}^\epsilon(t_{n+1}, P^{t,q}_{t_{n+1}}, e)(\partial_p P^{t,q}_{t_{n+1}})^2 - \partial^2_{pp}\mathcal{V}^\epsilon(t_{n+1}, P^{t,q}_{t_{n+1}}, e)(\partial_p P^{t,q'}_{t_{n+1}})^2| \mathrm{d}e\Big], \tag{3.4.57}$$

$$\leqslant \mathbb{E}\Big[\Big|(\partial_p P^{t,q}_{t_{n+1}})^2 - (\partial_p P^{t,q'}_{t_{n+1}})^2\Big| \int |\partial^2_{pp}\mathcal{V}^\epsilon(t_{n+1}, P^{t,q}_{t_{n+1}}, e)| \mathrm{d}e\Big], \tag{3.4.58}$$

$$\leqslant \frac{C}{\epsilon}\mathbb{E}\Big[\Big|(\partial_p P^{t,q}_{t_{n+1}})^2 - (\partial_p P^{t,q'}_{t_{n+1}})^2\Big|\Big], \tag{3.4.59}$$

where we used for the last inequality Lemma 3.2.1. Observing that

$$\Big|(\partial_p P^{t,q}_{t_{n+1}})^2 - (\partial_p P^{t,q'}_{t_{n+1}})^2\Big| \leqslant \Big|\partial_p P^{t,q}_{t_{n+1}} + \partial_p P^{t,q'}_{t_{n+1}}\Big| \cdot \Big|\partial_p P^{t,q}_{t_{n+1}} - \partial_p P^{t,q'}_{t_{n+1}}\Big|,$$

we combine Cauchy-Schwarz inequality with (3.4.53) to obtain

$$\mathbb{E}\Big[\Big|(\partial_p P^{t,q}_{t_{n+1}})^2 - (\partial_p P^{t,q'}_{t_{n+1}})^2\Big|\Big] \leqslant C|q-q'|\,. \tag{3.4.60}$$

Combining the previous inequality with (3.4.59), we get

$$\mathbb{E}\Big[\int |\partial^2_{pp}\mathcal{V}^\epsilon(t_{n+1}, P^{t,q}_{t_{n+1}}, e)(\partial_p P^{t,q}_{t_{n+1}})^2 - \partial^2_{pp}\mathcal{V}^\epsilon(t_{n+1}, P^{t,q}_{t_{n+1}}, e)(\partial_p P^{t,q'}_{t_{n+1}})^2| \mathrm{d}e\Big] \leqslant \frac{C}{\epsilon}|q-q'|\,. \tag{3.4.61}$$

We also compute

$$\begin{aligned} &\mathbb{E}\Big[\int |\partial^2_{pp}\mathcal{V}^\epsilon(t_{n+1}, P^{t,q}_{t_{n+1}}, e)(\partial_p P^{t,q'}_{t_{n+1}})^2 - \partial^2_{pp}\mathcal{V}^\epsilon(t_{n+1}, P^{t,q'}_{t_{n+1}}, e)(\partial_p P^{t,q'}_{t_{n+1}})^2| \mathrm{d}e\Big] \\ &\leqslant \mathbb{E}\Big[(\partial_p P^{t,q'}_{t_{n+1}})^2 \int |\partial^2_{pp}\mathcal{V}^\epsilon(t_{n+1}, P^{t,q}_{t_{n+1}}, e) - \partial^2_{pp}\mathcal{V}^\epsilon(t_{n+1}, P^{t,q'}_{t_{n+1}}, e)| \mathrm{d}e\Big] \\ &\leqslant \frac{C}{\epsilon^2}|q-q'| \end{aligned}$$

where we used Lemma 3.2.1 and (3.4.52), for the last inequality. Combining (3.4.61) with the previous inequality, we finally obtain that

$$B_1 \leqslant \frac{C}{\epsilon^2}|q-q'| + \frac{C}{\epsilon}|q-q'| \,. \tag{3.4.62}$$

For the term B_2 given in (3.4.56), we observe

$$\begin{aligned} B_2 \leqslant \mathbb{E}\Big[\int |\partial_p \mathcal{V}^\epsilon(t_{n+1}, P^{t,q}_{t_{n+1}}, e)\partial^2_{pp} P^{t,q}_{t_{n+1}} - \partial_p \mathcal{V}^\epsilon(t_{n+1}, P^{t,q}_{t_{n+1}}, e)\partial^2_{pp} P^{t,q'}_{t_{n+1}}|\mathrm{d}e\Big] \\ + \mathbb{E}\Big[\int |\partial_p \mathcal{V}^\epsilon(t_{n+1}, P^{t,q}_{t_{n+1}}, e)\partial^2_{pp} P^{t,q'}_{t_{n+1}} - \partial_p \mathcal{V}^\epsilon(t_{n+1}, P^{t,q'}_{t_{n+1}}, e)\partial^2_{pp} P^{t,q'}_{t_{n+1}}|\mathrm{d}e\Big] \end{aligned}$$

Combining Lemma 3.2.1, the estimates given in (3.4.53)-(3.4.52), with similar computations as done previously, we obtain

$$B_2 \leqslant \frac{C}{\epsilon}|q-q'| + C|q-q'| \,. \tag{3.4.63}$$

Inserting (3.4.62)-(3.4.63) back into (3.4.56), we obtain the

$$\int |\partial^2_{pp} w_n(t,q,e) - \partial^2_{pp} w_n(t,q',e)|\mathrm{d}e \leqslant \frac{C}{\epsilon}|q-q'| \,, \tag{3.4.64}$$

as $\epsilon \leqslant 1$.
Similar arguments allow to retrieve the estimates for the first order derivatives. □

Proposition 3.4.4 *Under Assumption 3.2.1, the following holds*

$$\mathcal{E}^D_n(p) \leqslant C\frac{\mathfrak{h}^{\frac{3}{2}}}{\epsilon^2}$$

for $0 \leqslant n \leqslant N-1$ *and* $p \in \mathbb{R}^d$.

Proof. For ease of presentation, we do the proof in dimension $d = 1$.
1. We first recall Definition 3.3.1 and (3.3.3). In this context, we introduce two new discrete processes:

$$\begin{aligned} \widehat{P}^{t_n,p}_t &= p + b(p)(t-t_n) + \bar{\sigma}\frac{\sqrt{t-t_n}}{\sqrt{\mathfrak{h}}}\Delta\widehat{W}_n \,, \\ \bar{P}^{t_n,p,\lambda}_t &= p + b(p)(t-t_n) + \lambda\bar{\sigma}\frac{\sqrt{t-t_n}}{\sqrt{\mathfrak{h}}}\Delta\widehat{W}_n, \end{aligned}$$

for $p \in \mathbb{R}$, $t \in [t_n, t_{n+1}]$, $\lambda \in [0,1]$ and $0 \leqslant n \leqslant N-1$.
Now, recalling (3.4.42), we first observe

$$\mathbb{E}[\mathcal{V}^\epsilon(t_{n+1}, \widehat{P}^{t_n,p}_{t_{n+1}}, e)] - \mathbb{E}[\mathcal{V}^\epsilon(t_{n+1}, P^{t_n,p}_{t_{n+1}}, e)] = \mathbb{E}[w_n(t_{n+1}, \widehat{P}^{t_n,p}_{t_{n+1}}, e)] - w_n(t_n, p, e) \,. \tag{3.4.65}$$

We apply the discrete Ito formula given of Proposition 14 in [24] to our much simpler framework, to obtain

$$\mathbb{E}[w_n(t_{n+1},\widehat{P}^{t_n,p}_{t_{n+1}},e)]-w_n(t_n,p,e)=\int_{t_n}^{t_{n+1}}\mathbb{E}\Big[\partial_t w_n(t,\widehat{P}^{t_n,p}_t,e)+b(p)\partial_p w_n(t,\widehat{P}^{t_n,p}_t,e)\Big]\,\mathrm{d}t \\ +\frac{\bar\sigma^2}{2}\mathbb{E}\Big[\int_{t_n}^{t_{n+1}}\int_0^1\partial^2_{pp}w_n(t,\bar P^{t_n,p,\lambda}_t,e)\mathrm{d}\lambda\mathrm{d}t\Big]\,.$$

Using the PDE (3.4.43) satisfied by w_n, the previous equality leads to

$$\mathbb{E}[w_n(t_{n+1},\widehat{P}^{t_n,p}_{t_{n+1}},e)]-w_n(t_n,p,e) \\ =\int_{t_n}^{t_{n+1}}\mathbb{E}\Big[\Big(b(p)-b(\widehat{P}^{t_n,p}_t)\Big)\,\partial_p w_n(t,\widehat{P}^{t_n,p}_t,e)\Big]\,\mathrm{d}t \tag{3.4.66}$$

$$+\frac{\bar\sigma^2}{2}\mathbb{E}\Big[\int_{t_n}^{t_{n+1}}\int_0^1[\partial^2_{pp}w_n(t,\bar P^{t_n,p,\lambda}_t,e)-\partial^2_{pp}w_n(t,\widehat{P}^{t_n,p}_t,e)]\mathrm{d}\lambda\mathrm{d}t\Big]\,. \tag{3.4.67}$$

2. For $e\in\mathbb{R}$, we denote by $A^1(e)$, the term in (3.4.66) and by $A^2(e)$, the term in (3.4.67) .
We compute

$$|A^1(e)|\leqslant\int_{t_n}^{t_{n+1}}\mathbb{E}\Big[|(b(p)-b(\widehat{P}^{t_n,p}_t)||\partial_p w_n(t,\widehat{P}^{t_n,p}_t,e)|\Big]\,\mathrm{d}t, \\ \leqslant C\mathfrak{h}^{\frac12}\int_{t_n}^{t_{n+1}}\mathbb{E}\Big[|\partial_p w_n(t,\widehat{P}^{t_n,p}_t,e)|\Big]\,\mathrm{d}t\,,$$

and thus

$$\int|A^1(e)|\mathrm{d}e\leqslant C\mathfrak{h}^{\frac12}\int_{t_n}^{t_{n+1}}\mathbb{E}\Big[\int|\partial_p w_n(t,\widehat{P}^{t_n,p}_t,e)|\mathrm{d}e\Big]\,\mathrm{d}t\,, \\ \leqslant C\mathfrak{h}^{\frac32}\,, \tag{3.4.68}$$

where we used (3.4.46) for the last inequality.
Using Proposition 3.4.3, we compute

$$\int|\partial^2_{pp}w_n(t,\bar P^{t_n,p,\lambda}_t,e)-\partial^2_{pp}w_n(t,\widehat{P}^{t_n,p}_t,e)|\mathrm{d}e\leqslant\frac{C}{\epsilon^2}|\bar P^{t_n,p,\lambda}_t-\widehat{P}^{t_n,p}_t|\,, \\ \leqslant\frac{C}{\epsilon^2}\sqrt{\mathfrak{h}}\,.$$

This yields

$$\int|A_2(e)|\mathrm{d}e\leqslant\frac{C}{\epsilon^2}\mathfrak{h}^{\frac32}\,. \tag{3.4.69}$$

Combining the previous inequality with (3.4.68) and (3.4.66)-(3.4.67), we get

$$\int|\mathbb{E}[w_n(t_{n+1},\widehat{P}^{t_n,p}_{t_{n+1}},e)]-w_n(t_n,p,e)|\mathrm{d}e\leqslant\frac{C}{\epsilon^2}\mathfrak{h}^{\frac32}\,.$$

The proof is concluded recalling (3.4.65) and (3.4.42). □

3.4.5 Proof of Theorem 3.3.1

The proof of our main is now almost straightforward. From Lemma 3.4.1, Corollary 3.4.1 and Proposition 3.4.4, we observe that

$$\mathbb{E}\Big[\mathcal{E}_n^{\mathrm{T}}(\widehat{P}_{t_n})\Big] \leqslant C\frac{\mathfrak{h}}{M}\ ,\ \mathbb{E}\Big[\mathcal{E}_n^{D}(\widehat{P}_{t_n})\Big] \leqslant C\frac{\mathfrak{h}^{\frac{3}{2}}}{\epsilon^2} \ \text{ and } \ \mathbb{E}\Big[\mathcal{E}_n^{S}(\widehat{P}_{t_n})\Big] \leqslant C\mathfrak{h}\left(\mathfrak{h}^{\frac{1}{2}}+\epsilon\right). \tag{3.4.70}$$

Summing over n, we get

$$\sum_{n=0}^{N-2}\mathbb{E}\Big[\mathcal{E}_n^{\mathrm{T}}(\widehat{P}_{t_n})+\mathcal{E}_n^{D}(\widehat{P}_{t_n})+\mathcal{E}_n^{S}(\widehat{P}_{t_n})\Big] \leqslant C(\frac{1}{M}+\frac{\sqrt{\mathfrak{h}}}{\epsilon^2}+\epsilon) \tag{3.4.71}$$

For the last step, we obtain

$$\mathbb{E}\Big[\mathcal{E}_{N-1}(\widehat{P}_{t_{N-1}})\Big] \leqslant C(\frac{h}{M}+\epsilon+\mathfrak{h}\left(\mathfrak{h}^{\frac{1}{2}}+\epsilon\right)) \tag{3.4.72}$$

combining (3.3.31) with Proposition 3.4.1 and Proposition 3.2.1. The previous inequality combined with (3.4.71) and Proposition 3.3.1 yields (3.3.37).
Balancing optimally the errors in (3.3.37) allows to conclude by proving (3.3.38). □

3.5 Numerics

In this section, we realize numerical experiments to test in practice the schemes introduced in Section 3.3.1.

We first introduce the models we will use. They have already been considered in [26], which facilitates the comparison with previous numerical results.
Let us first define the following toy model where the process P corresponds to a Brownian motion and is a multidimensional version of the model given in Remark 3.2.2:

Example 3.5.1 (Linear model)

$$dP_t = \sigma \mathrm{d}W_t, dE_t = \left(\frac{1}{\sqrt{d}}\sum_{\ell=1}^{d} P_t^\ell - Y_t\right)\mathrm{d}t \tag{3.5.1}$$

with terminal function $(p,e)\mapsto \phi(p,e)=\mathbf{1}_{\{e\geqslant 0\}}$ *and where* W *is a* d*-dimensional Brownian motion and* $\sigma>0$.

We will also consider a multiplicative model:

Example 3.5.2 (Multiplicative model) *Let* W *be a* d*-dimensional Brownian motion. For all* $\ell\in\{1,\dots,d\}$, *we set*

$$\mathrm{d}P_t^\ell = \mu P_t^\ell \mathrm{d}t + \sigma P_t^\ell \mathrm{d}W_t^\ell,\ P_0^\ell = 1,\ \textit{and}\ \mathrm{d}E_t = \tilde{\mu}(Y_t,P_t)\mathrm{d}t \tag{3.5.2}$$

with $(y,p)\mapsto\tilde{\mu}(y,p)=\left(\prod_{\ell=1}^d p^\ell\right)^{\frac{1}{\sqrt{d}}} e^{-\theta y}$, *for some* $\theta>0$. *The terminal condition is given by* $(p,e)\mapsto\phi(p,e)=\mathbf{1}_{\{e\geqslant 0\}}$.

As mentioned in [26], one advantage of these models is that they can be reduced to models with lower dimension (at most 2) whatever the value of d. For comparison, we will also use some numerical *proxy*: for the first model 3.5.1, we use the method considered in [9] applied to the one dimensional reduction of the model, for the second model 3.5.2 we use the NN & Upwind scheme. Both methods are introduced and discussed in [26].

We also observe that the above models fit into the setting of Section 3.3.1.2, recall Assumption 3.3.1. As shown below and as expected, they are thus numerically tractable. We shall use in this regard the scheme introduced in Definition 3.3.2, linked to CASE 1. We will also consider CASE 2, where the number of particles is capped. To this end, we need to define precisely the operator $\mathfrak{R}^{M,m}$ appearing in Definition 3.3.3.

Definition 3.5.1 (Operator $\mathfrak{R}^{M,m}$) *For $M \geqslant m \geqslant 1$, we first denote S^M the operator of sorting M particles in ascending order, namely*

$$\mathbb{R}^M \ni \xi \mapsto S^M(\xi) \in \mathcal{D}_M. \tag{3.5.3}$$

At each step n, for a set of $2dM$ particles namely $\xi \in \mathbb{R}^{2dM}$, $S^{2dM}(\xi)$ could be written as follows:

$$S^{2dM}(\xi) = (\widetilde{S}^{2d,1}(\xi), \cdots, \widetilde{S}^{2d,M}(\xi)), \tag{3.5.4}$$

where for $1 \leqslant i \leqslant M$, $\widetilde{S}^{2d,i}(\xi) := \left(S_j^{2dM}(\xi)\right)_{2d(i-1)<j\leqslant 2di} \in \mathcal{D}_{2d}$, with $S_i^{2dM}(\xi)$ denoting the i-th coordinate of vector $S^{2dM}(\xi)$. For $\psi^\xi \in \mathcal{I}^{2dM}$ associated to $\xi \in \mathcal{D}_{2dM}$, we recall that

$$\psi^\xi = H * \Big(\frac{1}{2dM} \sum_{m=1}^{2dM} \delta_{S_m^{2dM}(\xi)}\Big),$$

we then define the following operator

$$\psi^\xi \ni \mathcal{I}^{2dM} \mapsto \mathfrak{R}^{2dM,M}(\psi^\xi) := H * \Big(\frac{1}{M} \sum_{m=1}^{M} \delta_{\tilde{e}_m}\Big) \in \mathcal{I}^M, \tag{3.5.5}$$

where three different choices for $\tilde{e}_m$ are considered, leading to three different implementations. namely, for each $1 \leqslant m \leqslant M$,

`mean`*: The mean position of $2d$ particles of $\widetilde{S}^{2d,m}(\xi)$, namely*

$$\tilde{e}_m := \frac{1}{2d} \sum_{j=2d(m-1)+1}^{2dm} S_j^{2dM}(\xi). \tag{3.5.6}$$

`leftmost`*: The minimum position among the $2d$ particles of $\widetilde{S}^{2d,m}(\xi)$ is kept,*

$$\tilde{e}_m := \min\{S_j^{2dM}(\xi), 2d(m-1)+1 \leqslant j \leqslant 2dm\} = S^{2dM}_{2d(m-1)+1}(\xi). \tag{3.5.7}$$

`rightmost`: *The maximum position among the* $2d$ *particles of* $\widetilde{S}^{2d,m}(\xi)$ *is kept,*

$$\tilde{e}_m := \max\{S_j^{2dM}(\xi), 2d(m-1)+1 \leqslant j \leqslant 2dm\} = S_{2dm}^{2dM}(\xi). \tag{3.5.8}$$

First of all, to validate empirically our different implementations of operator $\mathfrak{R}$, we report the $L1$-error and $L\infty$-error against "proxy" solution for different numbers of particles, based on different reducing particle implementations defined in Definition 3.5.1 for $\sigma = 0.01, 0.3, 1.0$, see Table 3.1. We observe that those three implementations of $\mathfrak{R}$ including `leftmost`, `mean`, `rightmost` of positions of particles, have practically same numerical results for different levels of volatilities. The advantage of considering the CASE 2 scheme is that the number of particles does not grow exponentially during the iterations, hence it takes less computational time compared to CASE 1, see Table 3.2. We observe that as dimension d grows, the computational time of CASE 1 scheme increased exponentially. Hence in the following, we only consider the implemented operator $\mathfrak{R}$ `mean`.

Sigma	Number of particles	Method	$L1$-error	$L\infty$-error
1.0	1000	`leftmost`	0.00571	0.0167
		`mean`	0.00496	0.0150
		`rightmost`	0.00539	0.0180
	5000	`leftmost`	0.00505	0.0145
		`mean`	0.00492	0.0146
		`rightmost`	0.00492	0.0153
0.3	1000	`leftmost`	0.00134	0.0085
		`mean`	0.00088	0.0061
		`rightmost`	0.00125	0.0091
	5000	`leftmost`	0.00094	0.0068
		`mean`	0.00088	0.0061
		`rightmost`	0.00092	0.0065
0.01	1000	`leftmost`	0.00027	0.0039
		`mean`	0.00013	0.0020
		`rightmost`	0.00048	0.0043
	5000	`leftmost`	0.00009	0.0013
		`mean`	0.00008	0.0017
		`rightmost`	0.00013	0.0018

Table 3.1: $L1$-error and $L\infty$-error for model Example 3.5.1 with different numbers of particles with respect to `leftmost,mean,rightmost`, note that the time steps $N = 20$.

Dimension	$d = 1$	$d = 4$
Time for CASE 1	46.96s	784s
Time for CASE 2	0.3s	1.3s

Table 3.2: Computational cost in Example 3.5.1 for different dimension d (for the P-variable) for CASE 1 and CASE 2 schemes.

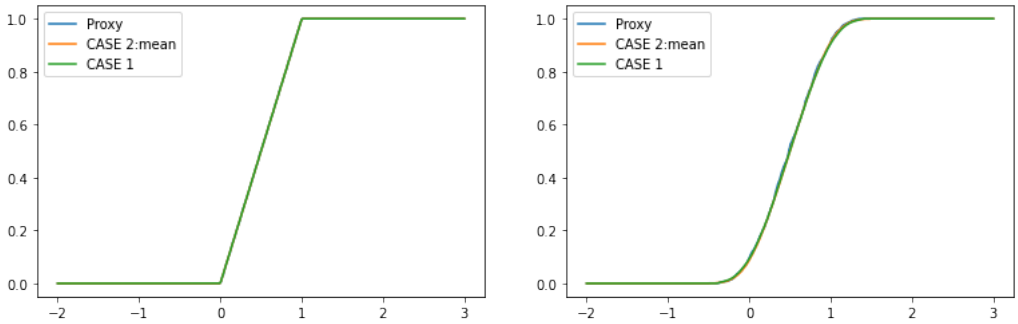

(a) $\sigma = 0.01$ (b) $\sigma = 0.3$

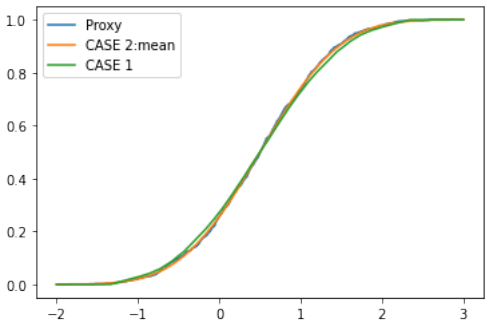

(c) $\sigma = 1.0$

Figure 3.1: Model of Example 3.5.1: Comparison of the two methods CASE 1 & CASE2 with $d = 4$. The Proxy solution is given by the same particle method on the one-dimensional PDE. For $BT\&SPD$: both CASE 1 and CASE 2, the number of particles is $M = 3500$ and the number of time steps $N = 20$.

To validate empirically our numerical schemes, we plot the value function $\mathcal{V}$ of model Example 3.5.1 using scheme CASE 1 and CASE 2 against the *proxy* solution presented in [9], see Figure 3.1. As expected, both CASE 1 and CASE 2 scheme could reproduce correctly the entropy solution of the PDE (3.2.1). We also observe that the solutions obtained by CASE 1 and CASE 2 scheme are quite close.

Apart from the linear model, we have also tested numerically our CASE 1 and CASE 2 schemes in model Example 3.5.2 against a NN & Upwind method based on splitting schemes presented in [26], see Figure 3.2. We note that the function μ in model Example 3.5.2 is always non negative, thus we take Upwind scheme which is less "diffusive" than Lax-Friedrisch scheme as argued in [26]. As expected, both CASE 1 and CASE 2 schemes give satisfying numerical results for different levels of volatility.

At last, we want to empirically estimate the convergence rate of the error introduced by our numerical scheme. We consider the model Example 3.5.1 where $\sigma = 1.0$. We consider a set of number of time steps $N := \{2, 4, 8, 16, 32, 64\}$ and time step $\mathfrak{h} := \frac{T}{N}$, and compute the $L1$-error for BT & SPD method. Note that the proxy solution is always given by method in [9] applied to one-dimensional equivalent model. The empirical convergence rate with respect to the time step is close to one see Figure 3.3, which is much better than the theoretical convergence order $\frac{1}{6}$

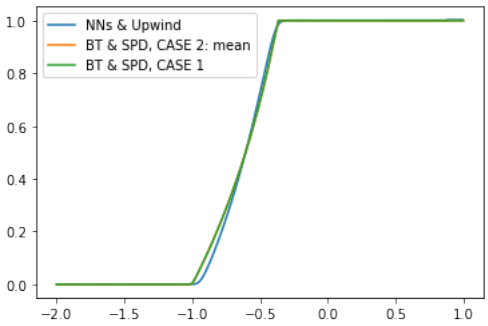

(a) $\sigma = 0.01$

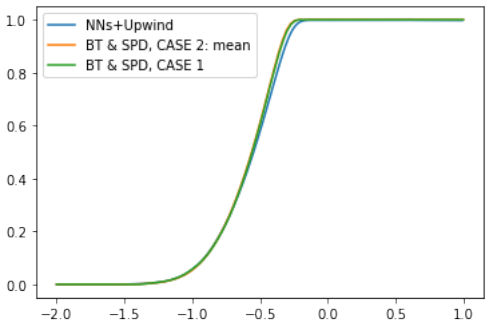

(b) $\sigma = 0.3$

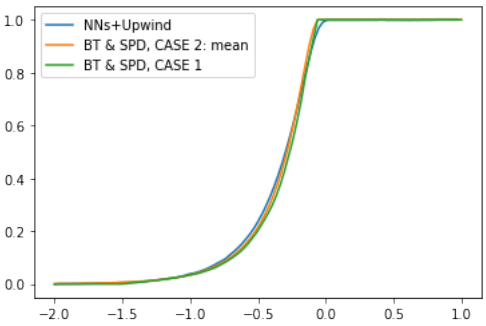

(c) $\sigma = 1.0$

Figure 3.2: Model of Example 3.5.2: Comparison of the two methods CASE 1 & CASE2 with $d = 4$. The Proxy solution is given by the Neural nets & Upwind in [26]. For $BT\&SPD$: both CASE 1 and CASE 2, the number of particles is $M = 3500$ and the number of time steps $N = 20$.

obtained in Theorem 3.3.1.

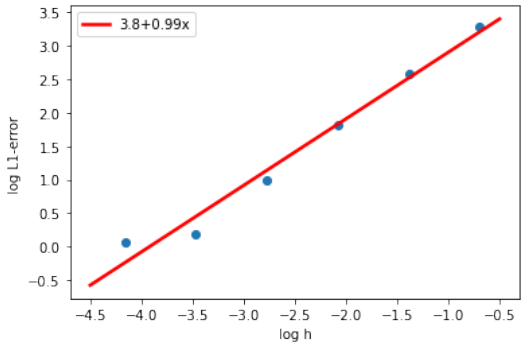

Figure 3.3: Convergence rate on $\mathfrak{h}$ for model Example 3.5.2 with parameters $d = 4, \sigma = 1.0$

Part II

A dual approach to weak hedging problem

Chapter 4

A dual approach to weak hedging problem

The content of this chapter is from a work in progress with Cyril Bénézet and Jean-François Chassagneux.

Contents

4.1 Introduction

In this work, we consider a class of non standard control problems. Indeed, we impose on the controlled process at a terminal time $T > 0$ a constraint which

involves its law. In finance, the classical example of such problem would be the so-called *quantile hedging problem*, see e.g. [36, 14]. In this case, the controlled process is a portfolio of financial assets. The key point is that the value of this portfolio at time T is not supposed to perfectly replicate a given contingent claim, as usual in mathematical finance. In the *quantile hedging problem*, the agent will seek to replicate the contingent claim with only a 95% (say) probability of success. This approach really puts a probability constraint or a quantile constraint on the total PnL of the position held by the agent. On a theoretical point of view, the problems of perfect replication and partial replication lead to quite different stochastic control problem. The first one has been generally recognized as a case of stochastic target problem see e.g. [65, 66]. The second one has been coined as a weak stochastic target problem and needs extra work to be solved, see e.g. [14]. In particular, it leads to a degenerate PDE representing its value function which is quite involved to work with and to approximate numerically, see e.g. [5]. A natural extension to the *quantile hedging problem* is the PnL matching problem introduced in [15]. In this article, the authors consider a finite number of quantile constraint, representing a given target PnL: in other words, the targeted law for the PnL is discrete and finite. The next step would be naturally to impose any possible law as target PnL, which, to the best of our knowledge has not been previously considered. The control problem that we introduce here encapsulates all this possible cases. Having in mind financial applications, we have called this more generic problem the *weak hedging problem*. It is, as we will show, closely related to partial hedging with controlled loss.

Our goal is thus to solve this *weak hedging problem* theoretically but also to propose a new numerical method to approximate its solution. Indeed, it is known that this kind of problem is difficult to tackle numerically [5, 11, 15]. The known approaches are usually based on PDE methods. Here, we follow a totally different road as we will rely on stochastic gradient algorithms. The first part of the work is thus dedicated to obtain a convenient formulation of the *weak hedging problem*. We rewrite it as a classical control problem involving the minimisation of non-linear expectation over a tailored class of random variables. We then make the new and crucial observation that this problem resembles optimal transportation problem 'à la Monge'. We then naturally introduce a 'Kantorovich version' and look for a dual characterization. In some important cases, we are able to obtain this dual characterization and this is the starting point of our numerical algorithms, which are proved to be efficient in practice.

The rest of the paper is organized as follows. In the next section, we introduce formally the *weak hedging problem* and we present some important properties in a non linear setting. Section 3 focuses on a linear framework in which we obtain duality results. The last Section presents the new numerical approach based on SGD algorithms. Various numerical experiments are run showing that the methods are reliable.

4.1.0.0.1 Notations that will be used throughout the paper:

- If $(\Omega, \mathcal{F}, \mathbb{F}, \mathbb{P})$ is a filtered probability space and E a normed space, we define $\mathscr{H}^2(\mathbb{F}, \mathbb{P}; E)$ as the set of progressively measurable processes $U : \Omega \times [0, T] \to E$

with $T > 0$ fixed satisfying

$$\mathbb{E}\left[\int_0^T |U_t|^2 \mathrm{d}t\right] < +\infty$$

and $\mathscr{S}^2(\mathbb{F}, \mathbb{P}; E))$ as the set of processes $U : \Omega \times [0,T] \to E$ continuous and adapted s.t.

$$\mathbb{E}\left[\sup_{t\in[0,T]} |U_t|^2 \mathrm{d}t\right] < +\infty.$$

- For $(\Omega, \mathcal{F}, \mathbb{P})$ a probability space, we denote $\mathcal{N}_{\mathbb{P}}$ the set of negligible sets, namely

$$\mathcal{N}_{\mathbb{P}} := \{A \in \mathcal{F} \,|\, \mathbb{P}(A) = 0\}\,.$$

- Given a measurable space $(E, \mathcal{E})$, the set of positive measures on E (resp. the subset probability measures) is denoted $\mathscr{M}_+(E)$ (resp. $\mathcal{P}(E)$). For $p \geqslant 1$, we consider

$$\mathcal{P}_p(\mathbb{R}) = \left\{\nu \in \mathcal{P}(\mathbb{R}) \,\middle|\, \int |x|^p \nu(\mathrm{d}x) < +\infty\right\}.$$

- For two probability measures μ, ν on $\mathbb{R}$, $\nu \succeq \mu$ denotes the *first order stochastic dominance*, i.e

$$\nu\left([\cdot, \infty)\right) := F_\nu \geqslant F_\mu =: \mu\left([\cdot, \infty)\right) \text{ on } \mathbb{R}.$$

We define

$$\mathcal{K}_\mu := \{\nu \in \mathcal{P}(\mathbb{R}) | \nu \succeq \mu\} \quad \text{and} \quad \mathcal{K}_\mu^p := \mathcal{K}_\mu \cap \mathcal{P}_p(\mathbb{R}),\ p \geqslant 1\,.$$

We also introduce

$$\mathcal{R}_\mu = \{\nu \in \mathcal{K}_\mu |\ \mathrm{supp}[\nu] \subset \mathrm{supp}[\mu]\} \quad \text{and} \quad \mathcal{R}_\mu^p := \mathcal{R}_\mu \cap \mathcal{P}_p(\mathbb{R}),\ p \geqslant 1\,,$$

where $\mathrm{supp}[\nu]$ is the support of the measure μ.

- For $(\Omega, \mathcal{F}, \mathbb{P})$ a *complete* probability space, we denote $\bar{\Omega} := \Omega \times \mathbb{R}$ and $\bar{\mathcal{F}} := \mathcal{F} \otimes \mathcal{B}(\mathbb{R})$, with $\mathcal{B}(\mathbb{R})$ the Borel sigma-algebra of $\mathbb{R}$. We define the following projections

$$\mathrm{pr}_1 : \bar{\Omega} \ni (\omega, \gamma) \mapsto \omega \in \Omega, \text{ and } \mathrm{pr}_2 : \bar{\Omega} \ni (\omega, \gamma) \mapsto \gamma \in \mathbb{R}.$$

We also introduce the following set of measures on $\bar{\Omega}$,

$$\mathcal{M}_+(\mathbb{P}) := \left\{\Pi \in \mathscr{M}_+(\bar{\Omega}) \,\middle|\, \forall (A,B) \in \mathcal{N}_{\mathbb{P}} \times \mathcal{B}(\mathbb{R}),\ \Pi(A \times B) = 0\right\} \tag{4.1.1}$$

$$\mathcal{M}_+^{\mathrm{r}}(\mathbb{P}, \mu) := \left\{\Pi \in \mathcal{M}_+(\mathbb{P}) \,|\, \mathrm{supp}[\mathrm{pr}_2 \sharp \Pi] \subset \mathrm{supp}[\mu]\right\}, \tag{4.1.2}$$

$$C(\mathbb{P}, \mu) := \left\{\Pi \in \mathcal{P}(\bar{\Omega}) \,\middle|\, (\mathrm{pr}_1)_\sharp \Pi = \mathbb{P}, (\mathrm{pr}_2)_\sharp \Pi \in \mathcal{K}_\mu\right\}, \tag{4.1.3}$$

$$C^{\mathrm{r}}(\mathbb{P}, \mu) := \left\{\Pi \in \mathcal{P}(\bar{\Omega}) \,\middle|\, (\mathrm{pr}_1)_\sharp \Pi = \mathbb{P}, (\mathrm{pr}_2)_\sharp \Pi \in \mathcal{R}_\mu\right\}. \tag{4.1.4}$$

- For E a topological space, the set of bounded (resp. continuous, resp. bounded continuous, resp. continuous with linear growth) functions with values in $\mathbb{R}$ is denoted $\mathscr{B}(E)$ (resp. $\mathscr{C}(E)$, resp. $\mathscr{C}_b(E) = \mathscr{C}(E) \cap \mathscr{B}(E)$, resp. $\mathscr{C}_l(E)$).
- Let $\mathscr{I}(\mathbb{R})$ be the set of increasing functions from $\mathbb{R}$ to $\mathbb{R}$.
- For all $d \geqslant 1$, we set $\Delta_+^d := \{x \in \mathbb{R}^d | 0 \leqslant x_1 \leqslant \cdots \leqslant x_d\}$.
- For two metric spaces E, E', $\mathbf{Lip}(E, E')$ is the set of Lipschitz continuous function from E to E'.

4.2 Approximate hedging: problem and general results

Let $(\Omega, \mathcal{A}, \mathbb{P})$ be a complete probability space supporting a m-dimensional Brownian Motion, where m is a positive integer. We denote by $\mathbb{F} = (\mathcal{F}_t)_{t \geqslant 0}$ the natural $\mathbb{P}$-augmented filtration of W. In the sequel, we work with a finite time horizon $T > 0$.

4.2.1 Problem formulation

We will consider controlled processes of the following form. For $y \in \mathbb{R}$ and $Z \in \mathscr{H}^2$,

$$Y_t^{y,Z} = y - \int_0^t \mathfrak{f}(s, Y_s, Z_s)\, \mathrm{d}s + \int_0^t Z_s \mathrm{d}W_s, \quad t \in [0, T], \tag{4.2.1}$$

where $(\mathfrak{f}(s, \cdot))_{s \in [0,T]}$ is a progressively measurable process taking values in $\mathbf{Lip}(\mathbb{R} \times \mathbb{R}^m, \mathbb{R})$ and such that $\mathbb{E}\Big[\int_0^T |\mathfrak{f}(s, 0, 0)|^2 \mathrm{d}s\Big] < +\infty$. Note that the assumptions on f guarantee the well-posedness in $\mathscr{S}^2$ of the above dynamics.

A key result in this context is given by the existence and uniqueness of BSDEs with a prescribed terminal value $\xi \in \mathscr{L}^2(\mathcal{F}_T)$, see e.g. [35]. Namely, there exists a unique $(\mathcal{Y}_0, \mathcal{Z}) \in \mathbb{R} \times \mathscr{H}^2$ such that $Y_T^{\mathcal{Y}_0, \mathcal{Z}} = \xi$. In this case, we define $\mathcal{Y}_t := Y_t^{\mathcal{Y}_0[\xi], \mathcal{Z}[\xi]}$ for all $t \in [0, T]$, so that $(\mathcal{Y}, \mathcal{Z})$ is the solution to the BSDE with driver $\mathfrak{f}$ and terminal condition ξ, namely

$$\mathcal{Y}_t = \xi + \int_t^T \mathfrak{f}(s, \mathcal{Y}_s, \mathcal{Z}_s)\mathrm{d}s - \int_t^T \mathcal{Z}_s \mathrm{d}W_s \,, 0 \leqslant t \leqslant T. \tag{4.2.2}$$

To insist on the dependence upon the terminal condition ξ, we shall sometimes denote the solution of the above BSDE by $(\mathcal{Y}_t[\xi], \mathcal{Z}_t[\xi])_{0 \leqslant t \leqslant T}$.

In the next section, we will consider the following linear setup for $\mathfrak{f}$.

Assumption 4.2.1 *There exists two bounded progressively measurable stochastic processes* $(\mathfrak{a}, \mathfrak{b})$ *such that*

$$\mathfrak{f}(t, y, z) = \mathfrak{a}_t y + \mathfrak{b}_t^\top z, \quad \textit{for } (t, y, z) \in [0, T] \times \mathbb{R} \times \mathbb{R}^m \,. \tag{4.2.3}$$

Remark 4.2.1 *Under Assumption 4.2.1, it is well known that* $\mathcal{Y}_0[\xi]$ *for* $\xi \in \mathscr{L}^2(\mathcal{F}_T)$ *rewrites as an expectation, see e.g. Proposition 2.2 in [35]. More precisely, let us introduce, the process* Γ *solution to*

$$\mathrm{d}\Gamma_t = \Gamma_t(\mathfrak{a}_s \mathrm{d}t + \mathfrak{b}_s^\top \mathrm{d}W_t) \text{ and } \Gamma_0 = 1 \,, \tag{4.2.4}$$

which satisfies, for any $p \geqslant 1$,

$$\mathbb{E}\left[\sup_{t\in[0,T]} |\Gamma_t|^p\right] \leqslant C_p \,. \tag{4.2.5}$$

Then, one has,

$$\mathcal{Y}_0[\xi] = \mathbb{E}[\Gamma_T \xi] \,. \tag{4.2.6}$$

Let us also be given a $(\mathcal{F}_T \otimes \mathcal{B}(\mathbb{R}), \mathcal{B}(\mathbb{R}))$-measurable random function

$$\Omega \times \mathbb{R} \ni (\omega, \gamma) \mapsto G(\omega, \gamma) \in \mathbb{R}$$

such that $\gamma \mapsto G(\gamma)$ is non-decreasing and left-continuous.
In the sequel, we shall also make use of the following

Assumption 4.2.2 *There exists* $\mathfrak{C} \in L^4(\mathcal{F}_T)$ *such that,* $\mathbb{P}$*-almost surely and for all* $\gamma \in \mathbb{R}$,

$$|G(\gamma)| \leqslant \mathfrak{C}(1 + |\gamma|). \tag{4.2.7}$$

Moreover, the following holds $\mathbb{P} - a.s.$

$$G(+\infty) := \lim_{\gamma\to+\infty} G(\gamma) = +\infty, \tag{4.2.8}$$

$$G(-\infty) := \lim_{\gamma\to-\infty} G(\gamma) \in [-\infty, +\infty), \tag{4.2.9}$$

$$\text{and } \; G(-\infty) < G(\gamma) \,, \; \forall \gamma \in \mathbb{R}. \tag{4.2.10}$$

We recall the definition of the generalized inverse of G,

$$\Psi(\omega, y) := \sup\{\gamma \in \mathbb{R} \,|\, y \geqslant G(\omega, \gamma)\} \in \mathbb{R} \cup \{-\infty, +\infty\} \,, (\omega, y) \in \overline{\Omega}. \tag{4.2.11}$$

Note that Ψ is a $(\mathcal{F}_T \otimes \mathcal{B}(\mathbb{R}), \mathcal{B}(\mathbb{R}))$-measurable random function, $\mathbb{P}$-almost surely non-decreasing and right-continuous. Under Assumption 4.2.2, the value $+\infty$ is avoided thanks to (4.2.8), and

$$\{\Psi(\omega, y) = -\infty\} = \{y \leqslant G(\omega, -\infty)\} \,. \tag{4.2.12}$$

We shall also use the following assumption.

Assumption 4.2.3 *There exists* $\mathfrak{C} \in L^4(\mathcal{F}_T)$ *such that,* $\mathbb{P}$*-almost surely and for all* $y \in \mathbb{R}$,

$$|\Psi(y)\mathbf{1}_{\{\Psi(y)>-\infty\}}| \leqslant \tilde{\mathfrak{C}}(1 + |y|) \,. \tag{4.2.13}$$

Observe that, by left-continuity of G and the right continuity of Ψ,

$$G \circ \Psi \leqslant \mathrm{Id} \leqslant \Psi \circ G\,. \tag{4.2.14}$$

We are now in position to introduce the *weak hedging problem.*
Denote, for $\mu \in \mathcal{P}(\mathbb{R})$, the set of super weak hedge price by

$$\mathfrak{H}(\mu) := \left\{ y \in \mathbb{R} \,\middle|\, \exists Z \in \mathscr{H}^2, \mathbb{P}(Y_T^{y,Z} \geqslant G(\gamma)) \geqslant F_\mu(\gamma), \forall \gamma \in \mathbb{R} \right\}. \tag{4.2.15}$$

We now define classicaly the *weak hedging price* as

$$\mathcal{V}_{\mathrm{WH}}(\mu) := \inf \mathfrak{H}(\mu)\ , \quad \text{for } \mu \in \mathcal{P}(\mathbb{R}). \tag{4.2.16}$$

We make directly the following observation, whose proof is postponed at the end of this introductory section. It says basically that the constraints are only binding for $\gamma \in \mathrm{supp}[\mu]$.

Proposition 4.2.1 *We have $\mathfrak{H}(\mu) = \tilde{\mathfrak{H}}(\mu)$, with*

$$\tilde{\mathfrak{H}}(\mu) := \left\{ y \in \mathbb{R} \,\middle|\, \exists Z \in \mathscr{H}^2,\ \mathbb{P}(Y_T^{y,Z} \geqslant G(\gamma)) \geqslant F_\mu(\gamma), \forall \gamma \in \mathrm{supp}[\mu] \right\}.$$

The weak hedging problem is general enough to encapsulate in particular the following problems, which will be studied extensively in the subsequent sections, see Section 4.3.1 and Section 4.3.2.

Example 4.2.1 (PnL matching problem) *For $n \geqslant 1$ and $0 \leqslant \xi_0 \leqslant \cdots \leqslant \xi_n \in L^2(\mathcal{F}_T)$, we define*

$$G(\omega, i) := \xi_i(\omega), \omega \in \Omega, 0 \leqslant i \leqslant n,$$

and $p_0, \ldots, p_n > 0$ such that $\sum_{i=0}^n p_i = 1$, we set $\mu = \sum_{i=0}^n p_i \delta_i$.
Then we recover the PnL matching problem with multiple constraints as introduced in [15]. Precisely, there are $n+1$ constraints, one super-replication constraint and n quantile constraints. Indeed, recalling Proposition 4.2.1,

$$\begin{aligned}
\mathcal{V}_{\mathrm{WH}}(\mu) &= \inf \left\{ y \in \mathbb{R} \,\middle|\, \exists Z \in \mathscr{H}^2, \mathbb{P}(Y_T^{y,Z} \geqslant G(i)) \geqslant F_\mu(i), 0 \leqslant i \leqslant n \right\} \\
&= \inf \left\{ y \in \mathbb{R} \,\middle|\, \exists Z \in \mathscr{H}^2, \mathbb{P}(Y_T^{y,Z} \geqslant \xi_i) \geqslant q_i, 0 \leqslant i \leqslant n \right\},
\end{aligned}$$

with $q_i := \sum_{j=i}^n p_j$, $1 \leqslant i \leqslant n$.
Two cases of the above multiple constraints problem are of particular interest.

- *For $n = 0$, one gets the super-replication problem (see e.g. [65], [66]): $G(\omega, 0) = \xi$ for some $\xi \in L^2(\mathcal{F}_T)$, $\mu = \delta_0$, and then*

$$\begin{aligned}
\mathcal{V}_{\mathrm{WH}}(\mu) &= \inf \left\{ y \in \mathbb{R} \,\middle|\, \exists Z \in \mathcal{U}_0, \mathbb{P}(Y_T^{y,Z} \geqslant \xi) \geqslant 1 \right\} \\
&= \inf \left\{ y \in \mathbb{R} \,\middle|\, \exists Z \in \mathcal{U}_0, Y_T^{y,Z} \geqslant \xi, \mathbb{P}-a.s. \right\}.
\end{aligned}$$

- *For $n = 1$, one recovers the classical quantile hedging problem (see e.g. [36], [14], [5]) and we denote $\mathcal{V}_{\mathrm{WH}}$ by $\mathcal{V}_{\mathrm{QH}}$ in this case: $G(\omega, 0) = 0$, $G(\omega, 1) = \xi$ for some $0 \leqslant \xi \in L^2(\mathcal{F}_T)$, $\mu = (1-p)\delta_0 + p\delta_1$ for $p \in [0,1]$, and then*

$$\mathcal{V}_{\mathrm{QH}}(\mu) = \inf\left\{ y \in \mathbb{R} \,\middle|\, \exists Z \in \mathscr{H}^2, Y_T^{y,Z} \geqslant 0, \mathbb{P}-a.s., \text{ and } \mathbb{P}(Y_T^{y,Z} \geqslant \xi) \geqslant p \right\}. \tag{4.2.17}$$

The discrete setting for μ, given in the example above is not the only one of interest. We can also consider more complex parametrization for μ. We give now an example, where the targeted PnL is possibly a continuous distribution.

Example 4.2.2 *Let $\xi \in \mathscr{L}^2(\mathcal{F}_T)$ and $\mu \in \mathcal{P}_2(\mathbb{R})$. Set $G(\omega, \gamma) = \xi(\omega) + \gamma$, for $(\omega, \gamma) \in \bar{\Omega}$, then one gets the following problem*

$$\mathcal{V}_{\mathrm{WH}}(\mu) = \inf\left\{ y \in \mathbb{R} \,\middle|\, \exists Z \in \mathscr{H}^2, \mathbb{P}(Y_T^{y,Z} \geqslant \xi + \gamma) \geqslant F_\mu(\gamma), \gamma \in \mathbb{R} \right\} \tag{4.2.18}$$

$$= \inf\left\{ y \in \mathbb{R} \,\middle|\, \exists Z \in \mathscr{H}^2, \left(Y_T^{y,Z} - \xi\right)_\sharp \mathbb{P} \in \mathcal{K}_\mu \right\}. \tag{4.2.19}$$

Remark 4.2.2 *Note that in the above examples, when G is only defined on $\Omega \times E$ with $E \subset \mathbb{R}$, it is easy to extend G to $\Omega \times \mathbb{R}$ as an almost-surely non-decreasing left-continuous map satisfying to (4.2.7)-(4.2.8), and such that its generalized inverse Ψ also satisfies to (4.2.13).*

Remark 4.2.3 *Proposition 4.2.1 sheds some light on the Assumption (4.2.9) on the random map G: if the support of the probability distribution μ is bounded from below, i.e. included in $[\gamma_-(\mu), \infty)$ for some $\gamma_- > -\infty$, then the map G can be arbitrarily modified on a neighbourhood of $-\infty$ for almost all $\omega \in \Omega$, in particular in a way so that (4.2.9) is satisfied.*
The assumption (4.2.9) is also obviously satisfied in the important application (4.2.18).

We conclude this section with the short
Proof of Proposition 4.2.1 We obviously have $\mathfrak{H}(\mu) \subset \tilde{\mathfrak{H}}(\mu)$.
Conversely, let $y \in \tilde{\mathfrak{H}}(\mu)$ and let $\gamma \in \mathbb{R} \backslash \mathrm{supp}[\mu]$. Let $\gamma^+ := \inf \mathrm{supp}[\mu] \cap [\gamma, \infty]$. Note that $\gamma^+ \in (\gamma, \infty]$, and we have either $\gamma^+ = \infty$ or $\gamma^+ \in \mathrm{supp}[\mu] \cap (\gamma, \infty)$, as $\mathrm{supp}[\mu]$ is closed.
If $\gamma^+ = +\infty$, then $F_\mu(\gamma) = 0$ and $\mathbb{P}(Y_T^{y,Z} \geqslant G(\gamma)) \geqslant F_\mu(\gamma) = 0$ is satisfied.
Otherwise, $\gamma^+ \in \mathrm{supp}[\mu] \cap (\gamma, \infty)$ and we have

$$F_\mu(\gamma) = F_\mu(\gamma^+) \leqslant \mathbb{P}(Y_T^{y,Z} \geqslant G(\gamma^+)) \leqslant \mathbb{P}(Y_T^{y,Z} \geqslant G(\gamma)),$$

the last inequality being true as, since G is non-decreasing, $\{Y_T^{y,Z} \geqslant G(\gamma^+)\} \subset \{Y_T^{y,Z} \geqslant G(\gamma)\}$. This proves that $y \in \mathfrak{H}(\mu)$, hence $\tilde{\mathfrak{H}}(\mu) \subset \mathfrak{H}(\mu)$. □

4.2.2 The Monge representation

Proposition 4.2.2 *Let $\mu \in \mathcal{P}_4(\mathbb{R})$. We have the equivalent formulations*

$$\mathcal{V}_{\rm WH}(\mu) = \widehat{\mathcal{V}}_{\rm RM} := \inf_{\chi \in \mathcal{T}_+(\mu)} \mathcal{Y}_0[G(\chi)]\,, \tag{4.2.20}$$

where $\mathcal{T}_+(\mu) = \big\{\chi \in \mathcal{L}^4(\mathcal{F}_T) \,\big|\, \chi_\sharp \mathbb{P} \in \mathcal{K}_\mu\big\}$, and

$$\mathcal{V}_{\rm WH}(\mu) = \inf \tilde{\mathfrak{H}}(\mu), \ \textit{with}\ \tilde{\mathfrak{H}}(\mu) := \Big\{ y \in \mathbb{R} | \exists Z \in \mathscr{H}^2, \Psi(Y_T^{y,Z})\sharp\mathbb{P} \in \mathcal{K}_\mu \Big\}\,, \tag{4.2.21}$$

recall (4.2.11).

Proof. 1. We first prove (4.2.20). Set $\widehat{\mathfrak{H}}(\mu) := \{\mathcal{Y}_0[G(\chi)] \,|\, \chi \in \mathcal{T}_+(\mu)\}$. First, since $\mu \in \mathcal{P}_4(\mathbb{R})$, notice that $\mathcal{T}_+(\mu)$ is not empty as there always exists a $\mathcal{F}_T$-measurable random variable with law μ, for example $F_\mu^{-1}(N(\frac{W_T}{\sqrt{T}}))$.
1.a Let $\chi \in \mathcal{T}_+(\mu)$ and set $\xi := G(\chi)$. Observe that, since G is non-decreasing, for each $\gamma \in \mathbb{R}$, we have $\{\chi \geqslant \gamma\} \subset \{\xi \geqslant G(\gamma)\}$. Thus $\mathbb{P}(\xi \geqslant G(\gamma)) \geqslant \mathbb{P}(\chi \geqslant \gamma) \geqslant F_\mu(\gamma)$ as $\chi_\sharp\mathbb{P} \succeq \mu$. Using (4.2.7) and the fact that $\chi \in \mathcal{L}^4(\mathcal{F}_T)$, we have that $\xi \in \mathcal{L}^2(\mathcal{F}_T)$ and then the BSDE $(\mathcal{Y}[\xi], \mathcal{Z}[\xi])$, recall (4.2.2), is well posed. We deduce $\mathcal{Y}_0[\xi] \in \mathfrak{H}(\mu)$. Thus $\widehat{\mathfrak{H}}(\mu) \subset \mathfrak{H}(\mu)$ and hence $\mathcal{V}_{\rm WH} \leqslant \widehat{\mathcal{V}}_{\rm RM}(\mu)$.
1.b Conversely, let $y \in \mathfrak{H}(\mu)$, so that there exists $Z \in \mathscr{H}^2$ s.t. $Y_T^{y,Z}$ satisfies to $\mathbb{P}(Y_T^{y,Z} \geqslant G(\gamma)) \geqslant F_\mu(\gamma)$ for all $\gamma \in \mathbb{R}$. We set $\chi := \Psi(Y_T^{y,Z})$: We first notice that $\mathbb{P}(Y_T^{y,Z} > G(-\infty)) \geqslant \mathbb{P}(Y_T^{y,Z} \geqslant G(\gamma))$, for all $\gamma \in \mathbb{R}$ since $\{\chi = -\infty\} = \{Y_T^{y,Z} \leqslant G(-\infty)\}$. Thus $\mathbb{P}(Y_T^{y,Z} > G(-\infty)) = \lim_{\gamma\to-\infty} \mathbb{P}(Y_T^{y,Z} \geqslant G(\gamma)) \geqslant \lim_{\gamma\to-\infty} F_\mu(\gamma) = 1$. Recalling (4.2.12), we have that $\{\chi = -\infty\} = \{Y_T^{y,Z} \leqslant G(-\infty)\}$ and thus deduce from the previous observation $\mathbb{P}(\chi > -\infty) = 1$. Then, using (4.2.13) and the fact that $Y_T^{y,Z} \in \mathcal{L}^2(\mathcal{F}_T)$, we obtain that $\chi \in \mathcal{L}^2(\mathcal{F}_T)$. Recalling (4.2.14), we have that $Y_T^{y,Z} \geqslant G(\gamma)$ implies $\chi = \Psi(Y_T^{y,Z}) \geqslant \Psi \circ G(\gamma) \geqslant \gamma$. Thus, $\mathbb{P}(\chi \geqslant \gamma) \geqslant \mathbb{P}(Y_T^{y,Z} \geqslant G(\gamma)) \geqslant F_\mu(\gamma)$ yielding $\chi_\sharp\mathbb{P} \succeq \mu$. Again from (4.2.14), we also observe that $G(\chi) = G(\Psi(Y_T^{y,Z})) \leqslant Y_T^{y,Z}$ leading to $\mathcal{Y}_0[G(\chi)] \leqslant \mathcal{Y}_0[Y_T^{y,Z}] = y$ by the comparison theorem for Lipschitz BSDEs. We then obtain $\widehat{\mathcal{V}}_{\rm RM}(\mu) \leqslant y$, hence $\widehat{\mathcal{V}}_{\rm RM}(\mu) \leqslant \mathcal{V}_{\rm WH}(\mu)$.
2. We now turn to the equivalent formulation (4.2.21). Denote $\tilde{v}(\mu)$ the quantity on the right hand side of (4.2.21). From the step 1.b above, we obtain that $\mathcal{V}_{\rm WH}(\mu) \geqslant \tilde{v}(\mu)$. Now, let $y \in \tilde{\mathfrak{H}}(\mu)$, then there exists Z, s.t. $\chi := \Psi(Y_T^{y,Z})$ satisfies $\chi\sharp\mathbb{P} \succeq \mu$. Using (4.2.14), we observe that $Y_T^{y,Z} \geqslant G(\chi)$. In particular on $\{\chi \geqslant \gamma\}$, we have, since G is non decreasing, that $Y_T^{y,Z} \geqslant G(\gamma)$. Thus $\mathbb{P}(Y_T^{y,Z} \geqslant G(\gamma)) \geqslant F_\mu(\gamma)$ proving that $y \in \mathfrak{H}(\mu)$. □

Remark 4.2.4 *1. The formulation (4.2.21) given in the previous proposition shows that the weak hedging problem is a particular instance of more generic weak stochastic target problem: Consider a set $\mathcal{M} \subset \mathcal{P}(\mathbb{R})$ and a right continuous non decreasing random function $\mathfrak{O}$ and solve*

$$\inf \Big\{ y \in \mathbb{R} | \exists Z \in \mathscr{H}^2, \mathfrak{O}(Y_T^{y,Z})\sharp\mathbb{P} \in \mathcal{M} \Big\}\,. \tag{4.2.22}$$

The weak hedging problem corresponds to the case $\mathfrak{O} = \Psi$ *and* $\mathcal{M} := \mathcal{K}_\mu$ *for a given* μ. *In [12], the authors introduce a similar problem to (4.2.22) where* $\mathcal{M} := \{\mu \in \mathcal{P}(\mathbb{R}) s.t. \int \gamma \mu(\mathrm{d}\gamma) \geqslant p\}$ *for a given level* $p \in \mathbb{R}$.

2. *The formulation (4.2.21) opens the way to a dynamic approach to characterize the solution of the quantile hedging problems as a BSDE, as done in [12] in a special case or to a PDE characterization in a Markovian setting, as done in [14]. The extension of these results to our framework is left for further research.*

Remark 4.2.5 *In the problem (4.2.20), "RM" stands for "Relaxed Monge". Indeed, let Assumption 4.2.1 hold. Then* $\mathcal{Y}_0$ *is a linear operator, since* $\mathcal{Y}_0[\xi] = \mathbb{E}[\Gamma_T \xi]$, *for some* $\Gamma_T \in L^2(\mathcal{F}_T)$, *recall Remark 4.2.1. Then, one has*

$$\widehat{\mathcal{V}}_{\mathrm{RM}}(\mu) = \inf_{\chi \in \mathcal{T}_+(\mu)} \mathbb{E}[\Gamma_T G(\chi)] = \inf_{\chi \in \mathcal{T}_+(\mu)} \int \Gamma_T(\omega) G(\omega, \chi(\omega)) \mathbb{P}(\mathrm{d}\omega),$$

which can be interpreted as an "à la Monge" optimal transport problem. We use the term 'relaxed' as the target distribution is not exactly μ, *but can be any square-integrable probability distribution stochastically dominating* μ. *This linear framework will be extensively studied in Section 4.3.*

4.2.3 The Kantorovitch representation

In this section, we will work with the following

Assumption 4.2.4 *The probability distribution* $\mu \in \mathcal{P}(\mathbb{R})$ *has discrete and finite support, namely* $\mathrm{supp}[\mu] = \{\gamma_1, \dots, \gamma_d\}$ *with* $\gamma_1 < \cdots < \gamma_d$. *We denote* $q_\ell = F_\mu(\gamma_\ell)$ *and* $p_\ell := q_\ell - q_{\ell+1} = \mu(\{\gamma_\ell\})$, *for* $\ell \in \{1, \dots, d\}$ *with the convention* $q_{d+1} = 0$.

The main point of the following result is that we are able to work with probability distribution whose support is included in the support of μ.

Lemma 4.2.1 *Under Assumption 4.2.4, the following holds*

$$\mathcal{V}_{\mathrm{WH}}(\mu) = \widehat{\mathcal{V}}_{\mathrm{RM}}(\mu) = \mathcal{V}_{\mathrm{RM}}(\mu) := \inf_{\chi \in \mathcal{T}_+^{\mathrm{r}}(\mu)} \mathcal{Y}_0[G(\chi)] \tag{4.2.23}$$

and where $\mathcal{T}_+^{\mathrm{r}}(\mu) = \{\chi \in \mathcal{L}^\infty(\mathcal{F}_T) \,|\, \chi_\sharp \mathbb{P} \in \mathcal{R}_\mu\}$.

Proof. Let $\mathfrak{H}^{\mathrm{r}}(\mu) := \{\mathcal{Y}_0[G(\chi)] \,|\, \chi \in \mathcal{T}_+^{\mathrm{r}}(\mu)\}$ and recall the definition of $\widehat{\mathfrak{H}}(\mu)$ in the proof of Proposition 4.2.2. Since $\mathcal{T}_+^{\mathrm{r}}(\mu) \subset \mathcal{T}_+(\mu)$, it is clear that $\mathfrak{H}^{\mathrm{r}}(\mu) \subset \widehat{\mathfrak{H}}(\mu)$, hence $\widehat{\mathcal{V}}_{\mathrm{RM}}(\mu) \leqslant \mathcal{V}_{\mathrm{RM}}(\mu)$. Conversely, for $\chi \in \mathcal{T}_+(\mu)$, we define, setting $\gamma_{d+1} := +\infty$,

$$\tilde{\chi} = \sum_{\ell=1}^{d} \gamma_\ell \mathbf{1}_{\chi \in [\gamma_\ell, \gamma_{\ell+1})} \in \mathcal{L}^\infty(\mathcal{F}_T), \tag{4.2.24}$$

we observe that $\chi \geqslant \tilde{\chi}$, thus $G(\chi) \geqslant G(\tilde{\chi})$. From the comparison theorem for one-dimensional Lipschitz BSDEs, we deduce $\mathcal{Y}_0[G(\chi)] \geqslant \mathcal{Y}_0[G(\tilde{\chi})]$. Moreover, we observe that $\mathrm{supp}[\tilde{\chi}\sharp\mathbb{P}] \subset \mathrm{supp}[\mu]$, by construction. Last, we easily compute, for

$\ell \in \{1, \dots, d\}$, $\mathbb{P}(\tilde{\chi} \geqslant \gamma_\ell) = \mathbb{P}(\chi \geqslant \gamma_\ell) \geqslant F_\mu(\gamma_\ell)$, which proves that $\tilde{\chi} \in \mathcal{T}_+^{\mathrm{r}}(\mu)$. We then have $\mathcal{V}_{\mathrm{RM}}(\mu) \leqslant \mathcal{Y}_0[G(\tilde{\chi})] \leqslant \mathcal{Y}_0[G(\chi)]$, hence $\mathcal{V}_{\mathrm{RM}}(\mu) \leqslant \widehat{\mathcal{V}}_{\mathrm{RM}}(\mu)$, which concludes the proof. □

We now introduce the Kantorovitch representation of the quantile hedging problem.

We define

$$\mathcal{V}_{\mathrm{KP}}(\mu) := \inf_{\Pi \in C^{\mathrm{r}}(\mathbb{P},\mu)} \mathcal{Y}_0 \left[\int G(\omega, \gamma) \rho^{\Pi}(\omega, \mathrm{d}\gamma) \right], \tag{4.2.25}$$

where ρ^{Π} is obtained from the disintegration of the measure Π, recall (4.1.4). More specifically, for all $\Pi \in C^{\mathrm{r}}(\mathbb{P}, \mu)$, there exists a map $\rho^{\Pi} : \Omega \times \mathcal{B}(\mathbb{R}) \to \mathbb{R}$ such that (see e.g. Villani [67])

- for all $\omega \in \Omega$, $\rho^{\Pi}(\omega, \cdot)$ is a probability distribution on $(\mathbb{R}, \mathcal{B}(\mathbb{R}))$,
- for all $A \in \mathcal{B}(\mathbb{R})$, $\rho^{\Pi}(\cdot, A)$ is $(\mathcal{F}_T, \mathcal{B}(\mathbb{R}))$-measurable,
- $\Pi(\mathrm{d}\omega, \mathrm{d}\gamma) = \rho^{\Pi}(\omega, \mathrm{d}\gamma)\mathbb{P}(\mathrm{d}\omega)$.

Remark 4.2.6 *In the linear setting of Remark 4.2.5, (4.2.23) writes*

$$\mathcal{V}_{\mathrm{RM}}(\mu) = \inf_{\chi \in \mathcal{T}_+^{\mathrm{r}}(\mu)} \int \Gamma_T(\omega) G(\omega, \chi(\omega)) \mathrm{d}\mathbb{P}(\omega),$$

and the associated Kantorovich (4.2.25) problem

$$\mathcal{V}_{\mathrm{KP}}(\mu) = \inf_{\Pi \in C^{\mathrm{r}}(\mathbb{P},\mu)} \int \Gamma(\omega) G(\omega, \gamma) \mathrm{d}\Pi(\omega, \gamma).$$

Moreover, using disintegration $\Pi(\mathrm{d}\omega, \mathrm{d}\gamma) = \rho^{\Pi}(\omega, \mathrm{d}\gamma)\mathbb{P}(\mathrm{d}\omega)$, we obtain

$$\begin{aligned} \mathcal{V}_{\mathrm{KP}}(\mu) &= \inf_{\Pi \in C^{\mathrm{r}}(\mathbb{P},\mu)} \int \Gamma_T(\omega) \int G(\omega, \gamma) \rho^{\Pi}(\omega, \mathrm{d}\gamma) \mathbb{P}(\mathrm{d}\omega) \\ &= \inf_{\Pi \in C^{\mathrm{r}}(\mathbb{P},\mu)} \mathbb{E}\left[\Gamma_T \int G(\gamma) \rho^{\Pi}(\mathrm{d}\gamma) \right], \end{aligned}$$

which motivates our definition (4.2.25). Theorem 4.2.1 shows that it is indeed the natural non-linear counterpart of the previous relation.

Lemma 4.2.2 *Under Assumption 4.2.4, the set $\mathcal{C}^{\mathrm{r}}(\mathbb{P}, \mu)$ is equal to*

$$\left\{ \Pi \in \mathcal{P}(\bar{\Omega}) \,|\, \mathrm{d}\Pi = \mathbb{P}(\mathrm{d}\omega) \sum_{i=1}^{d} \left(Q_i(\omega) - Q_{i+1}(\omega)\right) \delta_{\gamma_i}(\mathrm{d}\gamma)\,,\ (Q_i)_{i=1}^{d+1} \in \mathfrak{Q}_T(\mu) \right\}, \tag{4.2.26}$$

where, for all $t \in [0, T]$,

$$\mathfrak{Q}_t(\mu) := \left\{ (Q_i)_{i=1}^{d+1} \in \mathcal{L}^2(\mathcal{F}_t) \,\middle|\, 1 = Q_1 \geqslant \cdots \geqslant Q_d \geqslant Q_{d+1} = 0 \text{ and } \mathbb{E}[Q_i] \geqslant q_i, 1 \leqslant i \leqslant d \right\} \tag{4.2.27}$$

Proof. Let us denote $\tilde{\mathcal{C}}$ the set given in (4.2.26).
1. For $\Pi \in \tilde{\mathcal{C}}$, we have obviously $(\mathrm{pr}_1)_\sharp \Pi = \mathbb{P}$.
Moreover, for all $1 \leqslant i \leqslant d$, $\Pi(\Omega \times \{\gamma_i\}) = \mathbb{E}[Q_i - Q_{i+1}]$, so

$$\Pi(\Omega \times \mathrm{supp}[\mu]) = \sum_{i=1}^{d} \left(\mathbb{E}[Q_i] - \mathbb{E}[Q_{i+1}]\right) = \mathbb{E}[Q_1] - \mathbb{E}[Q_{d+1}] = 1,$$

as $Q_1 = 1$ and $Q_{d+1} = 0$, hence $\mathrm{supp}[(\mathrm{pr}_2)_\sharp \Pi] \subset \mathrm{supp}[\mu]$.
Last, for all $1 \leqslant i \leqslant d$,

$$(\mathrm{pr}_2)_\sharp \Pi([\gamma_i, \infty)) = \sum_{j=i}^{d} \mathbb{E}[Q_j] - \mathbb{E}[Q_{j+1}] = \mathbb{E}[Q_i] \geqslant q_i = F_\mu(\gamma_i),$$

which proves that $(\mathrm{pr}_2)_\sharp \Pi \succeq \mu$. Thus, $\Pi \in \mathcal{C}^{\mathrm{r}}(\mathbb{P}, \mu)$.

2. Conversely, let $\Pi(\mathrm{d}\omega, \mathrm{d}\gamma) = \rho^\Pi(\omega, \mathrm{d}\gamma)\mathbb{P}(\mathrm{d}\omega) \in \mathcal{C}^{\mathrm{r}}(\mathbb{P}, \mu)$. Define, for $1 \leqslant i \leqslant d$, $Q_i(\omega) = F_{\rho^\Pi(\omega)}(\gamma_i)$. Since $\mathrm{supp}[(\mathrm{pr}_2)_\sharp \Pi] \subset \mathrm{supp}[\mu]$, we have $\int_\Omega \rho^\Pi(\omega, \mathrm{supp}[\mu])\mathbb{P}(\mathrm{d}\omega) = 1$, implying that $\rho^\Pi(\omega, \mathrm{supp}[\mu]) = 1$ almost surely. Hence, for almost all ω, $1 = Q_1 \geqslant \cdots \geqslant Q_d \geqslant Q_{d+1} = 0$. We also observe

$$\mathrm{d}\Pi = \mathbb{P}(\mathrm{d}\omega) \sum_{i=1}^{d} \left(Q_i(\omega) - Q_{i+1}(\omega)\right) \delta_{\gamma_i}(\mathrm{d}\gamma).$$

Now, for $1 \leqslant i \leqslant d$, since $(\mathrm{pr}_2)_\sharp \Pi \succeq \mu$, we have

$$\mathbb{E}[Q_i] = \mathbb{E}\big[F_{\rho^\Pi}(\gamma_i)\big] = \int_\Omega \rho^\Pi(\omega, [\gamma_i, \infty))\mathbb{P}(\mathrm{d}\omega) \geqslant q_i,$$

which implies that $\Pi \in \tilde{\mathcal{C}}$ and concludes the proof. □

With the notations introduced in the previous Lemma, we obtain straightforwardly the following formulation.

Corollary 4.2.1 *Under Assumption 4.2.4, the Kantorovitch problem (4.2.25) then writes*

$$\mathcal{V}_{\mathrm{KP}}(\mu) = \inf_{(Q_i)_{i=1}^d \in \Omega_T(\mu)} \mathcal{Y}_0 \left[\sum_{i=1}^{d} G(\gamma_i)(Q_i - Q_{i+1})\right]. \tag{4.2.28}$$

We now state and prove the main result of this section, namely that the value of the Monge and Kantorovitch problems (4.2.23) and (4.2.25) coincide.

Theorem 4.2.1 *Under Assumption 4.2.4, the following holds true*

$$\mathcal{V}_{\mathrm{RM}}(\mu) = \mathcal{V}_{\mathrm{KP}}(\mu). \tag{4.2.29}$$

Proof. 1. We first observe that, for all $\epsilon > 0$, there exists a $\mathcal{F}_T$-measurable random variable $\mathfrak{U}^\epsilon$ with uniform distribution and independent of $\mathcal{F}_{T-\epsilon}$, for example $\mathfrak{U}^\epsilon = N\left(\frac{W_T - W_{T-\epsilon}}{\sqrt{\epsilon}}\right)$. Here, N denotes the c.d.f of the standard centered gaussian law.

2. Let $\chi \in \mathfrak{H}^{\mathrm{r}}(\mu)$. Since $\mathrm{supp}[\chi_\sharp \mathbb{P}] \subset \mathrm{supp}[\mu] = \{\gamma_1, \dots, \gamma_d\}$, we have

$$G(\chi) = \sum_{i=1}^{d} G(\gamma_i) \mathbf{1}_{\chi=\gamma_i} = \sum_{i=1}^{d} G(\gamma_i) \left(\mathbf{1}_{\chi \geqslant \gamma_i} - \mathbf{1}_{\chi \geqslant \gamma_{i+1}}\right),$$

where $\gamma_{d+1} := +\infty$. Defining the $\mathcal{F}_T$-measurable random variables $Q_i := \mathbf{1}_{\chi \geqslant \gamma_i}$ for all $1 \leqslant i \leqslant d+1$, one straightforwardly has $1 = Q_1 \geqslant \cdots \geqslant Q_d \geqslant Q_{d+1} = 0$ and $\mathbb{E}[Q_i] = \mathbb{P}(\chi \geqslant \gamma_i) \geqslant F_\mu(\gamma_i) = q_i$, as $\chi_\sharp \mathbb{P} \succeq \mu$. This proves that $(Q_i)_{i=1}^{d+1} \in \mathfrak{Q}_T(\mu)$. Hence

$$\mathcal{Y}_0\left[G(\chi)\right] = \mathcal{Y}_0\left[\sum_{i=1}^{d} G(\gamma_i)(Q_i - Q_{i+1})\right] \geqslant \mathcal{V}_{\mathrm{KP}}(\mu),$$

where we used Corollary 4.2.1 for the last inequality. Taking the infinimum over χ, we obtain $\mathcal{V}_{\mathrm{RM}}(\mu) \geqslant \mathcal{V}_{\mathrm{KP}}(\mu)$.

3. We now prove the converse inequality.
3.a Let $\eta > 0$ and $(Q_i^\eta)_{i=1}^{d+1} \in \mathfrak{Q}_T(\mu)$, such that

$$\mathcal{V}_{\mathrm{KP}}(\mu) \geqslant \mathcal{Y}_0\left[\sum_{i=1}^{d} G(\gamma_i)(Q_i^\eta - Q_{i+1}^\eta)\right] - \eta =: \mathcal{Y}_0\left[\sum_{i=1}^{d} G(\gamma_i) P_i^\eta\right] - \eta, \tag{4.2.30}$$

with $P_i^\eta := Q_i^\eta - Q_{i+1}^\eta$.
Let $\epsilon > 0$ and denote

$$Q_i^{\eta,\epsilon} := \mathbb{E}[Q_i^\eta \,|\, \mathcal{F}_{T-\epsilon}], \quad 1 \leqslant i \leqslant d+1, \text{ and} \tag{4.2.31}$$
$$P_i^{\eta,\epsilon} := Q_i^{\eta,\epsilon} - Q_{i+1}^{\eta,\epsilon} = \mathbb{E}[P_i^\eta \,|\, \mathcal{F}_{T-\epsilon}], \quad 1 \leqslant i \leqslant d. \tag{4.2.32}$$

Note that $(Q_i^{\eta,\epsilon})_{i=1}^{d+1} \in \mathfrak{Q}_{T-\epsilon}(\mu)$ as

$$1 = Q_1^{\eta,\epsilon} \geqslant \cdots \geqslant Q_d^{\eta,\epsilon} \geqslant Q_{d+1}^{\eta,\epsilon} = 0 \text{ and } \mathbb{E}[Q_i^{\eta,\epsilon}] = \mathbb{E}[Q_i^\eta] \geqslant q_i, \text{ for } i \in \{1, \dots, d\}.$$

We now introduce the $\mathcal{F}_T$-measurable random variable

$$\chi^{\eta,\epsilon} := \sum_{i=1}^{d} \gamma_i \mathbf{1}_{\{Q_i^{\eta,\epsilon} \geqslant \mathfrak{U}^\epsilon > Q_{i+1}^{\eta,\epsilon}\}}, \tag{4.2.33}$$

where $\mathfrak{U}^\epsilon$ is constructed in step 1.
One easily computes, for all $1 \leqslant i \leqslant d$,

$$\mathbb{E}\left[\mathbf{1}_{\{\chi^{\eta,\epsilon} \geqslant \gamma_i\}} \,\middle|\, \mathcal{F}_{T-\epsilon}\right] = \mathbb{E}\left[\mathbf{1}_{\{Q_i^{\eta,\epsilon} \geqslant \mathfrak{U}^\epsilon\}} \,\middle|\, \mathcal{F}_{T-\epsilon}\right] = Q_i^{\eta,\epsilon}, \tag{4.2.34}$$

Since $(Q_i^{\eta,\epsilon})_{i=1}^{d+1} \in \mathfrak{Q}_{T-\epsilon}(\mu)$, we deduce, for all $1 \leqslant i \leqslant d$,

$$\mathbb{P}\left(\chi^{\eta,\epsilon} \geqslant \gamma_i\right) = \mathbb{E}\left[\mathbb{E}\left[\mathbf{1}_{\{\chi^{\eta,\epsilon} \geqslant \gamma_i\}} \,\middle|\, \mathcal{F}_{T-\epsilon}\right]\right] = \mathbb{E}\left[Q_i^{\eta,\epsilon}\right] \geqslant q_i,$$

which implies that $\chi^{\eta,\epsilon} \in \mathcal{T}_+^{\mathrm{r}}(\mu)$. Assume that

$$\mathcal{Y}_0\left[\sum_{i=1}^{d} G(\gamma_i) P_i^{\eta}\right] \geqslant \mathcal{Y}_0\left[G(\chi^{\eta,\epsilon})\right] - w(\eta,\epsilon) \tag{4.2.35}$$

where $w(\eta,\epsilon) \to_{\epsilon\to 0} 0$ for all fixed $\eta > 0$.
From the definition of $\mathcal{V}_{\mathrm{RM}}(\mu)$, we straightforwardly obtain

$$\mathcal{Y}_0\left[\sum_{i=1}^{d} G(\gamma_i) P_i^{\eta}\right] \geqslant \mathcal{V}_{\mathrm{RM}}(\mu) - w(\eta,\epsilon), \tag{4.2.36}$$

which, combined with (4.2.30), leads to

$$\mathcal{V}_{\mathrm{KP}}(\mu) \geqslant \mathcal{V}_{\mathrm{RM}}(\mu) - w(\eta,\epsilon) - \eta.$$

Sending ϵ to 0 and then η to 0 yields the inequality for this step and then (4.2.29).
3.b To conclude, it remains to prove (4.2.35).
We define, for all $1 \leqslant i \leqslant d$, $G^{\epsilon}(\gamma_i) := \mathbb{E}[G(\gamma_i)|\mathcal{F}_{T-\epsilon}]$. Recalling (4.2.33), we observe that

$$\begin{aligned}\mathbb{E}\left[G^{\epsilon}(\chi^{\eta,\epsilon}) \,|\, \mathcal{F}_{T-\epsilon}\right] &= \sum_{i=1}^{d} G^{\epsilon}(\gamma_i)\mathbb{E}\left[\mathbf{1}_{Q^{\eta,\epsilon} \geqslant \mathfrak{U}^{\epsilon} > Q_{i+1}^{\eta,\epsilon}} \,\middle|\, \mathcal{F}_{T-\epsilon}\right] \\ &= \sum_{i=1}^{d} G^{\epsilon}(\gamma_i) P_i^{\eta,\epsilon} = \sum_{i=1}^{d} G^{\epsilon}(\gamma_i)\mathbb{E}\left[P_i^{\eta} \,|\, \mathcal{F}_{T-\epsilon}\right],\end{aligned} \tag{4.2.37}$$

where we used (4.2.32) for the last equality. For $\xi \in \mathcal{L}^2(\mathcal{F}_{T-\epsilon})$, let $(\mathcal{Y}_t^{\epsilon}[\xi], \mathcal{Z}_t^{\epsilon}[\xi])_{t\in[0,T-\epsilon]}$ be the solution of the BSDE with terminal condition ξ at terminal time $T-\epsilon$, driver $\mathfrak{f}$, namely

$$\mathcal{Y}_t^{\epsilon}[\xi] = \xi + \int_t^{T-\epsilon} \mathfrak{f}(s, \mathcal{Y}^{\epsilon}[\xi]_s, \mathcal{Z}^{\epsilon}[\xi]_s)\mathrm{d}s - \int_t^{T} \mathcal{Z}^{\epsilon}[\xi]_s \mathrm{d}W_s, \quad t \in [0, T-\epsilon].$$

For the reader's convenience, let us denote

$$\mathfrak{g} := \sum_{i=1}^{d} G(\gamma_i) P_i^{\eta}. \tag{4.2.38}$$

We have, by (4.2.37),

$$\begin{aligned}&\mathcal{Y}_0\left[\mathfrak{g}\right] - \mathcal{Y}_0\left[G(\chi^{\eta,\epsilon})\right] = A^{\eta,\epsilon} + B^{\eta,\epsilon} + C^{\eta,\epsilon} + D^{\eta,\epsilon}, \text{ with} \\ &A^{\eta,\epsilon} := \mathcal{Y}_0\left[\mathfrak{g}\right] - \mathcal{Y}_0^{\epsilon}\left[\mathbb{E}[\mathfrak{g} \,|\, \mathcal{F}_{T-\epsilon}]\right], \\ &B^{\eta,\epsilon} := \mathcal{Y}_0^{\epsilon}\left[\mathbb{E}[\mathfrak{g} \,|\, \mathcal{F}_{T-\epsilon}]\right] - \mathcal{Y}_0^{\epsilon}\left[\mathbb{E}[G^{\epsilon}(\chi^{\eta,\epsilon}) \,|\, \mathcal{F}_{T-\epsilon}]\right], \\ &C^{\eta,\epsilon} := \mathcal{Y}_0^{\epsilon}\left[\mathbb{E}[G^{\epsilon}(\chi^{\eta,\epsilon}) \,|\, \mathcal{F}_{T-\epsilon}]\right] - \mathcal{Y}_0^{\epsilon}\left[\mathbb{E}[G(\chi^{\eta,\epsilon}) \,|\, \mathcal{F}_{T-\epsilon}]\right], \text{ and} \\ &D^{\eta,\epsilon} := \mathcal{Y}_0^{\epsilon}\left[\mathbb{E}[G(\chi^{\eta,\epsilon}) \,|\, \mathcal{F}_{T-\epsilon}]\right] - \mathcal{Y}_0\left[G(\chi^{\eta,\epsilon})\right].\end{aligned}$$

We have, by the flow property and stability of Lipschitz BSDEs, that there exists $C, C' \geqslant 0$ such that

$$\begin{aligned}
|A^{\eta,\epsilon}| &= \left|\mathcal{Y}_0^\epsilon\left[\mathcal{Y}_{T-\epsilon}\left[\mathfrak{g}\right]\right] - \mathcal{Y}_0^\epsilon\left[\mathbb{E}[\mathfrak{g}\,|\,\mathcal{F}_{T-\epsilon}]\right]\right| \\
&\leqslant C\mathbb{E}\Big[\left|\mathcal{Y}_{T-\epsilon}\left[\mathfrak{g}\right] - \mathbb{E}[\mathfrak{g}\,|\,\mathcal{F}_{T-\epsilon}]\right|^2\Big]^{\frac{1}{2}} \\
&\leqslant C'\mathbb{E}\left[\int_{T-\epsilon}^T \left|f\left(s, \mathcal{Y}_s\left[\mathfrak{g}\right], \mathcal{Z}_s\left[\mathfrak{g}\right]\right)\right|^2 \mathrm{d}s\right]^{\frac{1}{2}} \\
&\leqslant C'\mathbb{E}\left[\int_{T-\epsilon}^T 4L^2\left|\mathcal{Y}_s\left[\mathfrak{g}\right]\right|^2 + 4L^2\left|\mathcal{Z}\left[\mathfrak{g}\right]_s\right|^2 + 2|f(s,0,0)|^2 \mathrm{d}s\right]^{\frac{1}{2}},
\end{aligned}$$

which goes to 0 with ϵ, as $\left(\mathcal{Y}\left[\mathfrak{g}\right], \mathcal{Z}\left[\mathfrak{g}\right], f(\cdot,0,0)\right) \in \mathscr{S}^2(\mathbb{F}) \times \mathscr{H}^2(\mathbb{F}) \times \mathscr{H}^2(\mathbb{F})$. Similarly,

$$|D^{\eta,\epsilon}| \leqslant C'\mathbb{E}\left[\int_{T-\epsilon}^T 4L^2\left|\mathcal{Y}_s\left[G(\chi^{\eta,\epsilon})\right]\right|^2 + 4L^2\left|\mathcal{Z}_s\left[G(\chi^{\eta,\epsilon})\right]\right|^2 + 2\left|f(s,0,0)\right|^2 \mathrm{d}s\right] \to_{\epsilon\to 0} 0.$$

We also have, by dominated convergence

$$\begin{aligned}
|B^{\eta,\epsilon}| &\leqslant C\mathbb{E}\left[\left|\mathbb{E}\left[\sum_{i=1}^d \left(G(\gamma_i) - G^\epsilon(\gamma_i)\right) P_i^\eta \,\middle|\, \mathcal{F}_{T-\epsilon}\right]\right|^2\right]^{\frac{1}{2}} \\
&\leqslant C\mathbb{E}\left[\left|\sum_{i=1}^d \left(G(\gamma_i) - G^\epsilon(\gamma_i)\right) P_i^\eta\right|^2\right]^{\frac{1}{2}} \to_{\epsilon\to 0} 0
\end{aligned}$$

and, again by dominated convergence,

$$\begin{aligned}
|C^{\eta,\epsilon}| &\leqslant C\mathbb{E}\Big[\left|\mathbb{E}[G^\epsilon(\chi^{\eta,\epsilon}) - G(\chi^{\eta,\epsilon})\,|\,\mathcal{F}_{T-\epsilon}]\right|^2\Big]^{\frac{1}{2}} \\
&\leqslant C\mathbb{E}\Big[\left|G^\epsilon(\chi^{\eta,\epsilon}) - G(\chi^{\eta,\epsilon})\right|^2\Big]^{\frac{1}{2}} \to_{\epsilon\to 0} 0,
\end{aligned}$$

which concludes the proof. □

4.3 Duality in the Linear case

We now focus on a special framework, useful for application, where tractable and implementable formula can be derived, namely the linear setting. We will thus assume that the Assumption 4.2.1 is in force throughout the section. We will use duality methods to solve the weak hedging problem, first for generic random function G in the setting of Assumption 4.2.4, then for a specific PnL matching problem with a more general target probability. In this last case, the duality method boils down to use classical optimal tools.

Recalling the setting of Remark 4.2.1, we define the random function

$$H(\omega, \gamma) := \Gamma_T(\omega) G(\omega, \gamma), \tag{4.3.1}$$

and Combining (4.2.5) and (4.2.7), we observe that, for all $\gamma \in \mathbb{R}$,

$$H(\gamma) \in \mathscr{L}^2(\mathcal{F}_T). \tag{4.3.2}$$

In this framework, Proposition 4.2.2, Lemma 4.2.1, Corollary 4.2.1 and Theorem 4.2.1 write

Corollary 4.3.1 *1. For all $\mu \in \mathcal{P}_4(\mathbb{R})$, we have $\mathcal{V}_{\mathrm{WH}}(\mu) = \widehat{\mathcal{V}}_{\mathrm{RM}}(\mu)$ with*

$$\widehat{\mathcal{V}}_{\mathrm{RM}}(\mu) = \inf_{\chi \in \mathcal{T}_+(\mu)} \mathbb{E}[H(\chi)]\,. \tag{4.3.3}$$

2. If, moreover, Assumption 4.2.4 holds, then $\mathcal{V}_{\mathrm{QH}}(\mu) = \mathcal{V}_{\mathrm{RM}}(\mu) = \mathcal{V}_{\mathrm{KP}}(\mu)$, with

$$\mathcal{V}_{\mathrm{RM}}(\mu) = \inf_{\chi \in \mathcal{T}_+^{\mathrm{t}}(\mu)} \mathbb{E}[H(\chi)]\,, \tag{4.3.4}$$

$$\mathcal{V}_{\mathrm{KP}}(\mu) = \inf_{(Q_i)_{i=1}^{d+1} \in \mathfrak{Q}_T(\mu)} \mathbb{E}\left[\sum_{i=1}^{d} H(\gamma_i)(Q_i - Q_{i+1})\right]. \tag{4.3.5}$$

4.3.1 μ has finite support

We work under Assumption 4.2.4.

We now introduce the dual formulation of the Kantorovitch problem. For μ satisfying to Assumption 4.2.4, we set

$$\mathcal{V}_{\mathrm{DP}}(\mu) := \sup_{(X,\Phi) \in \mathfrak{P}_{H,\mu}} \left(\mathbb{E}[X] + \sum_{i=1}^{d} \Phi_i \mu(\{\gamma_i\})\right), \tag{4.3.6}$$

where

$$\mathfrak{P}_{H,\mu} := \left\{(X,\Phi) \in \mathscr{L}^2(\mathcal{F}_T) \times \Delta_+^d \,\middle|\, H(\gamma_i) \geqslant X + \Phi_i, 1 \leqslant i \leqslant d, \mathbb{P}-\text{a.s.}\right\}. \tag{4.3.7}$$

Proposition 4.3.1 *Under Assumption 4.2.4, we have*

$$\mathcal{V}_{\mathrm{KP}}(\mu) \geqslant \mathcal{V}_{\mathrm{DP}}(\mu), \tag{4.3.8}$$

and

$$\mathcal{V}_{\mathrm{DP}}(\mu) = \sup_{\Phi \in \Delta_+^d} \left(\mathbb{E}\left[\Phi^\flat\right] + \sum_{i=1}^{d} \Phi_i \mu(\{\gamma_i\})\right), \tag{4.3.9}$$

with, for $\Phi \in \Delta_+^d$,

$$\Phi^\flat := \min_{1 \leqslant i \leqslant d} [H(\gamma_i) - \Phi_i] \in \mathscr{L}^2(\mathcal{F}_T), \tag{4.3.10}$$

so that in particular $(\Phi^\flat, \Phi) \in \mathfrak{P}_{H,\mu}$.

Proof. 1. For $\Pi \in \mathcal{C}^r(\mathbb{P}, \mu)$ and $(X, \Phi) \in \mathfrak{P}_{H,\mu}$, we have

$$\int H(\omega, \gamma)\Pi(\mathrm{d}\omega, \mathrm{d}\gamma) = \int_\Omega \sum_{i=1}^d H(\omega, \gamma_i)\Pi(\mathrm{d}\omega, \{\gamma_i\}) \tag{4.3.11}$$

$$\geqslant \int_\Omega \sum_{i=1}^d \left(X(\omega) + \Phi_i\right)\Pi(\mathrm{d}\omega, \{\gamma_i\}) \tag{4.3.12}$$

$$= \mathbb{E}[X] + \sum_{i=1}^d \Phi_i (\mathrm{pr}_2)_\sharp \Pi(\{\gamma_i\}) \tag{4.3.13}$$

$$\geqslant \mathbb{E}[X] + \sum_{i=1}^d \Phi_i \mu(\{\gamma_i\}), \tag{4.3.14}$$

where we used the definition of $\mathfrak{P}_{H,\mu}$ and the fact that $0 \leqslant \Phi_1 \leqslant \cdots \leqslant \Phi_d$ together with $(\mathrm{pr}_2)_\sharp \Pi \succeq \mu$.
2. From the definitions, we straightforwardly have that $(\Phi^\flat, \Phi) \in \mathfrak{P}_{H,\mu}$ for any $\Phi \in \Delta_+^d$. Hence

$$\mathcal{V}_{\mathrm{DP}}(\mu) \geqslant \sup_{\Phi \in \Delta_+^d} \left(\mathbb{E}\left[\Phi^\flat\right] + \sum_{i=1}^d \Phi_i \mu(\{\gamma_i\}) \right).$$

Conversely, for any $(X, \Phi) \in \mathfrak{P}_{H,\mu}$, it is clear that $X \leqslant \Phi^b$ and thus

$$\begin{aligned}\sup_{\hat{\Phi} \in \Delta_+^d} \left(\mathbb{E}\left[\hat{\Phi}^\flat\right] + \sum \hat{\Phi}_\ell \mu(\{\gamma_\ell\}) \right) &\geqslant \mathbb{E}\left[\Phi^\flat\right] + \sum \Phi_\ell \mu(\{\gamma_\ell\}) \\ &\geqslant \mathbb{E}[X] + \sum \Phi_\ell \mu(\{\gamma_\ell\}),\end{aligned}$$

hence

$$\sup_{\Phi \in \Delta_+^d} \left(\mathbb{E}\left[\Phi^\flat\right] + \sum_{i=1}^d \Phi_i \mu(\{\gamma_i\}) \right) \geqslant \mathcal{V}_{\mathrm{DP}}(\mu),$$

which concludes the proof. □

Regarding the dual problem (4.3.6), one can in fact reduce the dimension using (4.3.9). To this effect, for all $1 \leqslant i \leqslant d$, we set

$$\tilde{H}(\gamma_i) := H(\gamma_i) - H(\gamma_1) = \Gamma_T(G(\gamma_i) - G(\gamma_1)). \tag{4.3.15}$$

We then have

Corollary 4.3.2 *Under Assumption 4.2.4, we have*

$$\begin{aligned}\mathcal{V}_{\mathrm{DP}}(\mu) &= \mathbb{E}[H(\gamma_1)] + \mathfrak{V}(p_2, \ldots, p_d) \\ &= \mathbb{E}[H(\gamma_1)] + \mathfrak{W}(q_2, \ldots, q_d),\end{aligned} \tag{4.3.16}$$

where

$$\mathfrak{V}(p) = \sup_{\zeta\in\Delta_+^{d-1}} \left(\left(\sum_{i=1}^{d-1} \zeta_i p_{i+1} \right) - \mathbb{E}\left[\max_{1\leqslant i\leqslant d-1} \left(\zeta_i - \tilde{H}(\gamma_{i+1})\right)_+ \right] \right), \tag{4.3.17}$$

$$\mathfrak{W}(q) = \sup_{\theta\in\mathbb{R}_+^{d-1}} \sum_{j=1}^{d-1} \theta_j q_{j+1} - \mathbb{E}\left[\max_{1\leqslant i\leqslant d-1} \left(\sum_{j=1}^{i} \theta_j - \tilde{H}(\gamma_{i+1}) \right)_+ \right]. \tag{4.3.18}$$

Proof. For $\Phi \in \Delta_+^d$, we have, with $\zeta_i := \Phi_{i+1} - \Phi_1$, $1 \leqslant i \leqslant d-1$,

$$\Phi^\flat = H(\gamma_1) - \max_{1\leqslant i\leqslant d-1} \left(\zeta_i - \tilde{H}(\gamma_{i+1})\right)_+ - \Phi_1$$

Thus

$$\begin{aligned}
\mathcal{V}_{\mathrm{DP}}(\mu) &:= \sup_{\Phi\in\Delta_+^d} \mathbb{E}\left[\Phi^\flat\right] + \sum_{i=1}^{d} \Phi_i p_i \\
&= \sup_{\Phi\in\Delta_+^d} \mathbb{E}\left[H(\gamma_1) - \max_{1\leqslant i\leqslant d-1} \left(\zeta_i - \tilde{H}(\gamma_{i+1})\right)_+ \right] + \sum_{i=1}^{d} (\Phi_i - \Phi_1)\, p_i \\
&= \mathbb{E}[H(\gamma_1)] + \sup_{\zeta\in\Delta_+^{d-1}} \sum_{i=1}^{d-1} \zeta_i p_{i+1} - \mathbb{E}\left[\max_{1\leqslant i\leqslant d-1} \left(\zeta_i - \tilde{H}(\gamma_{i+1})\right)_+ \right].
\end{aligned}$$

Last, notice that Δ_+^{d-1} and $\mathbb{R}_+^{d-1}$ are in bijection, through $\Delta_+^{d-1} \ni \zeta \mapsto \theta = (\theta_i := \zeta_i - \zeta_{i-1})_{i=1}^{d-1} \in \mathbb{R}_+^{d-1}$ and its inverse $\mathbb{R}_+^{d-1} \ni \theta \mapsto \zeta = (\zeta_i := \sum_{j=1}^{i} \theta_i)_{i=1}^{d-1}$. We then have

$$\begin{aligned}
\mathcal{V}_{\mathrm{DP}} &= \mathbb{E}[H(\gamma_1)] + \sup_{\theta\in\mathbb{R}_+^{d-1}} \sum_{i=1}^{d-1} \left(\sum_{j=1}^{i} \theta_j \right) p_{i+1} - \mathbb{E}\left[\max_{1\leqslant i\leqslant d-1} \left(\sum_{j=1}^{i} \theta_j - \tilde{H}(\gamma_{i+1}) \right)_+ \right] \\
&= \mathbb{E}[H(\gamma_1)] + \sup_{\theta\in\mathbb{R}_+^{d-1}} \sum_{j=1}^{d-1} \sum_{i=j}^{d-1} p_{i+1} \theta_j - \mathbb{E}\left[\max_{1\leqslant i\leqslant d-1} \left(\sum_{j=1}^{i} \theta_j - \tilde{H}(\gamma_{i+1}) \right)_+ \right],
\end{aligned}$$

Recalling the notations in Assumption 4.2.4, we have $q_{j+1} = \sum_{i=j}^{d-1} p_{i+1}$, which concludes the proof. □

Remark 4.3.1

1. *In the applications, it is common to have $G(\gamma_1) = 0$, see e.g. [14, 15].*

2. *The function $\mathfrak{V}$ above appears as the Fenchel transform of the function*

$$\zeta \mapsto \mathbb{E}\left[\max_{i\in\{1,\dots,d-1\}} \left(\zeta_i - \tilde{H}_{i+1}\right)_+ \right].$$

This has already been observed and used in the context of one quantile constraint see e.g. [14, 11].

4.3.1.1 Proof of duality

The remaining of this section is dedicated to prove the reverse inequality $\mathcal{V}_{\mathrm{DP}} \geqslant \mathcal{V}_{\mathrm{KP}}$ in various settings. We obtain the duality for the case of one quantile constraint and two quantile constraints. This is obtained after tedious computations which allow us to characterise precisely the payoff to replicate, when one considers financial application, see Remark 4.3.3. The results for the general multi-dimensional are mostly conjectured in Section 4.3.1.4.
We shall use Corollary 4.3.2 and in particular the form given in (4.3.18). To this end, we define

$$\begin{aligned} \tilde{w} : \mathbb{R}_+^{d-1} &\to \mathbb{R} \\ \theta &\mapsto \sum_{j=1}^{d-1} \theta_j q_{j+1} - \mathbb{E}\left[\max_{1 \leqslant i \leqslant d-1} \left(\sum_{j=1}^{i} \theta_j - \tilde{H}(\gamma_{i+1}) \right)_+ \right]. \end{aligned} \tag{4.3.19}$$

In the following, we will often use the extended version of $\tilde{w}$ on $\mathbb{R}^{d-1}$ to apply general results of convex analysis (see e.g. [64]). Namely, we consider the function

$$w := \tilde{w} \mathbf{1}_{\mathbb{R}_+^{d-1}} + (-\infty) \mathbf{1}_{\mathbb{R}^d \setminus \mathbb{R}_+^{d-1}} . \tag{4.3.20}$$

We now list some general properties useful to solve the optimisation of the dual problem.

Lemma 4.3.1 *The function w is concave, continuous on $\mathbb{R}_+^{d-1}$ and satisfies*

$$\lim_{|\theta| \to \infty, \theta \in \mathbb{R}_+^{d-1}} w(\theta) = -\infty. \tag{4.3.21}$$

In particular, there exists $\theta^\star \in \mathbb{R}_+^{d-1}$ such that

$$\mathfrak{W}(q) = \sup_{\theta \in \mathbb{R}_+^{d-1}} w(\theta) = w(\theta^\star). \tag{4.3.22}$$

Proof. Continuity and concavity are straightforward consequences of (4.3.19), as the max operator is convex.
We have, since $1 > q_2 > \cdots > q_d > 0$,

$$\begin{aligned} w(\theta) &= \sum_{j=1}^{d-1} \theta_j q_{j+1} - \mathbb{E}\left[\max_{1 \leqslant i \leqslant d-1} \left(\sum_{j=1}^{i} \theta_j - \tilde{H}(\gamma_{i+1}) \right)_+ \right] \\ &\leqslant q_2 \sum_{j=1}^{d-1} \theta_j - \mathbb{E}\left[\left(\sum_{j=1}^{d-1} \theta_j - \tilde{H}(\gamma_d) \right)_+ \right] \\ &= \left(\sum_{j=1}^{d-1} \theta_j \right) \left(q_2 - \mathbb{P}\left[\sum_{j=1}^{d-1} \theta_j \geqslant \tilde{H}(\gamma_d) \right] \right) - \mathbb{E}\left[\tilde{H}(\gamma_d) \mathbf{1}_{\left\{ \sum_{j=1}^{d-1} \theta_j \geqslant \tilde{H}(\gamma_d) \right\}} \right]. \end{aligned}$$

Hence, as $|\theta| \to \infty$, we have, since $\theta_j \geqslant 0$ for all $1 \leqslant j \leqslant d-1$, recall (4.3.2),

$$\sum_{j=1}^{d-1} \theta_j \to \infty, \quad q_2 - \mathbb{P}\left[\sum_{j=1}^{d-1} \theta_j \geqslant \tilde{H}(\gamma_d)\right] \to q_2 - 1 < 0, \quad \text{and}$$
$$\mathbb{E}\Big[\tilde{H}(\gamma_d)\mathbf{1}_{\{\sum_{j=1}^{d-1}\theta_j \geqslant \tilde{H}(\gamma_d)\}}\Big] \to \mathbb{E}\big[\tilde{H}(\gamma_d)\big] > -\infty,$$

which proves that $w(\theta)$ goes to $-\infty$.
We note that the continuity and coercivity of w on $(\mathbb{R}_+)^{d-1}$ guarantee the existence of an argument maximum. □

4.3.1.2 The one quantile constraint case

We first consider the case $d = 2$ in Assumption 4.2.4, i.e. where $\mu = (1-q)\delta_{\gamma_1} + q\delta_{\gamma_2}$ with $0 < q < 1$. This case has already been well studied in the literature, see Remark 4.3.2 below.
In that setting, Corollary 4.3.1, Proposition 4.3.1 and Corollary 4.3.2 read simply

Corollary 4.3.3 *We have* $\mathcal{V}_{\mathrm{QH}}(\mu) = \mathcal{V}_{\mathrm{RM}}(\mu) = \mathcal{V}_{\mathrm{KP}}(\mu) \geqslant \mathcal{V}_{\mathrm{DP}}(\mu)$, *with*

$$\mathcal{V}_{\mathrm{RM}}(\mu) = \inf_{\chi \in \mathcal{T}_\mu^{\mathrm{r}}} \mathbb{E}\big[H(\chi)\big], \tag{4.3.23}$$
$$\mathcal{V}_{\mathrm{KP}}(\mu) = \inf_{(1,Q,0)\in\mathfrak{Q}_T(\mu)} \mathbb{E}\big[(1-Q)H(\gamma_1) + QH(\gamma_2)\big], \tag{4.3.24}$$

recall (4.2.27) *and*

$$\mathcal{V}_{\mathrm{DP}}(\mu) = H(\gamma_1) + \sup_{\theta \geqslant 0} w(\theta), \tag{4.3.25}$$

with $w(\theta) = \theta q - \mathbb{E}\big[(\theta - \tilde{H}(\gamma_2))^+\big]$, *recall* (4.3.19).

Remark 4.3.2 *Classically, see e.g. [36, 14, 5], the quantile hedging problem with one quantile constraint is formulated with a positivity contraint, namely* $H(\gamma_1) = 0$. *Moreover, one chooses* $\gamma_1 = 0$, $\gamma_2 = 1$, *setting* $G(0) = 0$ *and* $G(1) = \xi\gamma$ *for some payoff* $\xi \geqslant 0$ *to partially hedge. In particular the following formula for the quantile hedging price is stated, see [14],*

$$\mathcal{V}(\mu) = \inf_{P \in \mathscr{P}^p} \mathbb{E}\big[\Gamma_T \xi \mathbf{1}_{P>0}\big],$$

where $\mathscr{P}^p = \big\{P \in \mathcal{L}^2(\mathcal{F}_T) \,\big|\, P \in [0,1] \text{ and } \mathbb{E}[P] \geqslant p\big\}$, *which corresponds exactly to the Relaxed Monge problem* (4.3.23). *The classical dual approach (followed e.g. in [14, 11]) is then to introduce the quantity*

$$\tilde{\mathcal{V}}(p) = \inf_{P \in \mathscr{P}^p} \mathbb{E}\big[\Gamma_T \xi P\big],$$

which in turn corresponds exactly to the Kantorovich Problem problem (4.3.24).

We now prove the duality in this case.

Theorem 4.3.1 *We have* $\mathcal{V}_{\mathrm{KP}}(\mu) = \mathcal{V}_{\mathrm{DP}}(\mu)$ *and setting, for* $\theta^\star \in \operatorname{argmax} w$, *recall* (4.3.25),

$$Q^\star := \mathbf{1}_{\{\tilde{H}(\gamma_2)<\theta^\star\}} + \frac{q - \mathbb{P}\big[\tilde{H}(\gamma_2) < \theta^\star\big]}{\mathbb{P}\big[\tilde{H}(\gamma_2) = \theta^\star\big]}\mathbf{1}_{\{\tilde{H}(\gamma_2)=\theta^\star\}}\,, \tag{4.3.26}$$

which is such that $(1, Q^\star, 0) \in \mathfrak{Q}_T(\mu)$, *we have*

$$\mathcal{V}_{\mathrm{DP}}(\mu) = \mathbb{E}[(1-Q^\star)H(\gamma_1) + Q^\star H(\gamma_2)]\,.$$

Moreover, if $\mathbb{P}\big[\tilde{H}(\gamma_2) = \theta^\star\big] = 0$, *then*

$$\mathcal{V}_{\mathrm{DP}}(\mu) = \mathbb{E}[H(\chi^\star)]\,, \tag{4.3.27}$$

with

$$\chi^\star := \gamma_1 \mathbf{1}_{\{\tilde{H}(\gamma_2)\geqslant\theta^\star\}} + \gamma_2 \mathbf{1}_{\{\tilde{H}(\gamma_2)<\theta^\star\}} \in \mathcal{T}_+^{\mathrm{r}}(\mu). \tag{4.3.28}$$

Proof. Since $\mathcal{V}_{\mathrm{KP}}(\mu) \geqslant \mathcal{V}_{\mathrm{DP}}(\mu)$ by Proposition 4.3.1, we only need to prove that $\mathcal{V}_{\mathrm{DP}}(\mu) \geqslant \mathcal{V}_{\mathrm{KP}}(\mu)$. Recall that, for $\theta \geqslant 0$,

$$w(\theta) := \theta q - \mathbb{E}\big[(\theta - \tilde{H}(\gamma_2))^+\big] \tag{4.3.29}$$

$$= \theta\left(q - \mathbb{P}\big[\tilde{H}(\gamma_2) < \theta\big]\right) + \mathbb{E}\Big[\tilde{H}(\gamma_2)\mathbf{1}_{\{\tilde{H}(\gamma_2)<\theta\}}\Big]\,. \tag{4.3.30}$$

We have that w is concave, recall Lemma 4.3.1, and it admits left-hand derivatives at every point of $(0,\infty)$ and right-hand derivatives at every point of $[0,\infty)$ given by

$$w'_-(\theta) = q - \mathbb{P}\big[\tilde{H}(\gamma_2) < \theta\big]\,, \quad \theta > 0,$$
$$w'_+(\theta) = q - \mathbb{P}\big[\tilde{H}(\gamma_2) \leqslant \theta\big]\,, \quad \theta \geqslant 0.$$

Moreover, for all $0 \leqslant \theta \leqslant \theta' < \infty$ (setting in addition $w'_-(0) := +\infty$),

$$w'_-(\theta) \geqslant w'_+(\theta) \geqslant w'_-(\theta') \geqslant w'_+(\theta').$$

The classical result from convex optimisation states

$$\operatorname{argmax} w = \left\{\theta \in [0,\infty) \,\middle|\, w'_-(\theta) \geqslant 0 \geqslant w'_+(\theta)\right\},$$

here $[w'_+(\theta), w'_-(\theta)]$ is the subdifferential of w at θ.
Let $\theta^\star \in \operatorname{argmax} w$. We now discuss various cases.
1. If $w'_-(\theta^\star) = 0$, then $\mathbb{P}\big[\tilde{H}(\gamma_2) < \theta^\star\big] = q$, and $w(\theta^\star) = \mathbb{E}\Big[\tilde{H}(\gamma_2)\mathbf{1}_{\{\tilde{H}(\gamma_2)<\theta^\star\}}\Big]$, recall (4.3.30). Then, setting $\chi^\star$ as in (4.3.28), we obtain, recalling (4.3.25) and (4.3.15),

$$\mathcal{V}_{\mathrm{DP}}(\mu) = \mathbb{E}[H(\chi^\star)]\,.$$

Since $\mathbb{P}[\chi = \gamma_2] = \mathbb{P}\big[\tilde{H}(\gamma_2) < \theta^\star\big] = q$, we have that $\chi^\star \in \mathcal{T}_+^{\mathrm{r}}(\mu)$. This proves for this case $\mathcal{V}_{\mathrm{DP}}(\mu) \geqslant \mathcal{V}_{\mathrm{RM}}(\mu) = \mathcal{V}_{\mathrm{KP}}(\mu)$.
2. Otherwise, $0 < w'_-(\theta^\star) = q - \mathbb{P}\big[\tilde{H}(\gamma_2) < \theta^\star\big]$, and since $0 \geqslant w'_+(\theta^\star) = q -$

$\mathbb{P}\big[\tilde{H}(\gamma_2) \leqslant \theta\big]$, we have $\mathbb{P}\big[\tilde{H}(\gamma_2) < \theta^\star\big] < q \leqslant \mathbb{P}\big[\tilde{H}(\gamma_2) \leqslant \theta^\star\big]$, so $\mathbb{P}\big[\tilde{H}(\gamma_2) = \theta^\star\big] > 0$. We then compute, recall (4.3.25),

$$\begin{aligned}
\mathcal{V}_{\rm DP}(\mu) &= \mathbb{E}[H(\gamma_1)] + w(\theta^\star) \\
&= \mathbb{E}[H(\gamma_1)] + \theta^\star \left(q - \mathbb{P}\big[\tilde{H}(\gamma_2) < \theta^\star\big]\right) + \mathbb{E}\Big[\tilde{H}(\gamma_2)\mathbf{1}_{\{\tilde{H}(\gamma_2)<\theta^\star\}}\Big] \\
&= \mathbb{E}[H(\gamma_1)] + \mathbb{E}\Big[\tilde{H}(\gamma_2)\mathbf{1}_{\{\tilde{H}(\gamma_2)=\theta^\star\}}\Big] \frac{q - \mathbb{P}\big[\tilde{H}(\gamma_2) < \theta^\star\big]}{\mathbb{P}\big[\tilde{H}(\gamma_2) = \theta^\star\big]} + \mathbb{E}\Big[\tilde{H}(\gamma_2)\mathbf{1}_{\{\tilde{H}(\gamma_2)<\theta^\star\}}\Big] \\
&= \mathbb{E}[H(\gamma_1)] + \mathbb{E}[(H(\gamma_2) - H(\gamma_1))Q^\star]
\end{aligned}$$

recall (4.3.26). Note that $(1, Q^\star, 0) \in \mathfrak{Q}_T(\mu)$ as $\mathbb{E}[Q^\star] = q$, and $Q^\star \in \left\{1, \frac{q-\mathbb{P}[\tilde{H}(\gamma_2)<\theta^\star]}{\mathbb{P}[\tilde{H}(\gamma_2)=\theta^\star]}\right\} \subset [0,1]$ as

$$\frac{q - \mathbb{P}\big[\tilde{H}(\gamma_2) < \theta^\star\big]}{\mathbb{P}\big[\tilde{H}(\gamma_2) = \theta^\star\big]} = \frac{q - \mathbb{P}\big[\tilde{H}(\gamma_2) < \theta^\star\big]}{\mathbb{P}\big[\tilde{H}(\gamma_2) \leqslant \theta^\star\big] - \mathbb{P}\big[\tilde{H}(\gamma_2 < \theta^\star)\big]} \leqslant 1.$$

Hence $\mathcal{V}_{\rm DP}(\mu) = \mathbb{E}[(1 - Q^\star)H(\gamma_1) + Q^\star H(\gamma_2)] \geqslant \mathcal{V}_{\rm KP}(\mu)$. □

Remark 4.3.3 *1. We note that in the case (4.3.27), the infimum in the 'Relaxed Monge' problem (4.3.4) is a minimum.*

2. In financial applications, Theorem 4.3.1 gives the modified payoff to replicate. In the most general case, it is given by

$$\xi^\star := (1 - Q^\star)G(\gamma_1) + Q^\star G(\gamma_2), \tag{4.3.31}$$

since Γ_T interprets as the density of the risk neutral measure.

4.3.1.3 Application to two constraints case

We consider the case $d = 3$ in Assumption 4.2.4, i.e. where $\mu = (1 - q_2)\delta_{\gamma_1} + (q_2 - q_3)\delta_{\gamma_2} + q_3\delta_{\gamma_3}$, where $q_1 := 1 > q_2 > q_3 > 0$ and $\gamma_1 < \gamma_2 < \gamma_3$. In that setting, Corollary 4.3.1, Proposition 4.3.1 and Corollary 4.3.2 write

Corollary 4.3.4 *We have $\mathcal{V}_{\rm QH}(\mu) = \mathcal{V}_{\rm RM}(\mu) = \mathcal{V}_{\rm KP}(\mu) \geqslant \mathcal{V}_{\rm DP}(\mu)$, with*

$$\mathcal{V}_{\rm RM}(\mu) = \inf_{\chi \in \mathcal{T}_\mu^{\rm r}} \mathbb{E}[H(\chi)]\,, \tag{4.3.32}$$

$$\mathcal{V}_{\rm KP}(\mu) = \inf_{(1,Q_2,Q_3,0)\in\mathfrak{Q}_T(\mu)} \mathbb{E}[(1 - Q_2)H(\gamma_1) + (Q_2 - Q_3)H(\gamma_2) + Q_3 H(\gamma_3)]\,, \tag{4.3.33}$$

$$\mathcal{V}_{\rm DP}(\mu) = H(\gamma_1) + \mathfrak{W}(q), \tag{4.3.34}$$

with

$$\begin{aligned}
\mathfrak{W}(q_2, q_3) &= \sup_{\theta_1 \geqslant 0, \theta_2 \geqslant 0} w(\theta_1, \theta_2), \\
w(\theta_1, \theta_2) &= \theta_1 q_2 + \theta_2 q_3 - \mathbb{E}\big[\max\big(0, \theta_1 - \tilde{H}(\gamma_2), \theta_1 + \theta_2 - \tilde{H}(\gamma_3)\big)\big]\,.
\end{aligned}$$

We will now prove the duality in some particular cases. By Lemma 4.3.1, w is concave on $\mathbb{R}_+ \times \mathbb{R}_+$. Hence it admits left and right partial derivatives at every point, which we now compute. To this effect, we define, for $\theta = (\theta_1, \theta_2) \in \mathbb{R}_+ \times \mathbb{R}_+$,

$$\Phi_1(\theta) = (\theta_1 - \tilde{H}(\gamma_2) + \Phi_2(\theta))_+, \text{ and } \Phi_2(\theta) = (\theta_2 + \tilde{H}(\gamma_2) - \tilde{H}(\gamma_3))_+.$$

Lemma 4.3.2 *For all $\theta \in \mathbb{R}_+ \times \mathbb{R}_+$,*

$$\begin{aligned}
\partial_{1,-} w(\theta) &= q_2 - \mathbb{E}\big[\mathbf{1}_{\Phi_1(\theta)>0}\big] + (+\infty)\mathbf{1}_{\{\theta_1=0\}},\\
\partial_{1,+} w(\theta) &= q_2 - \mathbb{E}\Big[\mathbf{1}_{\theta-\tilde{H}(\gamma_2)+\Phi_2(\theta)\geqslant 0}\Big],\\
\partial_{2,-} w(\theta) &= q_3 - \mathbb{E}\big[\mathbf{1}_{\Phi_1(\theta)>0}\mathbf{1}_{\Phi_2(\theta)>0}\big] + (+\infty)\mathbf{1}_{\{\theta_2=0\}},\\
\partial_{2,+} w(\theta) &= q_3 - \mathbb{E}\Big[\mathbf{1}_{\theta_1-\tilde{H}(\gamma_2)+\Phi_2(\theta)\geqslant 0}\mathbf{1}_{\theta_2-\tilde{H}(\gamma_2)+\tilde{H}(\gamma_3)\geqslant 0}\Big].
\end{aligned}$$

Proof. We have, for all $\theta \in \mathbb{R}_+ \times \mathbb{R}_+$,

$$\begin{aligned}
w(\theta) =& \theta_1 q_2 + \theta_2 q_3 - \mathbb{E}\big[(\theta_1 + \theta_2 - \tilde{H}(\gamma_3))\mathbf{1}_{\Phi_1(\theta)>0}\mathbf{1}_{\Phi_2(\theta)>0}\big] - \mathbb{E}\big[(\theta_1 - \tilde{H}(\gamma_2))\mathbf{1}_{\Phi_1(\theta)>0}\mathbf{1}_{\Phi_2(\theta)=0}\big]\\
=& \theta_1\left(q_2 - \mathbb{E}\big[\mathbf{1}_{\Phi_1(\theta)>0}\big]\right) + \theta_2\left(q_3 - \mathbb{E}\big[\mathbf{1}_{\Phi_1(\theta)>0}\mathbf{1}_{\Phi_2(\theta)>0}\big]\right) \qquad (4.3.35)\\
&+ \mathbb{E}\big[\tilde{H}(\gamma_2)\left(\mathbf{1}_{\Phi_1(\theta)>0} - \mathbf{1}_{\Phi_1(\theta)>0}\mathbf{1}_{\Phi_2(\theta)>0}\right)\big] + \mathbb{E}\big[\tilde{H}(\gamma_3)\mathbf{1}_{\Phi_1(\theta)>0}\mathbf{1}_{\Phi_2(\theta)>0}\big]\\
=& \theta_1\left(q_2 - \mathbb{E}\big[\mathbf{1}_{\Phi_1(\theta)>0}\big]\right) + \theta_2\left(q_3 - \mathbb{E}\big[\mathbf{1}_{\Phi_1(\theta)>0}\mathbf{1}_{\Phi_2(\theta)>0}\big]\right)\\
&+ \mathbb{E}\big[\tilde{H}(\gamma_2)\mathbf{1}_{\Phi_1(\theta)>0}\big] + \mathbb{E}\big[(\tilde{H}(\gamma_3) - \tilde{H}(\gamma_2))\mathbf{1}_{\Phi_1(\theta)>0}\mathbf{1}_{\Phi_2(\theta)>0}\big].
\end{aligned}$$

We now compute the partial left and right derivatives.
1. Computing $\partial_{1,-} w$: We first have, for $\theta \in \mathbb{R}_+^* \times \mathbb{R}_+$, setting $\Phi_1 := \Phi_1(\theta)$, $\Phi_2 = \Phi_2(\theta)$, and for all $\epsilon > 0$, $\Phi_1^\epsilon := \Phi_1(\theta_1 - \epsilon, \theta_2)$ and $\Phi_2^\epsilon := \Phi_2(\theta_1 - \epsilon, \theta_2)$,

$$\begin{aligned}
\partial_{1,-} w(\theta) =& \left(q_2 - \lim_{0<\epsilon\to 0} \mathbb{E}\big[\mathbf{1}_{\Phi_1^\epsilon>0}\big]\right) - \theta_1 \partial_{1,-}\mathbb{E}\big[\mathbf{1}_{\Phi_1>0}\big] - \theta_2 \partial_{1,-}\mathbb{E}\big[\mathbf{1}_{\Phi_1>0}\mathbf{1}_{\Phi_2>0}\big]\\
&+ \partial_{1,-}\mathbb{E}\big[\tilde{H}(\gamma_2)\mathbf{1}_{\Phi_1>0}\big] + \partial_{1,-}\mathbb{E}\big[(\tilde{H}(\gamma_3) - \tilde{H}(\gamma_2))\mathbf{1}_{\Phi_1>0}\mathbf{1}_{\Phi_2>0}\big]\\
=& \left(q_2 - \lim_{0<\epsilon\to 0} \mathbb{E}\big[\mathbf{1}_{\Phi_1^\epsilon>0}\big]\right)\\
&+ \theta_1 \lim_{0<\epsilon\to 0} \frac{1}{\epsilon}\mathbb{E}\big[\mathbf{1}_{\Phi_1>0} - \mathbf{1}_{\Phi_1^\epsilon>0}\big] + \theta_2 \lim_{0<\epsilon\to 0} \frac{1}{\epsilon}\mathbb{E}\big[\mathbf{1}_{\Phi_1>0}\mathbf{1}_{\Phi_2>0} - \mathbf{1}_{\Phi_1^\epsilon>0}\mathbf{1}_{\Phi_2^\epsilon>0}\big]\\
&- \lim_{0<\epsilon\to 0} \frac{1}{\epsilon}\mathbb{E}\big[\tilde{H}(\gamma_2)\left(\mathbf{1}_{\Phi_1>0} - \mathbf{1}_{\Phi_1^\epsilon>0}\right)\big]\\
&- \lim_{0<\epsilon\to 0} \frac{1}{\epsilon}\mathbb{E}\big[\left(\tilde{H}(\gamma_3) - \tilde{H}(\gamma_2)\right)\left(\mathbf{1}_{\Phi_1>0}\mathbf{1}_{\Phi_2>0} - \mathbf{1}_{\Phi_1^\epsilon>0}\mathbf{1}_{\Phi_2^\epsilon>0}\right)\big]\\
=& \left(q_2 - \lim_{0<\epsilon\to 0} \mathbb{E}\big[\mathbf{1}_{\Phi_1^\epsilon>0}\big]\right)\\
&+ \lim_{0<\epsilon\to 0} \frac{1}{\epsilon}\mathbb{E}\big[\left(\theta_1 - \tilde{H}(\gamma_2)\right)\left(\mathbf{1}_{\Phi_1>0} - \mathbf{1}_{\Phi_1^\epsilon>0}\right)\big]\\
&+ \lim_{0<\epsilon\to 0} \frac{1}{\epsilon}\mathbb{E}\big[\left(\theta_2 + \tilde{H}(\gamma_2) - \tilde{H}(\gamma_3)\right)\left(\mathbf{1}_{\Phi_1>0}\mathbf{1}_{\Phi_2>0} - \mathbf{1}_{\Phi_1^\epsilon>0}\mathbf{1}_{\Phi_2^\epsilon>0}\right)\big].
\end{aligned}$$

We have, as $\Phi_2 = \Phi_2^\epsilon = \left(\theta_2 + \tilde{H}(\gamma_2) - \tilde{H}(\gamma_3)\right)_+$,

$$\left(\theta_2 + \tilde{H}(\gamma_2) - \tilde{H}(\gamma_3)\right)\left(\mathbf{1}_{\Phi_1>0}\mathbf{1}_{\Phi_2>0} - \mathbf{1}_{\Phi_1^\epsilon>0}\mathbf{1}_{\Phi_2^\epsilon>0}\right) = \Phi_2\left(\mathbf{1}_{\Phi_1>0} - \mathbf{1}_{\Phi_1^\epsilon>0}\right),$$

hence

$$\partial_{1,-}w(\theta) = \Big(q_2 - \lim_{0<\epsilon\to 0}\mathbb{E}\big[\mathbf{1}_{\Phi_1^\epsilon>0}\big]\Big) + \lim_{0<\epsilon\to 0}\frac{1}{\epsilon}\mathbb{E}\big[\big(\theta_1 - \tilde{H}(\gamma_2) + \Phi_2\big)\big(\mathbf{1}_{\Phi_1>0} - \mathbf{1}_{\Phi_1^\epsilon>0}\big)\big].$$

Using $\Phi_1^\epsilon = (\theta_1 - \epsilon - \tilde{H}(\gamma_2) + \Phi_2)_+ = (\Phi_1 - \epsilon)\mathbf{1}_{\Phi_1>\epsilon}$, we obtain

$$\begin{aligned}\big(\theta_1 - \tilde{H}(\gamma_2) + \Phi_2\big)\big(\mathbf{1}_{\Phi_1>0} - \mathbf{1}_{\Phi_1^\epsilon>0}\big) &= \big(\theta_1 - \tilde{H}(\gamma_2) + \Phi_2\big)\big(\mathbf{1}_{0<\Phi_1\leqslant\epsilon} + \mathbf{1}_{\epsilon<\Phi_1} - \mathbf{1}_{\Phi_1>\epsilon}\big)\\ &= \big(\theta_1 - \tilde{H}(\gamma_2) + \Phi_2\big)\mathbf{1}_{0<\Phi_1\leqslant\epsilon} = \Phi_1(\theta)\mathbf{1}_{0<\Phi_1\leqslant\epsilon}.\end{aligned}$$

This gives

$$0 \leqslant \lim_{0<\epsilon\to 0}\frac{1}{\epsilon}\mathbb{E}\big[\Phi_1\mathbf{1}_{0<\Phi_1\leqslant\epsilon}\big] \leqslant \lim_{0<\epsilon\to 0}\mathbb{E}\big[\mathbf{1}_{0<\Phi_1\leqslant\epsilon}\big] = 0,$$

and eventually

$$\partial_{1,-}w(\theta) = \Big(q_2 - \lim_{0<\epsilon\to 0}\mathbb{E}\big[\mathbf{1}_{\Phi_1^\epsilon>0}\big]\Big).$$

1. Computing $\partial_{1,+}w$: We have, for $\theta \in \mathbb{R}_+ \times \mathbb{R}_+$, setting $\Phi_1 := \Phi_1(\theta)$, $\Phi_2 := \Phi_2(\theta)$, and for all $\epsilon > 0$, $\Phi_1^\epsilon := \Phi_1(\theta_1 + \epsilon, \theta_2)$ and $\Phi_2^\epsilon := \Phi_2(\theta_1 + \epsilon, \theta_2)$,

$$\begin{aligned}\partial_{1,+}w(\theta) &= \Big(q_2 - \lim_{0<\epsilon\to 0}\mathbb{E}\big[\mathbf{1}_{\Phi_1^\epsilon>0}\big]\Big) - \theta_1\partial_{1,+}\mathbb{E}\big[\mathbf{1}_{\Phi_1>0}\big] - \theta_2\partial_{1,+}\mathbb{E}\big[\mathbf{1}_{\Phi_1>0}\mathbf{1}_{\Phi_2>0}\big]\\ &\quad + \partial_{1,+}\mathbb{E}\big[\tilde{H}(\gamma_2)\mathbf{1}_{\Phi_1>0}\big] + \partial_{1,+}\mathbb{E}\big[(\tilde{H}(\gamma_3) - \tilde{H}(\gamma_2))\mathbf{1}_{\Phi_1>0}\mathbf{1}_{\Phi_2>0}\big]\\ &= \Big(q_2 - \lim_{0<\epsilon\to 0}\mathbb{E}\big[\mathbf{1}_{\Phi_1^\epsilon>0}\big]\Big)\\ &\quad - \theta_1\lim_{0<\epsilon\to 0}\frac{1}{\epsilon}\mathbb{E}\Big[\mathbf{1}_{\Phi_1^\epsilon>0} - \mathbf{1}_{\Phi_1^>0}\Big] - \theta_2\lim_{0<\epsilon\to 0}\frac{1}{\epsilon}\mathbb{E}\big[\mathbf{1}_{\Phi_1^\epsilon>0}\mathbf{1}_{\Phi_2^\epsilon>0} - \mathbf{1}_{\Phi_1>0}\mathbf{1}_{\Phi_2>0}\big]\\ &\quad + \lim_{0<\epsilon\to 0}\frac{1}{\epsilon}\mathbb{E}\big[\tilde{H}(\gamma_2)\big(\mathbf{1}_{\Phi_1^\epsilon>0} - \mathbf{1}_{\Phi_1>0}\big)\big]\\ &\quad + \lim_{0<\epsilon\to 0}\frac{1}{\epsilon}\mathbb{E}\big[\big(\tilde{H}(\gamma_3) - \tilde{H}(\gamma_2)\big)\big(\mathbf{1}_{\Phi_1^\epsilon>0}\mathbf{1}_{\Phi_2^\epsilon>0} - \mathbf{1}_{\Phi_1>0}\mathbf{1}_{\Phi_2>0}\big)\big]\\ &= \Big(q_2 - \lim_{0<\epsilon\to 0}\mathbb{E}\big[\mathbf{1}_{\Phi_1^\epsilon>0}\big]\Big)\\ &\quad - \lim_{0<\epsilon\to 0}\frac{1}{\epsilon}\mathbb{E}\big[\big(\theta_1 - \tilde{H}(\gamma_2)\big)\big(\mathbf{1}_{\Phi_1^\epsilon>0} - \mathbf{1}_{\Phi_1>0}\big)\big]\\ &\quad - \lim_{0<\epsilon\to 0}\frac{1}{\epsilon}\mathbb{E}\big[\big(\theta_2 + \tilde{H}(\gamma_2) - \tilde{H}(\gamma_3)\big)\big(\mathbf{1}_{\Phi_1^\epsilon>0}\mathbf{1}_{\Phi_2^\epsilon>0} - \mathbf{1}_{\Phi_1>0}\mathbf{1}_{\Phi_2>0}\big)\big].\end{aligned}$$

We have, as $\Phi_2 = \Phi_2^\epsilon = \big(\theta_2 + \tilde{H}(\gamma_2) - \tilde{H}(\gamma_3)\big)_+$,

$$\big(\theta_2 + \tilde{H}(\gamma_2) - \tilde{H}(\gamma_3)\big)\big(\mathbf{1}_{\Phi_1>0}\mathbf{1}_{\Phi_2>0} - \mathbf{1}_{\Phi_1^\epsilon>0}\mathbf{1}_{\Phi_2^\epsilon>0}\big) = \Phi_2\big(\mathbf{1}_{\Phi_1>0} - \mathbf{1}_{\Phi_1^\epsilon>0}\big),$$

hence

$$\partial_{1,+}w(\theta) = \Big(q_2 - \lim_{0<\epsilon\to 0}\mathbb{E}\big[\mathbf{1}_{\Phi_1^\epsilon>0}\big]\Big) - \lim_{0<\epsilon\to 0}\frac{1}{\epsilon}\mathbb{E}\big[\big(\theta_1 - \tilde{H}(\gamma_2) + \Phi_2\big)\big(\mathbf{1}_{\Phi_1^\epsilon>0} - \mathbf{1}_{\Phi_1>0}\big)\big].$$

Using $\Phi_1 = (\theta_1 - \tilde{H}(\gamma_2) + \Phi_2)_+ = (\Phi_1^\epsilon - \epsilon)\mathbf{1}_{\Phi_1^\epsilon > \epsilon}$, we obtain

$$\begin{aligned}\left(\theta_1 - \tilde{H}(\gamma_2) + \Phi_2\right)\left(\mathbf{1}_{\Phi_1^\epsilon>0} - \mathbf{1}_{\Phi_1>0}\right) &= \left(\theta_1 - \tilde{H}(\gamma_2) + \Phi_2\right)\left(\mathbf{1}_{0<\Phi_1^\epsilon\leqslant\epsilon} + \mathbf{1}_{\Phi_1^\epsilon>\epsilon} - \mathbf{1}_{\Phi_1^\epsilon>\epsilon}\right)\\ &= \left(\theta_1 - \tilde{H}(\gamma_2) + \Phi_2\right)\mathbf{1}_{0<\Phi_1^\epsilon\leqslant\epsilon} = \left(\Phi_1^\epsilon - \epsilon\right)\mathbf{1}_{0<\Phi_1^\epsilon\leqslant\epsilon}\end{aligned}$$

This gives

$$0 \geqslant \lim_{0<\epsilon\to 0}\frac{1}{\epsilon}\mathbb{E}\left[\left(\Phi_1^\epsilon - \epsilon\right)\mathbf{1}_{0<\Phi_1^\epsilon\leqslant\epsilon}\right] \geqslant \lim_{0<\epsilon\to 0} -\mathbb{E}\left[\mathbf{1}_{0<\Phi_1\leqslant\epsilon}\right] = 0,$$

and eventually

$$\partial_{1,+}w(\theta) = \left(q_2 - \lim_{0<\epsilon\to 0}\mathbb{E}\left[\mathbf{1}_{\Phi_1^\epsilon>0}\right]\right).$$

3. Computing $\partial_{2,-}w$: We have, for $\theta \in \mathbb{R}_+ \times \mathbb{R}_+^*$, setting $\Phi_1 := \Phi_1(\theta)$, $\Phi_2 := \Phi_2(\theta)$, and for all $\epsilon > 0$, $\Phi_1^\epsilon := \Phi_1(\theta_1, \theta_2 - \epsilon)$ and $\Phi_2^\epsilon := \Phi_2(\theta_1, \theta_2 - \epsilon)$,

$$\begin{aligned}\partial_{2,-}w(\theta) =& -\theta_1\partial_{2,-}\mathbb{E}\left[\mathbf{1}_{\Phi_1>0}\right] + \left(q_3 - \lim_{0<\epsilon\to 0}\mathbb{E}\left[\mathbf{1}_{\Phi_1^\epsilon>0}\mathbf{1}_{\Phi_2^\epsilon>0}\right]\right) - \theta_2\partial_{2,-}\mathbb{E}\left[\mathbf{1}_{\Phi_1>0}\mathbf{1}_{\Phi_2>0}\right]\\ &+ \partial_{2,-}\mathbb{E}\left[\tilde{H}(\gamma_2)\mathbf{1}_{\Phi_1>0}\right] + \partial_{2,-}\mathbb{E}\left[(\tilde{H}(\gamma_3) - \tilde{H}(\gamma_2))\mathbf{1}_{\Phi_1>0}\mathbf{1}_{\Phi_2>0}\right]\\ =&\left(q_3 - \lim_{0<\epsilon\to 0}\mathbb{E}\left[\mathbf{1}_{\Phi_1^\epsilon>0}\mathbf{1}_{\Phi_2^\epsilon>0}\right]\right)\\ &+ \theta_1\lim_{0<\epsilon\to 0}\frac{1}{\epsilon}\mathbb{E}\left[\mathbf{1}_{\Phi_1>0} - \mathbf{1}_{\Phi_1^\epsilon>0}\right] + \theta_2\lim_{0<\epsilon\to 0}\frac{1}{\epsilon}\mathbb{E}\left[\mathbf{1}_{\Phi_1>0}\mathbf{1}_{\Phi_2>0} - \mathbf{1}_{\Phi_1^\epsilon>0}\mathbf{1}_{\Phi_2^\epsilon>0}\right]\\ &- \lim_{0<\epsilon\to 0}\frac{1}{\epsilon}\mathbb{E}\left[\tilde{H}(\gamma_2)\left(\mathbf{1}_{\Phi_1>0} - \mathbf{1}_{\Phi_1^\epsilon>0}\right)\right]\\ &- \lim_{0<\epsilon\to 0}\frac{1}{\epsilon}\mathbb{E}\left[\left(\tilde{H}(\gamma_3) - \tilde{H}(\gamma_2)\right)\left(\mathbf{1}_{\Phi_1>0}\mathbf{1}_{\Phi_2>0} - \mathbf{1}_{\Phi_1^\epsilon>0}\mathbf{1}_{\Phi_2^\epsilon>0}\right)\right]\\ =&\left(q_3 - \lim_{0<\epsilon\to 0}\mathbb{E}\left[\mathbf{1}_{\Phi_1^\epsilon>0}\mathbf{1}_{\Phi_2^\epsilon>0}\right]\right)\\ &+ \lim_{0<\epsilon\to 0}\frac{1}{\epsilon}\mathbb{E}\left[\left(\theta_1 - \tilde{H}(\gamma_2)\right)\left(\mathbf{1}_{\Phi_1>0} - \mathbf{1}_{\Phi_1^\epsilon>0}\right)\right]\\ &+ \lim_{0<\epsilon\to 0}\frac{1}{\epsilon}\mathbb{E}\left[\left(\theta_2 + \tilde{H}(\gamma_2) - \tilde{H}(\gamma_3)\right)\left(\mathbf{1}_{\Phi_1>0}\mathbf{1}_{\Phi_2>0} - \mathbf{1}_{\Phi_1^\epsilon>0}\mathbf{1}_{\Phi_2^\epsilon>0}\right)\right].\end{aligned}$$

We have, as $\Phi_2^\epsilon = \left(\theta_2 - \epsilon + \tilde{H}(\gamma_2) - \tilde{H}(\gamma_3)\right)_+ = (\Phi_2 - \epsilon)\mathbf{1}_{\Phi_2>\epsilon}$,

$$\begin{aligned}&\left(\theta_2 + \tilde{H}(\gamma_2) - \tilde{H}(\gamma_3)\right)\left(\mathbf{1}_{\Phi_1>0}\mathbf{1}_{\Phi_2>0} - \mathbf{1}_{\Phi_1^\epsilon>0}\mathbf{1}_{\Phi_2^\epsilon>0}\right)\\ &= \left(\theta_2 + \tilde{H}(\gamma_2) - \tilde{H}(\gamma_3)\right)\left(\mathbf{1}_{\Phi_1>0}\mathbf{1}_{\Phi_2>0} - \mathbf{1}_{\Phi_1^\epsilon>0}\mathbf{1}_{\Phi_2>\epsilon}\right)\\ &= \mathbf{1}_{0<\Phi_2\leqslant\epsilon}\Phi_2\mathbf{1}_{\Phi_1>0} + \mathbf{1}_{\epsilon<\Phi_2}\Phi_2\left(\mathbf{1}_{\Phi_1>0} - \mathbf{1}_{\Phi_1^\epsilon>0}\right)\end{aligned}$$

hence

$$\begin{aligned}\partial_{2,-}w(\theta) =&\left(q_3 - \lim_{0<\epsilon\to 0}\mathbb{E}\left[\mathbf{1}_{\Phi_1^\epsilon>0}\mathbf{1}_{\Phi_2^\epsilon>0}\right]\right)\\ &+ \lim_{0<\epsilon\to 0}\frac{1}{\epsilon}\mathbb{E}\left[\left(\theta_1 - \tilde{H}(\gamma_2) + \Phi_2\right)\left(\mathbf{1}_{\Phi_1>0} - \mathbf{1}_{\Phi_1^\epsilon>0}\right)\mathbf{1}_{\epsilon<\Phi_2}\right]\\ &+ \lim_{0<\epsilon\to 0}\frac{1}{\epsilon}\mathbb{E}\left[\left(\theta_1 - \tilde{H}(\gamma_2)\right)\left(\mathbf{1}_{\Phi_1>0} - \mathbf{1}_{\Phi_1^\epsilon>0}\right)\mathbf{1}_{0\leqslant\Phi_2\leqslant\epsilon}\right]\\ &+ \lim_{0<\epsilon\to 0}\frac{1}{\epsilon}\mathbb{E}\left[\mathbf{1}_{0<\Phi_2\leqslant\epsilon}\Phi_2\mathbf{1}_{\Phi_1>0}\right].\end{aligned}$$

Using $\Phi_1^\epsilon = (\theta_1 - \tilde{H}(\gamma_2) + \Phi_2^\epsilon)_+ = \mathbf{1}_{\Phi_2>\epsilon}(\theta_1 - \tilde{H}(\gamma_2) + \Phi_2 - \epsilon)_+ + \mathbf{1}_{0\leqslant\Phi_2\leqslant\epsilon}(\theta_1 - \tilde{H}(\gamma_2))_+ = \mathbf{1}_{\Phi_2>\epsilon}\mathbf{1}_{\Phi_1>\epsilon}(\Phi_1 - \epsilon) + \mathbf{1}_{0\leqslant\Phi_2\leqslant\epsilon}(\theta_1 - \tilde{H}(\gamma_2))_+$, we obtain

$$\begin{aligned}
&\left(\theta_1 - \tilde{H}(\gamma_2) + \Phi_2\right)\left(\mathbf{1}_{\Phi_1>0} - \mathbf{1}_{\Phi_1^\epsilon>0}\right)\mathbf{1}_{\epsilon<\Phi_2} \\
&= \left(\theta_1 - \tilde{H}(\gamma_2) + \Phi_2\right)\left(\mathbf{1}_{\Phi_1>0} - \mathbf{1}_{\Phi_1>\epsilon}\right)\mathbf{1}_{\epsilon<\Phi_2} = \Phi_1\mathbf{1}_{0<\Phi_1\leqslant\epsilon}\mathbf{1}_{\epsilon<\Phi_2},
\end{aligned}$$

and

$$\begin{aligned}
&\left(\theta_1 - \tilde{H}(\gamma_2)\right)\left(\mathbf{1}_{\Phi_1>0} - \mathbf{1}_{\Phi_1^\epsilon>0}\right)\mathbf{1}_{0\leqslant\Phi_2\leqslant\epsilon} \\
&= \left(\theta_1 - \tilde{H}(\gamma_2)\right)\left(\mathbf{1}_{\theta_1-\tilde{H}(\gamma_2)+\Phi_2>0} - \mathbf{1}_{\theta_1-\tilde{H}(\gamma_2)>0}\right)\mathbf{1}_{0\leqslant\Phi_2\leqslant\epsilon} \\
&= \left(\theta_1 - \tilde{H}(\gamma_2)\right)\mathbf{1}_{-\Phi_2<\theta_1-\tilde{H}(\gamma_2)\leqslant 0}\mathbf{1}_{0<\Phi_2\leqslant\epsilon}
\end{aligned}$$

Hence

$$\begin{aligned}
\partial_{2,-}w(\theta) =&(q_3 - \lim_{0<\epsilon\to 0}\mathbb{E}\left[\mathbf{1}_{\Phi_1^\epsilon>0}\mathbf{1}_{\Phi_2^\epsilon>0}\right]) \\
&+ \lim_{0<\epsilon\to 0}\frac{1}{\epsilon}\mathbb{E}\left[\Phi_1\mathbf{1}_{0<\Phi_1\leqslant\epsilon}\mathbf{1}_{\epsilon<\Phi_2}\right] \\
&+ \lim_{0<\epsilon\to 0}\frac{1}{\epsilon}\mathbb{E}\left[\left(\theta_1 - \tilde{H}(\gamma_2)\right)\mathbf{1}_{-\Phi_2<\theta_1-\tilde{H}(\gamma_2)\leqslant 0}\mathbf{1}_{0<\Phi_2\leqslant\epsilon}\right] \\
&+ \lim_{0<\epsilon\to 0}\frac{1}{\epsilon}\mathbb{E}\left[\mathbf{1}_{0<\Phi_2\leqslant\epsilon}\Phi_2\mathbf{1}_{\Phi_1>0}\right].
\end{aligned}$$

We eventually have

$$\begin{aligned}
&0 \leqslant \lim_{0<\epsilon\to 0}\frac{1}{\epsilon}\mathbb{E}\left[\Phi_1\mathbf{1}_{0<\Phi_1\leqslant\epsilon}\mathbf{1}_{\epsilon<\Phi_2}\right] \leqslant \mathbb{E}\left[\mathbf{1}_{0<\Phi_1\leqslant\epsilon}\right] \to 0, \\
&0 \geqslant \lim_{0<\epsilon\to 0}\frac{1}{\epsilon}\mathbb{E}\left[\left(\theta_1 - \tilde{H}(\gamma_2)\right)\mathbf{1}_{-\Phi_2<\theta_1-\tilde{H}(\gamma_2)\leqslant 0}\mathbf{1}_{0<\Phi_2\leqslant\epsilon}\right] \geqslant -\mathbb{E}\left[\mathbf{1}_{0<\Phi_2\leqslant\epsilon}\right] \to 0 \\
&0 \leqslant \lim_{0<\epsilon\to 0}\frac{1}{\epsilon}\mathbb{E}\left[\mathbf{1}_{0<\Phi_2\leqslant\epsilon}\Phi_2\mathbf{1}_{\Phi_1>0}\right] \leqslant \lim_{0<\epsilon\to 0}\mathbb{E}\left[\mathbf{1}_{0<\Phi_2\leqslant\epsilon}\right] \to 0,
\end{aligned}$$

hence

$$\partial_{2,-}w(\theta) = q_3 - \lim_{0<\epsilon\to 0}\mathbb{E}\left[\mathbf{1}_{\Phi_1^\epsilon>0}\mathbf{1}_{\Phi_2^\epsilon>0}\right].$$

4. Computing $\partial_{2,+}w$: for $\theta \in \mathbb{R}_+ \times \mathbb{R}_+$, setting $\Phi_1 := \Phi_1(\theta)$, $\Phi_2 := \Phi_2(\theta)$, and for all

$\epsilon > 0$, $\Phi_1^\epsilon := \Phi_1(\theta_1, \theta_2 + \epsilon)$ and $\Phi_2^\epsilon := \Phi_2(\theta_1, \theta_2 + \epsilon)$,

$$\begin{aligned}
\partial_{2,+} w(\theta) =& -\theta_1 \partial_{2,+} \mathbb{E}\big[\mathbf{1}_{\Phi_1>0}\big] + (q_3 - \lim_{0<\epsilon\to 0} \mathbb{E}\big[\mathbf{1}_{\Phi_1^\epsilon>0}\mathbf{1}_{\Phi_2^\epsilon>0}\big]) - \theta_2 \partial_{2,+}\mathbb{E}\big[\mathbf{1}_{\Phi_1>0}\mathbf{1}_{\Phi_2>0}\big] \\
&+ \partial_{2,+}\mathbb{E}\big[\tilde{H}(\gamma_2)\mathbf{1}_{\Phi_1>0}\big] + \partial_{2,+}\mathbb{E}\big[(\tilde{H}(\gamma_3) - \tilde{H}(\gamma_2))\mathbf{1}_{\Phi_1>0}\mathbf{1}_{\Phi_2>0}\big] \\
=&(q_3 - \lim_{0<\epsilon\to 0} \mathbb{E}\big[\mathbf{1}_{\Phi_1^\epsilon>0}\mathbf{1}_{\Phi_2^\epsilon>0}\big]) \\
&- \theta_1 \lim_{0<\epsilon\to 0} \frac{1}{\epsilon}\mathbb{E}\big[\mathbf{1}_{\Phi_1^\epsilon>0} - \mathbf{1}_{\Phi_1>0}\big] - \theta_2 \lim_{0<\epsilon\to 0} \frac{1}{\epsilon}\mathbb{E}\big[\mathbf{1}_{\Phi_1^\epsilon>0}\mathbf{1}_{\Phi_2^\epsilon>0} - \mathbf{1}_{\Phi_1>0}\mathbf{1}_{\Phi_2>0}\big] \\
&+ \lim_{0<\epsilon\to 0} \frac{1}{\epsilon}\mathbb{E}\big[\tilde{H}(\gamma_2)\left(\mathbf{1}_{\Phi_1^\epsilon>0} - \mathbf{1}_{\Phi_1>0}\right)\big] \\
&+ \lim_{0<\epsilon\to 0} \frac{1}{\epsilon}\mathbb{E}\big[\left(\tilde{H}(\gamma_3) - \tilde{H}(\gamma_2)\right)\left(\mathbf{1}_{\Phi_1^\epsilon>0}\mathbf{1}_{\Phi_2^\epsilon>0} - \mathbf{1}_{\Phi_1>0}\mathbf{1}_{\Phi_2>0}\right)\big] \\
=&(q_3 - \lim_{0<\epsilon\to 0} \mathbb{E}\big[\mathbf{1}_{\Phi_1^\epsilon>0}\mathbf{1}_{\Phi_2^\epsilon>0}\big]) \\
&- \lim_{0<\epsilon\to 0} \frac{1}{\epsilon}\mathbb{E}\big[\left(\theta_1 - \tilde{H}(\gamma_2)\right)\left(\mathbf{1}_{\Phi_1^\epsilon>0} - \mathbf{1}_{\Phi_1>0}\right)\big] \\
&- \lim_{0<\epsilon\to 0} \frac{1}{\epsilon}\mathbb{E}\big[\left(\theta_2 + \tilde{H}(\gamma_2) - \tilde{H}(\gamma_3)\right)\left(\mathbf{1}_{\Phi_1^\epsilon>0}\mathbf{1}_{\Phi_2^\epsilon>0} - \mathbf{1}_{\Phi_1>0}\mathbf{1}_{\Phi_2>0}\right)\big].
\end{aligned}$$

We have, as $\Phi_2 = \left(\theta_2 + \tilde{H}(\gamma_2) - \tilde{H}(\gamma_3)\right)_+ = (\Phi_2^\epsilon - \epsilon)\mathbf{1}_{\Phi_2^\epsilon>\epsilon}$,

$$\begin{aligned}
&\left(\theta_2 + \tilde{H}(\gamma_2) - \tilde{H}(\gamma_3)\right)\left(\mathbf{1}_{\Phi_1^\epsilon>0}\mathbf{1}_{\Phi_2^\epsilon>0} - \mathbf{1}_{\Phi_1>0}\mathbf{1}_{\Phi_2>0}\right) \\
&= \left(\theta_2 + \tilde{H}(\gamma_2) - \tilde{H}(\gamma_3)\right)\left(\mathbf{1}_{\Phi_1^\epsilon>0}\mathbf{1}_{\Phi_2^\epsilon>0} - \mathbf{1}_{\Phi_1>0}\mathbf{1}_{\Phi_2^\epsilon>\epsilon}\right) \\
&= \Phi_2\mathbf{1}_{\Phi_2^\epsilon>\epsilon}(\mathbf{1}_{\Phi_1^\epsilon>0} - \mathbf{1}_{\Phi_1>0}),
\end{aligned}$$

hence

$$\begin{aligned}
\partial_{2,+} w(\theta) =&(q_3 - \lim_{0<\epsilon\to 0} \mathbb{E}\big[\mathbf{1}_{\Phi_1^\epsilon>0}\mathbf{1}_{\Phi_2^\epsilon>0}\big]) \\
&- \lim_{0<\epsilon\to 0} \frac{1}{\epsilon}\mathbb{E}\big[\left(\theta_1 - \tilde{H}(\gamma_2)\right)\left(\mathbf{1}_{\Phi_1^\epsilon>0} - \mathbf{1}_{\Phi_1>0}\right)\mathbf{1}_{0\leqslant\Phi_2^\epsilon\leqslant\epsilon}\big] \\
&- \lim_{0<\epsilon\to 0} \frac{1}{\epsilon}\mathbb{E}\big[\left(\theta_1 - \tilde{H}(\gamma_2) + \Phi_2\right)\left(\mathbf{1}_{\Phi_1^\epsilon>0} - \mathbf{1}_{\Phi_1>0}\right)\mathbf{1}_{\Phi_2^\epsilon>\epsilon}\big].
\end{aligned}$$

Using $\Phi_1 = (\theta_1 - \tilde{H}(\gamma_2) + \Phi_2)_+ = \mathbf{1}_{\Phi_2^\epsilon>\epsilon}(\theta_1 - \tilde{H}(\gamma_2) + \Phi_2^\epsilon - \epsilon)_+ + \mathbf{1}_{0\leqslant\Phi_2^\epsilon\leqslant\epsilon}(\theta_1 - \tilde{H}(\gamma_2))_+ = \mathbf{1}_{\Phi_2^\epsilon>\epsilon}\mathbf{1}_{\Phi_1^\epsilon>\epsilon}(\Phi_1^\epsilon - \epsilon) + \mathbf{1}_{0\leqslant\Phi_2\leqslant\epsilon}(\theta_1 - \tilde{H}(\gamma_2))_+$, we obtain

$$\begin{aligned}
&\left(\theta_1 - \tilde{H}(\gamma_2) + \Phi_2\right)\left(\mathbf{1}_{\Phi_1^\epsilon>0} - \mathbf{1}_{\Phi_1>0}\right)\mathbf{1}_{\epsilon<\Phi_2^\epsilon} \\
&= \left(\theta_1 - \tilde{H}(\gamma_2) + \Phi_2\right)\left(\mathbf{1}_{\Phi_1^\epsilon>0} - \mathbf{1}_{\Phi_1^\epsilon>\epsilon}\right)\mathbf{1}_{\epsilon<\Phi_2^\epsilon} = (\Phi_1^\epsilon - \epsilon)\mathbf{1}_{0<\Phi_1^\epsilon\leqslant\epsilon}\mathbf{1}_{\epsilon<\Phi_2^\epsilon},
\end{aligned}$$

and

$$\begin{aligned}
&\left(\theta_1 - \tilde{H}(\gamma_2)\right)\left(\mathbf{1}_{\Phi_1^\epsilon>0} - \mathbf{1}_{\Phi_1>0}\right)\mathbf{1}_{0\leqslant\Phi_2^\epsilon\leqslant\epsilon} \\
&= (\theta_1 - \tilde{H}(\gamma_2))(\mathbf{1}_{\theta_1-\tilde{H}(\gamma_2)>-\Phi_2^\epsilon} - \mathbf{1}_{\theta_1-\tilde{H}(\gamma_2)>0})\mathbf{1}_{0<\Phi_2^\epsilon\leqslant\epsilon} \\
&= (\theta_1 - \tilde{H}(\gamma_2))\mathbf{1}_{-\Phi_2^\epsilon<\theta_1-\tilde{H}(\gamma_2)\leqslant 0}\mathbf{1}_{0<\Phi_2^\epsilon\leqslant\epsilon}.
\end{aligned}$$

Hence

$$\begin{aligned}\partial_{2,+}w(\theta) =&(q_3 - \lim_{0<\epsilon\to 0}\mathbb{E}\big[\mathbf{1}_{\Phi_1^\epsilon>0}\mathbf{1}_{\Phi_2^\epsilon>0}\big])\\ &- \lim_{0<\epsilon\to 0}\frac{1}{\epsilon}\mathbb{E}\Big[(\theta_1 - \tilde{H}(\gamma_2))\mathbf{1}_{-\Phi_2^\epsilon<\theta_1-\tilde{H}(\gamma_2)\leqslant 0}\mathbf{1}_{0<\Phi_2^\epsilon\leqslant\epsilon}\Big]\\ &- \lim_{0<\epsilon\to 0}\frac{1}{\epsilon}\mathbb{E}\big[(\Phi_1^\epsilon - \epsilon)\mathbf{1}_{0<\Phi_1^\epsilon\leqslant\epsilon}\mathbf{1}_{\epsilon<\Phi_2^\epsilon}\big].\end{aligned}$$

We eventually have

$$\begin{aligned}0 \geqslant \lim_{0<\epsilon\to 0}\frac{1}{\epsilon}\mathbb{E}\Big[(\theta_1 - \tilde{H}(\gamma_2))\mathbf{1}_{-\Phi_2^\epsilon<\theta_1-\tilde{H}(\gamma_2)\leqslant 0}\mathbf{1}_{0<\Phi_2^\epsilon\leqslant\epsilon}\Big] \geqslant -\mathbb{E}\big[\mathbf{1}_{0<\Phi_2^\epsilon\leqslant\epsilon}\big] \to 0,\\ 0 \geqslant \lim_{0<\epsilon\to 0}\frac{1}{\epsilon}\mathbb{E}\big[(\Phi_1^\epsilon - \epsilon)\mathbf{1}_{0<\Phi_1^\epsilon\leqslant\epsilon}\mathbf{1}_{\epsilon<\Phi_2^\epsilon}\big] \geqslant -\mathbb{E}\big[\mathbf{1}_{0<\Phi_1^\epsilon\leqslant\epsilon}\big] \to 0,\end{aligned}$$

hence

$$\partial_{2,+}w(\theta) = q_3 - \lim_{0<\epsilon\to 0}\mathbb{E}\big[\mathbf{1}_{\Phi_1^\epsilon>0}\mathbf{1}_{\Phi_2^\epsilon>0}\big].$$

To summarize, we have

$$\begin{aligned}\partial_{1,-}w(\theta) &= q_2 - \lim_{0<\epsilon\to 0}\mathbb{E}\big[\mathbf{1}_{\Phi_1(\theta_1-\epsilon,\theta_2)>0}\big],\\ \partial_{1,+}w(\theta) &= q_2 - \lim_{0<\epsilon\to 0}\mathbb{E}\big[\mathbf{1}_{\Phi_1(\theta_1+\epsilon,\theta_2)>0}\big],\\ \partial_{2,-}w(\theta) &= q_3 - \lim_{0<\epsilon\to 0}\mathbb{E}\big[\mathbf{1}_{\Phi_1(\theta_1,\theta_2-\epsilon)>0}\mathbf{1}_{\Phi_2(\theta_1,\theta_2-\epsilon)>0}\big],\\ \partial_{2,+}w(\theta) &= q_3 - \lim_{0<\epsilon\to 0}\mathbb{E}\big[\mathbf{1}_{\Phi_1(\theta_1,\theta_2+\epsilon)>0}\mathbf{1}_{\Phi_2(\theta_1,\theta_2+\epsilon)>0}\big],\end{aligned}$$

and the lemma is proved as these limits are easily computed. □

We now prove the duality in two particular cases. Note that for $\theta^\star \in \arg\sup_{\mathbb{R}^2_+} w$, we have, by Lemma 4.3.2,

$$q_2 - \mathbb{E}\big[\mathbf{1}_{\Phi_1(\theta^\star)>0}\big] \geqslant 0 \geqslant q_2 - \mathbb{E}\Big[\mathbf{1}_{\theta_1^\star-\tilde{H}(\gamma_2)+\Phi_2(\theta^\star)\geqslant 0}\Big], \text{ and} \tag{4.3.36}$$

$$q_3 - \mathbb{E}\big[\mathbf{1}_{\Phi_1(\theta^\star)>0}\mathbf{1}_{\Phi_2(\theta^\star)>0}\big] \geqslant 0 \geqslant q_3 - \mathbb{E}\Big[\mathbf{1}_{\theta_1^\star-\tilde{H}(\gamma_2)+\Phi_2(\theta^\star)\geqslant 0}\mathbf{1}_{\theta_2^\star+\tilde{H}(\gamma_2)-\tilde{H}(\gamma_3)\geqslant 0}\Big]. \tag{4.3.37}$$

Theorem 4.3.2 *Assume that there exists $\theta^\star \in \arg\sup_{\theta\in\mathbb{R}^2_+} w$ such that*

$$\mathbb{E}\big[\mathbf{1}_{\Phi_1(\theta^\star)>0}\big] = \mathbb{E}\Big[\mathbf{1}_{\theta_1^\star-\tilde{H}(\gamma_2)+\Phi_2(\theta^\star)\geqslant 0}\Big], \text{ and} \tag{4.3.38}$$

$$\mathbb{E}\big[\mathbf{1}_{\Phi_1(\theta^\star)>0}\mathbf{1}_{\Phi_2(\theta^\star)>0}\big] = \mathbb{E}\Big[\mathbf{1}_{\theta_1^\star-\tilde{H}(\gamma_2)+\Phi_2(\theta^\star)\geqslant 0}\mathbf{1}_{\theta_2^\star+\tilde{H}(\gamma_2)-\tilde{H}(\gamma_3)\geqslant 0}\Big]. \tag{4.3.39}$$

We then have $\mathcal{V}_{\mathrm{DP}}(\mu) = \mathcal{V}_{\mathrm{KP}}(\mu)$.

Proof. By (4.3.38)-(4.3.39) and (4.3.36), we obtain

$$q_2 - \mathbb{E}\big[\mathbf{1}_{\Phi_1(\theta^\star)>0}\big] = q_3 - \mathbb{E}\big[\mathbf{1}_{\Phi_1(\theta^\star)>0}\mathbf{1}_{\Phi_2(\theta^\star)>0}\big] = 0, \tag{4.3.40}$$

and we deduce from (4.3.34), (4.3.35) and (4.3.40) that

$$\begin{aligned}\mathcal{V}_{\mathrm{DP}}(\mu) &= \mathbb{E}\big[H(\gamma_1)\big] + \mathbb{E}\Big[\tilde{H}(\gamma_2)\mathbf{1}_{\Phi_1(\theta^\star)>0}\mathbf{1}_{\Phi_2(\theta^\star)=0}\Big] + \mathbb{E}\Big[\tilde{H}(\gamma_3)\mathbf{1}_{\Phi_1(\theta^\star)>0}\mathbf{1}_{\Phi_2(\theta^\star)>0}\Big] \\ &= \mathbb{E}\Big[H(\gamma_1)\mathbf{1}_{\Phi_1(\theta^\star)=0} + H(\gamma_2)\mathbf{1}_{\Phi_1(\theta^\star)>0}\mathbf{1}_{\Phi_2(\theta^\star)=0} + H(\gamma_3)\mathbf{1}_{\Phi_1(\theta^\star)>0}\mathbf{1}_{\Phi_2(\theta^\star)>0}\Big] \\ &= \mathbb{E}\big[H(\chi^\star)\big]\,,\end{aligned} \tag{4.3.41}$$

with $\chi^\star := \gamma_1\mathbf{1}_{\Phi_1(\theta^\star)=0} + \gamma_2\mathbf{1}_{\Phi_1(\theta^\star)>0}\mathbf{1}_{\Phi_2(\theta^\star)=0} + \gamma_3 1_{\Phi_1(\theta^\star)>0}\mathbf{1}_{\Phi_2(\theta^\star)>0}$.
One has $F_{\chi^\star_\sharp\mathbb{P}}(\gamma_2) = \mathbb{P}[\Phi_1(\theta^\star) > 0] = q_2$ and $F_{\chi^\star_\sharp\mathbb{P}}(\gamma_3) = \mathbb{P}[\Phi_1(\theta^\star) > 0, \Phi_2(\theta^\star) > 0] = q_3$, so $\chi^\star_\sharp\mathbb{P} \succeq \mu$. Hence $\mathcal{V}_{\mathrm{DP}}(\mu) \geqslant \mathcal{V}_{\mathrm{RM}}(\mu) = \mathcal{V}_{\mathrm{KP}}(\mu)$. □

Theorem 4.3.3 *Assume that there exists* $\theta^\star \in \arg\sup_{\theta\in\mathbb{R}^2_+} w$ *such that*

$$\mathbb{E}\big[\mathbf{1}_{\Phi_1(\theta^\star)>0}\big] < \mathbb{E}\Big[\mathbf{1}_{\theta^\star_1 - \tilde{H}(\gamma_2)+\Phi_2(\theta^\star)\geqslant 0}\Big]\,, \text{ and} \tag{4.3.42}$$

$$\mathbb{E}\big[\mathbf{1}_{\Phi_1(\theta^\star)>0}\mathbf{1}_{\Phi_2(\theta^\star)>0}\big] = \mathbb{E}\Big[\mathbf{1}_{\theta^\star_1 - \tilde{H}(\gamma_2)+\Phi_2(\theta^\star)\geqslant 0}\mathbf{1}_{\theta^\star_2 + \tilde{H}(\gamma_2) - \tilde{H}(\gamma_3)\geqslant 0}\Big]\,. \tag{4.3.43}$$

We then have $\mathcal{V}_{\mathrm{DP}}(\mu) = \mathcal{V}_{\mathrm{KP}}(\mu)$.

Proof. By (4.3.43) and (4.3.36), we have

$$q_3 - \mathbb{E}\big[\mathbf{1}_{\Phi_1(\theta^\star)>0}\mathbf{1}_{\Phi_2(\theta^\star)>0}\big] = 0. \tag{4.3.44}$$

In addition, by (4.3.42) and (4.3.36), we have either

$$q_2 - \mathbb{E}\big[\mathbf{1}_{\Phi_1(\theta^\star)>0}\big] > 0 \geqslant q_2 - \mathbb{E}\Big[\mathbf{1}_{\theta^\star_1 - \tilde{H}(\gamma_2)+\Phi_2(\theta^\star)\geqslant 0}\Big]\,, \text{ or} \tag{4.3.45}$$

$$q_2 - \mathbb{E}\big[\mathbf{1}_{\Phi_1(\theta^\star)>0}\big] = 0 > q_2 - \mathbb{E}\Big[\mathbf{1}_{\theta^\star_1 - \tilde{H}(\gamma_2)+\Phi_2(\theta^\star)\geqslant 0}\Big]\,. \tag{4.3.46}$$

If (4.3.44)-(4.3.46) are satisfied, then the computations (4.3.41) are still valid and we obtain $\mathcal{V}_{\mathrm{DP}}(\mu) \geqslant \mathcal{V}_{\mathrm{KP}}(\mu)$.
Otherwise, if (4.3.44)-(4.3.45) are satisfied, we easily have that

$$0 < \mathbb{E}\Big[\mathbf{1}_{\theta^\star_1 - \tilde{H}(\gamma_2)+\Phi_2(\theta^\star)=0}\Big] = \mathbb{E}\Big[\mathbf{1}_{\theta^\star_1 - \tilde{H}(\gamma_2)=0}\mathbf{1}_{\Phi_2(\theta^\star)=0}\Big] + \mathbb{E}\Big[\mathbf{1}_{\theta^\star_1 - \tilde{H}(\gamma_2)+\Phi_2(\theta^\star)=0}\mathbf{1}_{\Phi_2(\theta^\star)>0}\Big]\,.$$

If $\mathbb{E}\Big[\mathbf{1}_{\theta^\star_1 - \tilde{H}(\gamma_2)+\Phi_2(\theta^\star)=0}\mathbf{1}_{\Phi_2(\theta^\star)>0}\Big] > 0$, then in particular one would have

$$\mathbb{E}\Big[\mathbf{1}_{\theta^\star_1 - \tilde{H}(\gamma_2)+\Phi_2(\theta^\star)\geqslant 0}\mathbf{1}_{\theta^\star_2 + \tilde{H}(\gamma_2) - \tilde{H}(\gamma_3)\geqslant 0}\Big] - \mathbb{E}\big[\mathbf{1}_{\Phi_1(\theta^\star)>0}\mathbf{1}_{\Phi_2(\theta^\star)>0}\big] > 0,$$

contradicting (4.3.43). We thus necessarily have $\mathbb{E}\Big[\mathbf{1}_{\theta_1^\star-\tilde{H}(\gamma_2)=0}\mathbf{1}_{\Phi_2(\theta^\star)=0}\Big] > 0$. Then

$$\begin{aligned}
\mathcal{V}_{\mathrm{DP}}(\mu) =& \mathbb{E}[H(\gamma_1)] + \theta_1^\star\left(q_2 - \mathbb{E}\big[\mathbf{1}_{\Phi_1(\theta^\star)>0}\big]\right) \\
&+ \mathbb{E}\big[\tilde{H}(\gamma_2)\mathbf{1}_{\Phi_1(\theta^\star)>0}\mathbf{1}_{\Phi_2(\theta^\star)=0}\big] + \mathbb{E}\big[\tilde{H}(\gamma_3)\mathbf{1}_{\Phi_1(\theta^\star)>0}\mathbf{1}_{\Phi_2(\theta^\star)>0}\big] \\
=& \mathbb{E}[H(\gamma_1)] + \frac{q_2 - \mathbb{E}\big[\mathbf{1}_{\Phi_1(\theta^\star)>0}\big]}{\mathbb{E}\Big[\mathbf{1}_{\theta_1^\star=\tilde{H}(\gamma_2)}\mathbf{1}_{\Phi_2(\theta^\star)=0}\Big]}\mathbb{E}\Big[\tilde{H}(\gamma_2)\mathbf{1}_{\theta_1^\star=\tilde{H}(\gamma_2)}\mathbf{1}_{\Phi_2(\theta^\star)=0}\Big] \\
&+ \mathbb{E}\big[\tilde{H}(\gamma_2)\mathbf{1}_{\Phi_1(\theta^\star)>0}\mathbf{1}_{\Phi_2(\theta^\star)=0}\big] + \mathbb{E}\big[\tilde{H}(\gamma_3)\mathbf{1}_{\Phi_1(\theta^\star)>0}\mathbf{1}_{\Phi_2(\theta^\star)>0}\big] \\
=& \mathbb{E}[H(\gamma_1)] + \mathbb{E}\left[\tilde{H}(\gamma_2)\left(\mathbf{1}_{\Phi_1(\theta^\star)>0}\mathbf{1}_{\Phi_2(\theta^\star)=0} + \frac{q_2 - \mathbb{E}\big[\mathbf{1}_{\Phi_1(\theta^\star)>0}\big]}{\mathbb{E}\Big[\mathbf{1}_{\theta_1^\star=\tilde{H}(\gamma_2)}\mathbf{1}_{\Phi_2(\theta^\star)=0}\Big]}\mathbf{1}_{\theta_1^\star=\tilde{H}(\gamma_2)}\mathbf{1}_{\Phi_2(\theta^\star)=0}\right)\right] \\
&+ \mathbb{E}\big[\tilde{H}(\gamma_3)\mathbf{1}_{\Phi_1(\theta^\star)>0}\mathbf{1}_{\Phi_2(\theta^\star)>0}\big] \\
=& \mathbb{E}[H(\gamma_1)(1-Q_2) + H(\gamma_2)(Q_2-Q_3) + H(\gamma_3)Q_3]\,,
\end{aligned}$$

where

$$Q_2 = \mathbf{1}_{\Phi_1(\theta^\star)>0}\mathbf{1}_{\Phi_2(\theta^\star)=0} + \mathbf{1}_{\Phi_1(\theta^\star)>0}\mathbf{1}_{\Phi_2(\theta^\star)>0} + \frac{q_2 - \mathbb{E}\big[\mathbf{1}_{\Phi_1(\theta^\star)>0}\big]}{\mathbb{E}\Big[\mathbf{1}_{\theta_1^\star=\tilde{H}(\gamma_2)}\mathbf{1}_{\Phi_2(\theta^\star)=0}\Big]}\mathbf{1}_{\theta_1^\star=\tilde{H}(\gamma_2)}\mathbf{1}_{\Phi_2(\theta^\star)=0},$$

$$Q_3 = \mathbf{1}_{\Phi_1(\theta^\star)>0}\mathbf{1}_{\Phi_2(\theta^\star)>0}$$

satisfy $1 \geqslant Q_2 \geqslant Q_3 \geqslant 0$, $\mathbb{E}[Q_2] = \mathbb{E}\big[\mathbf{1}_{\Phi_1(\theta^\star)>0}\big] + q_2 - \mathbb{E}\big[\mathbf{1}_{\Phi_1(\theta^\star)>0}\big] = q_2$ and $\mathbb{E}[Q_3] = \mathbb{E}\big[\mathbf{1}_{\Phi_1(\theta^\star)>0}\mathbf{1}_{\Phi_2(\theta^\star)>0}\big] = q_3$, so that $(1, Q_2, Q_3, 0) \in \mathfrak{Q}_T(\mu)$. Hence $\mathcal{V}_{\mathrm{DP}}(\mu) \geqslant \mathcal{V}_{\mathrm{KP}}(\mu)$. □

4.3.1.4 The multidimensional case

We now give a partial duality result in the general case of arbitrary dimension $d \geqslant 2$, generalising Theorem 4.3.2. We need first to know the left and right partial derivatives of the function w.

To compute these derivatives, we generalise (4.3.35). Observe that, for all $\theta \in \mathbb{R}_+^{d-1}$,

$$w(\theta) = \sum_{j=1}^{d-1}\theta_j q_{j+1} - \mathbb{E}[\Phi_j(\theta)]\,,$$

with, for all $1 \leqslant i \leqslant d-1$,

$$\begin{aligned}
&\Phi_i : \Omega \times \mathbb{R}_+^{d-i} \to \mathbb{R}, \qquad (4.3.47)\\
&(\omega, (\theta_i, \ldots, \theta_{d-1})) \mapsto \max\left(0, \max_{i\leqslant j\leqslant d-1}\left(\sum_{k=i}^{j}\theta_k + \tilde{H}(\omega,\gamma_i) - \tilde{H}(\omega,\gamma_{j+1})\right)\right).
\end{aligned}$$

We easily show that, almost surely and for all $1 \leqslant i \leqslant d-1$ and $\theta \in \mathbb{R}^{d-1}$, setting $\theta^{(i)} := (\theta_i, \ldots, \theta_{d-1}) \in \mathbb{R}^{d-i}$,

$$\Phi_i(\theta^{(i)}) = \Big(\theta_i + \tilde{H}(\gamma_i) - \tilde{H}(\gamma_{i+1}) + \Phi_{i+1}(\theta^{(i+1)})\Big)_+\,, \qquad (4.3.48)$$

where, by convention $\theta^{(d)} := \varnothing$ and $\Phi_d(\varnothing) = 0$.
We define

$$A_i(\theta^{(i)}) := \left\{\Phi_i(\theta^{(i)}) > 0\right\} = \left\{\theta_i + \tilde{H}(\gamma_i) - \tilde{H}(\gamma_{i+1}) + \Phi_{i+1}(\theta^{(i+1)}) > 0\right\}, \quad 1 \leqslant i \leqslant d-1, \tag{4.3.49}$$

$$Q_i(\theta) := \mathbf{1}_{\bigcap_{k=1}^{i-1} A_k(\theta^{(k)})}, \quad 2 \leqslant i \leqslant d+1, \tag{4.3.50}$$

with $A_d(\varnothing) := \varnothing$ by convention so that $Q_{d+1}(\theta) = 0$. We also set $Q_1(\theta) := 1$.
We immediately observe that, for all $\theta \in \mathbb{R}_+^{d-1}$ and $1 \leqslant i \leqslant d$,

$$Q_{d+1}(\theta) = 0 \leqslant Q_{i+1}(\theta) = Q_i(\theta)\mathbf{1}_{A_i(\theta^{(i)})} \leqslant Q_i(\theta) \leqslant 1 = Q_1(\theta).$$

Lemma 4.3.3 *We have, for all $\theta \in \mathbb{R}_+^{d-1}$,*

$$w(\theta) = \sum_{j=1}^{d-1} \theta_j \left(q_{j+1} - \mathbb{E}[Q_{j+1}(\theta)]\right) + \sum_{j=2}^{d} \mathbb{E}\left[\tilde{H}(\gamma_j)\left(Q_j(\theta) - Q_{j+1}(\theta)\right)\right]. \tag{4.3.51}$$

Proof. We prove more generally by induction that, for all $1 \leqslant i \leqslant d-1$,

$$\begin{aligned} w(\theta) = &\sum_{j=1}^{i} \theta_j \left(q_{j+1} - \mathbb{E}[Q_{j+1}(\theta)]\right) + \sum_{j=i+1}^{d-1} \theta_j q_{j+1} \\ &+ \sum_{j=2}^{i} \mathbb{E}\left[\tilde{H}(\gamma_j)\left(Q_j(\theta) - Q_{j+1}(\theta)\right)\right] + \mathbb{E}\left[\tilde{H}(\gamma_{i+1})Q_{i+1}(\theta)\right] \\ &- \mathbb{E}\left[\Phi_{i+1}(\theta^{(i+1)})Q_{i+1}(\theta)\right], \end{aligned} \tag{4.3.52}$$

noticing that (4.3.52) for $i = d-1$ is (4.3.51), as $Q_{d+1}(\theta) = 0$ and $\Phi_d(\theta^{(d)}) = 0$.

First, notice that, by (4.3.48), for $A \subset \mathcal{F}_T$, $1 \leqslant i \leqslant d-1$ and $\theta \in \mathbb{R}^{d-1}$,

$$\begin{aligned} \mathbb{E}\left[\Phi_i(\theta^{(i)})\mathbf{1}_A\right] &= \mathbb{E}\left[\left(\theta_i + \tilde{H}(\gamma_i) - \tilde{H}(\gamma_{i+1}) + \Phi_{i+1}(\theta^{(i+1)})\right)_+ \mathbf{1}_A\right] \\ &= \theta_i \mathbb{E}\left[\mathbf{1}_{A \cap A_i(\theta^{(i)})}\right] + \mathbb{E}\left[\tilde{H}(\gamma_i)\mathbf{1}_{A \cap A_i(\theta^{(i)})}\right] \\ &\quad - \mathbb{E}\left[\tilde{H}(\gamma_{i+1})\mathbf{1}_{A \cap A_i(\theta^{(i)})}\right] + \mathbb{E}\left[\Phi_{i+1}(\theta^{(i+1)})\mathbf{1}_{A \cap A_i(\theta^{(i)})}\right]. \end{aligned} \tag{4.3.53}$$

For $i = 1$, we have, using (4.3.53) with $A = \Omega$, as $\tilde{H}(\gamma_1) = 0$,

$$\begin{aligned} w(\theta) &= \sum_{j=1}^{d-1} \theta_j q_{j+1} - \mathbb{E}[\Phi_1(\theta)] \\ &= \theta_1 \left(q_2 - \mathbb{E}\left[\mathbf{1}_{A_1(\theta)}\right]\right) + \sum_{j=2}^{d-1} \theta_j q_{j+1} + \mathbb{E}\left[\tilde{H}(\gamma_2)\mathbf{1}_{A_1(\theta)}\right] - \mathbb{E}\left[\Phi_2(\theta_2, \ldots, \theta_{d-1})\mathbf{1}_{A_1(\theta)}\right] \\ &= \theta_1 \left(q_2 - \mathbb{E}[Q_2(\theta)]\right) + \sum_{j=2}^{d-1} \theta_j q_{j+1} + \mathbb{E}\left[\tilde{H}(\gamma_2)Q_2(\theta)\right] - \mathbb{E}\left[\Phi_2(\theta^{(2)})Q_2(\theta)\right], \end{aligned}$$

which is equality (4.3.52) for $i = 1$. Assume now that (4.3.52) is true for some $1 \leqslant i < d-1$, we prove it for $i+1$. By (4.3.52) for i, using also (4.3.53) as $\mathbb{E}\big[\Phi_{i+1}(\theta^{(i+1)})Q_{i+1}(\theta)\big] = \mathbb{E}\Big[\Phi_{i+1}(\theta^{(i+1)})\mathbf{1}_{\bigcap_{k=1}^{i} A_k(\theta^{(k)})}\Big]$, we obtain

$$
\begin{aligned}
w(\theta) &= \sum_{j=1}^{i} \theta_j \left(q_{j+1} - \mathbb{E}[Q_{j+1}(\theta)]\right) + \theta_{i+1} q_{i+2} + \sum_{j=i+2}^{d-1} \theta_j q_{j+1} \\
&\quad + \sum_{j=2}^{i} \mathbb{E}\big[\tilde{H}(\gamma_j)\left(Q_j(\theta) - Q_{j+1}(\theta)\right)\big] + \mathbb{E}\big[\tilde{H}(\gamma_{i+1})Q_{i+1}(\theta)\big] \\
&\quad - \theta_{i+1}\mathbb{E}\Big[\mathbf{1}_{\bigcap_{k=1}^{i} A_k(\theta^{(k)}) \cap A_{i+1}(\theta^{(i+1)})}\Big] - \mathbb{E}\Big[\tilde{H}(\gamma_{i+1})\mathbf{1}_{\bigcap_{k=1}^{i} A_k(\theta^{(k)}) \cap A_{i+1}(\theta^{(i+1)})}\Big] \\
&\quad + \mathbb{E}\Big[\tilde{H}(\gamma_{i+2})\mathbf{1}_{\bigcap_{k=1}^{i} A_k(\theta^{(k)}) \cap A_{i+1}(\theta^{(i+1)})}\Big] - \mathbb{E}\Big[\Phi_{i+2}(\theta^{(i+2)})\mathbf{1}_{\bigcap_{k=1}^{i} A_k(\theta^{(k)}) \cap A_{i+1}(\theta^{(i+1)})}\Big] \\
&= \sum_{j=1}^{i+1} \theta_j \left(q_{j+1} - \mathbb{E}[Q_{j+1}(\theta)]\right) + \sum_{j=i+2}^{d-1} \theta_j q_{j+1} + \sum_{j=2}^{i} \mathbb{E}\big[\tilde{H}(\gamma_j)P_j(\theta)\big] \\
&\quad + \mathbb{E}\big[\tilde{H}(\gamma_{i+1})\left(Q_{i+1}(\theta) - Q_{i+2}(\theta)\right)\big] + \mathbb{E}\big[\tilde{H}(\gamma_{i+2})Q_{i+2}(\theta)\big] - \mathbb{E}\Big[\Phi_{i+2}(\theta^{(i+2)})Q_{i+2}(\theta)\Big],
\end{aligned}
$$

which is equality (4.3.52) for $i+1$. We are done. □

One could then use the previous Lemma to obtain the following generalization of Lemma 4.3.2, in which we compute each left and right partial derivatives of w. We conjecture that:

Lemma 4.3.4 (conjecture) *For all $1 \leqslant i \leqslant d-1$ and $\theta \in \mathbb{R}_+^{d-1}$, we have*

$$
\begin{aligned}
\partial_{i,-} w(\theta) &= (+\infty)\mathbf{1}_{\theta_i = 0} + \left(q_{i+1} - \mathbb{E}[Q_{i+1}(\theta)]\right), \\
\partial_{i,+} w(\theta) &= q_{i+1} - \mathbb{E}\big[Q_{i+1}^{+}(\theta)\big],
\end{aligned}
$$

with $Q_{i+1}^{+}(\theta) := \mathbf{1}_{\bigcap_{j=1}^{i}\{\theta_j + \tilde{H}(\gamma_j) - \tilde{H}(\gamma_{j+1}) + \Phi_{j+1}(\theta^{(j+1)}) \geqslant 0\}}$.

This in turn allows to prove the duality in an important particular case, which is the generalization of Theorem 4.3.2. Note that for $\theta^\star \in \arg\sup_{\mathbb{R}_+^{d-1}} w$, we would then have, by Lemma 4.3.4,

$$
q_{i+1} - \mathbb{E}[Q_{i+1}(\theta)] \geqslant 0 \geqslant q_{i+1} - \mathbb{E}\big[Q_{i+1}^{+}(\theta)\big], \quad 1 \leqslant i \leqslant d-1. \tag{4.3.54}
$$

Theorem 4.3.4 (conjecture) *Assume that there exists $\theta^\star \in \arg\sup_{\theta \in \mathbb{R}_+^{d-1}} w$ such that*

$$
\mathbb{E}[Q_{i+1}(\theta^\star)] = \mathbb{E}\big[Q_{i+1}^{+}(\theta^\star)\big], \quad 1 \leqslant i \leqslant d-1. \tag{4.3.55}
$$

We then have $\mathcal{V}_{\mathrm{DP}}(\mu) = \mathcal{V}_{\mathrm{KP}}(\mu)$.

Proof. By (4.3.55) and (4.3.54), we have

$$
q_{i+1} - \mathbb{E}[Q_{i+1}(\theta)] = 0, \quad 1 \leqslant i \leqslant d-1. \tag{4.3.56}
$$

We then compute, using (4.3.16), (4.3.51) and (4.3.56),

$$\mathcal{V}_{\mathrm{DP}}(\mu) = \mathbb{E}[H(\gamma_1)] + \sum_{j=2}^{d} \mathbb{E}\big[\tilde{H}(\gamma_j)\,(Q_j(\theta^\star) - Q_{j+1}(\theta^\star))\big] = \mathbb{E}[H(\chi^\star)]\,,$$

with $\chi^\star := \sum_{i=1}^d \gamma_i\,(Q_i(\theta^\star) - Q_{i+1}(\theta^\star)) = \sum_{i=1}^d \gamma_i \mathbf{1}_{\bigcap_{j=1}^{i-1} A_j(\theta^\star)\cap A_i(\theta^\star)^c}$.

Last, notice that $\chi^\star \in \mathcal{T}_+^{\mathrm{r}}(\mu)$ as $Q_1(\theta^\star) = 1 \geqslant Q_2(\theta^\star) \geqslant \cdots \geqslant Q_d(\theta^\star) \geqslant 0 = Q_{d+1}(\theta^\star)$ and $\mathbb{E}[Q_i(\theta^\star)] = q_i$ for all $2 \leqslant i \leqslant d$. Hence $\mathcal{V}_{\mathrm{DP}}(\mu) \geqslant \mathcal{V}_{\mathrm{RM}}(\mu) = \mathcal{V}_{\mathrm{DP}}(\mu)$. □

4.3.2 PnL hedging with given probability

In this section, we study how to weakly hedge a position when a constraint on the PnL target is given in a set of probability. We have to specialize the setting to linear G function namely, given a fixed random payoff ξ, we assume in this part that

$$G(\gamma) := \xi + \gamma\,. \tag{4.3.57}$$

In this setting, we observe that, recall (4.3.1) and (4.3.3),

$$\widehat{\mathcal{V}}_{\mathrm{RM}}(\mu) = \inf_{\chi\in\mathcal{T}_+(\mu)} \mathbb{E}[H(\chi)] \tag{4.3.58}$$

$$= \mathbb{E}[\Gamma_T\xi] + \inf_{\chi\in\mathcal{T}_+(\mu)} \mathbb{E}[\Gamma_T\chi]\,. \tag{4.3.59}$$

To solve this problem, we use directly results from optimal transportation problem. In particular, we will first solve the problem above when the constraint is saturated namely when $\chi\sharp\mathbb{P} = \mu$. We shall rely on the following:

Assumption 4.3.1 *The law of Γ_T is absolutely continuous with respect to the Lebesgue measure.*

We define the following (more restrictive) problem, for $\mu \in \mathcal{P}_4$,

$$\mathcal{V}_{\mathrm{OT}}(\mu) := \inf_{\chi\in\mathcal{T}_\mu} \mathbb{E}[\Gamma_T\,(\xi + \chi)]\,, \tag{4.3.60}$$

where $\mathcal{T}_\mu = \big\{\chi \in \mathcal{L}^2(\mathcal{F}_T)\,\big|\,\chi_\sharp\mathbb{P} \in \mathcal{K}_\mu\big\}$.

Lemma 4.3.5 *Under Assumptions 4.3.1, for $\mu \in \mathcal{P}_4$, we have*

$$\mathcal{V}_{\mathrm{OT}}(\mu) = \mathbb{E}[\Gamma_T\xi] - \frac{1}{2}\mathbb{E}\Big[(\Gamma_T)^2\Big] - \frac{1}{2}\int x^2\mu(\mathrm{d}x) + \frac{1}{2}\mathcal{W}_2^2(\mathcal{L}(-\Gamma_T),\mu).$$

In addition, there exists $\chi^\star \in \mathcal{T}_\mu$ such that

$$\mathcal{V}_{\mathrm{OT}}(\mu) = \mathbb{E}[\Gamma_T\,(\xi + \chi^\star)]\,,$$

which writes explicitely $\chi^\star = N_\mu^{-1} \circ N_{\mathcal{L}(-\Gamma_T)}(-\Gamma_T)$. Here, N_μ stands for the c.d.f. of the law μ and N_μ^{-1} its generalized inverse.

Proof. We compute, starting from (4.3.60), as each $\theta \in \mathcal{T}_\mu$ has law μ,

$$\begin{aligned}\mathcal{V}_{\mathrm{OT}}(\mu) &= \mathbb{E}[\Gamma_T \xi] + \inf_{\theta \in \mathcal{T}_\mu} \mathbb{E}[\Gamma_T \theta] \\ &= \mathbb{E}[\Gamma_T \xi] + \inf_{\theta \in \mathcal{T}_\mu} -\mathbb{E}[(-\Gamma_T)\theta] \\ &= \mathbb{E}[\Gamma_T \xi] + \frac{1}{2} \inf_{\theta \in \mathcal{T}_\mu} \left(\mathbb{E}\left[(-\Gamma_T - \theta)^2\right] - \mathbb{E}\left[(-\Gamma_T)^2\right] - \mathbb{E}\left[\theta^2\right]\right) \\ &= \mathbb{E}[\Gamma_T \xi] - \frac{1}{2}\mathbb{E}\left[(\Gamma_T)^2\right] - \frac{1}{2}\int x^2 \mu(\mathrm{d}x) + \frac{1}{2} \inf_{\theta \in \mathcal{T}_\mu} \mathbb{E}\left[(-\Gamma_T - \theta)^2\right].\end{aligned}$$

Since $\mathcal{L}(-\Gamma_T)$ is absolutely continuous with respect to the Lebesgue measure by Assumption 4.3.1, using Brenier's theorem (see for example [21, Theorem 5.20]), there exists an optimal transport map T from $\nu := \mathcal{L}(-\Gamma_T)$ to μ, i.e. such that $T_\sharp \nu = \mu$ and

$$\mathcal{W}_2^2(\nu, \mu) = \int (x - T(x))^2 \nu(\mathrm{d}x).$$

Defining $\theta^\star := T(-\Gamma_T) \in \mathcal{T}_\mu$, we have

$$\mathcal{W}_2^2(\nu, \mu) = \mathbb{E}\left[(-\Gamma_T - \theta^\star)^2\right] = \inf_{\theta \in \mathcal{T}_\mu} \mathbb{E}\left[(-\Gamma_T - \theta)^2\right].$$

It is well-known, see for example [21, Remark 5.15], that $\theta^\star = N_\mu^{-1} \circ N_\nu(-\Gamma_T)$ as Γ_T has no atom by assumtion. □

Lemma 4.3.6 *Under Assumptions 4.3.1, for any $\nu, \mu \in \mathcal{P}_2$ such that $\nu \succeq \mu$, we have $\mathcal{V}_{\mathrm{OT}}(\nu) \geqslant \mathcal{V}_{\mathrm{OT}}(\mu)$.*

Proof. By Lemma 4.3.5, we have that

$$\begin{aligned}\mathcal{V}_{\mathrm{OT}}(\nu) - \mathcal{V}_{\mathrm{OT}}(\mu) &= \mathbb{E}\left[\Gamma_T \left(N_\nu^{-1}(N_{\mathcal{L}(-\Gamma_T)}(-\Gamma_T)) - N_\mu^{-1}(N_{\mathcal{L}(-\Gamma_T)}(-\Gamma_T))\right)\right] \\ &= \mathbb{E}\left[\Gamma_T \left(N_\nu^{-1}(U) - N_\mu^{-1}(U)\right)\right],\end{aligned}$$

with $U := N_{\mathcal{L}(-\Gamma_T)}(-\Gamma_T)$ is uniformly distributed on $[0,1]$ as Γ_T has no atom. Since $\nu \succeq \mu$, we have $N_\nu^{-1} \geqslant N_\mu^{-1}$, hence the result, as $\Gamma_T > 0$, $\mathbb{P}$-almost surely. □

Proposition 4.3.2 *Under Assumption 4.3.1, for all $\mu \in \mathcal{P}_2$, we have*

$$\hat{\mathcal{V}}_{\mathrm{RM}}(\mu) = \mathcal{V}_{\mathrm{OT}}(\mu).$$

Proof. Since $\mathcal{T}(\mu) \subset \mathcal{T}_+(\mu)$, we have $\hat{\mathcal{V}}_{\mathrm{RM}}(\mu) \leqslant \mathcal{V}_{\mathrm{OT}}(\mu)$.
Conversely, let $(\chi_n, n \geqslant 1)$, a sequence of elements of $\mathcal{T}_+(\mu)$ such that $\mathcal{V}_{\mathrm{RM}}(\mu) + \frac{1}{n} \geqslant \mathbb{E}[\Gamma_T(\xi + \chi_n)]$. We have $\mathbb{E}[\Gamma_T(\xi + \chi_n)] \geqslant \mathcal{V}_{\mathrm{OT}}(\chi_n \sharp \mathbb{P}) \geqslant \mathcal{V}_{\mathrm{OT}}(\mu)$, thanks to Lemma 4.3.6, as $\chi_n \sharp \mathbb{P} \succeq \mu$ for all $n \geqslant 1$. We then have $\hat{\mathcal{V}}_{\mathrm{RM}}(\mu) + \frac{1}{n} \geqslant \mathcal{V}_{\mathrm{OT}}(\mu)$ and sending n to infinity gives the reverse inequality. □

Remark 4.3.4 *In this case, the infimum in the weak hedging problem is attained by replicating the payoff $\xi + \chi^\star$ given in Lemma 4.3.5. Obviously, the value Kantorovich problem (4.2.25) (adapted to the linear setting) is obtained for $\mathrm{d}\Pi^\star(\omega, \gamma) = \delta_{\chi^\star}(\mathrm{d}\gamma)\mathrm{d}\mathbb{P}(\omega)$.*

4.4 Numerical studies

We now turn to numerical consideration associated to the above problem having in mind possible application. We thus first introduced a Markovian setting where our previous results can be straightforwardly restated.

We introduce a Markovian setting where our previous results can be straightforwardly restated.

$$X_t = X_0 + \int_0^t b(X_s)\mathrm{d}s + \int_0^t \sigma(X_s)\mathrm{d}W_s \ , \tag{4.4.1}$$

where $b : \mathbb{R}^m \to \mathbb{R}^m$, $\sigma : \mathbb{R}^m \to \mathbb{R}^{m\times m}$ are Lipschitz continuous functions. As usual, the starting point $X_0 \in \mathbb{R}^m$ at time 0 is arbitrary and we omit it in the notation. In this setting, the controlled process $Y^{y,Z}$, recall (4.2.1), satisfies

$$Y_s^{y,Z} = y - \int_t^s f(r, X_r, Y_r^{y,Z}, Z_r)\,\mathrm{d}r + \int_t^s Z_r \mathrm{d}W_r \ , \tag{4.4.2}$$

where $f : [0,T] \times \mathbb{R}^m \times \mathbb{R} \times \mathbb{R}^m \to \mathbb{R}$ is a Lipschitz continuous function.
Let us mention that all our numerical tests will be done in the linear framework, basically considering that the following holds:

Assumption 4.4.1 *There exists a bounded continuous map $(\alpha, \beta) : [0,T]\times(0,\infty) \to \mathbb{R} \times \mathbb{R}^m$ such that*

$$f\,(t,x,y,z) = \alpha(t,x)y + \beta(t,x)^\top z, \quad (t,x,y,z) \in [0,T] \times (0,\infty) \times \mathbb{R} \times \mathbb{R}^m.$$

Under Assumption 4.4.1, the process Γ, recall Remark 4.2.1, is solution to

$$\Gamma_t = 1 + \int_0^t \Gamma_s \alpha(s, X_s)\mathrm{d}s + \int_0^t \Gamma_s \beta(s, X_s)^\top \mathrm{d}W_s, \quad 0 \leqslant t \leqslant T. \tag{4.4.3}$$

Regarding the terminal constraint, we consider a continuous function:

$$\mathbb{R}^d \times \mathbb{R} \ni (x,\gamma) \mapsto g(x,\gamma) \in \mathbb{R}\,, \tag{4.4.4}$$

such that $\gamma \mapsto g(\cdot,\gamma)$ is non decreasing. And we set, for all $\gamma \in \mathbb{R}$,

$$G(\gamma) = g(X_T, \gamma) \ \text{ and } \ H(\gamma) = \Gamma_T g(X_T, \gamma). \tag{4.4.5}$$

4.4.1 Numerical solution for the PnL hedging problem

We consider here the case where $\mu \in \mathcal{P}_4(\mathbb{R})$ but g has the following form

$$g(x,\gamma) := \tilde{g}(x) + \gamma\,. \tag{4.4.6}$$

Assuming that $\mathcal{L}(-\Gamma_T)$ is absolutely continuous w.r.t. Lebesgue measure, we have, from Proposition 4.3.2 adapted to our setting,

$$\widehat{\mathcal{V}}_{\mathrm{RM}}(\mu) = \mathbb{E}[\Gamma_T \tilde{g}(X_T)] - \frac{1}{2}\mathbb{E}\Big[(\Gamma_T)^2\Big] - \frac{1}{2}\int x^2 \mu(\mathrm{d}x) + \frac{1}{2}\mathcal{W}_2^2(\mathcal{L}(-\Gamma_T), \mu). \tag{4.4.7}$$

$$= \mathbb{E}[\Gamma_T\,(\tilde{g}(X_T) + \chi^\star)]\,, \tag{4.4.8}$$

with $\chi^\star = N_\mu^{-1} \circ N_{\mathcal{L}(-\Gamma_T)}(-\Gamma_T)$.

We apply the previous result, to the Black & Scholes model, already studied in [5, 36].

Example 4.4.1 (Black & Scholes Model) *The process X satisfies*

$$X_t = X_0 + \int_0^t \hat{b} X_s \mathrm{d}s + \int_0^t \sigma X_s \, \mathrm{d}W_s \ ,$$

with $\hat{b} \in \mathbb{R}, \sigma > 0$ and $X_0 > 0$. The function f is given by:

$$f(t,x,y,z) = -ry - \frac{\hat{b}-r}{\sigma} z =: -ry - \lambda z, \tag{4.4.9}$$

where $r \geqslant 0$ the interest rate, and $\lambda := \frac{\hat{b}-r}{\sigma}$ the risk premium. The Radon-Nikodym derivative defined in (4.4.3) is thus:

$$\Gamma_T = \frac{\mathrm{d}\mathbb{Q}}{\mathrm{d}\mathbb{P}}\Big|_T = \exp\Big(\frac{r-\hat{b}}{\sigma} W_T - \frac{1}{2}\frac{(r-\hat{b})^2}{\sigma^2} T\Big).$$

Using the (almost) explicit formula (4.4.7), we first test the model Example 4.4.1 for a one-constraint target measure μ, see Figure 4.1 (note that we consider the set $p := \{\frac{i}{1000}, 0 \leqslant i \leqslant 1000\}$). We also plot the histogram of distribution of $\tilde{g}(X_T^{t,x}) + \chi^\star$ under the probability measure $\mathbb{P}$ at the terminal time T, recall (4.4.8), in Figure 4.2.

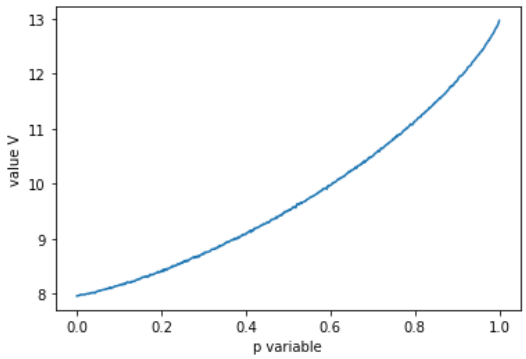

Figure 4.1: $\mathcal{V}_{\mathrm{OT}}(p)$ for model Example 4.4.1 for call option $x \mapsto \tilde{g}(x) = (x-K)_+$ with target measure $\mu = (1-p)\delta_0 + p\delta_5$ with following parameters: $X_0 = 100$, interest rate $r = 0$, volatility $\sigma = 0.2$ and drift term $\hat{b} = 0.1$, strike $K = 100$, time horizon $T = 1$.

4.4.2 The multiple quantile constraint case

We now turn to the numerical study of the general case under Assumption 4.2.4. When $d = 2$ in Assumption 4.2.4, the setting essentially corresponds to the quantile hedging problem. When $d > 2$, the setting corresponds to the PnL matching problem introduced in [15]. Obtaining numerical solution for these weak hedging problem is quite involved see e.g. [15, 11, 5].

We propose here a new method based on the dual representation obtained (in some cases) in the previous section. We shall then focus on the computation of $\mathcal{V}_{\mathrm{DP}}$ and more particularly $\mathfrak{W}$, recall Corollary 4.3.2. Based on the shape of $\mathfrak{W}$, it completely natural to rely on SGD algorithms.

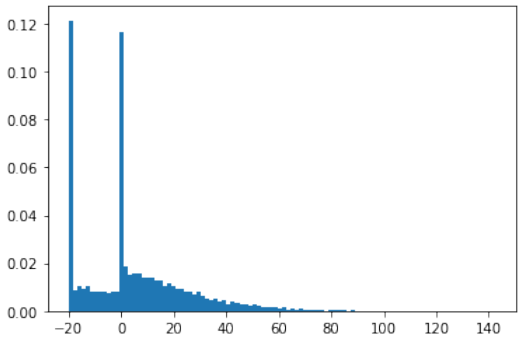

Figure 4.2: Model Example 4.4.1. Histogram of law $g(X_T)+\theta^\star$ for call option $x \mapsto (x-K)_+$ at terminal time T for the probability measure $\mu = \frac{1}{2}\delta_{-20} + \frac{1}{2}\delta_0$ with following parameters: $X_0 = 100$, interest rate $r = 0$, volatility $\sigma = 0.2$ and drift term $\hat{b} = 0.1$, strike $K = 100$, time horizon $T = 1$. As expected, the graph presents two Dirac masses around the quantiles 0 and -20.

4.4.2.1 SGD algorithms

We consider various SGD algorithms to compute $\theta^\star$, recall Lemma 4.3.1. Once this is achieved, we recompute by Monte Carlo simulation the quantity $\mathfrak{W}$. Note that, to slightly simplify the practical implementation, in the following we take the parameterization using the survival probability $q_\ell = \sum_{j=\ell}^d p_j$ and thus compute $\mathfrak{W}$ instead of $\mathfrak{V}$ in Corollary 4.3.2. Indeed, the range of parameter for θ is $\mathbb{R}_+^{d-1}$ instead of the simplex Δ_+^{d-1} for ζ, recall (4.3.17). As already mentioned, in order to compute the optimal $\theta^\star$ so, we will use stochastic gradient descent algorithms. This technique has been already demonstrated to be quite efficient for quantile estimation problems (corresponding to the computation of quantile hedging price here). We refer, to e.g. [3] for a detailed description of computing VaR as well as CVaR (unidimensional, however could be extended to multi-dimensional) using stochastic approximation. We note that the stochastic approximation in [3] is originally without any constraint, however in our case, parameter θ is constrained on a convex set $C := \mathbb{R}_+^{d-1}$, thus it is more suitable here to use the Projected Stochastic Gradient (PSG), see e.g. [37, 59] where at each step, the algorithm move in the direction of the negative gradient and then project parameters into feasible set.

We now describe the algorithms.
Given a random variable θ_0, independent of Brownian motion W with $\mathbb{E}[|\theta_0|] < \infty$, N_{iter} the maximal iteration steps, and $(\eta_n)_{n\geqslant 1}$ a deterministic sequence verifying

$$\sum_{n\geqslant 1} \eta_n = +\infty \text{ and } \sum_{n\geqslant 1} \eta_n^2 < +\infty, \tag{4.4.10}$$

the scheme to compute $\hat{\theta}^\star$ approximation of $\theta^\star$ in Theorem 4.3.4 is given as follows, and we suppose in addition that $\mathfrak{W}$ is differentiable with respect to $\theta \in \mathbb{R}_+^{d-1}$.

Definition 4.4.1 *1. At initial step $n = 0$, set $\hat{\theta}_0^\star = \theta_0$.*

2. *For* $n = 1, \cdots, N_{iter}$*: generate*[1] (Γ_n, X_n) *independent from* $(\Gamma_1, X_1), \cdots, (\Gamma_{n-1}, X_{n-1})$ *(with law* (Γ_T, X_T) *given by* (4.4.3) *and* (4.4.1) *respectively),* θ_0 *and* $\eta_n > 0$ *step size,*

$$\hat{\theta}^\star_n = \pi_C\Big(\hat{\theta}^\star_{n-1} - \eta_n \mathfrak{h}(\hat{\theta}^\star_{n-1}, \Gamma_n, X_n)\Big)\,. \tag{4.4.11}$$

Where $\pi_C(u) := \underset{w\in C}{\operatorname{argmin}}\ ||u - w||$ *the orthogonal projection on convex* $C = \mathbb{R}^{d-1}_+$*. And the gradient* $\mathfrak{h}(\theta, \Gamma, X) := (\mathfrak{h}_1, \cdots, \mathfrak{h}_{d-1}) \in \mathbb{R}^{d-1}$*, where we define* $\mathfrak{h}_i(\theta, \Gamma, X) = \hat{\partial}_{i,+} w(\theta), 1 \leqslant i \leqslant d-1$*, recall Lemma 4.3.4.*

The convergence of projected gradient descent for a convex objective and a convex constraint is well-studied, see e.g. [37, Theorem 3.6] in Hilbert space, also in [50], the author proves the convergence of projected gradient descent in the case of a convex objective, and [59] proves a convergence rate $O(\frac{1}{T})$ with T iteration number, if the additional constraint keeps the feasible set convex and the algorithm used is projected stochastic subgradient descent with a suitable step size rule.

Remark 4.4.1 *We have the following remarks on SGD algorithm:*

1. *This method is easy to apply provided we can compute the projection. In our special cases, we project onto* $C = \mathbb{R}^{d-1}_+$ *for* θ *or* Δ^{d-1}_+ *for* ζ*, recall Corollary 4.3.2. There exist efficient projection methods in linear time, e.g. if* C *is a polyhedron, i.e. a set of* x *such that* $Ax \leqslant b$ *for some matrix* A *and vector* b*, see e.g. Liu and Ye [61], or projection on a simplex, see e.g. [27].*

2. *In one-dimensional case, for extreme values* $p = 0$ *or* 1*, there is no issue concerning the convergence see e.g. Figure 4.3 , however when using the above stopping criteria for SGD algorithm with* $p = 1$*, this could lead to a gradient vanishing problem since during the stochastic gradient descent, the negative gradient*

$$-\theta_n \mathfrak{h} = \theta_n \mathbf{1}_{\{\theta_n - \Gamma_T \mathfrak{g} \geqslant 0\}},$$

could be initially 0 and trigger the stopping criteria, hence for a probability p *close to 1 such as 0.99 or 0.999, the above SGD algorithm with stopping criteria still works and converges well, see Figure 4.4. For higher-dimensional case, there is no such gradient vanishing issue with above stopping criteria.*

3. *For* $p < p^\star := \mathbb{E}[\mathbf{1}_{0 \geqslant \Gamma_T \mathfrak{g}}]$*, the exact formula of quantile hedging in [36] is not valid, this issue is resolved automatically in our numerical scheme. To illustrate this numerically, we consider constraints such that* $\mathbb{P}(Y_T^{y,Z} \geqslant 0) = 1, \mathbb{P}(Y_T^{y,Z} \geqslant g(X_T) + \gamma) = p$ *with* $p < p^\star$*. As expected, we observe that the estimated quantile* $\theta^\star$ *converges well to zero, see Figure 4.5.*

One of the difficulties of the above maximization problem is saddle points, i.e. points where one-dimension slopes up and another slopes down, which makes it very hard for vanilla SGD to escape, as the gradient becomes vanishing. The advantage

[1] We assume here that the law (Γ_T, X_T) is perfectly simulatable. If not, a proxy (given e.g. by an Euler scheme) has to be used.

of adaptive gradient algorithms that change learning rates for each parameter, e.g. ADAM optimizer is that they could potentially escape saddle points unlike the vanilla SGD algorithm. We thus also consider this alternative algorithm.

Definition 4.4.2 (ADAM optimizer [57]) *1. At initial step $n = 0$, set $\hat{\theta}_0^\star = \theta_0$.*

2. Initialize first moment $m_0 = 0$, and second moment $v_0 = 0$.

3. For $n = 1, \cdots, N_{iter}$: generate (Γ_n, X_n) independant from $(\Gamma_1, X_1), \cdots, (\Gamma_{n-1}, X_{n-1})$, θ_0 and $\eta_n > 0$ step size, then we calculate

$$g_n = \pi_C\Big(\mathfrak{h}(\hat{\theta}_{n-1}^\star, \Gamma_n, X_n)\Big), \tag{4.4.12}$$

$$m_n = \beta_1 m_{n-1} + (1-\beta_1) g_n, \tag{4.4.13}$$

$$v_n = \beta_2 v_{n-1} + (1-\beta_2) g_n^2, \tag{4.4.14}$$

$$\hat{m}_n = \frac{m_n}{1-\beta_1^n}, \hat{v}_n = \frac{v_n}{1-\beta_2^n}, \tag{4.4.15}$$

$$\hat{\theta}_n^\star = \pi_C\Big(\hat{\theta}_{n-1}^\star - \eta_n \frac{\hat{m}_n}{\sqrt{\hat{v}_n} + \epsilon}\Big). \tag{4.4.16}$$

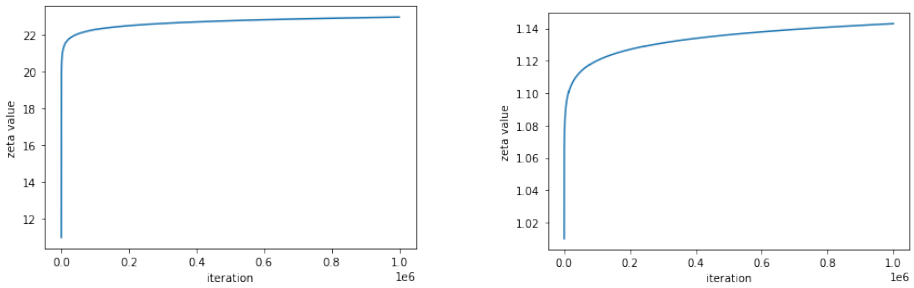

(a) $p = 1.0$ (b) $p = 0$

Figure 4.3: Evolution of quantile $\theta^\star$ in the setting $\gamma_1 = 10, \gamma_2 = 100$ during the stochastic gradient descent without stopping criteria.

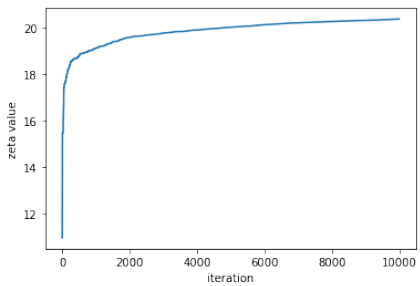

Figure 4.4: Evolution of $\theta^\star$ for $\mu = (1-p)\delta_0 + p\delta_{10}$, with $p = 0.999$ and $\gamma = 0$, $\hat{b} = 0.1, r = 0, K = 100, X_0 = 100, \sigma = 0.2$.

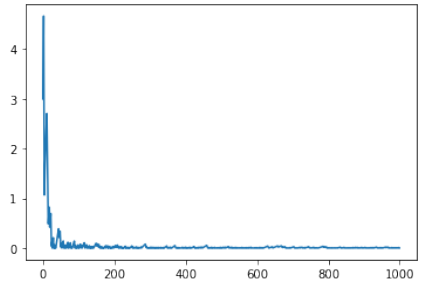

Figure 4.5: Evolution of $\theta^\star$ in quantile hedging with probability $p < p^\star$, as well as with parameters $\gamma = 0$, $\hat{b} = 0.1, r = 0, K = 100, X_0 = 100, \sigma = 0.2$, with stopping criteria $\epsilon = 10^{-6}$.

Probability p	$p = 0.01$	$p = 0.1$	$p = 0.5$	$p = 0.9$	$p = 0.99$
Computation time of SGD	17.89s	18.14s	19.17s	17.88s	18.93s
SGD algorithm	7.99	8.36	11.08	15.72	17.81
Optimal transport	7.94	8.36	11.15	15.78	17.78

Table 4.1: Numerics of measure $\mu = (1-p)\delta_0 + p\delta_\gamma$ with different probabilities with SGD algorithm and OT-APPROACH.

4.4.2.2 Numerical experiments

In this section, we report the findings of our numerical tests we performed on the model Example 4.4.1 given in the above, using stochastic gradient descent method of Definition 4.4.1 and the formula (4.4.7), called below OT-APPROACH, obtained by optimal transport method and used in Section 4.4.1.

Concerning the stochastic gradient descent, we use a common structure in all our numerical tests, namely:

- The maximum of number of iterations N_{iter} set to 10^6.
- The deterministic step $\eta_n = \frac{10}{n}$.
- Initial value θ_0 is drawn randomly from an exponential distribution exp(1) of parameter $\lambda = 1$.
- Stopping criteria: if the absolute value of all coefficients of increment vector $-\eta_n \mathfrak{h}$ less than a predefined tolerance which we set to 10^{-6}.

4.4.2.2.1 One constraint We consider a target measure $\mu = (1-p)\delta_0 + p\delta_\gamma$, which corresponds to an "almost sure" constraint on 0 and a quantile constraint on γ. We have tested numerical results by SGD algorithm against OT-APPROACH, and results are reported in Table 4.1. We note that the number of simulations of trajectories of brownian motion is $N = 100000$, European claim payoff function $g(x) = (x-K)+$ with $K = 100$. Concerning the dynamics of X, we take $X_0 = 100$, $r = 0, \hat{b} = 0.1, \sigma = 0.2$, and time horizon $T = 1.0$.

One can see in Table 4.1 that SGD algorithm performs well compared to the OT-APPROACH and we also plot the learning curves of quantile $\theta^\star$ during the SGD algorithm, see Figure 4.6, we observe that they all converge and verify the convex constraint.

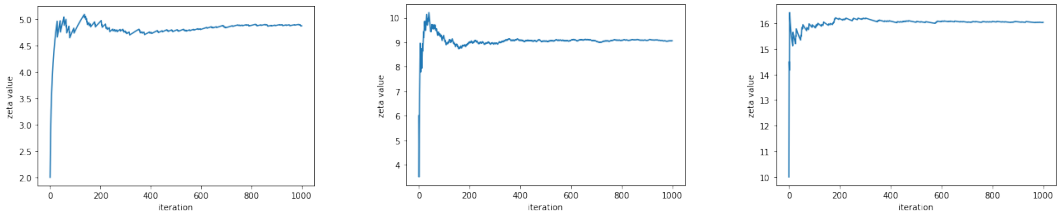

(a) $p = 0.1$ (b) $p = 0.5$ (c) $p = 0.9$

Figure 4.6: Numerical convergence of $\theta^\star$ for different values of quantiles $p = 0.1, 0.5, 0.9$ and $\gamma = 10$ by SGD algorithm.

Quantiles p_1, p_2	γ_1, γ_2	SGD	OT	Computation time of SGD
(0.3,0.5)	(10,20)	17.38	17.48	30.66s
(0.05,0.05)		8.48	8.41	30.31s
(0.05,0.9)		24.41	24.44	29.46s
(0.3,0.5)	(10,100)	42.07	42.19	32.47s
(0.05,0.05)		9.57	9.62	31.40s
(0.05,0.9)		87.89	87.57	30.68s

Table 4.2: Numerics of measure $\mu = (1-p_1-p_2)\delta_0 + p_1\delta_{\gamma_1} + p_2\delta_{\gamma_2}$ with different probabilities and quantiles with SGD algorithm and OT-APPROACH.

4.4.2.2.2 Two constraints We consider in this part a discrete measure with two constraints $\mu = (1 - p_1 - p_2)\delta_0 + p_1\delta_{\gamma_1} + p_2\delta_{\gamma_2}$. The numerical results are reported in the Table 4.2. Again we observe that the numerical solutions by SGD perform well in comparison to the OT-APPROACH. Besides we also report the evolution of quantile vector $\theta^\star = (\theta_1^\star, \theta_2^\star)$ for a particular case where $p_1 = 0.05, p_2 = 0.9$ and $\gamma_1 = 10, \gamma_2 = 100$ in Figure 4.7, to illustrate the numerical convergence of SGD algorithm. We note that the other parameters are same as above.

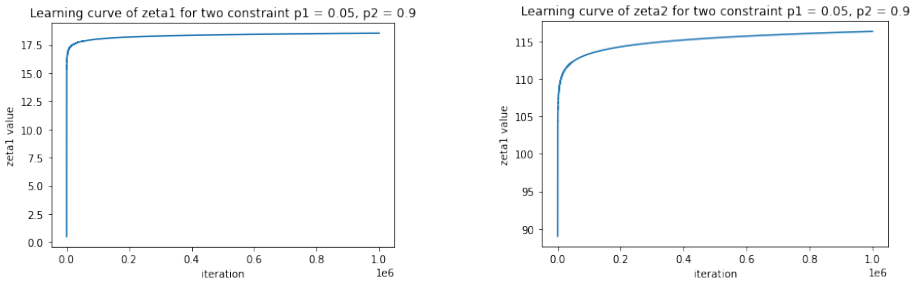

(a) Evolution of $\theta_1^\star$ (b) Evolution of $\theta_2^\star$

Figure 4.7: Evolution of quantiles $\theta^\star = (\theta_1^\star, \theta_2^\star)$ in the setting $p_1 = 0.05, p_2 = 0.9$ and $\gamma_1 = 10, \gamma_2 = 100$ during the stochastic gradient descent.

4.4.2.2.3 Quantile hedging problem In this part, we want to validate our numerical methods by comparison with some theoretical quantile hedging results see

e.g. [5, 36, 11]. In this setting, it presents two following constraints: $\mathbb{P}(Y_T \geqslant 0) = 1$ and $\mathbb{P}(Y_T \geqslant g(X_T)) = p$. We consider a set of probabilites $p := \{\frac{i}{100}, 0 \leqslant i \leqslant 100\}$. We have tested our numerical scheme for classical European call and put option claims against theoretical price see e.g. [36]. We first observe that our numerical scheme is able to reproduce correctly the true solution of call option claim, even for extreme values of p, as reported in Figure 4.8. However we note that SGD algorithm does not work pretty well for put option as reported in Figure 4.8: we observe that the values given by SGD and theoretical values by e.g. Föllmer-Leukert [36] are quite close for p below 0.8, however it seems that SGD algorithm could not reproduce the correct value for extreme values p (above 0.8). This numerical phenomenon comes from the difficulty of computation of extreme quantiles in the case of put option, since the distribution of law $\Gamma_T\mathfrak{g}$ is much rarer in terms of extreme values : this fact is illustrated on Figure 4.9. And this results in an unstable and inaccurate computation of rare extreme quantiles during the gradient descent algorithm.

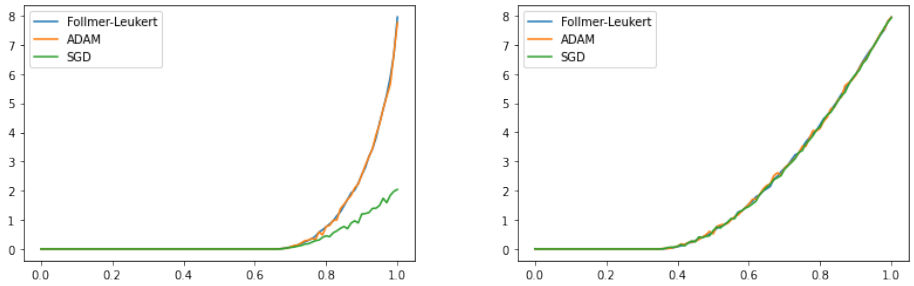

(a) Put option $(K - S)_+$ (b) Call option $(S - K)_+$

Figure 4.8: Comparison of the three methods: SGD algorithm, ADAM optimizer & Exact solution [5, 36] for put and call options, with parameters $X_0 = 100$, $r = 0$, $\sigma = 0.2$ and $\hat{b} = 0.1$, strike $K = 100$, terminal time $T = 1$.

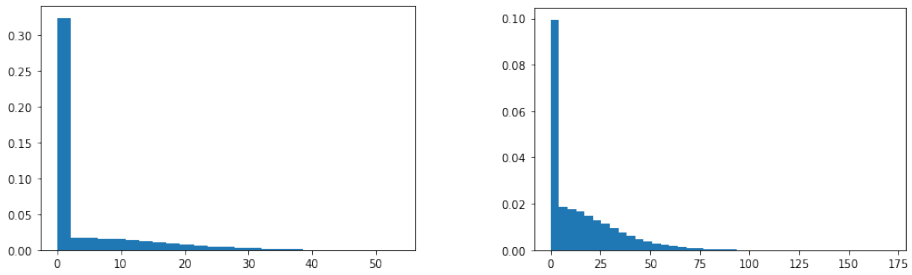

(a) Put option (b) Call option

Figure 4.9: Comparison of histograms of distribution of law $\Gamma_T\mathfrak{g}$ for put and call option, note that other parameters of processes are same as the above.

Finally, to illustrate empirically this rare extreme quantile fact, we tested our algorithm on a simpler setting where we take $\hat{b} = r = 0$ and hence $\mathbb{P} = \mathbb{Q}$. The result of SGD algorithm against theoretical price is reported on the graph in Figure 4.10. As expected, we observe that this phenomenon is much less severe for extreme

values of p. For comparison, the distribution of law $\Gamma_T \mathfrak{g}$ in this setting is reported in Figure 4.11 and we observe that it presents less rare extreme quantiles compared to Figure 4.8 where $\hat{b} = 0.1, r = 0$. Besides we also try to increase the maximal iteration number N_{iter} to 10^8 and decrease the stopping criteria to 10^{-8} particularly for the extreme case $p = 0.99$, although we observe that there is an improvement compared to before, the computation time is much longer and improvement is barely mild.

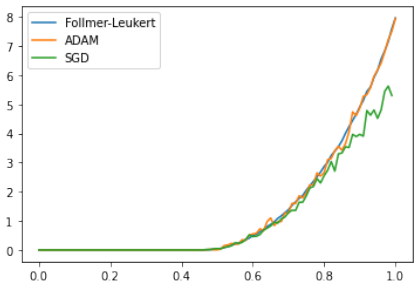

Figure 4.10: Comparison of the three methods: SGD algorithm, ADAM optimizer & Exact solution [5, 36] for put option with $\hat{b} = r = 0$, other parameters are same as above.

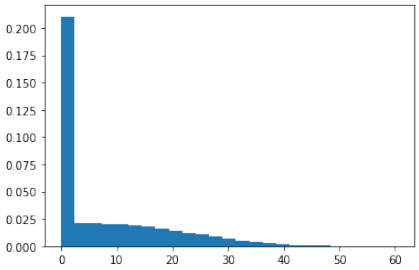

Figure 4.11: Distribution of law of $\Gamma_T \mathfrak{g}$ for put option with $\hat{b} = r = 0$, other parameters of processes are kept same as the above.

As we observed, although there is an improvement for the case $\hat{b} = r$, for both cases, the vanilla SGD could not capture correctly the extreme quantile, we think it is largely because of the trapping in a saddle point: as we increase the learning rate or step size, the performance of vanilla SGD becomes much better, as we plotted in Figure 4.12, since a larger step size can help alleviating the gradient vanishing in a degree. We mention that for put with $\hat{b} = 0.1, r = 0$, we chose an initial step size $\eta_0 = 200$, and for put $\hat{b} = r = 0$, we chose it as 50. This numerical phenomenon suggests us using an adaptive gradient descent method such as ADAM optimiser given in Definition 4.4.2. Concerning the ADAM optimiser, we tested two cases mentioned in the above: $\hat{b} = 0.1, r = 0$ and $\hat{b} = r = 0$, see in the Figure 4.8 and 4.10 , note that we choose parameters $\beta_1 = 0.9, \beta_2 = 0.999$ as well as a batch size $= 256$. We observe that ADAM optimiser captures quite well the extreme quantiles compared to vanilla SGD.

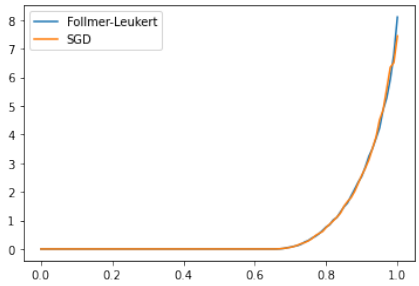

(a) Put option with $\mu = 0.1, r = 0, \eta_0 = 200$.

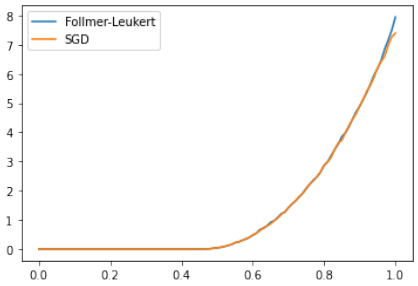

(b) Put option with $\mu = r = 0, \zeta_0 = 50$.

Figure 4.12: Comparison of the two methods SGD with larger initial step size & Exact solution [5, 36] for put options, with parameters $X_0 = 100$, $\sigma = 0.2$, strike $K = 100$, terminal time $T = 1$.

Bibliography

[1] Bally, V., and Pagès, G. Error analysis of the optimal quantization algorithm for obstacle problems. *Stochastic Processes and their Applications 106*, 1 (2003), 1 – 40.

[2] Bally, V., and Pagès, G. A quantization algorithm for solving multidimensional discrete-time optimal stopping problems. *Bernoulli 9*, 6 (2003), 1003–1049.

[3] Bardou, O., Frikha, N., and Pages, G. Computing var and cvar using stochastic approximation and adaptive unconstrained importance sampling.

[4] Bender, C., and Zhang, J. Time discretization and markovian iteration for coupled fbsdes. *The Annals of Applied Probability 18*, 1 (2008), 143–177.

[5] Bénézet, C., Chassagneux, J.-F., and Reisinger, C. A numerical scheme for the quantile hedging problem. *SIAM Journal on Financial Mathematics 12*, 1 (2021), 110–157.

[6] Bernard, P., Talay, D., and Tubaro, L. Rate of convergence of a stochastic particle method for the kolmogorov equation with variable coefficients. *Mathematics of Computation 63*, 208 (1994), 555–587.

[7] Bianchini, S., and Bressan, A. Vanishing viscosity solutions of nonlinear hyperbolic systems. *Annals of mathematics* (2005), 223–342.

[8] Bossy, M. *Vitesse de convergence d'algorithmes particulaires stochastiques et application à l'équation de Burgers*. PhD thesis, Aix-Marseille 1, 1995.

[9] Bossy, M., and Talay, D. Convergence rate for the approximation of the limit law of weakly interacting particles: application to the burgers equation. *The Annals of Applied Probability 6*, 3 (1996), 818–861.

[10] Bossy, M., and Talay, D. A stochastic particle method for the mckean-vlasov and the burgers equation. *Mathematics of computation 66*, 217 (1997), 157–192.

[11] Bouchard, B., Bouveret, G., and Chassagneux, J.-F. A backward dual representation for the quantile hedging of bermudan options. *SIAM Journal on Financial Mathematics 7*, 1 (2016), 215–235.

[12] Bouchard, B., Elie, R., and Réveillac, A. Bsdes with weak terminal condition. *The Annals of Probability 43*, 2 (2015), 572–604.

[13] Bouchard, B., Elie, R., and Touzi, N. Discrete-time approximation of bsdes and probabilistic schemes for fully nonlinear pdes. In *Advanced financial modelling*. De Gruyter, 2009, pp. 91–124.

[14] Bouchard, B., Elie, R., and Touzi, N. Stochastic target problems with controlled loss. *SIAM Journal on Control and Optimization 48*, 5 (2010), 3123–3150.

[15] Bouchard, B., and Nam Vu, T. A stochastic target approach for p&l matching problems. *Mathematics of Operations Research 37*, 3 (2012), 526–558.

[16] Bouchard, B., and Touzi, T. Discrete-time approximation and monte-carlo simulation of backward stochastic differential equations. *Stochastic Processes and their Applications 111*, 2 (2004), 175 – 206.

[17] Brenier, Y., and Grenier, E. Sticky particles and scalar conservation laws. *SIAM journal on numerical analysis 35*, 6 (1998), 2317–2328.

[18] Bressan, A. Hyperbolic systems of conservation laws. *Revista matemática complutense 12*, 1 (1999), 135–200.

[19] Carmona, R., and Delarue, F. Singular FBSDEs and scalar conservation laws driven by diffusion processes. *Probability Theory and Related Fields 157*, 1-2 (2013), 333–388.

[20] Carmona, R., Delarue, F., Espinosa, G.-E., and Touzi, N. Singular forward–backward stochastic differential equations and emissions derivatives. *The Annals of Applied Probability 23*, 3 (2013), 1086–1128.

[21] Carmona, R., Delarue, F., et al. *Probabilistic Theory of Mean Field Games with Applications I-II*. Springer, 2018.

[22] Chassagneux, J.-F., Chotai, H., and Crisan, D. Modelling multiperiod carbon markets using singular forward-backward sdes. *Mathematics of Operations Research* (2022).

[23] Chassagneux, J.-F., Chotai, H., and Muûls, M. *A Forward-Backward SDEs Approach to Pricing in Carbon Markets*. SpringerBriefs in Mathematics of Planet Earth, Springer, 2017.

[24] Chassagneux, J.-F., Crisan, D., and Delarue, F. Numerical method for fbsdes of mckean–vlasov type. *The Annals of Applied Probability 29*, 3 (2019), 1640–1684.

[25] Chassagneux, J.-F., and Garcia Trillos, C. Cubature method to solve bsdes: Error expansion and complexity control. *Mathematics of Computation 89*, 324 (2020), 1895–1932.

[26] Chassagneux, J.-F., and Yang, M. Numerical approximation of singular forward-backward sdes. *Journal of Computational Physics 468* (2022), 111459.

[27] Chen, Y., and Ye, X. Projection onto a simplex. *arXiv preprint arXiv:1101.6081* (2011).

[28] Chollet, F., et al. Keras, 2015.

[29] Chotai, H. Forward-backward stochastic differential equations and applications to carbon emissions markets, 2019. PhD thesis, Imperial College London.

[30] Crisan, D., and Manolarakis, K. Solving backward stochastic differential equations using the cubature method: application to nonlinear pricing. *SIAM Journal on Financial Mathematics 3*, 1 (2012), 534–571.

[31] Crisan, D., and Manolarakis, K. Second order discretization of backward sdes and simulation with the cubature method. *The Annals of Applied Probability 24*, 2 (2014), 652–678.

[32] Crisan, D., Manolarakis, K., and Nizar, T. On the monte carlo simulation of bsdes: An improvement on the malliavin weights. *Stochastic Processes and their Applications 120*, 7 (2010), 1133 – 1158.

[33] Delarue, F., and Menozzi, S. A forward-backward stochastic algorithm for quasi-linear PDEs. *The Annals of Applied Probability* (2006), 140–184.

[34] Ec.europa.eu. Structural reform of the european carbon market - european commission, 2015.

[35] El Karoui, N., Peng, S., and Quenez, M. C. Backward stochastic differential equations in finance. *Mathematical finance 7*, 1 (1997), 1–71.

[36] Föllmer, H., and Leukert, P. Quantile hedging. *Finance and Stochastics 3*, 3 (1999), 251–273.

[37] Geiersbach, C., and Pflug, G. C. Projected stochastic gradients for convex constrained problems in hilbert spaces. *SIAM Journal on Optimization 29*, 3 (2019), 2079–2099.

[38] Gobet, E., Lemor, J.-P., and Warin, X. A regression-based Monte Carlo method to solve backward stochastic differential equations. *The Annals of Applied Probability 15*, 3 (2005), 2172–2202.

[39] Gobet, E., López-Salas, J. G., Turkedjiev, P., and Vázquez, C. Stratified regression monte-carlo scheme for semilinear pdes and bsdes with large scale parallelization on gpus. *SIAM Journal on Scientific Computing 38*, 6 (2016), C652–C677.

[40] Gobet, E., and Turkedjiev, P. Approximation of backward stochastic differential equations using malliavin weights and least-squares regression. *Bernoulli 22*, 1 (2016), 530–562.

[41] Gyurkó, L. G., and Lyons, T. J. Efficient and practical implementations of cubature on wiener space. In *Stochastic analysis 2010*. Springer, 2011, pp. 73–111.

[42] Han, J., Jentzen, A., and E, W. Overcoming the curse of dimensionality: Solving high-dimensional partial differential equations using deep learning. *arXiv preprint arXiv:1707.02568* (2017).

[43] Han, J., Jentzen, A., and Weinan, E. Solving high-dimensional partial differential equations using deep learning. *Proceedings of the National Academy of Sciences 115*, 34 (2018), 8505–8510.

[44] Han, J., and Long, J. Convergence of the deep bsde method for coupled fbsdes. *Probability, Uncertainty and Quantitative Risk 5*, 1 (2020), 1–33.

[45] Hornik, K., Stinchcombe, M., and White, H. Multilayer feedforward networks are universal approximators. *Neural networks 2*, 5 (1989), 359–366.

[46] Howison, S., and Coulon, M. C. Stochastic behaviour of the electricity bid stack: from fundamental drivers to power prices. *The Journal of Energy Markets 2*, 1 (2009).

[47] Howison, S., and Schwarz, D. Risk-neutral pricing of financial instruments in emission markets: a structural approach. *SIAM Journal on Financial Mathematics 3*, 1 (2012), 709–739.

[48] Huré, C., Pham, H., and Warin, X. Deep backward schemes for high-dimensional nonlinear pdes. *Mathematics of Computation 89*, 324 (2020), 1547–1579.

[49] Hutzenthaler, M., Jentzen, A., Kruse, T., and Nguyen, T. A. Overcoming the curse of dimensionality in the numerical approximation of backward stochastic differential equations. *Journal of Numerical Mathematics* (2022).

[50] Iusem, A. N. On the convergence properties of the projected gradient method for convex optimization. *Computational & Applied Mathematics 22* (2003), 37–52.

[51] Jourdain, B. Probabilistic characteristics method for a one-dimensional inviscid scalar conservation law. *The Annals of Applied Probability 12*, 1 (2002), 334–360.

[52] Jourdain, B. Signed sticky particles and 1d scalar conservation laws. *COMPTES RENDUS MATHEMATIQUE 334*, 3 (2002), 233–238.

[53] Jourdain, B., and Reygner, J. Optimal convergence rate of the multitype sticky particle approximation of one-dimensional diagonal hyperbolic systems with monotonic initial data. *Discrete & Continuous Dynamical Systems-A 36*, 9, 4963.

[54] Jourdain, B., and Reygner, J. The small noise limit of order-based diffusion processes. *Electronic Journal of Probability 19* (2014), 1–36.

[55] Jourdain, B., and Reygner, J. A multitype sticky particle construction of wasserstein stable semigroups solving one-dimensional diagonal hyperbolic systems with large monotonic data. *Journal of Hyperbolic Differential Equations 13*, 03 (2016), 441–602.

[56] Jourdain, B., and Roux, R. Convergence of a stochastic particle approximation for fractional scalar conservation laws. *Stochastic Processes and their Applications 121*, 5 (2011), 957–988.

[57] Kingma, D. P., and Ba, J. Adam: A method for stochastic optimization. *arXiv preprint arXiv:1412.6980* (2014).

[58] Kružkov, S. N. First order quasilinear equations in several independent variables. *Mathematics of the USSR-Sbornik 10*, 2 (1970), 217.

[59] Lacoste-Julien, S., Schmidt, M., and Bach, F. A simpler approach to obtaining an o (1/t) convergence rate for the projected stochastic subgradient method. *arXiv preprint arXiv:1212.2002* (2012).

[60] LeVeque, R. J. *Numerical methods for conservation laws*, vol. 132. Springer, 1992.

[61] Liu, J., and Ye, J. Efficient euclidean projections in linear time. In *Proceedings of the 26th Annual International Conference on Machine Learning* (2009), pp. 657–664.

[62] Pagès, G., and Sagna, A. Improved error bounds for quantization based numerical schemes for bsde and nonlinear filtering. *Stochastic Processes and their Applications 128*, 3 (2018), 847 – 883.

[63] Pardoux, E., and Peng, S. Backward stochastic differential equations and quasilinear parabolic partial differential equations. In *Stochastic partial differential equations and their applications*. Springer, 1992, pp. 200–217.

[64] Rockafellar, R. T. *Convex analysis*, vol. 18. Princeton university press, 1970.

[65] Soner, H. M., and Touzi, N. Dynamic programming for stochastic target problems and geometric flows. *Journal of the European Mathematical Society 4*, 3 (2002), 201–236.

[66] Soner, H. M., and Touzi, N. Stochastic target problems, dynamic programming, and viscosity solutions. *SIAM Journal on Control and Optimization 41*, 2 (2002), 404–424.

[67] Villani, C. *Optimal transport: old and new*, vol. 338. Springer, 2009.

[68] Zhang, J. *Some fine properties of backward stochastic differential equations*. PhD thesis, purdue University, 2001.